

P 230931 (1)

UNCLASSIFIED

92

AGARD-AG-241

AGARD-AG-241

AGARD

ADVISORY GROUP FOR AEROSPACE RESEARCH & DEVELOPMENT

7 RUE ANCELLE 92200 NEUILLY SUR SEINE FRANCE

AGARDograph No. 241

A Comparison of Panel Methods for Subsonic Flow Computation

by

H.S. Sytsma, B.L. Hewitt and P.E. Rubbert

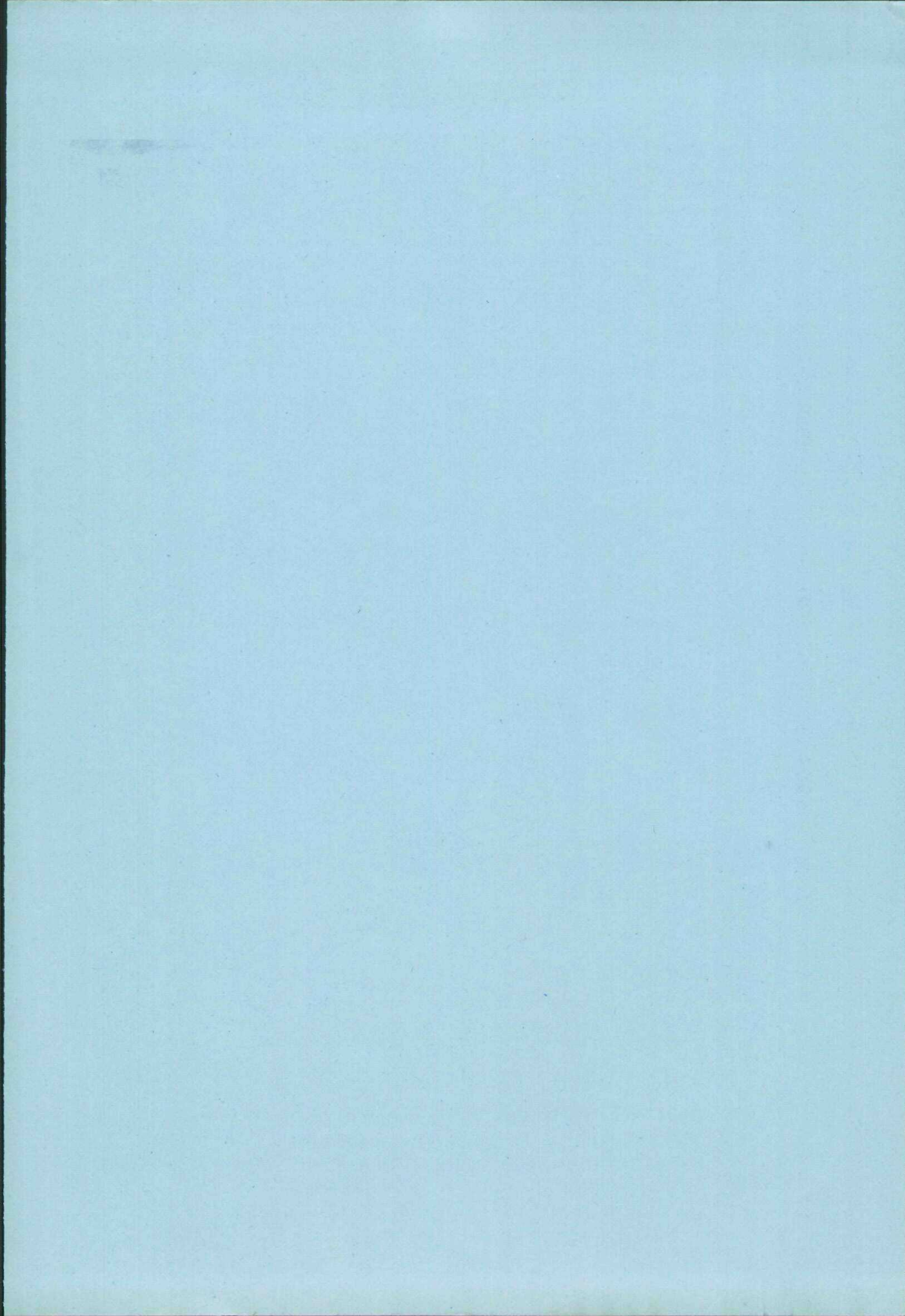
A

NORTH ATLANTIC TREATY ORGANIZATION



DISTRIBUTION AND AVAILABILITY
ON BACK COVER

UNCLASSIFIED



NORTH ATLANTIC TREATY ORGANIZATION
ADVISORY GROUP FOR AEROSPACE RESEARCH AND DEVELOPMENT
(ORGANISATION DU TRAITE DE L'ATLANTIQUE NORD)

AGARDograph No.241

**A COMPARISON OF PANEL METHODS FOR
SUBSONIC FLOW COMPUTATION**

by

H.S.Sytsma
Research Engineer
National Aerospace Laboratory (NLR)
Anthony Fokkerweg 2
1059 CM Amsterdam, Netherlands

B.L.Hewitt
Principal Aerodynamicist
British Aerospace
Warton Division
Preston
Lancashire PR4 1AX, UK

and

P.E.Rubbert
Engineering Manager
Boeing Military Airplane Development
P.O.Box 3999
Seattle
Washington 98124, USA

THE MISSION OF AGARD

The mission of AGARD is to bring together the leading personalities of the NATO nations in the fields of science and technology relating to aerospace for the following purposes:

- Exchanging of scientific and technical information;
- Continuously stimulating advances in the aerospace sciences relevant to strengthening the common defence posture;
- Improving the co-operation among member nations in aerospace research and development;
- Providing scientific and technical advice and assistance to the North Atlantic Military Committee in the field of aerospace research and development;
- Rendering scientific and technical assistance, as requested, to other NATO bodies and to member nations in connection with research and development problems in the aerospace field;
- Providing assistance to member nations for the purpose of increasing their scientific and technical potential;
- Recommending effective ways for the member nations to use their research and development capabilities for the common benefit of the NATO community.

The highest authority within AGARD is the National Delegates Board consisting of officially appointed senior representatives from each member nation. The mission of AGARD is carried out through the Panels which are composed of experts appointed by the National Delegates, the Consultant and Exchange Programme and the Aerospace Applications Studies Programme. The results of AGARD work are reported to the member nations and the NATO Authorities through the AGARD series of publications of which this is one.

Participation in AGARD activities is by invitation only and is normally limited to citizens of the NATO nations.

The content of this publication has been reproduced directly from material supplied by AGARD or the authors.

Published February 1979

Copyright © AGARD 1979
All Rights Reserved

ISBN 92-835-1312-6



*Printed by Technical Editing and Reproduction Ltd
Harford House, 7-9 Charlotte St, London, W1P 1HD*

FOREWORD

A brief unpublished report on the subject of this AGARDograph was made by Mr B.Hung (BAe) at the Euromech 75 Colloquium in May of 1976. The authors, who had prepared that report, were commissioned by the Fluid Dynamics Panel of AGARD to prepare the work for this publication. The AGARDograph Editor was Dr G.G.Pope (RAE).

CONTENTS

	page
SUMMARY	1
LIST OF SYMBOLS	2
1. INTRODUCTION	2
2. THEORETICAL BACKGROUND OF PANEL METHODS	3
3. SHORT OUTLINE OF THE PANEL METHODS INVOLVED IN THE COMPARISON	4
3.1 Introduction	4
3.2 The NLR Panel Method	4
3.3 Hunt - Semple Panel Methods	5
3.3.1 The "lines" model	5
3.3.2 The "sheets" model	6
3.4 Boeing's Interim Higher Order Panel Method	7
3.5 Roberts' Spline - Neumann Method	7
4. DEFINITION OF THE TEST CASES	8
4.1 Definition of the Geometry of the Test Cases	8
4.2 Flow Conditions	8
4.3 Panel Distributions	8
5. EVALUATION OF THE RESULTS	9
5.1 Datum Results	9
5.1.1 Introductory remarks	9
5.1.2 Discussion	9
5.2 Comparison of "first-order" Method Results	10
5.2.1 Introduction	10
5.2.2 Discussion	10
5.2.3 Comparison of some NLR method results with Hunt - Semple "lines" method results	12
6. SENSITIVITY OF THE RESULTS TO THE NUMBER OF PANELS USED	12
6.1 Introduction	12
6.2 Results from "first-order" Methods	12
6.3 Results from "higher-order" Methods	13
6.3.1 Rubbert's method	13
6.3.2 Roberts' method	13
7. ACCURACY VERSUS COMPUTATION TIMES	14
8. CONCLUSIONS	15
REFERENCES	16
5 TABLES	
112 FIGURES	

A COMPARISON OF PANEL METHODS FOR
SUBSONIC FLOW COMPUTATIONS

by

H.A. Sytsma *

B.L. Hewitt **

P.E. Rubbert ***

SUMMARY

Surface singularity or panel methods have, in recent years, been developed to a stage where, in principle at least, they are capable of providing nominally exact numerical solutions for incompressible potential flow around complicated, real aircraft configurations. As such they have proved to be very useful, particularly to the wing designer.

There is at present, a large variety of surface singularity methods in use or under development throughout the world. In general, each method has its own modeling, accuracy limitations, convergence characteristics, computational time per case etc.. The variety of methods together with the importance attached to them by the wing designers et.al.means that there is a real need for a data base against which the various programs (either existing or under development) may be checked.

This report contains such a data base for a number of relatively simple wing configurations and nacelle configurations. The datum results have been obtained from the Roberts (BAe) Spline-Neumann Program, and a pilot version of the Boeing Advanced Panel-Type Influence Coefficient Method.

In addition, results from the practical, engineering type application of several methods are compared with the datum solutions. These comparisons suggest that of the methods considered, i.e. the NLR Panel Method, Hunt-Semple "sheets" method, Roberts Spline-Neumann program and the pilot version of the Boeing Advanced Panel-Type Influence Coefficient Method, the latter is the most efficient, in terms of the accuracy/computation time ratio, for the simple test cases considered. However, it must be realised that these test cases are not representative of the production cases which are normally required by aircraft designers, and that the calculations related to the results in this document were carried out in 1976; many improvements to programs have been incorporated since then.

*) Research Engineer, National Aerospace Laboratory(NLR), Anthony Fokkerweg 2, 1059 CM AMSTERDAM, The Netherlands

**) Principal Aerodynamicist, British Aerospace, Warton Division, Preston, Lancashire PR4 1AX, UK

***) Engineering Manager, Boeing Military Airplane Development, P.O.Box 3999, Seattle, Washington 98124, USA

LIST OF SYMBOLS

C	local chord	α	free stream incidence (degrees)
C_{LL}	local lift coefficient	Γ	sectional circulation
C_p	pressure coefficient	μ	doublet strength
\bar{n}	unit normal vector (outward positive)	η	fractional spanwise distance
\bar{U}_∞	free stream velocity vector	σ	source strength
X, Y, Z	rectangular co-ordinate system	θ	circumferential angle (degrees)
V_x, V_y	velocity components in X, Y, Z system	ϕ	perturbation velocity potential
T/C	thickness/chord ratio	Φ	total velocity potential
C/D_E	chord/exit diameter ratio		

1. INTRODUCTION

Surface singularity or so-called panel methods for the computation of incompressible flows with linear compressibility corrections, have been in use for more than 15 years. During these years they have been developed (mainly because of the advent of fast computers) into an important and frequently used tool for aerodynamicists.

Although the basic theorem (i.e. Green's theorem) underlying all panel methods is the same, there exists at present a large variety of panel methods. This is due to several factors. First of all, Green's theorem leaves, in principle, a freedom of choice from a variety of combinations of singularity (source, doublet) distributions. Secondly, panel methods are numerical by nature, leaving for each method developer the possibility of choosing his own numerical scheme with regard to e.g. the discretisation of the singularity distributions, geometry representation, type of boundary conditions used, solution method etc.

This multichoice situation naturally gives rise to questions about which type of method is most efficient in terms of the accuracy/computation time ratio for a given type of flow problem. The present report presents the results of a joint NLR-BAE-Boeing effort (with some participation by McDonnell - Douglas) to establish and compare this "efficiency" for a limited number of panel methods that have been generally accepted in literature as viable programs for aeronautical applications. Three of the methods involved in the comparison are of the "first - order" type (truncation error of order (panel dimension)). These methods are known as the NLR-Panel method (Ref. 1), the Hunt-Semple "lines" method (Ref. 2) and the Hunt-Semple "sheets" method (Ref. 2) the last two being developed at BAE (Warton). Results of a "pseudo-second-order" method are available from Boeing, using their Interim Higher-Order method (developed by P.E. Rubbert et. al.), which is a pilot program for Boeings' Advanced Panel-Type Influence Coefficient Method (Ref. 3).

The aim of establishing and comparing the efficiency of the various numerical methods encounters two main problems.

Firstly, no exact solutions currently exist for three-dimensional lifting potential flow problems. However, in order to obtain some kind of measure with regard to accuracy, the following approach was adopted. For a selected set of, relatively, simple geometries (a family of wings and nacelles) rather costly "converged*" solutions were obtained by means of the "third-order" panel method developed by A. Roberts at BAE (Weybridge) (Ref. 4). In this report it is assumed that this method provides results with datum accuracy against which the results of the other methods can be checked. Results with datum accuracy were also provided by Boeing.

Secondly, there remains the problem of comparing computing times. Computing costs related to the methods are very difficult to compare in a truly fair manner. Even if it were possible to run all programs individually on the same computer with access to the full storage capacity, the computation times could only give a rather narrow comparison. For example, a versatile program would probably use more computation time than a specialised one. In the comparative study being described the situation was even more complicated, since the calculations were carried out on different computers. Nevertheless, a comparison of computation times is presented. This was constructed by scaling all computation times to a reference computer, which in this case was chosen as the CDC 6600. However, it will be clear that the scaling factors should be interpreted with care, and therefore the actual computation times for each computer are also

*) Within the scope of this report, converged should be interpreted in the sense that an increase of the number of panels used did not affect the results significantly.

presented.

In the next chapter the mathematical background of the calculation of inviscid incompressible flow around arbitrary lifting bodies will be briefly outlined. Some details about the particular numerical schemes used in the methods being currently compared are presented in chapter 3. The geometrical details of the selected set of test configurations, together with flow conditions and the chosen panel distributions are given in chapter 4. A discussion of the results in terms of chordwise pressure distributions, velocity components, quantities such as sectional load and circulation is presented in chapter 5. The sensitivity of the results to the number of panels used is subject of chapter 6. In chapter 7 an attempt is made to relate accuracy, number of panels used, and computation time for the various methods compared. Finally some concluding remarks are given in chapter 8.

Some provisional results of this study were presented by B. Hunt (BAe) at the Euromech 75 colloquium at Braunschweig in May '76. It was felt by the participants to be worthwhile to make the results available to a wider audience, and consequently publication through the AGARD-FDP was sought and granted.

2. THEORETICAL BACKGROUND OF PANEL METHODS

In this chapter the mathematical basis for the treatment of 3-D irrotational incompressible flow around arbitrary configurations will briefly be outlined. Only this type of flow is considered in this report. More details of the theory can be found in standard references (Refs. 5,6,7).

Flows of this type are characterized by a perturbation velocity potential ϕ . This potential satisfies Laplace's equation:

$$\phi_{xx} + \phi_{yy} + \phi_{zz} = 0 \quad (1)$$

in a region R surrounding the body, and is subject to certain boundary conditions. The body is bounded by the surface S. In order to obtain a unique solution in lifting cases, a potential discontinuity surface W (the so-called wake), leaving the sharp trailing edge and extending to infinity, has to be introduced (Fig. 1).

According to Green's third identity, a solution of eqn. (1) may be expressed at any point P as the potential induced by a combination of so-called source singularities of strength σ and doublet singularities of strength μ , distributed on the surfaces S and W:

$$\phi(P) = \iint \sigma(Q) \left(\frac{-1}{4\pi r} \right) \partial S + \iint \mu(Q) \frac{\partial}{\partial n_Q} \left(\frac{1}{4\pi r} \right) \partial S \quad (2)$$

where r is the distance from the field point P to the surface point Q, and $\frac{\partial}{\partial n_Q}$ is the derivative in the direction of the outward surface normal. A required solution may be found by imposing suitable boundary conditions on S and W. Within the scope of this report only the Neumann type of boundary condition is considered, which can be imposed directly:

$$\frac{\partial \phi}{\partial n_Q} = -\bar{U}_\infty \cdot \bar{n}_Q \quad (3)$$

or (indirectly) by requiring the Dirichlet condition that

$$\phi = 0 \quad (4)$$

on the inner surface of the body. Upon making an "a priori" choice for the doublet strength distribution when using eqn. (3), or an "a priori" choice for the source strength distribution when using eqn. (4), a Fredholm integral equation of the 2nd kind for the remaining unknown singularity strength is obtained*). It should be noted that for flows with circulation, doublet singularities must be used somewhere in the field.

Common to all panel methods is the subdivision of the surfaces S and W into so-called panels that approximate the geometric surfaces to a certain order. Further the singularity strengths may be chosen to vary in a convenient prescribed way over each panel, e.g. in a "first-order" method, constant strength source/doublet strengths, or possibly bi-linear doublet strength variations are employed on flat panels.

Selecting a number of control points per panel (this number depending on the order of the singularity distribution) i.e. points where the boundary condition is applied, leads (after integration) to a linear system of algebraic equations in the unknown singularity strengths. This system may then be numerically solved in several ways e.g. directly through matrix inversion or through some iterative process.

*) Other choices may lead to an integral equation of the 1st kind.

The above brief description contains the basic elements underlying all the panel methods involved in the current comparative study. In the next chapter these methods will be described in more detail, paying regard to the schemes adopted for geometry approximation, the location, type and variation of singularities used, the type of boundary conditions employed and the formation and solution of the linear systems of algebraic equations.

3. SHORT OUTLINE OF THE PANEL METHODS INVOLVED IN THE COMPARISON

3.1 Introduction

In this chapter the methods involved in the current comparison will be discussed in some detail. More details about a particular method or its scope of applications may be found in the relevant references. It should be noted that the description relates to the situation at the time that the calculations were carried out (1976). Since then some of the methods have been changed, or have evolved in some respect.

3.2 The NLR Panel Method

The NLR Panel Method follows, at least with regard to the solution of incompressible lifting flow problems, the lines of the method developed by P.E. Rubbert et. al. (Ref. 8). This method is a "first order" method, and this implies that generally the truncation error is of $O(h)$, where h is a characteristic panel dimension. It should be noted, however, that for reasons explained below the error becomes of $O(1)$ in the limiting case of vanishing thickness.

In this method the body and/or wing surfaces are approximated by flat panels in the same way as originally defined by Hess and Smith (Ref. 9).

The singularities used in the NLR Panel Method are: (i) constant strength sources distributed on each body and/or wing surface panel, and (ii) constant strength doublet panels on all wake surfaces of lifting configurations. For numerical reasons the wing wake is extended inside the wing, along the camber surface. From the well-known induced-velocity equivalence between a constant strength doublet panel and a line vortex along the edge of the panel, it follows that the constant doublet panels on wake and camber surface may be re-interpreted as a vortex network or lattice. For the doublet panels on the camber surface, the shape of the chordwise variation of doublet strength (which is equivalent to the variation of the internal vortex strengths) is prescribed and kept constant spanwise. However, an unknown scaling factor is associated with each streamwise strip and is effectively determined by locally applying the Kutta condition. In the NLR-method a standard parabolic shape is used for the chordwise variation of discrete vortex strengths (see Fig. 2). As a precaution the suitability of this shape may be checked for a typical 2-D section of the wing under consideration.

The surface boundary condition is of the Neumann type, i.e. (eqn. (3))

$$\frac{\partial \Phi}{\partial n} = -\bar{U}_{\infty} \cdot \bar{n} \quad ,$$

where \bar{n} is the outward normal to the body, and \bar{U}_{∞} the free stream velocity vector. This b.c. is applied at the geometric centroid of each flat surface panel; i.e. at the so-called "collocation points". In lifting cases the wake doublet strength is determined by forcing the flow to leave the wing tangential to a plane that bisects the wing trailing edge at a small ($\sim 10^{-7}$ x local chord) distance downstream (i.e. the Kutta-condition, see Fig.3). The general source panel and vortex lattice arrangement is depicted in figure 4.

The matrix equation stating that the unknown source and doublet strengths must satisfy the Neumann boundary condition (eqn.(3)) at all collocation points, together with the Kutta-condition, may be written in matrix form as follows:

$$\begin{bmatrix} A \end{bmatrix} \begin{bmatrix} X \end{bmatrix} = \begin{bmatrix} B \end{bmatrix} \tag{5}$$

or

$$\sum_{j=1}^N a_{ij} x_j = b_i \quad (i = 1, N) \tag{6}$$

where the a_{ij} are so-called normal velocity influence coefficients, expressing the normal velocity at collocation point i due to a unit strength singularity on panel j . Here b_i stands for the boundary condition pertaining to collocation point i , and x_j for the unknown singularity strength on panel j . The normal velocity influence coefficients are calculated and stored on disc column-wise, since then only the data pertaining to one panel has to reside in central memory. The velocity components V_x , V_y and V_z are likewise calculated and stored columnwise. Use is made of far- and near-field approximations given by Hess and Smith (Ref.9).

The linear system of algebraic equations is solved iteratively. For this purpose the matrix $[A]$ and the vectors $[X]$ and $[B]$ are organized in a special way, as depicted in figure 5. The coefficients relating to a streamwise source panel strip are grouped together in blocks (within the sub-matrix $[Sc]$) on the main diagonal. This structure allows the solution of the system by means of an adapted (note the column wise storage of the influence coefficients) block Gauss-Seidel approach. Convergence is tested on $\Delta\sigma$ and $\Delta\Gamma$ for two consecutive iteration steps ($\Delta\sigma = \sigma^{n+1} - \sigma^n$, n being the iteration number). The process is stopped when both $\Delta\sigma$ and $\Delta\Gamma$ are $< .0001$. For a simple lifting wing configuration a number of 10 -15 iterations is typical.

More details about the method with regard to the formation and the solution of the system of equations can be found in reference 10. Reference 11 contains a program listing on micro-fiche. Examples of applications can be found in references 12, 13.

3.3 Hunt - Semple Panel Methods

The Hunt - Semple "Mark 1A" panel program contains within a single program the option of using a "lines" model or a "sheets" model.

3.3.1 The "lines" model

The Hunt - Semple "lines" method, like the NLR-Panel method, is a "first-order" method. Both the NLR-method and the Hunt - Semple "lines" method use the same type of singularity distributions and boundary conditions (see Fig. 4), but differ in two important respects: (i) in the method of applying the Kutta-condition and (ii) in the Hunt - Semple use of an "optimiser" to determine an "optimal" chordwise shape for the strengths of the internal constant doublet panels; n.b. a new shape is calculated for each wing.

In the Hunt - Semple "lines" panel method the following approach is adopted for determining a characteristic "optimal" variation or shape of the chordwise doublet strength. It is argued that for a three-dimensional lifting component this chordwise shape may be conveniently chosen from a quasi-two dimensional argument. For each lifting strip the set of doublet strengths is chosen such that for an onset flow of 90° , with the internal vortices extended indefinitely spanwise, and all other influences, including the source panels neglected, the doublet distribution on the camber line satisfies (in a weighted least squares sense), the surface boundary conditions at the surface collocation points. An example of such an "optimised" distribution is given in figure 6a. The corresponding vortex distribution (Fig. 6b) can differ, significantly, from the type used at NLR (see Fig. 2), and from the distribution usually used at MBB (Ref. 14) where the strengths are chosen proportional to local thickness.

In the currently described Hunt - Semple methods, in order to make use of a 2-D "optimised" chordwise doublet shape in 3-D calculations, the shape values of doublet along each chordwise strip are scaled by the associated trailing edge value of doublet; which is regarded as the unknown for each chordwise strip. Figure 6c shows the source strengths associated with these "optimised" doublet distributions. It can be seen that the "optimised" distribution produces much smaller source strengths than e.g. does the thickness-based distribution. The objective of this procedure is to reduce the discretisation errors due to the fairly crude constant strength source panel modelling. It is to be noted that, thinking similar to that underlying the Hunt - Semple "optimiser" is expressed by Rubbert et. al. in Reference 15.

With respect to satisfying the Kutta-condition the following remarks can be made. In the Hunt - Semple "lines" method a set of Kutta-points is first constructed downstream of the wing trailing edge on the extension of its camber surface. Whereas in the NLR-method a tangential flow condition is fulfilled at such points, the technique adopted here could be described as a "calculated" Kutta-condition.

The approach is based on an exact analysis of the 2-D flow around a particular family of analytical airfoils, and is characterized by the chord length C and the trailing-edge angle A . The following function has been derived describing the velocity component normal to the trailing-edge bisector as a function of A , the circulation Γ and the distance δ downstream of the trailing edge.

$$v_n = \frac{\Gamma}{\pi C} \left(\frac{\delta}{C} \right)^{\frac{\pi + A}{2\pi - A}} \quad (7)$$

This formula is applied directly in the 3-D program, where the Kutta-points are placed at about $\frac{1}{3}$ % of the local chord downstream of the trailing edge along the mean spanwise position of the surface collocation points in the relevant strip. The reasoning behind this approach is to allow the Kutta-points to be sufficiently far removed from the trailing edge that flow field induced at these points by the actual constant

strength source panels closely matches that which would be induced by a corresponding "higher-order" source distribution. The circulation used in eqn (7) is found directly as part of the solution of the system of linear equations represented by eqn (6). The solution of this system depends on the normal velocity induced by all the singularities at collocation points. Thus because of implied small source strengths the normal velocity induced by the internal vortex system is of primary importance. Now it can be shown (Ref.8) that the normal velocity induced by a discrete vortex system is much less sensitive to the parameter h/Δ than e.g. the tangential velocity (Fig.7). From this it also follows that the circulation Γ will be less sensitive to a decrease in h/Δ than the sectional integrated load. More details about this approach can be found in reference 2.

The matrix formation is essentially the same as in the NLR-method, except that the matrix is written to disc row-wise, and the chordwise shape of the doubletivity variation may vary spanwise (n.b. usually this shape will not vary spanwise and is calculated by the so-called "optimiser", as described earlier).

The linear equations are solved by a point Gauss-Seidel method, (optionally, by over- or underrelaxation) except that the influences of the vortex chordwise vortex "ladders" on the Kutta-points are inverted as a single diagonal block; as in the MBB-method (see Ref. 14). The solution is considered to have converged when the residues $(b_i - \sum_j a_{ij} x_j)$ computed during an iterative cycle are all less than .0003.

3.3.2 The "sheets" model

The Hunt - Semple "sheets" method differs from the "lines" method only in the sense that, on the (flat) camber surface panels, the doubletivity on each panel is built up from a linear combination of four bilinear Lagrangian interpolation modes, one mode being associated with each of the four panel corners. A main requirement for the currently described "sheets" model is to provide sensible estimates for both the "tangential" first derivatives of doubletivity, and the doubletivity values, at panel centroids (see Fig. 8). For the purpose approximating the tangential derivatives, doubletivity values at adjacent centroids are locally fitted, three at a time, by quadratics. Independent fits are made in both the chordwise and spanwise directions. These local fits provide analytical estimates for first derivatives of doubletivity at panel centroids, which involve doubletivity values at adjacent centroids. As described previously, the only unknown associated with the doubletivity variation along each chordwise strip of panels is the value at the trailing edge. Thus, using the first derivative estimates there results a doubletivity representation over each panel which depends, in general, on three unknown trailing edge values of doubletivity. This doubletivity is equivalent to distributed vorticity $-\bar{n} \times \text{grad } \mu$ on each panel, together with a discrete line vortex of linearly varying strength μ along each panel edge. It can be shown that for the "sheet" approach, particularly in the case of lifting wings with small thickness, the tangential velocity at surface collocation points will be better represented than for the "lines" model, where a discrete internal vortex lattice is employed. The effect is demonstrated for a simplified model in figure 7. Further it should be noted that due to the discretisation of the lifting vortex system in a "lines" model, the jump in the spanwise velocity component at the trailing edge can never be predicted correctly, whereas a "sheets" model allows for this discontinuity. With regard to the errors for a "lines" model associated with the chordwise and the spanwise velocity components at the wing surface, it should be noted that the parameter Δ from figure 7 should be interpreted respectively as the chordwise panel length (error in V_x), or as the spanwise strip width (error in V_y). It may be noted that these errors in the velocity may lead to an error in the pressure distribution and, indirectly, to an error in integrated quantities such as the sectional load. This does not apply, however, to the circulation, as explained earlier in 3.3.1.

The chordwise shape of the doubletivity on the camber surface panels is found through essentially the same "optimising" process as for the "lines" model. It should be noted, however, that because of the 2-D nature of the optimisation process, the truncation error for vanishing thickness in the 3-D case is still formally of $O(1)$, as for other "first-order" panel methods.

The Kutta-condition is the same "calculated" one as employed in the "lines" method, and was outlined in chapter 3.3.1.

The matrix formation for the "sheets" model is somewhat more complex than that for the "lines" model. As previously explained, the doubletivity on each panel is generally dependent on three unknown trailing edge values of doubletivity. This dependence carries through directly into the panel influence expressions, and it is this fact which slightly complicates the "sheets" model matrix formation procedure relative to that for the "lines" model; further details are given in reference 7.

The solution of the linear system of equations is the same as for the "lines" model.

3.4 Boeing's Interim "Higher-Order" Panel Method

The type of geometry approximation in Boeing's method is "first-order", i.e. flat panels were employed on the surface and the wake of the test configurations. The wake is not extended inside the wing. Generally, a configuration is divided into so-called "networks". A "network" is viewed as a portion of the boundary surface which is subdivided into panels, and is logically independent in the sense that it contributes as many equations to the overall problem as it contributes unknowns.

In contrast to the methods discussed in the preceding sections, for this method the singularity distribution on the surface (and wake) panels is of doublet type only. The doublet strength distribution on each surface panel is chosen to vary quadratically in two orthogonal directions; a local 2-D Taylor expansion involving 6 parameters. Discrete values of the doublet strength are assigned to certain standard points on each "network". The location of these points (i.e. doublet parameter points) is shown in figure 9. The doublet distribution on a surface panel is then found by fitting the 6 parameter quadratic form, in a weighted least-squares sense, using the doublet value at its centre point and at those of the adjacent panels (9 points in all). The weight is chosen to be relatively very large only for the doublet value point on the panel considered. For a panel adjacent to a "network" edge, doublet value points on the edge are also included in the fit (Fig. 9).

The control points on a network, i.e. points where boundary conditions are applied, are also indicated in figure 9. These points include panel centre points as well as edge points (very slightly displaced from "network" edges).

At panel centre points a Dirichlet condition is employed which requires the vanishing of the total potential on the interior surface of the wing. The edge control points serve to facilitate matching between "networks". Thus at network edges, continuity of the doublet strength and its gradient is ensured to a certain order. At the trailing edge (where the wing and wake "networks" abut) the Kutta-condition is satisfied implicitly. For such a model the local doublet strength may be identified with the total potential Φ ; which is the basic unknown in this particular version of the Boeing's method.

This approach leads to a linear system of algebraic equations in the unknown doublet strength parameters. This system is solved by employing a Crout decomposition algorithm with pivoting in diagonal blocks only. Also use is made of a very fast Compass-coded vector product subroutine. After solving this system the velocity components at any point are directly found from the analytic gradient of the total potential Φ .

Note that the truncation error of the approach described above is generally $O(h)$, but becomes $O(h^2)$ in case of vanishing surface curvature (h being a characteristic panel dimension).

More details about this method can be found in reference 3.

3.5 Roberts' Spline - Neumann Method

In Roberts' method (Ref. 4) the aircraft's wetted surfaces are subdivided into a set of convenient "carpets", which are analogous to the "networks" in the Boeing method (see chapter 3.4). Each carpet is subdivided into curvilinear panels whose corners form a grid of points. These carpets are first mapped into a set of rectangles in convenient parametric u, v planes. The Cartesian components of the vector position of each grid point are specified as part of the input. Each of these components is regarded as a regular bi-cubic spline function of the parameters u and v in the parametric plane. Using this representation, the surface shape associated with any single panel is defined by sixteen basic bi-cubic spline modes (one mode is shown in Fig. 10). Thus continuity upto the second derivative between panel edges is preserved. The same approximation is used to represent the rigid wake surface and its extension inside the wing.

The type and location of the singularities used in Roberts' method correspond to those of the "first-order" NLR and Hunt - Semple methods. Sources are employed on the wetted surfaces and doublet strength on the wake and its extension along the camber surface inside the wing. As in the Hunt - Semple and NLR methods the chordwise shape of the internal doublet distribution is prescribed. Roberts' chordwise shape is given by the integral of a mixture of Birnbaum vorticity modes. The unknown source and doublet strength distributions over the set of "carpet" rectangles in the parametric plane are cubic. Again a bi-cubic spline approach is used and any single panel is covered by sixteen basic spline modes (see Fig. 10). By applying the boundary condition of zero normal velocity at the corners of each panel, a one-to-one correspondence

with the unknown singularity strength in the middle of each mode (point A in Fig. 10) is obtained.

In contrast with the "first-order" methods described earlier the Kutta-condition (i.e. the requirement that velocities remain finite at the wing trailing edge) is satisfied implicitly. Over a certain number of panels on both the upper and lower surfaces of the wing adjacent to the trailing edge, special singular types of source strength modes are employed. These modes are based on the analysis of a wedge type of flow, thus implicitly ensuring the correct flow behaviour at the trailing edge. Wing tips are treated in a similar way.

The influence coefficient of each singularity mode for the normal velocity at each collocation point is found numerically through specially developed Gauss quadrature techniques.

The resulting linear system of algebraic equations is solved directly by Crout matrix inversion.

Note that the truncation error of this method is generally of $O(h^3)$ (h being a characteristic panel dimension) but, because of the fixed choice of the internal doublet distribution, this becomes formally of $O(1)$ in the limiting case of 3-D lifting wings with vanishing thickness.

More details can be found in reference 4.

4. DEFINITION OF THE TEST CASES

4.1 Definition of the Geometry of the Test Configurations

Three different types of relatively simple test configurations were chosen for the current comparison. The first configuration is a swept tapered wing with RAE wing "A" planform, without camber or twist and without dihedral. The second one is a more complex configuration of the straked-wing type. The third configuration considered is an annular duct or flow-through nacelle. This latter configuration was introduced because it has been observed that the computation of such "partially internal" flow poses accuracy problems to several panel methods. The planforms of these wings and the cross-section of the nacelle are defined in figure 11.

For all configurations the same airfoil section was used for simplicity of definition, this was taken from the NACA-Four-Digit series. This appeared to be of importance for the methods of Boeing (Rubbert) and Roberts since these methods cannot easily handle open trailing edges without including a thick wake representation. Consequently the trailing edges had to be handled in a special way. Rubbert solved this problem by altering the slope of the trailing edge panels, whereas Roberts extrapolated the trailing edge slightly beyond the original trailing edge to enable closure.

In order to study the capability of the various methods to treat wings of different thicknesses, a "family" of wings was defined, i.e. calculations were carried out for three thickness/chord ratios for the RAE WING planform ($T/C = .15, .05$ and $.02$) and for two T/C ratios for the straked-wing planforms ($T/C = .05$ and $.02$).

Although the extremely thin wing configurations ($T/C = .02$) are not "realistic" in the sense that wings of this thickness are not practical from a constructional point of view, they were introduced for the following reason. In the computation of flows with allowance for linear compressibility, the correction, according to Goethert's rule, requires the computation of the incompressible flow around an effectively thinner configuration. This means e.g. that for a 5 % thick configuration at $M = .8$, the incompressible flow is calculated around a configuration only 3 % thick. Also two nacelles were studied, with two chord/exit diameter ratios, i.e. 1.0 and 3.333.

4.2 Flow Conditions

With one exception the calculations were carried out for $\alpha = 5^\circ$ and with a rigid wake. For the wing cases the latter was located in the horizontal plane of symmetry downstream the wing. The wake of the nacelles is located on a cylindrical surface with its diameter equal to the exit diameter of the nacelle. Only one wing case (i.e. RAE WING, $T/C = .15$) is included for $\alpha = 0^\circ$ since it can be argued that none of the methods involved should have problems calculating non-lifting potential flow.

4.3 Panel Distributions

Apart from defining the test configurations geometrically, it was also deemed necessary to require the use of identical panel distributions for at least the "first-order" methods. Both the spanwise and the chordwise panelling was therefore prescribed. The two chosen distributions are tabulated in table 1 (chordwise) and table 2 (spanwise). In this way, differences between the results will be revealed more clearly

and will not be obscured by the use of different panel distributions. Thus, some useful information will also be obtained about the sensitivity of the results to the number of panels used in the computations.

Panelling for the "higher-order" methods was left open to choice in order to create the best conditions for obtaining supposedly datum accuracy. Furthermore, it was also requested that the "higher-order" methods provide so-called "engineering solutions" (i.e. results with acceptable accuracy in terms of chordwise pressure distributions) again with freedom of panelling.

5. EVALUATION OF THE RESULTS

5.1 Datum Results

5.1.1 Introductory Remarks

In this chapter datum solutions from the methods of Roberts and Rubbert will be discussed. The results are compared graphically in terms of chordwise pressure distributions, velocity distributions, and circulation. Unfortunately sectional load distributions could not be compared since Roberts' program did not provide this data. Corresponding tabulated data can be found in table 3.

The panel distributions used to generate the datum results were the following. Rubbert employed 40 panels chordwise and 12 spanwise strips for the RAE WING cases. Roberts used 39 panels chordwise and 13 spanwise strips for these cases.

For the STRAKED WING cases Rubbert employed 38 panels chordwise and 12 spanwise strips, whereas Roberts used 39 panels chordwise and 18 spanwise strips (thickness/chord ratio .05) and 24 strips spanwise for $T/C = .02$. On the nacelles, the number of chordwise panels used were 40 and 55, by Rubbert and Roberts, respectively. Both used 10 circumferential strips.

It should be noted that the set of data is not complete, in the sense that datum results from both methods are not available for all test cases. With regard to Rubbert's results it should be noted that an anomaly in the immediate vicinity of the trailing-edge is present; this is due to the alteration of the trailing edge slopes to enable closure (see 4.1). The consequences of this procedure were checked two-dimensionally and appeared to have no other effects.

5.1.2 Discussion

RAE WING Cases

Results for the RAE WING cases are presented graphically in figures 12 to 33. Chordwise pressure distributions show generally a high level of agreement for both ($T/C = .05$ and $.02$) thickness/chord ratios (Figs. 12 to 14, 19). The velocity components agree also very well for both thickness/chord ratios (Figs. 15, 16 and 21, 22). From drag loop comparisons (Figs. 17 and 20a, b) at near mid semi-span only slight differences can be noted in the peak region. From figures 18 and 23 it can be seen that there is also good agreement along the span between the circulation distributions.

STRAKED WING Cases

Only results for the $T/C = .02$ case are available for datum result comparison. The agreement between the chordwise pressure distributions on the inboard wing (Figs. 24, 25) is definitely worse than for the corresponding thickness/chord ratio for the RAE WING case. On the outboard wing next to the kink the agreement is of the same order (Fig. 26). Velocity components are compared for the two stations on either side of the kink. The agreement is fair for the chordwise velocity component (Figs. 27 and 29). The differences in the spanwise velocity component, in particular at the inboard section, are significant (Figs 28, 30). Consequently the flow directions as predicted by one or both methods are in error. This would obviously be of some importance for boundary layer calculations. It should here be mentioned that there is some indication that Roberts' results are not fully converged. In chapter 6.3.2 this will be discussed in some detail. Spanwise circulation distributions again show good agreement (Fig. 31).

NACELLE Cases

Datum results for the nacelle cases, are presented in figures 32 and 33. For these cases results are also available from calculations by J.L. Hess (McDonnell - Douglas). These results were obtained using a special "higher-order" axi-symmetric program, using 240 panels chordwise. From figures 32, 33 it can be seen that there is a fair agreement between all three methods. Since in Hess' method no circumferential discretisation is employed, and this discretisation contributes significantly to be the error in internal flow problems (Hess, Ref. 9), this solution is probably the best of the datum solutions presented.

5.2 Comparison of "first-order" Method Results

5.2.1 Introduction

In this chapter results from the Hunt - Semple "sheets" method and the NLR-method are compared graphically in terms of chordwise pressure distributions, drag loops, velocity components and integrated quantities such as circulation and sectional load. It may be noted that the NLR-method is considered as representative of the first-generation panel methods.

At the end of this section a few NLR results are also compared with results obtained from calculations carried out with the Hunt - Semple "lines" method. As outlined in chapters 3.2 and 3.3.1 these methods employ essentially the same numerical scheme.

The test cases were run with prescribed panel distributions defined in tables 1A and 2. These distributions are considered as typical engineering distributions for most "first-order" panel method applications in which detailed pressure distributions are required. However, it should be noted that, although 60 chordwise panels have been used in both the NLR and the Hunt - Semple "sheets" method in the calculations discussed in this section, 30 chordwise panels are usually adequate for use with the Hunt - Semple "sheets" method, as is illustrated by the results discussed in chapter 6.2.

5.2.2 Discussion

RAE WING Cases

The chordwise pressure distributions predicted by the various methods for the RAE WING with $T/C = .15$ and $\alpha = 0^\circ$ were found to be practically identical. An example is shown in figure 34. It can be seen that for this non-lifting case agreement between the first-order NLR results and Roberts' solution is very good.

Results for the RAE WING with $T/C = .15$ and $\alpha = 5^\circ$ are presented in figures 35 - 38. The picture is generally similar to that at $\alpha = 0^\circ$. However, the drag loop comparison presented in figure 36 shows some discrepancies in the leading edge region for the Hunt - Semple "sheets" results. Since the output points used by both NLR and Hunt - Semple program are nominally at flat panel centroids, the difference in C_p values near the leading edge must be associated with the fact that NLR effectively optimise their chordwise camber surface doublet variation with respect to sectional local lift. Which means that the leading edge C_p suction peak values are probably overestimated to compensate for the inescapable ΔC_p underestimates near the trailing edge, associated with the "lines" modelling. Thus, the accurate NLR drag loop peak values would appear to be the result of a rather fortuitous cancellation of independent errors associated with the Z/C and the C_p values. There is also a noticeable difference in the spanwise distribution of the sectional load (Fig. 38, note that a datum solution for this case is not available). The reason for this difference was not well understood. However, the spanwise distributions of circulation (Fig. 37) are virtually identical.

For $T/C = .05$ results are presented in figures 39 - 46. For the chordwise pressure distributions there is again good agreement between the various solutions, although some discrepancy is noticeable in the NLR results near the tip (Fig. 41). The Hunt - Semple results again differ significantly from the datum solution in the leading edge region, as can be seen from the drag loop comparisons presented in figure 42. Regarding the spanwise velocity component, it can be seen from figure 44 that the values calculated by the NLR panel method are in error over a large part of the wing. The explanation of this discrepancy has already been given in section 3.3.2. The agreement between spanwise distributions of circulation and load is good for both the "first-order" methods (Fig. 45 and 46).

Results for the extremely thin RAE WING case, i.e. $T/C = .02$ are given in figures 47 - 52. Regarding the chordwise pressure distributions, it can be seen from figure 47 that there is poor agreement between the NLR results and the datum solution. This can also be seen from the drag loop comparisons presented in figures 48a, b. Details of the pressure distribution in the leading edge region are again poorly predicted by the Hunt - Semple method. It can be seen that in the NLR results for this case an error in V_x is apparent, whereas the error in V_y has increased significantly in comparison with the situation for $T/C = .05$ (Figs. 49, 50). Also, there is a significant error in the spanwise load distribution predicted by the NLR method (Fig. 52).

From the observations made above it can be concluded that a "lines" model (as employed in the NLR panel method) generally is not adequate to predict aerodynamic quantities accurately and in sufficient detail for wings with a thickness/chord ratio below .05, at least not with a panel distribution as used for these calculations. For this low thickness/chord ratio only the circulation can be calculated with

reasonable accuracy using such a method.

The Hunt - Semple results generally agree quite well with Roberts' datum solutions, except in the nose region. This is possibly explained by the following. From figure 6c, it can be seen that the use of the "optimiser" reduces the source strength gradient over the greater part of the chord, but not in the immediate vicinity of the leading edge. Consequently the discretisation errors, which are proportional to the source strength gradient, can still be significant in this region.

STRAKED WING Cases

Results for the STRAKED WING case with $T/C = .05$ are presented in figures 53 - 64. From the comparisons of pressure distributions at three inboard and three outboard stations it can be seen that the agreement with Roberts' datum solution is reasonable, both inboard and outboard for both methods (Figs. 53 - 58), the worst errors being shown by the NLR results just inboard of the crank station (Fig. 55). Spanwise and chordwise velocity components are presented for the stations at either side of the kink in figures 59 - 62. It can be seen that the error in V_y at the inboard section is significant for the NLR results (Fig. 60). In contrast, the Hunt - Semple results exhibit a much smaller error. This error is probably due to the fact that in the Hunt - Semple method a 2-D "optimiser" is used for the determination of the internal doublet distribution (see 3.3.1), whereas the flow at this station is highly 3-D.

For $T/C = .02$, results are presented in figures 65 - 73. Inboard, the pressures are again predicted reasonably well by both methods; however, the NLR errors are larger than those of the Hunt - Semple method. At the outboard station next to the kink, the errors in the NLR results are similar to those in the mid-semispan results for the corresponding RAE WING case (Fig. 47; $T/C = .02$). Regarding the V_x comparisons, it can be noted from figure 68 that at the inboard station the error in V_x has increased slightly for both methods in comparison with the corresponding plot for $T/C = .05$ (Fig. 59).

At the outboard section next to the kink the situation is similar to the RAE WING case with $T/C = .02$ i.e. the Hunt - Semple results agree well with the datum solution, whereas the NLR results are seriously in error. Regarding the V_y comparisons the situation is quite different. Inboard both methods are seriously in error (Fig. 69); n.b. two datum solutions are shown. However, figure 69 indicates some uncertainty in datum solution accuracy. At the outboard section, however, the results again agree reasonably well with Roberts' datum solution.

The sectional load distributions are presented in figure 73. Apart from small differences on the inboard part of the wing, the Hunt - Semple results agree very well with Rubbert's solution. For the NLR results the situation is different, in that on the outboard wing the comparison is similar to that for the RAE WING with $T/C = .02$, i.e. the error in the load is significant, whereas on the inboard part of the wing the agreement with Rubbert's results is relatively good. However, the distinct jump in the NLR results across the crank seems unrealistic.

Summarizing the "first-order" method comparisons for the STRAKED WING cases it may be said that, for the results on the outboard wing the same conclusions apply as those already given for the RAE WING cases. Regarding the inboard part of the wing, errors in the predicted spanwise velocity component become very apparent, particularly for the $T/C = .02$ case. For the Hunt - Semple results, this may possibly be due to the 2-D nature of the "optimiser" used in this method (see chapter 3.3.1). However, it should be mentioned that, apart from "sheets" modelling being inherently better than that of the "lines" type, the Hunt - Semple method does allow the user to modify the results of the usual 2-D "optimiser", if it is felt advantageous to do so.

NACELLE Cases

Chordwise pressure distributions for the NACELLE case with chord/exit diameter ratio 1.0 and an angle of attack of 5° are compared at three circumferential stations, and are shown in figures 74 - 76. At all three stations the Hunt - Semple results agree well with Rubbert's datum solution on the outside of the nacelle. On the innerside, some discrepancies can be seen. Generally, the NLR results do not show such good agreement as those from the Hunt - Semple method.

In figure 77 results are compared for chord/exit diameter ratio 3.333, at an angle of 0° . The flow for this type of configuration can be characterized as being more of the "internal" type than in the case discussed above. It can be seen from figure 77 that inside the nacelle, both "first-order" methods are seriously in error. These errors can be associated with the fact that, for internal flows of this type, the conservation of mass is not satisfied, the leakage being due to "first-order" modelling deficiencies.

5.2.3 Comparison of NLR Results with Hunt - Semple "lines" Method Results

A comparison is presented to illustrate the type of differences that may occur when calculations are carried out with two methods, that basically employ an identical numerical model with regard to surface approximation and the use of a discrete vortex system (i.e. a "lines" model). Differences between the results then are only due to a different chordwise variation of the internal vortex strengths (note the use of the "optimiser" in the Hunt - Semple "lines" method, see chapter 3.3.1) and the formulation of the Kutta-condition ("calculated" in the Hunt - Semple method).

Results for the RAE WING with $T/C = .05$ are given in figures 78 -82. From figure 78 it can be seen that the pressure distributions at the section near mid-semispan agree to about the same level of accuracy with Roberts' results. This applies also to the comparisons of the velocity distributions (Figs. 79,80). Agreement between the circulation distributions is again very good(Fig. 81). From figure 82 it can be noted that the Hunt - Semple "lines" method tends to underpredict the load slightly.

6. SENSITIVITY OF THE RESULTS TO THE NUMBER OF PANELS USED

6.1 Introduction

In this section some results are presented and discussed which were obtained from calculations carried out using different numbers of panels. For both the NLR panel method and the Hunt - Semple "sheets" method a common panel distribution was prescribed in which only 30 panels chordwise were used. Spanwise the distribution is the same as for the preceding comparisons (see table 1B and 2). Also there are some results available from the methods of Rubbert and Roberts' which were obtained for fewer panels than were used to obtain datum accuracy. For both these methods the panelling used was left entirely to the choice of the user.

6.2 Results from "first-order" Methods

RAE WING Cases

Results from the NLR method for the RAE WING, with $T/C = .15$ are presented in figure 83 - 85. These indicate that, for a relatively thick wing, 30 chordwise panels are sufficient to give good accuracy.

Some results for the RAE WING with $T/C = .05$ are given in figures 86 - 89. From the pressure distributions near mid-semispan it appears that, in order to get a good quantitative prediction of the pressures, 30 chordwise panels suffice when the Hunt - Semple "sheets" method is used. For a "lines" method like that of NLR, 30 chordwise panels are not sufficient to predict the pressure distribution in detail. The spanwise velocity component at mid-semispan is given in figure 87. Apparently the results obtained from the Hunt - Semple "sheets" method with 30 chordwise panels are practically as accurate as the (60 x 12) results. The NLR results show a worsening of the type of error already present in the (60 x 12) results, as the number of panels is decreased. However, for the circulation distribution (Fig. 88), the agreement with Roberts' datum solution for both the Hunt - Semple "sheets" method and the NLR method is seen to be remarkably good for only 30 chordwise panels. Figure 89 illustrates that, in order to predict the spanwise loading with acceptable accuracy the NLR method must be used with many more than 30 chordwise panels.

Results for the $T/C = .02$ case are given in figures 90 - 93. From figure 90 it can be seen that the pressure distribution calculated with the Hunt - Semple "sheets" method, and employing only 30 chordwise panels, still show a good accuracy. For this case, results from the NLR-method are available with up to 90 chordwise panels. The NLR results using a (90 x 12) panel distribution show a distinct improvement in comparison with the corresponding (60 x 12) results. For this case, the (30 x 12) NLR results are very inaccurate. The spanwise velocity component comparison is presented in figure 91. The Hunt - Semple "sheets" results are accurate for both the panel distributions used. On the other hand the NLR results show that, increasing the number of chordwise panels up to 90 does not lead to a significant improvement in accuracy of the spanwise velocity component. However, from figure 92, it can be seen that even for such a low thickness/chord ratio (i.e. .02) the circulation is still predicted with good accuracy by all methods. With regard to the sectional load distributions presented in figure 93, the situation is quite different. The Hunt - Semple "sheets" method is capable of predicting the load distribution with good accuracy; even using only (30 x 12) panels. However, the NLR results again show, in particular for the (30 x 12) distribution, a rather poor agreement with the datum solution. Furthermore, it can be noted that even the use of the (90 x 12) panel distribution is not sufficient to obtain acceptable accuracy.

STRAKED WING Cases

In figures 94 - 100, results are presented for the two STRAKED WING cases i.e. for $T/C = .05$ and $.02$.

For $T/C = .05$, figure 94 shows the chordwise pressure distributions plotted at the inboard section next to the crank; this section is considered to be the most difficult section for this particular configuration. The agreement of the (30 x 12) results ranges from good (Hunt - Semple "sheets" method) to reasonable (NLR-method). The good agreement between the NLR (30 x 12) results and the datum solution is unexpected in view of the relatively poor agreement for the RAE WING case with $T/C = .05$ (see Fig. 86). The spanwise velocity components for this case are compared in figure 95. It can be seen that, though the pressure distributions agree fairly well at this section, the V_y results do not; the Hunt - Semple "sheets" results, though in error, being considerably better than the best from the NLR-method. The sectional load distributions obtained from both the NLR and the Hunt - Semple methods are presented in figure 97. It can be seen that a decrease of the number of panels used, to 30, corresponds to a significant decrease in the accuracy of the calculated load distribution for the NLR-method, whereas the agreement between the Hunt - Semple results for (30 x 12) and (60 x 12) results is very good (n.b. no datum solution for this case is available). In figures 98 - 100 results are presented for the extremely thin STRAKED WING case, i.e. $T/C = .02$. The chordwise pressure distributions for the most critical section i.e. the section just inboard of the crank are given in figure 98. Please note that two extra sets of results have been introduced, which were obtained using the NLR panel method. It can be seen that for the NLR-method 30 chordwise panels are definitely inadequate to predict the pressure distribution with sufficient detail. Further, it can be noted that an increase from 60 to 90 chordwise panels hardly changes the pressure distribution. An increase, however, of the number of spanwise strips from 12 to 18 (n.b. 6 extra strips in the vicinity of the crank were used) leads to some improvement.

A spanwise velocity component comparison is given in figure 99. Here it can also be seen that an increase of the number of chordwise panels hardly improves the level of accuracy. In fact, increasing the number of spanwise strips clearly gives the most significant improvement in accuracy. Sectional load distributions are compared in figure 100. The agreement of the NLR results, obtained using 30 chordwise panels, with Rubbert's datum solution is rather poor. Further, it can be seen that even when using a (90 x 12) distribution the predicted load is still about 10 % in error.

6.3 Results from "higher-order" methods

6.3.1 Rubbert's method

From Rubbert's method results are available for the RAE WING case with $T/C = .05$, obtained using two "engineering" panel distributions, i.e. one with 22 chordwise panels, and 12 spanwise strips and one in which only 12 chordwise panels are employed, but again with 12 spanwise strips. In practice, a distribution with 22 chordwise panels and only 8 spanwise strips could be used to give reasonably accurate results for such a simple wing configuration.

In figure 101 the chordwise pressure distributions near mid-semispan are presented and compared with Roberts' datum solution. It can be seen that the (22 x 12) distribution gives very accurate results. Using a (12 x 12) distribution, which is characterized by a coarser panelling near the leading edge, leads to a loss of accuracy in this region. From figure 102 it can be seen that the spanwise velocity component is predicted very well even when only 22 chordwise panels are used. The sectional load distributions plotted in figure 103 show that, although the chordwise pressure distributions are not correct in detail, the sectional load is still predicted with good accuracy; even when the (12 x 12) distribution is used.

6.3.2 Roberts'-method

The sensitivity of the results from Roberts'-method to the number of panels used is demonstrated for both the "thin" RAE WING and the "thin" STRAKED WING case. For the RAE WING, results are available from calculations carried out with two different panel distributions, i.e. one with 27 chordwise panels, and 9 spanwise strips and a second one which has 19 chordwise panels and only 6 spanwise strips.

In figure 104 the chordwise pressure distributions near mid-semispan are presented for the RAE WING case. The agreement between the datum solution and the results from both panel distributions is very good over a large part of the chord. From figure 104 it can be noted, however, that when the number of panels used is decreased, the pressures show a rapid increase of error. It could even be questioned whether the datum solution is "fully converged" near the trailing edge. Spanwise velocity components are presented in

figure 105. Generally, the agreement between the solutions is very good, although the same tendency, i.e. the rapid increase of error near the trailing edge can be seen. Circulation distributions are presented in figure 106. Apparently, the use of fewer panels results in an overprediction of the circulation along the span.

For the STRAKED WING results are available for the $T/C = .02$ case. Chordwise pressure distributions at the inboard station next to the crank are presented in figure 107. A decrease (in the vicinity of the crank) of the number of spanwise strips used, leads to relatively small changes in the pressure distribution at this section. A similar comparison is obtained for the spanwise velocity components (Fig. 108). The circulation distribution apparently is hardly altered, as can be seen from figure 109.

7. ACCURACY VERSUS COMPUTATION TIMES

In this chapter a crude attempt is made to evaluate the relative merits of the methods compared, in terms of the computational effort required to obtain a certain level of accuracy. As mentioned already in chapter 1, this poses two problems. Firstly, the calculations with the various programs were carried out on different computers. This makes it impossible to compare the respective computation times in a direct way. Secondly, the level of the accuracy must be defined in some appropriate manner.

The first problem has been approached by scaling all computing times to the time required on a reference computer; for this purpose the CDC 6600 has been chosen. The scaling factors used (see table 4) have been estimated by the individual participants in this investigation. It will be clear that these factors should be interpreted with care. For reference purposes, some of the actual computation times are presented in table 5. For three of the test cases two different times are given. Firstly, the time for the computer on which the case was actually run and, between brackets, the estimated time for a CDC 6600, using the scaling factors from table 4.

The level of accuracy has been defined by means of a so-called "L₂-error norm". This L₂-error norm E is given over some interval l by:

$$E = \sqrt{\frac{\int_0^l (\delta)^2 ds}{\int_0^l ds}} \tag{8}$$

In particular the following discretised form of eqn (8) has been used:

$$E = \sqrt{\frac{\sum_{i=1}^N (\delta)_i^2 (\Delta x/c)_i}{\sum_{i=1}^N (\Delta x/c)_i}} \tag{9}$$

The error norm E according to eqn (9) has been determined for pressure distributions ($\delta \equiv \Delta C_p$) and spanwise velocity component distributions ($\delta \equiv \Delta V_y$), wherein $(\delta)_i$ is the difference between Roberts' datum solution, calculated at N (= 100) equidistant points on the interval l (= chord), and any other solution. The values at the points i were found through a spline interpolation procedure.

Some results, obtained from the procedure outlined above, are plotted in figures 110, 111. Error norms for chordwise pressure distributions and spanwise velocity distributions are considered at mid-semispan ($\eta = .549$) for two RAE WING cases ($T/C = .05$ and $.02$), and at $\eta = .219$ (just inboard next to the crank) for the two STRAKED WING cases.

Regarding the RAE WING cases, it can be seen from figure 110a, c that for all methods the error in C_p increases significantly when the thickness/chord ratio decreases from .05 to .02. Further, it may be noted that, for a given computational effort the error in Rubbert's results is smaller than that of all other methods. Further, it can be seen that the difference in error norm E between the NLR and the Hunt - Semple "sheets" results is somewhat smaller than might be expected from the corresponding pressure distribution plots. This is possibly due to the relatively large errors in the Hunt - Semple "sheets" results present in the leading edge region. Also, it can be seen in figure 110c, that the error norm for Rubbert's datum solution and for Roberts' engineering case (27 x 9) panels is of the same order of magnitude but that the corresponding computation times differ significantly.

Regarding the spanwise velocity components the situation is very similar.

In figure 111 results of the same type are presented for the STRAKED WING cases at the section just inboard of the crank. Generally the same conclusions apply as have already been drawn for the RAE WING cases. In addition, it can be noted from the NLR results that an increase of the number of spanwise strips

(with the number of chordwise panels kept fixed) gives a significantly better prediction of the spanwise velocity component than a chordwise increase with the spanwise distribution fixed.

The C_p -error norm results from the NLR-method for the RAE WING cases are plotted as function of the thickness/chord ratio in figure 112. This figure shows the rapid increase of the error, when only 30 x 12 panels are used, for decreasing thickness/chord ratio. Also it can be seen clearly that when 60 x 12 panels are used, good results can be obtained employing a "lines" model (as used in the NLR-method) for relatively thick wings, i.e. with the thickness/chord ratio not below .05.

Finally, it is worthwhile bringing attention to the fact that both the NLR and the Hunt - Semple programs are very general in terms of application scope and are extremely "user oriented" in terms of input/output facilities etc.. Because of their generality of scope and design for ease of use, such programs are always liable to be less efficient, for any particular simple case, than programs having a smaller practical all-round utility value.

8. CONCLUSIONS

A comparative study has been made of the capabilities and efficiency of several so-called "panel methods", with respect to the prediction of aerodynamic quantities such as pressure distributions, velocity distributions, circulation, and integrated quantities such as sectional load. The methods currently compared are: i) Roberts' Spline-Neumann Program, developed at BAe (Weybridge), ii) Boeing's Interim Higher Order Method, developed by Rubbert et. al., iii) the Hunt - Semple "sheets" method and iv) the NLR Panel method.

The configurations for which calculations have been carried out are: i) a set of simple swept wings (RAE WING cases), ii) a set of wings with strake (STRAKED WING cases) and iii) a set of ring-wings or nacelles (NACELLE cases).

High accuracy (datum) solutions were provided by the methods of Roberts and Rubbert.

Regarding the wing test cases, the following has been observed:

- i) It appears that generally the agreement between the datum solutions from Roberts' "third-order" Spline-Neumann program and Rubbert's "pseudo second-order" method is very good. However, on the inboard part of the STRAKED WING case, with thickness/chord ratio .02, some discrepancies can be noted in particular for the spanwise velocity component. Unfortunately it cannot be decided which of the solutions, if any, is the "correct one".
- ii) It appears that first generation panel methods employing discretized vortex sheets (like the NLR panel method, the MBB method, the Boeing TEA 230 program and the Hunt - Semple program using the "lines" option) are adequate for predicting aerodynamic quantities for relatively thick wings (i.e. thickness/chord ratio not below .05).
- iii) The Hunt - Semple program using the "sheets" option offers an improved capability for "thin wing" applications; and is also relatively more efficient for calculating "thick wings".
- iv) Considering relative merits in terms of accuracy versus associated computation time, with different numbers of panels being used for each method, strongly suggests that the Boeing Interim Higher Order Method is the most efficient. However, it should be noted that some of the methods have evolved considerably since the currently compared results were actually calculated (i.e. in 1976).

With regard to the nacelle test cases the following has observed:

- i) Discrepancies can be noted between the datum solutions for all the nacelle cases considered, in particular on the innerside.
- ii) On the innerside of the slender NACELLE case (chord/exit diameter ratio 3.333), there is poor agreement with the datum solution for both "first-order" methods (i.e. NLR and Hunt - Semple "sheets" method). However, it may be inferred that these discrepancies are not so much due to "lines" versus "sheets" modelling differences, but rather to the chosen chordwise shapes of doublet variation on the mean surface used in conjunction with constant strength source panels on the geometric surface.

REFERENCES

1. Labrujere, Th.E, Loeve, W and Slooff, J.W.: "An approximate Method for the Calculation of the Pressure Distribution on Wing-Body Combinations at Sub-Critical Speeds," AGARD CP 71, also published as NLR MP 70014 U (1970).
2. Hunt, B and Semple, W.G.: "Economic Improvements to the Mathematical Model in a Plane/Constant-Strength Panel Method", Paper presented at Euromech Colloquium 75 at Braunschweig (1976).
3. Johnson, F.T. and Rubbert, P.E.: "Advanced Panel-Type Influence Coefficient Methods Applied to Subsonic Flows", AIAA Paper No. 75 - 50.
4. Roberts, A and Rundle, K.: "Computation of Incompressible Flow About Bodies and Thick Wings Using the Spline-Mode System", BAC(CAD) Report Aero Ma 19 (1972).
5. Kellogg, O.D.: "Foundations of Potential Theory", Dover Publish. Cy (1932).
6. Lamb, H.: "Hydrodynamics", Dover Publish. Cy (1945).
7. Hunt, B.: "The Panel Method for Subsonic Flows: a Surrey of Mathematical Formulations and an Outline of the New British Aerospace Scheme", VKI Lecture Series 1978-4.
8. Rubbert, P.E. and Saaris, G.R. et. al.: "A General Method for Determining the Characteristics of Fan-in-Wing Configurations", USAAVLABS Technical Report 67-61A (1967).
9. Hess, J.L. and Smith, A.M.O.: "Calculation of Non-Lifting Potential Flow About Arbitrary Three-Dimensional Bodies", Douglas Aircraft Report No. E.S. 40622 (1962).
10. Labrujere, Th.E. and Bleekrode, A.L.: "A Survey of Current Collocation Methods in Inviscid Subsonic Lifting Surface Theory (Part I: Numerical Aspects, Part II: Calculation Aspects of Solving the Large System of Equations on a Digital Computer)", VKI Lecture Series 1972-44.
11. Nijhuis, G.H.: "A Program for the Prediction of Stationary Flow about Airplane Configurations; A User-Guide for the NLR Panel Method", NLR TR 75052 U (1975).
12. Labrujere, Th.E. and Sytsma, H.A.: "Aerodynamic Interference Between Aircraft Components; Illustration of the Possibility of Prediction", NLR MP 72020 U (1972).
13. Loeve, W. and Slooff, J.W.: "On the Use of Panel Methods for Predicting Subsonic Flow About Airfoils and Aircraft Configurations", NLR MP 71018 U (1971).
14. Kraus, W.: "Das MBB-UFE Unterschall Panel Verfahren", MBB-UFE 633-70 (1970).
15. Rubbert, P.E. and Saaris, G.R.: "Review and Evaluation of a 3-D Lifting Potential Flow Analysis Method for Arbitrary Configurations", AIAA Paper 72 - 188 (1972).

TABLE 1A
Chordwise definition of fixed panel distribution (60 panels)

NACA FOUR-DIGIT SERIES			NACA FOUR-DIGIT SERIES			NACA FOUR-DIGIT SERIES		
T/C = 0.020000			T/C = 0.050000			T/C = 0.150000		
	x/c	z/c		x/c	z/c		x/c	z/c
0	0.0	0.0	0	0.0	0.0	0	0.0	0.0
1	0.002084	0.001329	1	0.002084	0.003322	1	0.002084	0.009967
2	0.008319	0.002601	2	0.008319	0.006502	2	0.008319	0.019506
3	0.018656	0.003808	3	0.018656	0.009520	3	0.018656	0.028561
4	0.033014	0.004941	4	0.033014	0.012353	4	0.033014	0.037060
5	0.051281	0.005989	5	0.051281	0.014971	5	0.051281	0.044914
6	0.073311	0.006937	6	0.073311	0.017343	6	0.073311	0.052028
7	0.098933	0.007774	7	0.098933	0.019436	7	0.098933	0.058308
8	0.127944	0.008489	8	0.127944	0.021223	8	0.127944	0.063668
9	0.160117	0.009071	9	0.160117	0.022679	9	0.160117	0.068036
10	0.195199	0.009515	10	0.195199	0.023787	10	0.195199	0.071362
11	0.232913	0.009816	11	0.232913	0.024540	11	0.232913	0.073620
12	0.272963	0.009975	12	0.272963	0.024936	12	0.272963	0.074809
13	0.315035	0.009994	13	0.315035	0.024986	13	0.315035	0.074957
14	0.358797	0.009882	14	0.358797	0.024705	14	0.358797	0.074115
15	0.403905	0.009647	15	0.403905	0.024118	15	0.403905	0.072353
16	0.450004	0.009301	16	0.450004	0.023253	16	0.450004	0.069759
17	0.496733	0.008858	17	0.496733	0.022144	17	0.496733	0.066432
18	0.543724	0.008330	18	0.543724	0.020825	18	0.543724	0.062476
19	0.590606	0.007733	19	0.590606	0.019333	19	0.590606	0.057998
20	0.637012	0.007080	20	0.637012	0.017701	20	0.637012	0.053102
21	0.682576	0.006385	21	0.682576	0.015964	21	0.682576	0.047891
22	0.726941	0.005661	22	0.726941	0.014153	22	0.726941	0.042460
23	0.769757	0.004920	23	0.769757	0.012300	23	0.769757	0.036900
24	0.810687	0.004173	24	0.810687	0.010433	24	0.810687	0.031300
25	0.849411	0.003432	25	0.849411	0.008581	25	0.849411	0.025744
26	0.885622	0.002709	26	0.885622	0.006772	26	0.885622	0.020316
27	0.919038	0.002013	27	0.919038	0.005033	27	0.919088	0.015100
28	0.949394	0.001358	28	0.949394	0.003394	28	0.949394	0.010182
29	0.976452	0.000753	29	0.976452	0.001882	29	0.976452	0.005646
30	1.000000	0.000210	30	1.000000	0.000525	30	1.000000	0.001575

TABLE 1B
Chordwise definition of fixed panel distributions (30 panels)

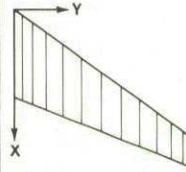
NACA FOUR-DIGIT SERIES T/C = 0.020000			NACA FOUR-DIGIT SERIES T/C = 0.050000			NACA FOUR-DIGIT SERIES T/C = 0.150000		
	x/c	z/c		x/c	z/c		x/c	z/c
0	0.0	0.0	0	0.0	0.0	0	0.0	0.0
1	0.006234	0.002264	1	0.006234	0.005661	1	0.006234	0.016982
2	0.025317	0.004383	2	0.025317	0.010957	2	0.025317	0.032872
3	0.057991	0.006306	3	0.057991	0.015766	3	0.057991	0.047297
4	0.105167	0.007946	4	0.105167	0.019865	4	0.105167	0.059596
5	0.167863	0.009185	5	0.167863	0.022962	5	0.167863	0.068887
6	0.246917	0.009889	6	0.246917	0.024722	6	0.246917	0.074165
7	0.342298	0.009939	7	0.342298	0.024847	7	0.342298	0.074541
8	0.451964	0.009284	8	0.451964	0.023211	8	0.451964	0.069633
9	0.570710	0.007994	9	0.570710	0.019986	9	0.570710	0.059958
10	0.690027	0.006267	10	0.690027	0.015668	10	0.690027	0.047003
11	0.799534	0.004380	11	0.799534	0.010951	11	0.799534	0.032853
12	0.889014	0.002639	12	0.889014	0.006599	12	0.889014	0.019796
13	0.950584	0.001331	13	0.950584	0.003329	13	0.950584	0.009986
14	0.984054	0.000579	14	0.984054	0.001448	14	0.984054	0.004344
15	1.000000	0.000210	15	1.000000	0.000525	15	1.000000	0.001575

Airfoil section: Symmetrical NACA FOUR-DIGIT AIRFOIL

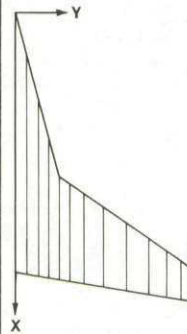
$$z/c = \frac{T/C}{.2} \left[.29690(x/c)^{\frac{1}{2}} - .12600(x/c) - .35160(x/c)^2 + .28430(x/c)^3 - .10150(x/c)^4 \right]$$

TABLE 2
Spanwise (c.q. circumferential) panel distribution

RAE WING a planform	
η Values of Panel Edges	η Values of Output Stations (Centroids)
0.0	0.0243
0.049	0.0788
0.107	0.1456
0.185	0.2314
0.279	0.3307
0.384	0.4380
0.494	0.5489
0.606	0.6583
0.713	0.7604
0.810	0.8506
0.893	0.9244
0.957	0.9782
1.0	



STRAKED WING planform	
η Values of Panel Edges	η Values of Output Stations (Centroids)
0.0	0.03394
0.07	0.09906
0.13	0.15884
0.19	0.21850
0.25	0.27972
0.31	0.34948
0.39	0.44391
0.50	0.56325
0.63	0.69291
0.76	0.80851
0.86	0.89886
0.94	0.96925
1.0	



Circular NACELLE
Circumferential Panel Edges in Terms of the Angle θ in Degrees
0.0
18.0
36.0
54.0
72.0
90.0
108.0
126.0
144.0
162.0
180.0

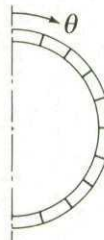


TABLE 3
Presentation of datum results

A) Contents

1 :	ROBERTS, RAE WING	, T/C = .15	, ALFA = .0	(CP-, VELOCITY-DATA)
2 :	" , " "	, T/C = .15	, ALFA = 5.0	(CP-, DRAGLOOP-DATA)
3 :	" , " "	, T/C = .05	, ALFA = 5.0	(CP-, VELOCITY-, DRAGLOOP-, GAMMA-DATA)
4 :	" , " "	, T/C = .02	, ALFA = 5.0	(CP-, VELOCITY-, DRAGLOOP-, GAMMA-DATA)
5 :	" , STRAKED WING	, T/C = .05	, ALFA = 5.0	(CP-, VELOCITY-, GAMMA-DATA)
6 :	" , " "	, T/C = .02	, ALFA = 5.0	(CP-, VELOCITY-, GAMMA-DATA)
7 :	" , NACELLE	, C/D _E = 1.0	, ALFA = .0	(CP-DATA)
8 :	" , " "	, C/D _E = 3.333	, ALFA = .0	(CP-DATA)
9 :	RUBBERT, RAE WING	, T/C = .05	, ALFA = 5.0	(CP-, VELOCITY-, DRAGLOOP-, GAMMA-, LOAD-DATA)
10 :	" , " "	, T/C = .02	, ALFA = 5.0	(CP-, VELOCITY-, DRAGLOOP-, GAMMA-, LOAD-DATA)
11 :	" , STRAKED WING	, T/C = .02	, ALFA = 5.0	(VELOCITY-, CP-, GAMMA-, LOAD-DATA)
12 :	" , NACELLE	, C/D _E = 1.0	, ALFA = .0	(CP-DATA)
13 :	" , " "	, C/D _E = 1.0	, ALFA = 5.0	(CP-DATA)
14 :	HESS , " "	, C/D _E = 1.0	, ALFA = .0	(CP-DATA)
15 :	" , " "	, C/D _E = 3.333	, ALFA = .0	(CP-DATA)

B) Data key

The datum results are given in part C of this table. The results pertaining to some test case are subdivided in one or more of the following data-blocks.

- Case-identification block

RUBBERT

DATUM

RAE WING

.02 ----- T/C (or C/D_E for NACELLE cases)

5.0 ----- ALFA

- Pressure-data block

CP-DATA

3 ----- n; number of spanwise stations for which data are given

40 ----- m; " " chordwise " " " " " "

	.079	.549	.924	η_i	$i = 1(1)n$
.9937	.04855	.05068	.05394	X/C ; CP(η_i)	$i = 1(1)n$
.9690	.00065	.00291	.01226		
.9207	-.02209	-.01908	-.00421		

- Velocity-data block

VELOCITY-DATA

1 ----- n; number of spanwise stations for which data are given

40 ----- m; " " chordwise " " " " " "

	.549	η_i	$i = 1(1)n$
.9937	.92978	.00269	-.09288
.9690	.98301	-.01936	-.05578
.9207	.99988	-.02663	-.05373

X/C ; V_x(η_i), V_y(η_i), V_z(η_i) $i = 1(1)n$

- Dragloop-data block

DRAGLOOP-DATA

1 ----- n, number of spanwise stations for which data are given

40 ----- m, " " chordwise " " " " " "

	.549	η_i	$i = 1(1)n$
.0006	.12688		
.0024	.03020	Z/C ; CP(η_i)	$i = 1(1)n$
.0049	-.00336		

TABLE 3 (continued)
Presentation of datum results

- Gamma-data block

GAMMA-DATA

12 - - - - - n; number of spanwise stations for which data are given

.0245 .14528

.078 .14528 $\eta ; \Gamma$

.146 .14645

- Load-data block

LOAD-DATA

12 - - - - - n; number of spanwise stations for which data are given

.0245 .14359

.078 .14463 $\eta ; C_{LL} C/2$

.146 .145529

⋮ ⋮

0.99601	0.10720	0.11121	0.09749
0.98002	0.08596	0.09039	0.07456
0.95807	0.07165	0.07738	0.05783
0.89752	0.05262	0.05919	0.03428
0.81815	0.04218	0.05047	0.02132
0.72478	0.03808	0.04705	0.01383
0.62287	0.03428	0.04911	0.01218
0.51806	0.03687	0.05373	0.01715
0.41574	0.04212	0.06316	0.02856
0.32059	0.05367	0.08129	0.05035
0.23626	0.07100	0.11031	0.08553
0.16520	0.09888	0.15324	0.13944
0.10851	0.14152	0.21862	0.21102
0.06601	0.20407	0.30643	0.30817
0.03644	0.29698	0.42313	0.43263
0.01769	0.43016	0.56312	0.57141
0.00717	0.59216	0.63693	0.62469
0.00222	0.62003	0.27447	0.17397
0.00044	0.17914	-0.95560	-1.22167
0.00003	-0.44263	-2.18088	-2.55460

VELOCITY-DATA

1			
42			
	0.549		
1.00565	0.92889	0.00326	-0.05454
0.99601	0.95310	-0.00666	-0.05550
0.98002	0.97133	-0.01454	-0.05577
0.95807	0.98638	-0.02101	-0.05563
0.89752	1.00959	-0.03141	-0.05295
0.81815	1.03011	-0.04037	-0.04928
0.72478	1.04970	-0.05024	-0.04517
0.62287	1.07052	-0.06133	-0.03931
0.51806	1.09216	-0.07386	-0.03073
0.41574	1.11566	-0.08811	-0.01954
0.32059	1.14217	-0.10506	-0.00312
0.23626	1.17197	-0.12559	0.01825
0.16520	1.20590	-0.14986	0.04851
0.10851	1.24888	-0.17997	0.09013
0.06601	1.30217	-0.21835	0.15036
0.03644	1.37266	-0.27136	0.24786
0.01769	1.46478	-0.35920	0.42075
0.00717	1.55265	-0.40450	0.75199
0.00222	1.48765	-0.35628	1.32489
0.00044	1.04647	-0.02906	1.85278
0.00003	0.53402	0.35186	1.90420
1.00565	0.91751	0.04966	-0.05291
0.99601	0.94035	0.04030	-0.05382
0.98002	0.95155	0.03603	-0.05343
0.95807	0.95854	0.03318	-0.05209
0.89752	0.96824	0.02998	-0.04939
0.81815	0.97300	0.02697	-0.04546
0.72478	0.97500	0.02645	-0.04017
0.62287	0.97814	0.02725	-0.03429
0.51806	0.97194	0.02920	-0.02724
0.41574	0.96720	0.03264	-0.01698
0.32059	0.95767	0.03925	-0.00434
0.23626	0.94176	0.05107	0.01236
0.16520	0.91705	0.06996	0.03078
0.10851	0.87701	0.09795	0.05123
0.06601	0.81757	0.14101	0.07247
0.03644	0.72428	0.21097	0.08811
0.01769	0.57021	0.32466	0.07952
0.00717	0.32036	0.50973	-0.02452
0.00222	0.00548	0.74382	-0.41498
0.00044	-0.06741	0.79771	-1.14660
0.00003	0.20441	0.59627	-1.66840

DRAGLOOP-DATA

1			
42			
	0.549		
0.00019	0.13417		
0.00076	0.08846		
0.00168	0.05319		
0.00291	0.02350		
0.00616	-0.02308		
0.01008	-0.06518		
0.01424	-0.10693		
0.01821	-0.15132		
0.02157	-0.19922		
0.02392	-0.25284		
0.02497	-0.31560		
0.02459	-0.38963		
0.02287	-0.47902		
0.02008	-0.60022		
0.01663	-0.76595		
0.01291	-1.01927		
0.00929	-1.43759		
0.00606	-2.13968		
0.00343	-3.09538		
0.00154	-3.52876		
0.00039	-3.03498		
-0.00019	0.15289		
-0.00075	0.11121		
-0.00168	0.09039		
-0.00291	0.07738		
-0.00616	0.05919		
-0.01008	0.05047		
-0.01424	0.04705		
-0.01821	0.04911		
-0.02157	0.05373		
-0.02392	0.06316		
-0.02497	0.08129		
-0.02459	0.11031		
-0.02287	0.15324		
-0.02008	0.21862		
-0.01663	0.30643		
-0.01291	0.42313		
-0.00929	0.56312		
-0.00606	0.63693		
-0.00343	0.27447		
-0.00154	-0.95560		
-0.00039	-2.18088		

GAMMA-DATA

14			
0	1.4489		
0.00737	1.4502		
0.03028	1.4539		
0.07078	1.4602		
0.13131	1.4640		
0.21342	1.4564		
0.31655	1.4263		
0.43708	1.3622		
0.56802	1.2629		
0.69937	1.1272		
0.81929	0.9538		
0.91573	0.7213		
0.97831	0.3996		
1.00000	0.00000		

ROBERTS 39X13(=DATUM) 4

RAE WING
0.02
5.0
CP-DATA

1			
42			
	0.549		
1.00134	0.02644		
0.97907	0.01194		
0.94305	-0.01327		
0.89504	-0.03563		
0.77166	-0.07280		
0.62848	-0.11464		
0.48450	-0.16243		
0.35420	-0.21878		
0.24588	-0.28716		
0.16211	-0.37241		
0.10136	-0.49834		
0.05987	-0.66887		
0.03318	-0.93471		
0.01709	-1.39790		
0.00809	-2.19493		
0.00348	-3.69393		
0.00137	-6.49278		
0.00051	-10.76293		
0.00019	-15.00187		
0.00006	-17.58981		
0.00001	-18.10731		
1.00134	0.07656		
0.97907	0.05280		
0.94305	0.05249		
0.89504	0.05533		
0.77166	0.06280		
0.62848	0.07836		
0.48450	0.10002		
0.35420	0.12877		
0.24588	0.16649		
0.16211	0.21510		
0.10136	0.28724		
0.05987	0.37113		
0.03318	0.47205		
0.01709	0.58724		
0.00809	0.64440		
0.00348	0.43184		
0.00137	-0.67394		
0.00051	-3.56720		
0.00019	-7.98097		
0.00006	-12.43020		
0.00001	-16.15535		

VELOCITY-DATA

1			
42			
	0.549		
1.00134	0.98623	-0.01897	-0.02310
0.97907	0.99353	-0.02060	-0.02278
0.94305	1.00602	-0.02663	-0.02189
0.89504	1.01693	-0.03181	-0.02159
0.77166	1.03478	-0.04070	-0.01909
0.62848	1.05438	-0.05169	-0.01544
0.48450	1.07624	-0.06335	-0.01118
0.35420	1.10119	-0.07831	-0.00335
0.24588	1.13012	-0.09968	0.00632
0.16211	1.16456	-0.12592	0.01846
0.10136	1.21328	-0.15750	0.03838
0.05987	1.27428	-0.20261	0.06343
0.03318	1.36054	-0.27031	0.10285
0.01709	1.49395	-0.36744	0.17603
0.00809	1.68420	-0.50648	0.31917
0.00348	1.95922	-0.70902	0.59384
0.00137	2.28590	-0.95685	1.16269
0.00051	2.47038	-1.09344	2.11294
0.00019	2.25613	-0.93065	3.16947
0.00006	1.67828	-0.50240	3.93964
0.00001	0.82863	0.12853	4.29000
1.00134	0.96005	0.03517	-0.02237
0.97907	0.97257	0.02864	-0.02186
0.94305	0.97272	0.02931	-0.02129
0.89504	0.97126	0.03040	-0.01942
0.77166	0.96738	0.03285	-0.01667
0.62848	0.95916	0.03809	-0.01374
0.48450	0.94760	0.04405	-0.00897
0.35420	0.93185	0.05352	-0.00408
0.24588	0.91025	0.07021	0.00323
0.16211	0.88095	0.09306	0.01250
0.10136	0.85505	0.12274	0.01921
0.05987	0.77463	0.16739	0.02825
0.03318	0.68605	0.23672	0.03521
0.01709	0.54445	0.33978	0.02941
0.00809	0.33154	0.49552	-0.01131
0.00348	-0.00336	0.74194	-0.13288
0.00137	-0.47303	1.09585	-0.49927
0.00051	-0.92900	1.43430	-1.28332
0.00019	-1.05524	1.52489	-2.35417
0.00006	-0.76383	1.30938	-3.33650
0.00001	-0.09117	0.81054	-4.06079

DRAGLOOP-DATA

1			
42			
	0.549		
0.00018	0.02644		
0.00069	0.01194		
0.00150	-0.01327		
0.00252	-0.03563		
0.00489	-0.07280		
0.00720	-0.11464		
0.00898	-0.16243		
0.00990	-0.21878		
0.00988	-0.28716		
0.00910	-0.37241		
0.00784	-0.49834		
0.00639	-0.66887		
0.00495	-0.93471		
0.00366	-1.39790		
0.00257	-2.19493		
0.00171	-3.69393		
0.00108	-6.49278		
0.00067	-10.76293		
0.00041	-15.00187		
0.00023	-17.58981		
0.00008	-18.10731		
-0.00018	0.07656		
-0.00069	0.05280		
-0.00150	0.05249		
-0.00252	0.05533		
-0.00489	0.06280		
-0.00720	0.07836		
-0.00898	0.10002		
-0.00990	0.12877		
-0.00988	0.16649		
-0.00910	0.21510		
-0.00784	0.28724		
-0.00639	0.37113		
-0.00495	0.47205		
-0.00366	0.58724		
-0.00257	0.64440		

.81696 .04675
 .89161 .04675
 .95001 .03305
 .98722 .01722
 1.00000 0.00000

0.14398 0.73137
 0.18941 0.69447
 0.24197 0.66076
 0.30116 0.62515
 0.36615 0.58572
 0.43577 0.54579
 0.50858 0.50272
 0.58289 0.45906
 0.65681 0.42054
 0.72836 0.38017
 0.79550 0.34230
 0.85627 0.30461
 0.90884 0.27210
 0.95155 0.25325
 0.98308 0.23898
 0.99432 0.23622
 1.00242 0.24371
 1.00730 0.27376

ROBERTS
 DATUM
 MACELLE
 1.0
 0.0
 CP-DATA
 1
 58

7

0.0
 1.00730 0.23142
 1.00242 0.18299
 0.99432 0.14873
 0.98308 0.12217
 0.95155 0.07976
 0.90884 0.04375
 0.85627 0.00899
 0.79550 -0.01281
 0.72836 -0.03818
 0.65681 -0.06460
 0.58289 -0.08991
 0.50858 -0.12119
 0.43577 -0.15044
 0.36615 -0.18854
 0.30116 -0.23278
 0.24197 -0.28104
 0.18941 -0.35010
 0.14398 -0.43432
 0.10583 -0.53296
 0.07483 -0.66758
 0.05054 -0.86046
 0.03230 -1.12978
 0.01928 -1.54276
 0.01056 -2.17350
 0.00517 -3.17041
 0.00217 -4.60860
 0.00073 -6.07078
 0.00017 -6.53910
 0.00001 -5.95896
 0.00001 -4.91847
 0.00017 -3.31615
 0.00073 -1.19243
 0.00217 0.34122
 0.00517 0.91834
 0.01056 0.99582
 0.01928 0.91496
 0.03230 0.80246
 0.05054 0.70139
 0.07483 0.61285
 0.10583 0.54041
 0.14398 0.47930
 0.18941 0.43229
 0.24197 0.39098
 0.30116 0.35873
 0.36615 0.32924
 0.43577 0.30424
 0.50858 0.28309
 0.58289 0.26336
 0.65681 0.24321
 0.72836 0.22652
 0.79550 0.21076
 0.85627 0.19732
 0.90884 0.19123
 0.95155 0.18923
 0.98308 0.19523
 0.99432 0.20291
 1.00242 0.21813
 1.00730 0.25373

RUBBERT
 DATUM
 RAE WING
 .05
 5.0
 CP-DATA
 3
 40

9

.079 .549 .924
 .9937 .12176 .12688 .13251
 .9690 .02462 .03020 .04044
 .9207 -.01067 -.00336 .01299
 .8513 -.05507 -.04689 -.02405
 .7643 -.09509 -.08815 -.05786
 .6641 -.13399 -.13184 -.09723
 .5556 -.17324 -.18066 -.14316
 .4443 -.21456 -.23771 -.20003
 .3358 -.25950 -.30662 -.27647
 .2356 -.31002 -.39282 -.37638
 .1487 -.37567 -.51391 -.51623
 .0870 -.46103 -.67340 -.69712
 .0475 -.58835 -.91693 -.96850
 .0225 -.78615 -1.30338 -1.39656
 .0110 -1.04320 -1.83492 -1.98843
 .0050 -1.32657 -2.51022 -2.75215
 .00205 -1.54277 -3.20090 -3.55447
 .00075 -1.56044 -3.60103 -4.05138
 .00024 -1.34611 -3.53612 -4.02996
 .00004 -.96905 -3.07072 -3.55791
 .00004 -.54510 -2.40074 -2.84381
 .00024 -.08627 -1.54522 -1.90721
 .00075 .32789 -.62070 -.87066
 .00205 .59460 .17024 .04079
 .0050 .63494 .57816 .53809
 .0110 .52896 .62912 .63143
 .0225 .39231 .52740 .54295
 .0475 .26468 .38314 .39633
 .0870 .17115 .25918 .26352
 .1487 .11450 .17604 .16894
 .2356 .07394 .11432 .09505
 .3358 .05210 .07980 .05198
 .4443 .04086 .06083 .02852
 .5556 .03568 .05101 .01603
 .6641 .03453 .04684 .01332
 .7643 .03697 .04701 .01755
 .8513 .04321 .05134 .02520
 .9207 .05617 .06267 .04042
 .9690 .06337 .06893 .05274
 .9937 .13758 .14094 .13024

VELOCITY-DATA
 1
 40

.549
 .9937 .92978 .00269 -.09288
 .9690 .98301 -.01936 -.05578
 .9207 .99988 -.02663 -.05373
 .8513 1.02127 -.03626 -.05080
 .7643 1.04109 -.04578 -.04678
 .6641 1.06157 -.05640 -.04153
 .5556 1.08386 -.06888 -.03418
 .4443 1.10910 -.08408 -.02318
 .3358 1.13841 -.10293 -.00637
 .2356 1.17321 -.12659 .01930
 .1487 1.21867 -.15879 .05956
 .0870 1.27298 -.19829 .11666
 .0475 1.34575 -.25180 .20609
 .0225 1.43855 -.32048 .36228
 .0110 1.52757 -.38643 .59340
 .0050 1.56469 -.41390 .94375
 .00205 1.46390 -.33889 1.35933
 .00075 1.19649 -.14005 1.77478
 .00024 .85414 .11447 1.94768
 .00004 .50831 .37156 1.91684
 .00004 .22388 .58301 1.73514
 .00024 .00094 .74875 1.40875
 .00075 -.09733 .82184 .96737
 .00205 -.02666 .76936 .48696
 .0050 .19280 .60630 .13063
 .0110 .42909 .43076 -.03494
 .0225 .16170 .29142 -.08573
 .0475 .75855 .18612 -.08260
 .0870 .85030 .11830 -.06176
 .1487 .90353 .07900 -.03672
 .2356 .93954 .05271 -.01272
 .3358 .95846 .03897 .00592
 .4443 .96839 .03174 .01976
 .5556 .97330 .02809 .02975
 .6641 .97524 .02649 .03702
 .7643 .97493 .02628 .04260
 .8513 .97247 .02722 .04715
 .9207 .96637 .02981 .05073
 .9690 .96293 .03123 .05349
 .9937 .92119 .04846 .09014

DRAGLOOP-DATA
 1
 40

.549
 .0006 .12688
 .0024 .03020
 .0049 -.00336
 .0085 -.04689
 .0125 -.08815
 .0166 -.13184
 .0203 -.18066
 .0232 -.23771
 .0246 -.30662
 .0243 -.39282
 .0219 -.51391
 .0183 -.67340
 .0142 -.91693
 .0103 -1.30338

ROBERTS
 DATUM
 MACELLE
 3.33333
 0.0
 CP-DATA
 1
 58

8

0.0
 1.00730 0.23528
 1.00242 0.18803
 0.99432 0.14975
 0.98308 0.12358
 0.95155 0.07996
 0.90884 0.04362
 0.85627 0.02626
 0.79550 0.00767
 0.72836 -0.00863
 0.65681 -0.02635
 0.58289 -0.04138
 0.50858 -0.06798
 0.43577 -0.09458
 0.36615 -0.12242
 0.30116 -0.15159
 0.24197 -0.19344
 0.18941 -0.24347
 0.14398 -0.31412
 0.10583 -0.39755
 0.07483 -0.52508
 0.05054 -0.69601
 0.03230 -0.96254
 0.01928 -1.35784
 0.01056 -2.00191
 0.00517 -3.04416
 0.00217 -4.62050
 0.00073 -6.33717
 0.00017 -7.09828
 0.00001 -6.69920
 0.00001 -5.73892
 0.00017 -4.11746
 0.00073 -1.82456
 0.00217 -0.02511
 0.00517 0.76767
 0.01056 0.98418
 0.01928 0.98836
 0.03230 0.93443
 0.05054 0.87288
 0.07483 0.81529
 0.10583 0.77023

.3358	.93553	.04775	.00364	.94649	.03302	.00240
.4443	.95101	-.02581	.00822	.95729	.02585	.00790
.5556	.96119	.01806	.01200	.96467	.02143	.01190
.6641	.96793	.01479	.01489	.96990	.01874	.01485
.7643	.97250	.01312	.01718	.97362	.01721	.01716
.8513	.97549	.01232	.01912	.97597	.01639	.01910
.9207	.97641	.01226	.02074	.97638	.01617	.02071
.9690	.97810	.01168	.02199	.97788	.01588	.02197
.9937	.96325	.01416	.03845	.96249	.01838	.03839

CP-DATA
6

.9937	.034	.099	.219	.280	.693	.899
.9690	.04590	.05006	.05559	.05790	.05403	.05626
.9207	-.00686	-.00087	.00798	.01027	.00595	.00775
.8513	-.03173	-.02447	-.01244	-.00846	-.01485	-.00965
.7643	-.06089	-.05265	-.03730	-.03287	-.04087	-.03133
.6641	-.08689	-.07950	-.06152	-.05593	-.06718	-.05212
.5556	-.10395	-.10445	-.08750	-.08032	-.09657	-.07603
.4443	-.10344	-.12008	-.11705	-.10752	-.13117	-.10632
.3358	-.09067	-.11932	-.15308	-.13934	-.17344	-.14702
.2356	-.07970	-.10921	-.20186	-.17894	-.22691	-.20357
.1487	-.07500	-.10521	-.26486	-.23228	-.29845	-.28353
.0870	-.07484	-.11576	-.30788	-.31615	-.40650	-.40397
.0475	-.08033	-.13969	-.34483	-.43883	-.55513	-.56691
.0225	-.09525	-.18456	-.46628	-.65786	-.80401	-.83394
.0105	-.12544	-.26299	-.71679	-.10355	-.122748	-.128564
.004	-.17041	-.38558	-.110065	-.170859	-.199257	-.210026
.00125	-.22018	-.55386	-.172507	-.315180	-.367026	-.389733
.00030	-.24214	-.69957	-.238021	-.637678	-.7580801	-.803603
.00005	-.22158	-.74676	-.273361	-.1184412	-.1420618	-.1532786
.00005	-.17682	-.70883	-.274885	-.1563761	-.1916852	-.2083585
.00005	-.11958	-.61788	-.255987	-.1215572	-.1534576	-.1684682
.00030	-.05065	-.47649	-.216779	-.498500	-.667086	-.746556
.00125	.03014	-.24625	-.147004	-.61175	-.115454	-.140915
.004	.08596	-.06014	-.69063	.57920	.48037	.42913
.0105	.09684	.04609	-.18802	.63723	.66417	.66452
.0225	.08658	.07550	.03226	.50220	.56304	.57328
.0475	.07341	.07585	.13817	.36249	.43028	.43854
.0870	.06226	.06735	.16580	.25267	.31453	.31664
.1487	.05475	.06048	.17508	.18391	.23347	.22667
.2356	.05028	.05860	.15938	.13342	.16952	.15221
.3358	.05197	.06766	.12286	.10306	.12800	.10315
.4443	.06199	.08186	.09485	.08286	.09931	.07047
.5556	.07452	.08537	.07564	.06882	.07901	.04937
.6641	.07629	.07550	.06266	.05873	.06439	.03641
.7643	.06689	.06268	.04378	.05147	.05404	.02916
.8513	.05885	.05271	.04790	.04685	.04739	.02616
.9207	.04907	.04760	.04605	.04598	.04517	.02744
.9690	.04125	.04154	.04270	.04301	.04157	.02751
.9937	.06657	.06809	.07047	.07180	.06905	.05608

GAMMA-DATA
12

LOAD-DATA
12

.0350	.09909
.1000	.09877
.1600	.09802
.2200	.09681
.2800	.09516
.3500	.09268
.4450	.08836
.5650	.08130
.6950	.07128
.8100	.05932
.9000	.04580
.9700	.02670

RUBBERT
DATUM
NACELLE
1.0
0.0
CP-DATA
1
40

12

.9937	.0	.19611
.9690	.0	.10295
.9207	.0	.05841
.8513	.0	.01906
.7643	.0	-.02010
.6641	.0	-.05754
.5556	.0	-.09868
.4443	.0	-.14988
.3358	.0	-.21467
.2356	.0	-.30074
.1487	.0	-.43596
.0870	.0	-.63409
.0475	.0	-.94970
.0225	.0	-1.47750
.0110	.0	-2.18192
.0050	.0	-3.42854
.00205	.0	-5.18919
.00075	.0	-6.90959
.00024	.0	-7.36612
.00004	.0	-6.85258
.00004	.0	-5.54966
.00024	.0	-3.69810
.00075	.0	-1.69136
.00205	.0	.12382
.005	.0	.88411
.011	.0	.99536
.0225	.0	.89275
.0475	.0	.73535
.0870	.0	.59255
.1487	.0	.49316
.2356	.0	.41205
.3358	.0	.35495
.4443	.0	.31069
.5556	.0	.27366
.6641	.0	.24255
.7643	.0	.21572
.8513	.0	.19401
.9207	.0	.18491
.969	.0	.16611
.9937	.0	.23054

RUBBERT
DATUM
NACELLE
1.0
5.0
CP-DATA
3
40

13

.9937	9.0	81.0	171.0	.19803
.9690	.20743	.17522	.15412	.10054
.9207	.11628	.00388	.00567	.01748
.8513	.07395	.04036	.00204	-.01903
.7643	.03425	-.03628	-.07317	-.05146
.6641	-.00681	-.04898	-.11412	-.08402
.5556	-.04804	-.16210	-.23177	-.16547
.4443	-.08689	-.24734	-.32077	-.21849
.3358	-.12610	-.35729	-.46228	-.29580
.2356	-.16210	-.46055	-.62707	-.40482
.1487	-.19804	-.56055	-.80929	-.56505
.0870	-.23177	-.62707	-.100929	-.83897
.0475	-.26291	-.746461	-.234441	-.118819
.0225	-.28353	-.85826	-.371575	-.162931
.0110	-.30788	-.95972	-.467922	-.226506
.0050	-.33494	-.100775	-.567296	-.276614
.00205	-.36394	-.1395229	-.675990	-.258747
.00075	-.39486	-.18105	-.775990	-.201970
.00024	-.42678	-.23105	-.859105	-.120915
.00004	-.46037	-.28386	-.92261	-.32047
.00005	-.49482	-.33854	-.969226	-.48027
.00005	-.52931	-.39457	-.100929	-.95487
.00024	-.56397	-.45145	-.31785	.97464
.00075	-.59852	-.50837	.011	.99365
.00205	-.63307	-.56538	.0225	.99365
.0050	-.66762	-.62238	.0475	.91315
.0110	-.70217	-.68033	.0870	.76155
.0225	-.73672	-.73704	.1487	.61794
.0475	-.77127	-.79335	.2356	.51534
.0870	-.80582	-.84966	.3358	.41958
.1487	-.84037	-.90600	.4443	.36088
.2356	-.87492	-.96234	.5556	.31821
.3358	-.90947	-.10163	.6641	.29077
.4443	-.94402	-.14297	.7643	.26831
.5556	-.97857	-.18431	.8513	.24669
.6641	-.10163	-.22566	.9207	.22615
.7643	-.14297	-.26700	.9690	.20622
.8513	-.18431	-.30834	.9937	.18931
.9207	-.22566	-.34968		.18259
.9690	-.26700	-.39102		.16695
.9937	-.30834	-.43236		.22960

HESS
DATUM
NACELLE
1.0
0
CP-DATA
1
42

14

.0005	0.0	-6.6364
.0040	0.0	-3.7979
.0165	0.0	-1.7516
.0285	0.0	-1.2614
.0445	0.0	-.9575
.0715	0.0	-.7096
.0985	0.0	-.5750
.1525	0.0	-.4249
.1975	0.0	-.3500
.2605	0.0	-.2764
.3235	0.0	-.2235
.3955	0.0	-.1772
.4765	0.0	-.1342
.5755	0.0	-.0916
.6745	0.0	-.0537
.7735	0.0	-.0167
.8545	0.0	.0185
.9085	0.0	.0449
.9535	0.0	.0774
.9785	0.0	.1269
.9985	0.0	.2676
.0005	-2.9374	
.0040	-7.628	
.0165	9.545	
.0285	8.470	
.0445	7.449	
.0715	6.375	
.0985	5.695	
.1525	4.889	
.1975	4.394	
.2605	3.955	
.3235	3.594	
.3955	3.281	
.4765	2.986	
.5755	2.674	
.6745	2.393	
.7735	2.134	
.8545	1.945	
.9085	1.804	
.9535	1.759	
.9785	1.868	
.9985	2.676	

HESS
DATUM
NACELLE
3.3333
0
CP-DATA
1
42

15

.0005	0.0	-7.529
.0040	0.0	-3.834
.0165	0.0	-1.617
.0285	0.0	-1.113
.0445	0.0	-.8104
.0715	0.0	-.5733
.0985	0.0	-.4487
.1525	0.0	-.3147
.1975	0.0	-.2495
.2605	0.0	-.1909

.3235 -.1455
 .3955 -.1109
 .4765 -.0756
 .5755 -.0418
 .6745 -.0143
 .7735 .0108
 .8545 .0353
 .9085 .0626
 .9535 .0830
 .9785 .1340
 .9985 .2028
 .9985 .2028
 .9785 .2215
 .9535 .2289
 .9085 .2618
 .8545 .2994
 .7735 .3563
 .6745 .4218
 .5755 .4889
 .4765 .5552
 .3955 .6076
 .3235 .6527
 .2605 .6913
 .1975 .7314
 .1525 .7645
 .0985 .8178
 .0715 .8585
 .0445 .9193
 .0285 .9707
 .0165 .9999
 .0040 .4610
 .0005 -4.0603

TABLE 4

Computers used and their relative speeds (estimated)

	COMPUTER USED	SCALE FACTOR USED TO OBTAIN CDC 6600 TIME
RUBBERT	CDC 6600	1.0
ROBERTS	ICL 1906S	.6
HUNT - SEMPLE	IBM 370/158	1.5
NLR	CDC Cyber 7214	3.0

(e.g. NLR : 1 hr CDC 6600 = 3.0 hrs Cyber 7214)

CASE: RAE WING

T/C = .02

$\alpha = 5.0^\circ$

TABLE 5A

Comparison of calculation times

METHOD	PANEL DISTRIBUTION ON HALF WING						CPU - MINUTES (FIGURES BETWEEN BRACKETS ARE CDC - 6600 TIMES ACCORDING TO TABLE 4)			
	CHORD	SPAN	WAKE	TIP	NUMB. OF MODES	TOT. NUMBER OF SINGULARITIES	AERODYN.	SOL. OF LIN	NUMBER OF	TOTAL
							INFL. COEFF.	SYST. OF EQS	ITERATIONS	
ROBERTS ¹⁾ DATUM	39	13	13		630		11.90(39.74)	8.9 (14.80)		39.6 (117.33)
	27	9	9		330		4.95(16.5)	1.35(2.30)		15.6 (49.33)
	19	6	6		176		2.60(8.70)	.3 (.5)		8.5 (28.00)
RUBBERT(DATUM)	40	12	12	40		684	6.36(6.36)	2.53(2.53)		11.36(11.36)
	22	8	8	22		296	1.37(1.37)	.32(.32)		2.46(2.46)
	12	12	12	12		264	1.00(1.00)	.24(.24)		1.90(1.90)
HUNT - SEMPLE (SHEETS)	60	12	12			732	31.2 (20.80)	8.0 (5.33) ²⁾	54	40.0 (26.67)
	30	12	12			372	8.47(5.65)	2.17(1.45) ²⁾	56	10.9 (7.27)
NLR	90	12	12			1092	48.94(16.31)	4.60(1.53)	12	60.0 (20.0)
	60	12	12			732	21.66(7.22)	2.44(.81)	14	28.38(9.46)
	30	12	12			372	6.02(2.00)	.72(.24)	15	9.06(3.02)

1) Roberts took advantage of the non-cambered nature of the wings, and the axi-symmetry of the nacelle. This is accounted for in the figures presented between brackets. The other participants employed only the XZ-plane as plane of symmetry.

2) For the RAE WING with T/C = .05 these times are less than one half those for T/C = .02

TABLE 5B

Comparison of calculation times.

CASE: STRAKED WING
 $T/C = .02$
 $\alpha = 5.0$

METHOD	PANEL DISTRIBUTION ON HALF WING					CPU - MINUTES (FIGURES BETWEEN BRACKETS ARE CDC - 6600 TIMES ACCORDING TO TABLE 4)				
	CHORD	SPAN	WAKE	TIP	NUMB.OF MODES	TOTAL NUMB.OF SINGULARITIES	AERODYN INFL.COEFF.	SOL.OF LIN. SYST.OF EQS.	NUMB. OF ITERATIONS	TOTAL
ROBERTS	39	18				966	24.8 (82.67)	31.02(51.73)		81.3 (219.33)
RUBBERT (DATUM)	38	12	12	38		734	6.91(6.91)	3.17(3.17)		12.55(12.55)
	22	8	8	22		371	1.96(1.96)	.55(.55)		3.43(3.43)
	12	12	12	12		298	1.20(1.20)	.33(.33)		2.19(2.19)
HUNT - SEMPLE (SHEETS)	60	12	12			732	31.30(20.87)	8.80(5.87) ³⁾		40.8 (27.20)
	30	12	12			372	8.83(5.89)	2.32(1.55) ³⁾	60 ¹⁾	11.39(7.59)
NLR	90	12	12			1092	49.20(16.40)	4.15(1.38)	11	59.83(19.94)
	60	18	18			1046	42.94(14.31)	7.51(2.54)	20 ²⁾	55.69(18.56)
	60	12	12			732	22.17(7.39)	2.44(.81)	14	28.93(9.64)
	30	12	12			372	6.13(2.04)	.67(.22)	14	9.17(3.06)

1) 90° solution not fully converged.

2) Not fully converged.

3) For $T/C = .05$ these times are less than one half those for $T/C = .02$.

TABLE 5C

Comparison of calculation times

CASE: NACELE
 $C/D_E = 1.0$
 $\alpha = 0^\circ$

METHOD	PANEL DISTRIBUTION ON HALF NACELE					CPU - MINUTES (FIGURES BETWEEN BRACKETS ARE CDC - 6600 TIMES ACCORDING TO TABLE 4)			
	CHORD	CIRCUMF.	WAKE	NUMB.OF MODES	TOTAL NUMB.OF SINGULARITIES	AERODYN INFL.COEFF.	SOL.OF SYST. OF LIN.EQS	NUMBER OF ITER.	TOTAL TIME
ROBERTS(DATUM)	55	10			58	1.10(14.67)	.033(.053)		2.90(38.0)
RUBBERT(DATUM)	40	10	10		516	3.74(3.74)	1.17 (1.17)		6.52(6.52)
HUNT - SEMPLE (SHEETS)	60	10	10		610	21.50(14.33)	2.60 (1.93)	25	24.6 (16.4)
NLR	60	10	10		610	14.96(4.99)	1.59 (.53)	15	19.35(6.63)

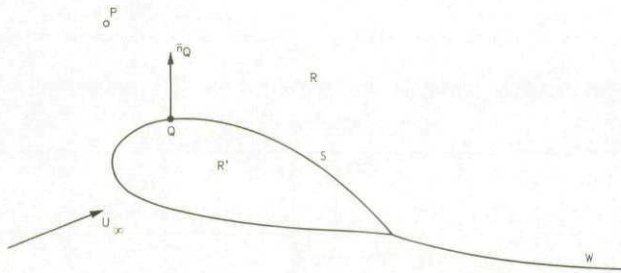


Fig. 1 Definition of flow region for 3D lifting flow problem

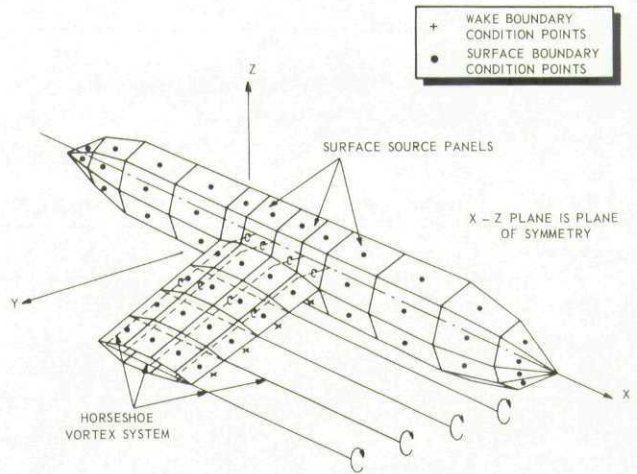


Fig. 4 Schematic view of selected system of singularity distributions for the NLR panel method

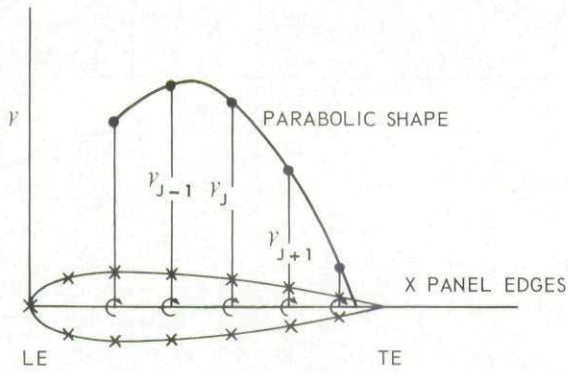


Fig. 2 Chordwise parabolic shape of internal vortex strength variation used in the NLR panel method

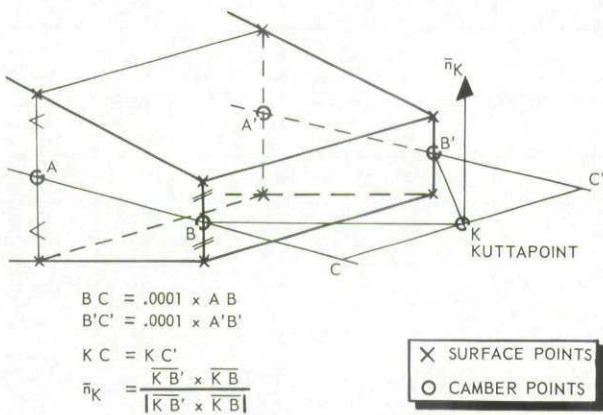


Fig. 3 Definition of kutta-point location in the NLR panel method (N.B. the trailing edge is open)

$$\begin{bmatrix} S_c & V_c \\ S_k & V_k \end{bmatrix} \cdot \begin{bmatrix} \sigma \\ \Gamma \end{bmatrix} = \begin{bmatrix} R_c \\ R_k \end{bmatrix}$$

- S_c = normal velocity influence coefficient matrix of sources on surface collocation points
- S_k = refers to the influence of sources on Kutta points
- V_c = refers to the influence of vortices on surface collocation points
- V_k = refers to the influence of vortices on Kutta points
- σ = unknown source singularities
- Γ = unknown vortex or doublet strength
- R_c = boundary condition at surface collocation points
- R_k = boundary condition at Kutta points

Fig. 5 Structure of normal velocity influence coefficient matrix, unknown singularity vector and right-hand side vector in the NLR panel method

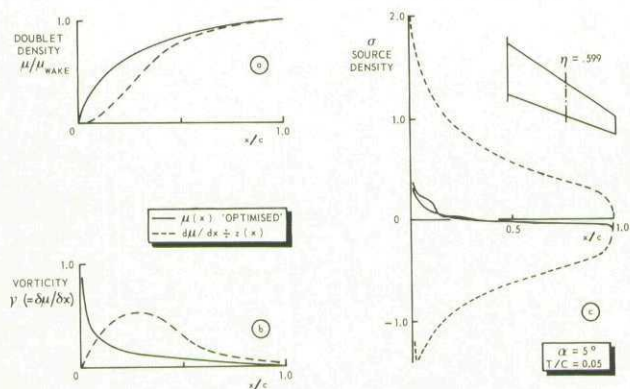


Fig. 6 Influence of optimising on source and vortex density in the Hunt-Semple panel method (REF. 7)

TYPICAL PANEL ON WHICH 16 MODES OVERLAP

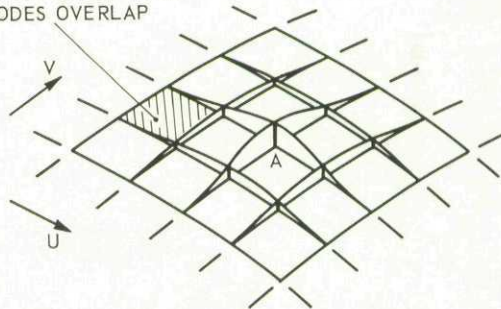


Fig. 9 Basic bicubic spline used in Roberts' Spline-Neumann method

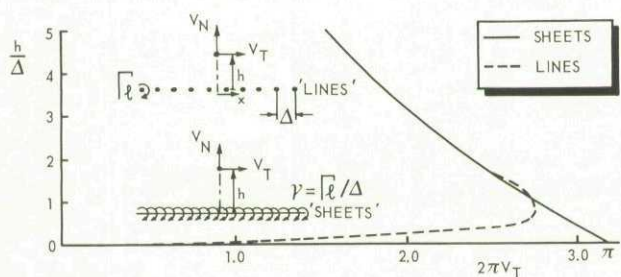


Fig. 7 Comparison of tangential velocity induced by vortex lines and vortex sheets (REF. 7)

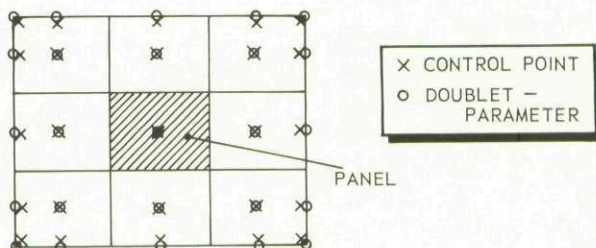


Fig. 10 Definition of control point and doublet parameter point location in a network for Rubbert's method

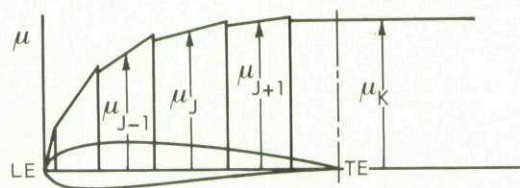


Fig. 8 Chordwise doublet shape in the Hunt-Semple 'sheets' method (REF. 2)

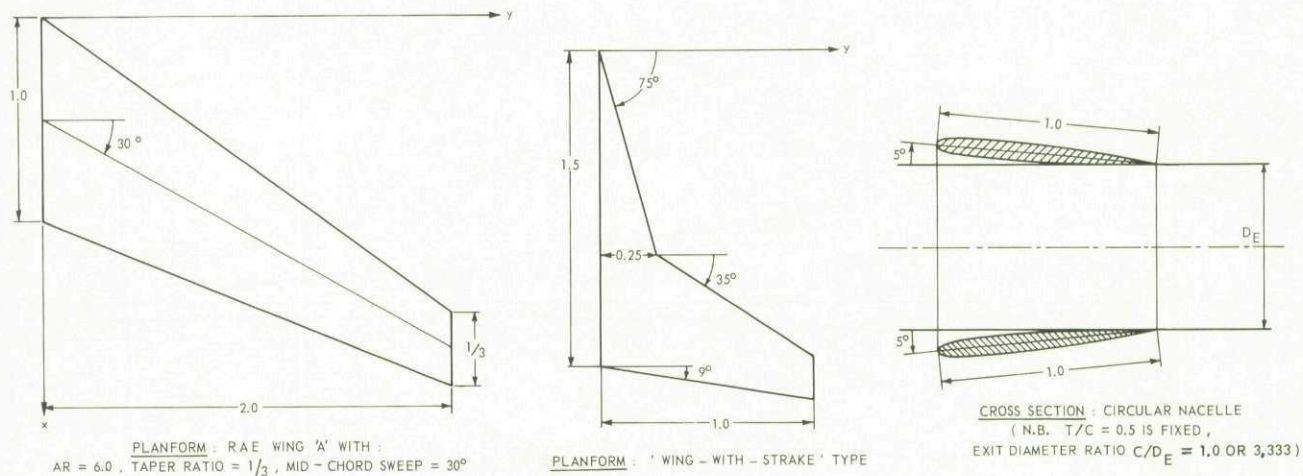


Fig. 11 Definition of test configurations (symmetrical Naca-four-digit airfoil used for all configurations)

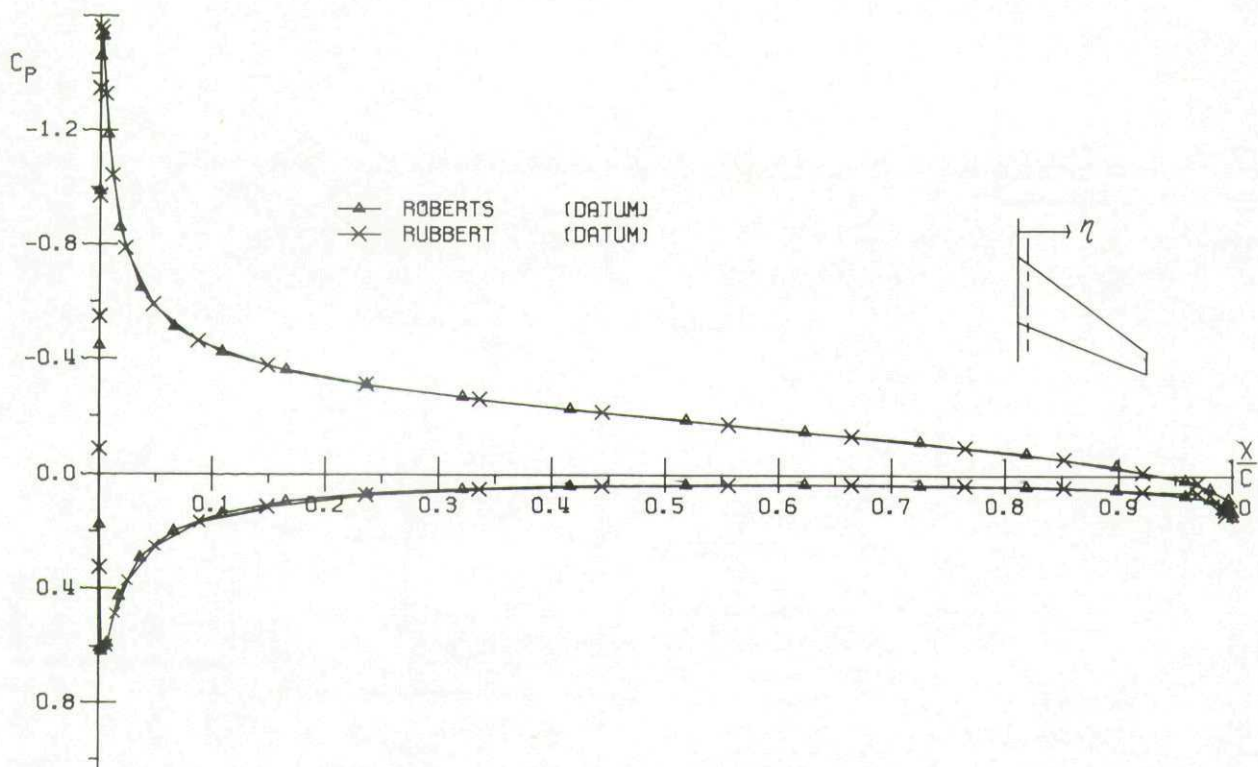


FIG. 12 COMPARISON OF DATUM RESULTS
CHORDWISE PRESSURE DISTRIBUTION
RAE WING . $T/C = .05$. $\alpha = 5.0$. $\eta = .079$

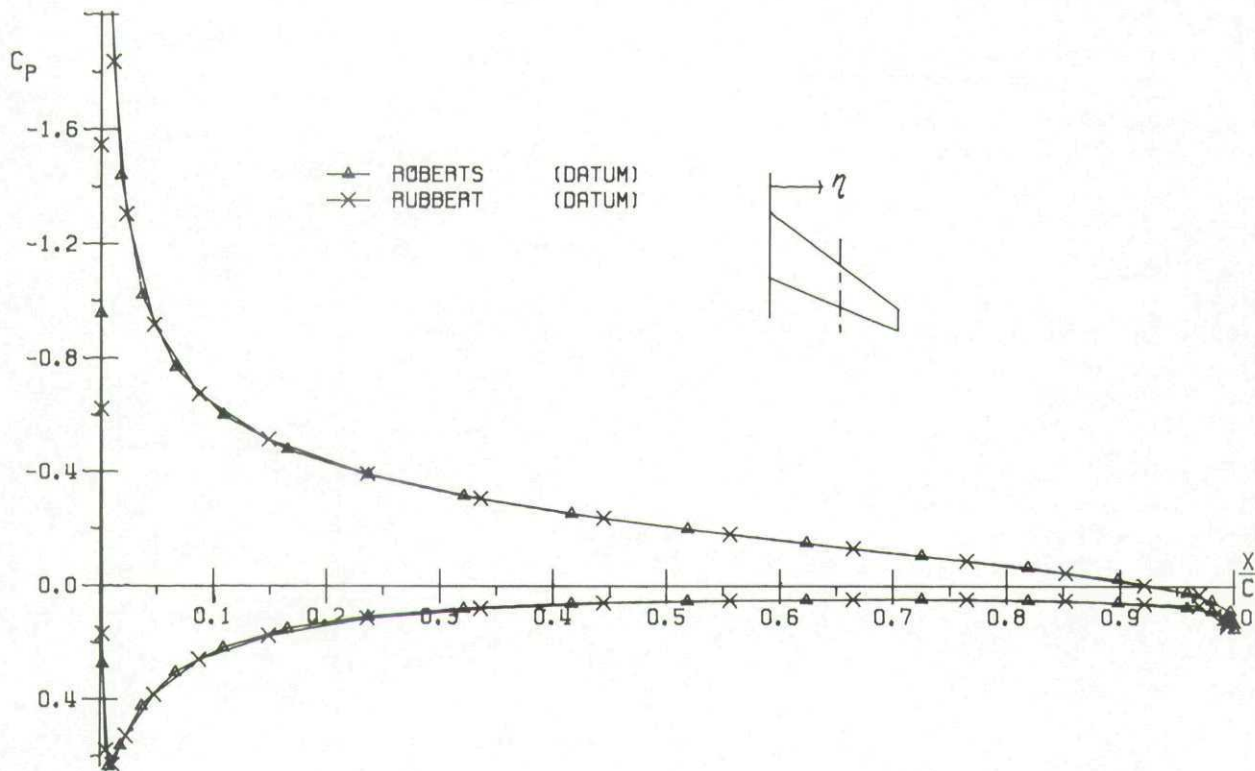


FIG. 13 COMPARISON OF DATUM RESULTS
CHORDWISE PRESSURE DISTRIBUTION
RAE WING . $T/C = .05$. $\alpha = 5.0$. $\eta = .549$

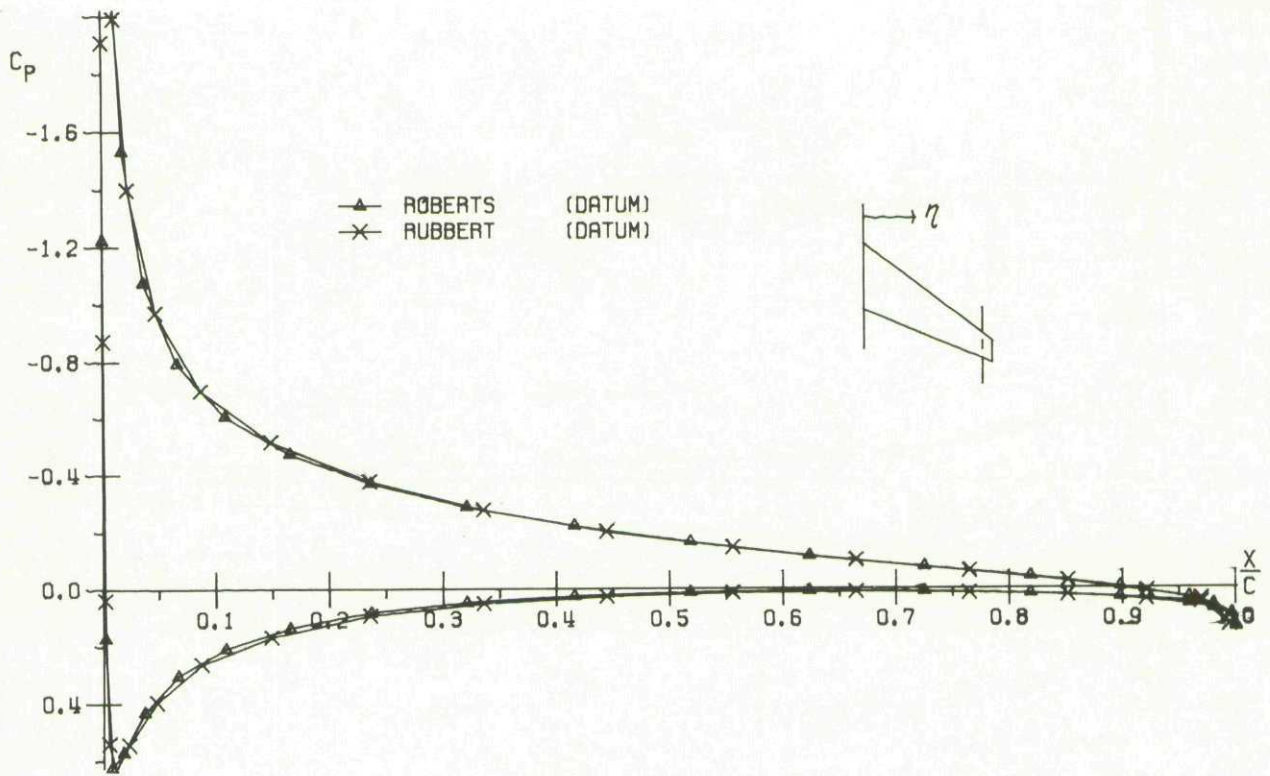


FIG. 74 COMPARISON OF DATUM RESULTS
CHORDWISE PRESSURE DISTRIBUTION
RAE WING . $T/C = .05$. $\alpha = 5.0$. $\eta = .924$

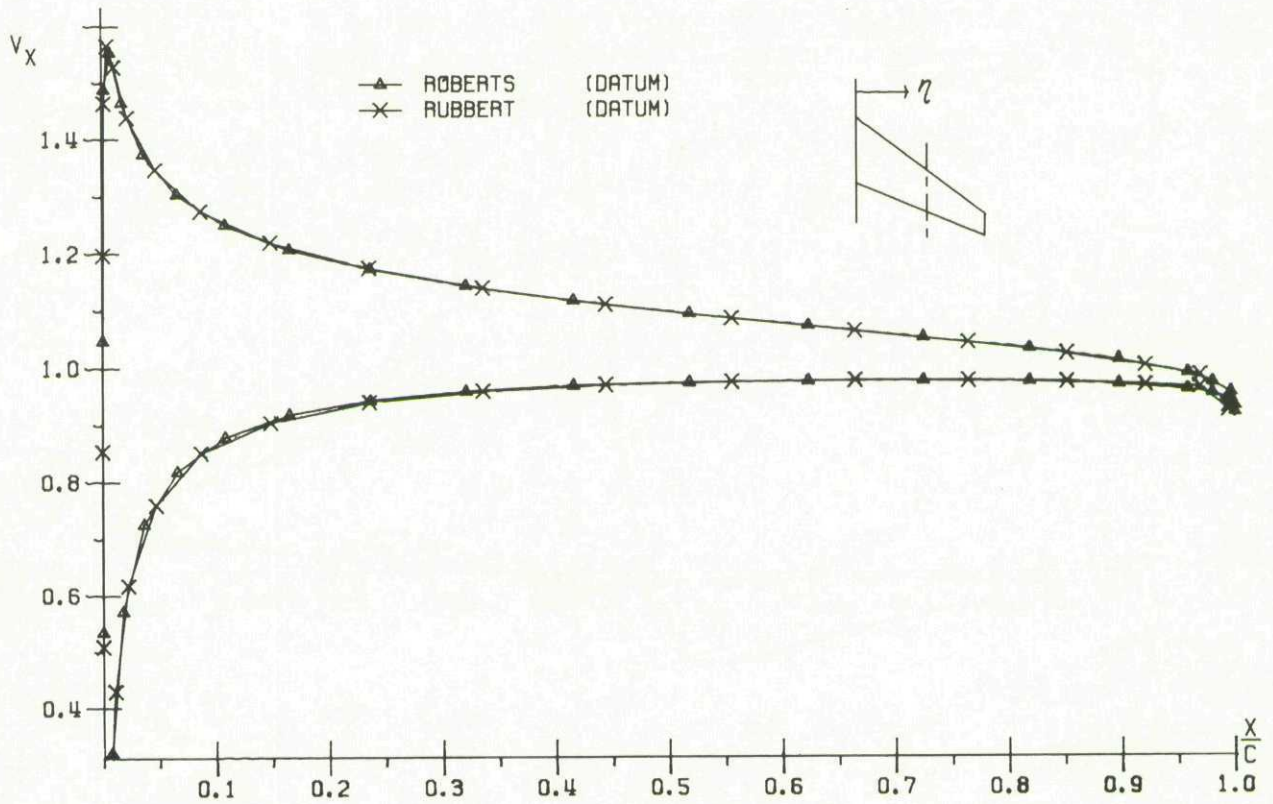


FIG. 75 COMPARISON OF DATUM RESULTS
X-COMPONENT OF VELOCITY
RAE WING . $T/C = .05$. $\alpha = 5.0$. $\eta = .549$

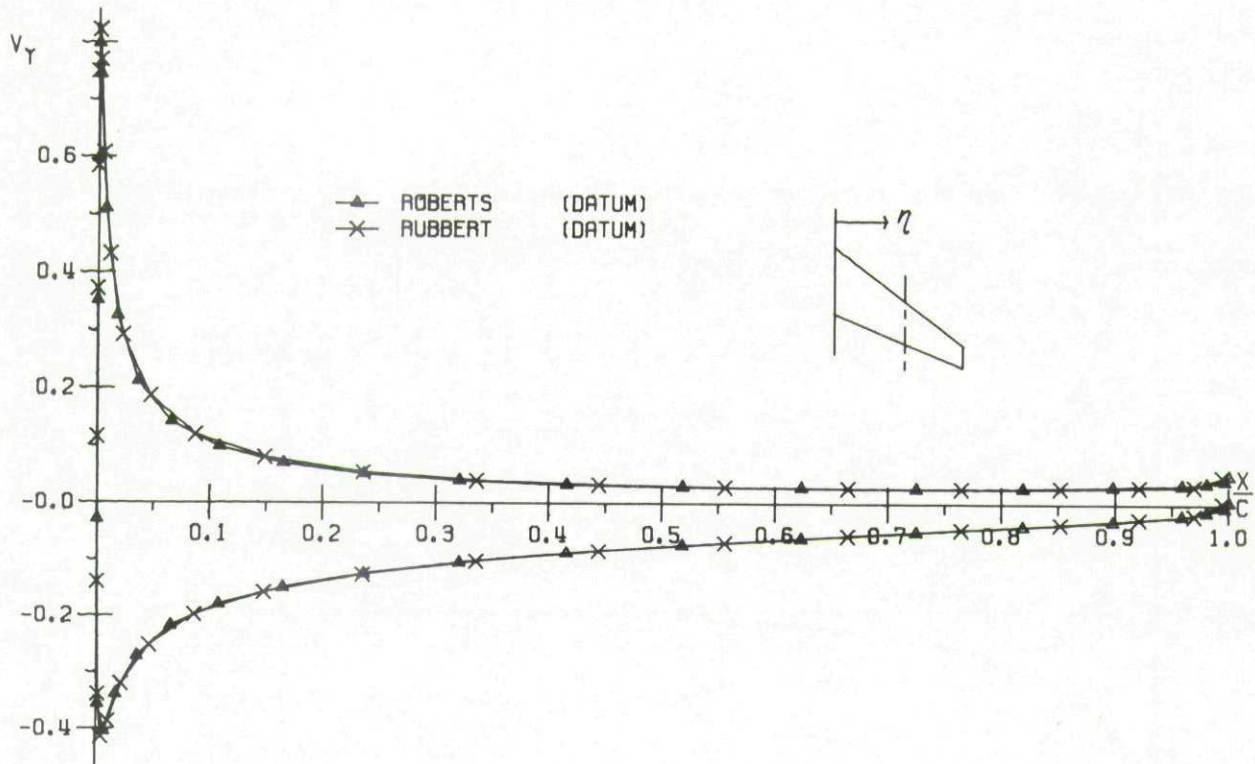


FIG. 16 COMPARISON OF DATUM RESULTS
 Y-COMPONENT OF VELOCITY
 RAE WING • T/C = .05 • $\alpha = 5.0$ • $\eta = .549$

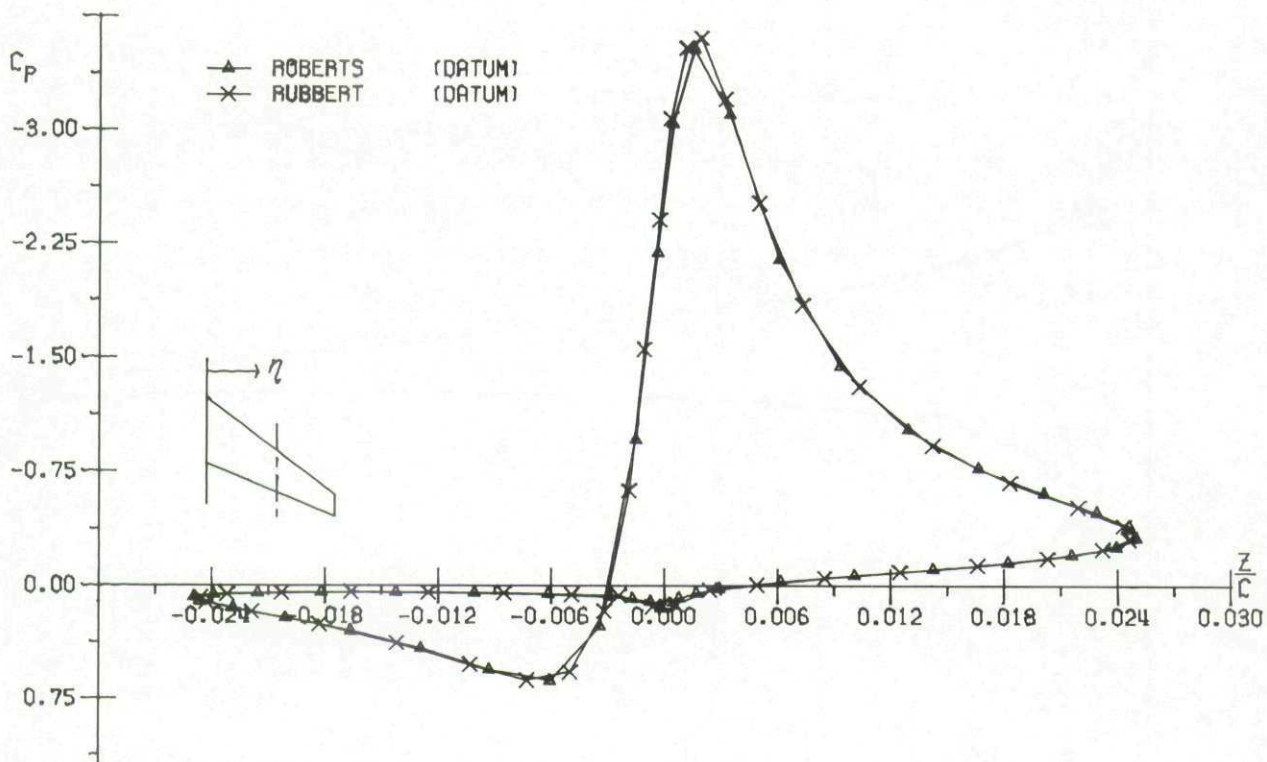


FIG. 17 COMPARISON OF DATUM RESULTS
 DRAG LOOP
 RAE WING • T/C = .05 • $\alpha = 5.0$ • $\eta = .549$

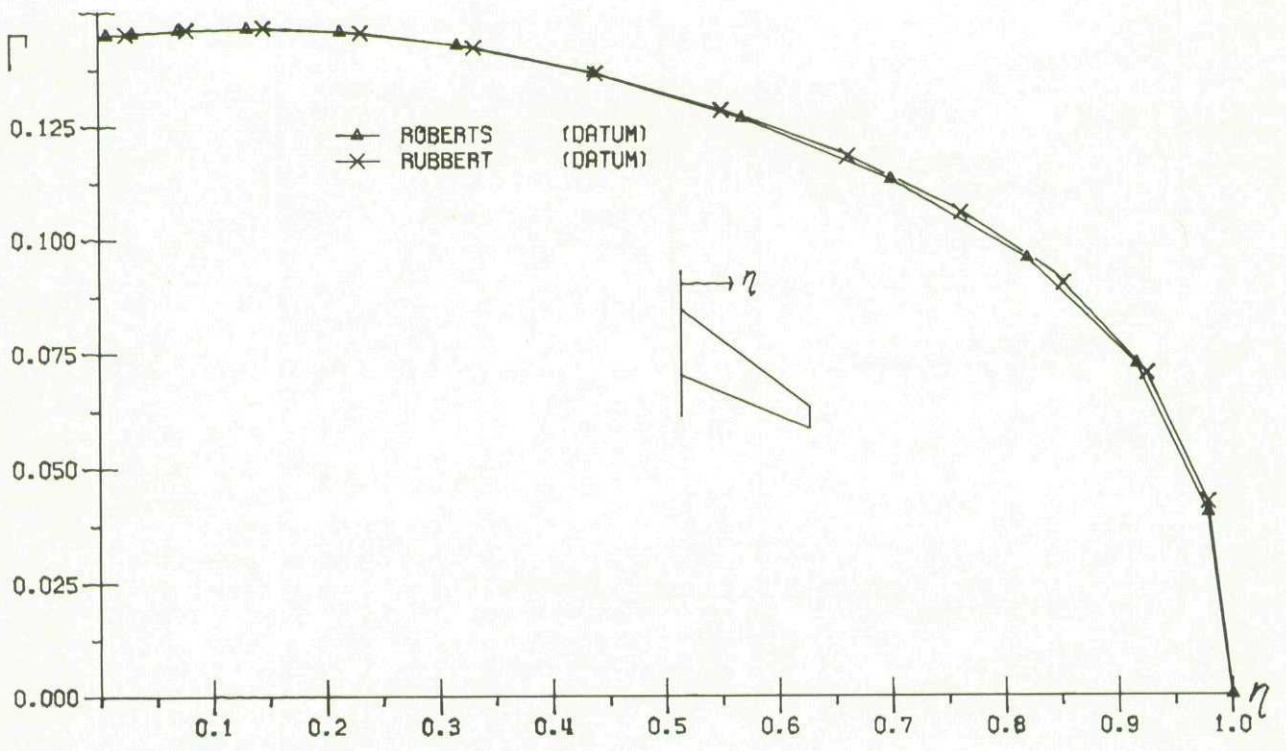


FIG. 18 COMPARISON OF DATUM RESULTS
CIRCULATION
RAE WING . $T/C = .05$. $\alpha = 5.0$

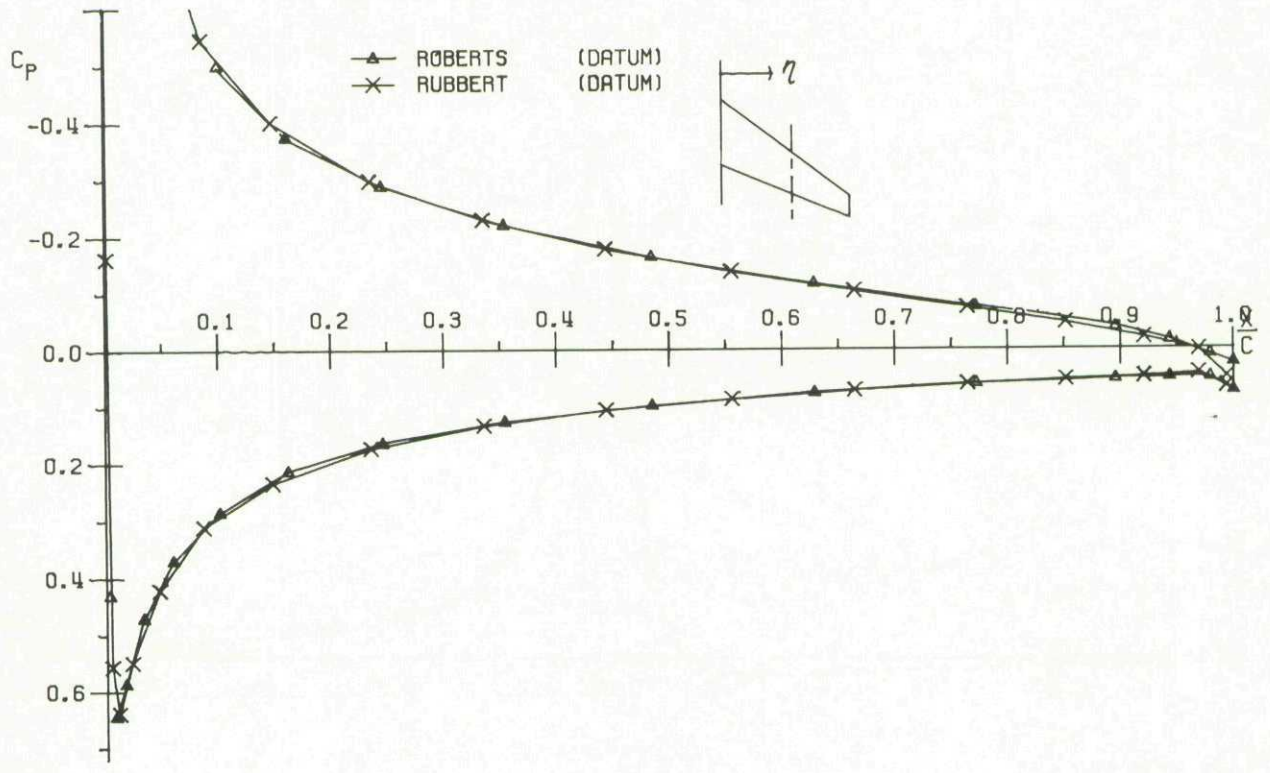


FIG. 19 COMPARISON OF DATUM RESULTS
CHORDWISE PRESSURE DISTRIBUTION
RAE WING . $T/C = .02$. $\alpha = 5.0$. $\eta = .549$

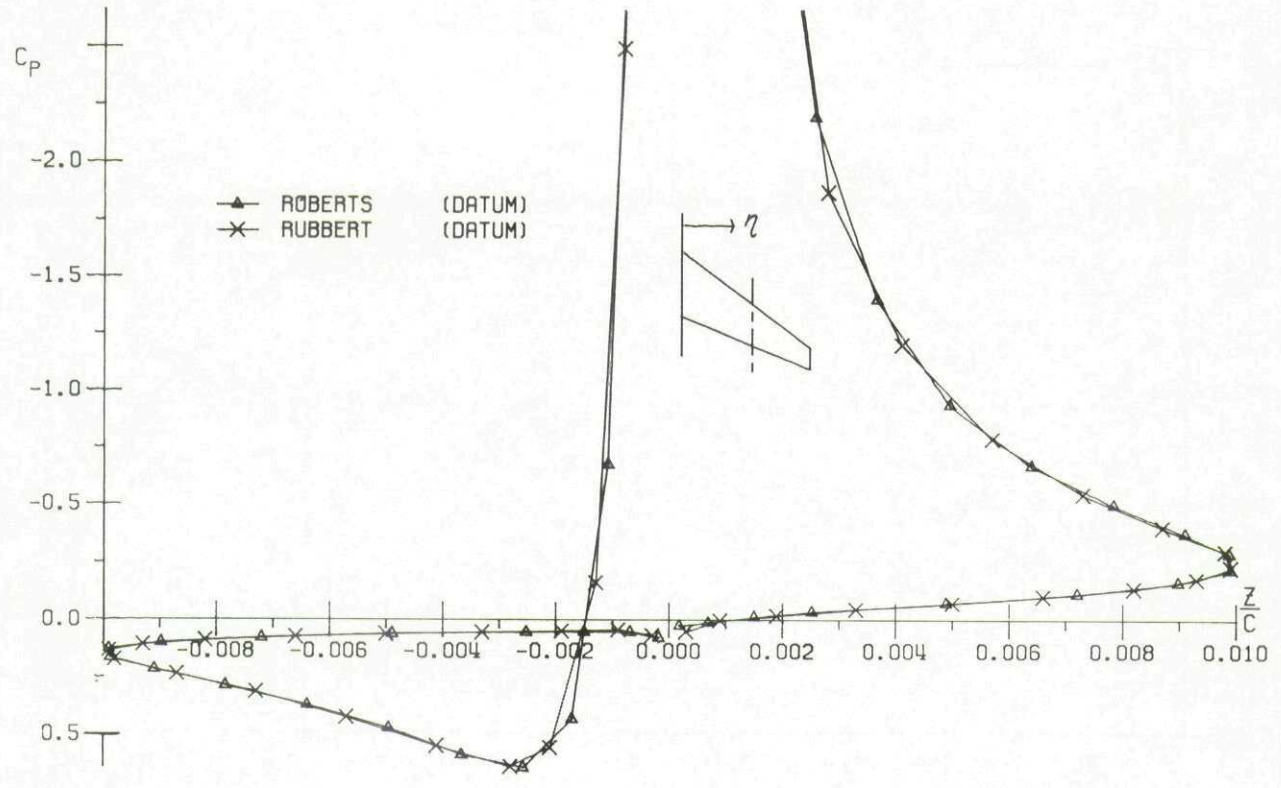


FIG. 20a COMPARISON OF DATUM RESULTS
DRAG LOOP
RAE WING , $T/C = .02$, $\alpha = 5.0$, $\eta = .549$

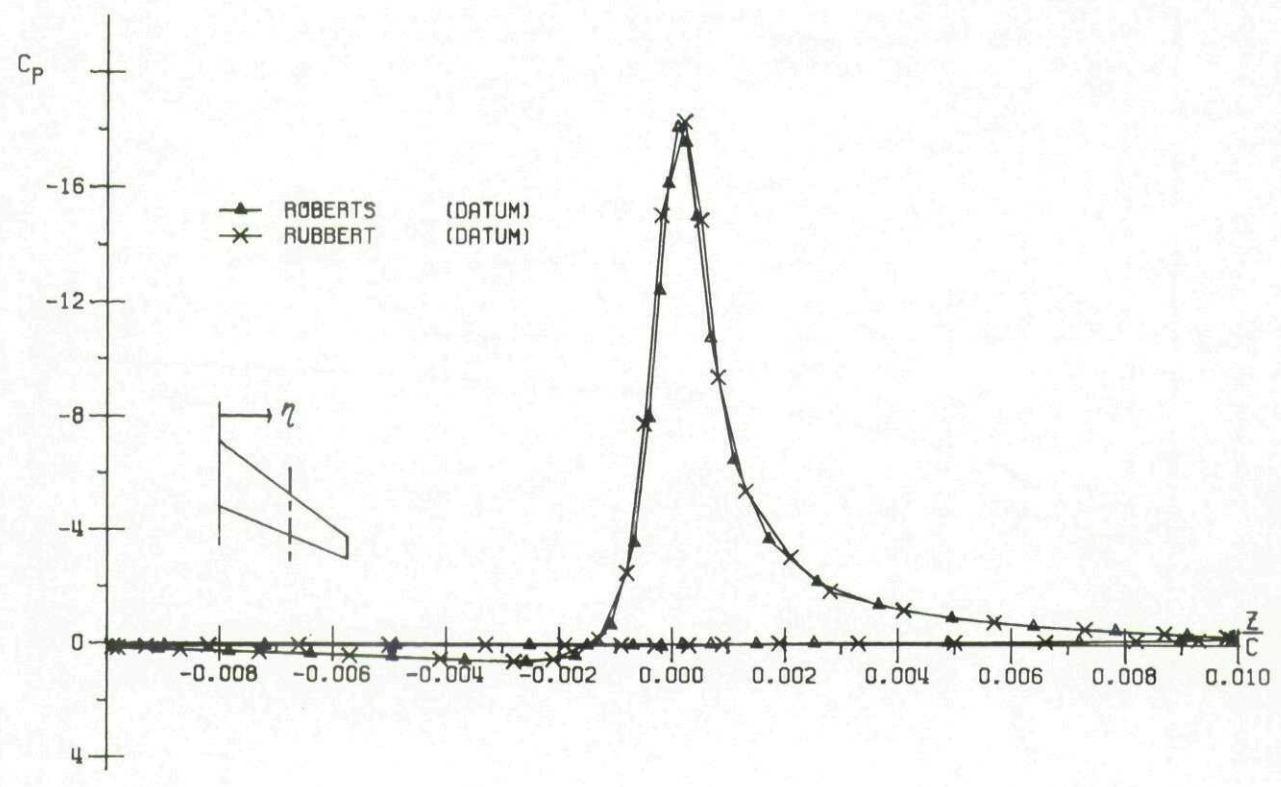


FIG. 20b COMPARISON OF DATUM RESULTS
DRAG LOOP
RAE WING , $T/C = .02$, $\alpha = 5.0$, $\eta = .549$

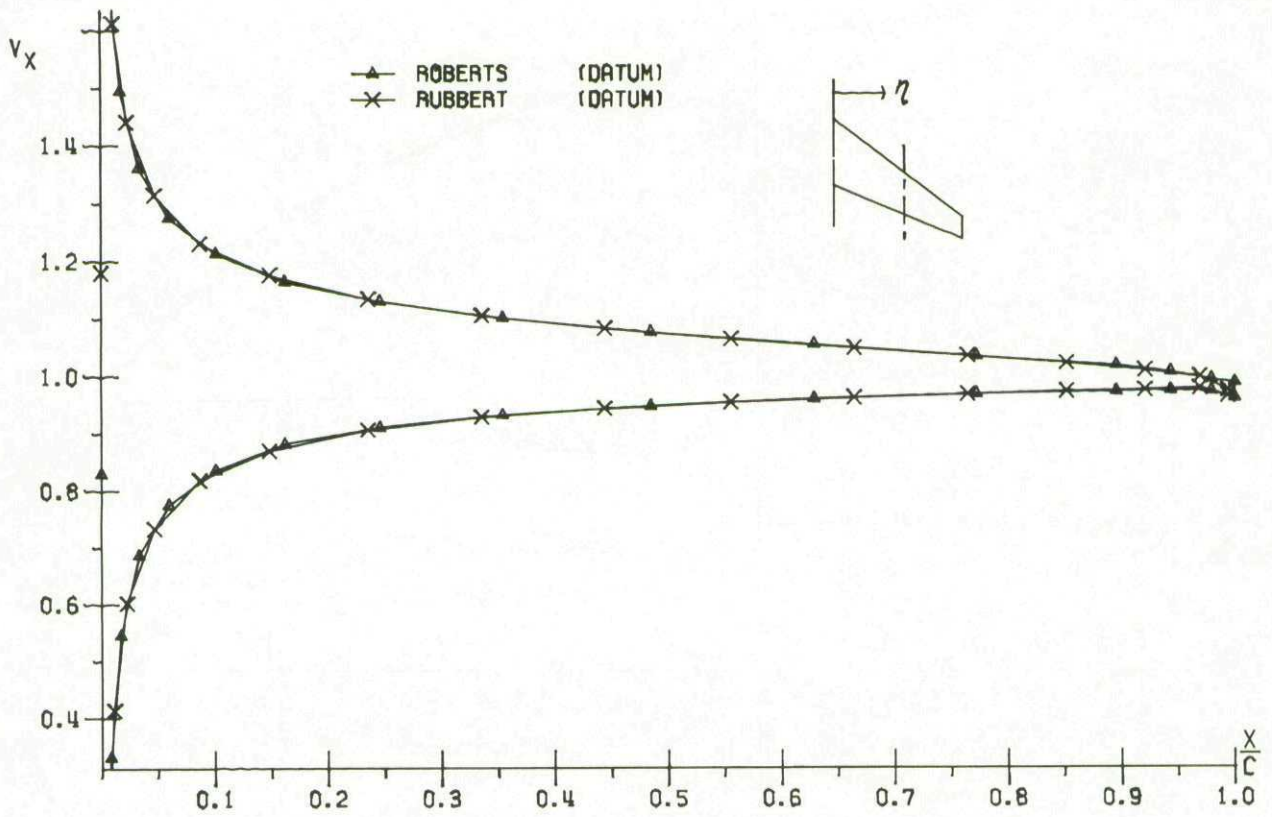


FIG. 27 COMPARISON OF DATUM RESULTS
X-COMPONENT OF VELOCITY
RAE WING . T/C = .02 . $\alpha = 5.0$. $\eta = .549$

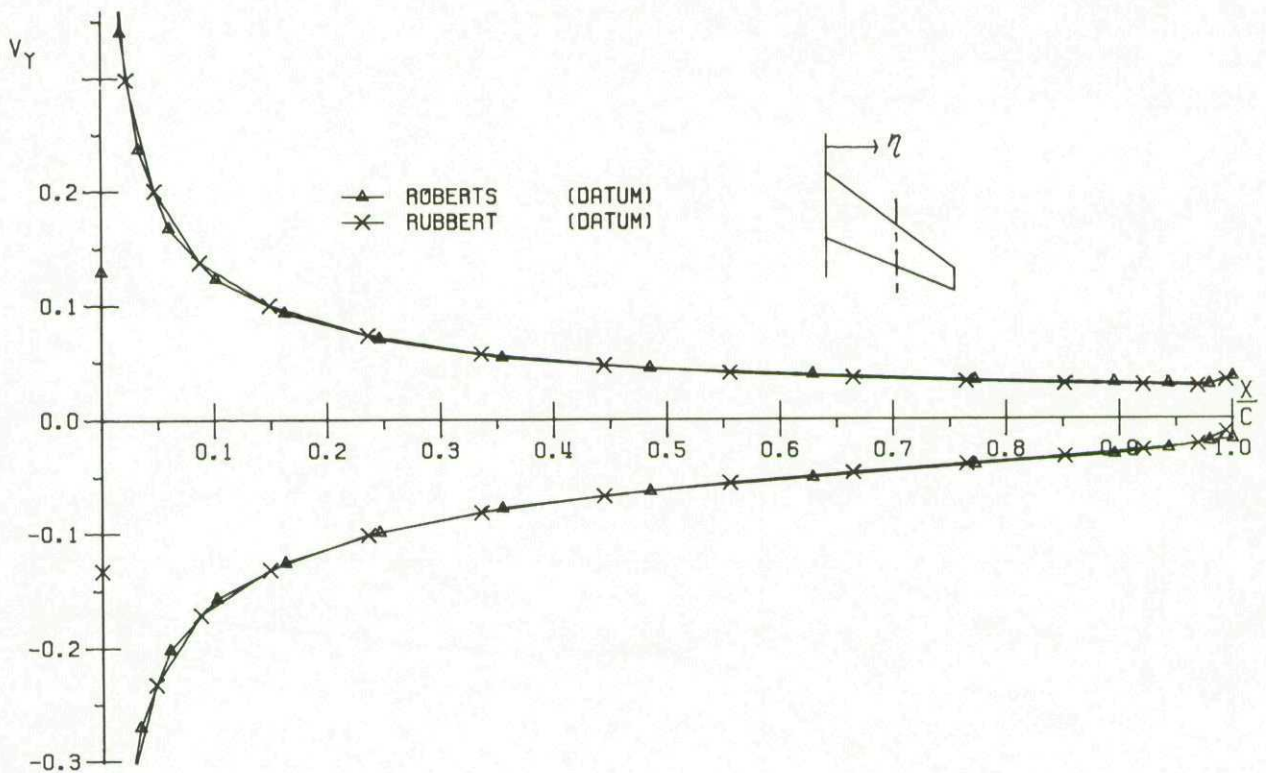


FIG. 22 COMPARISON OF DATUM RESULTS
Y-COMPONENT OF VELOCITY
RAE WING , T/C = .02 , $\alpha = 5.0$, $\eta = .549$

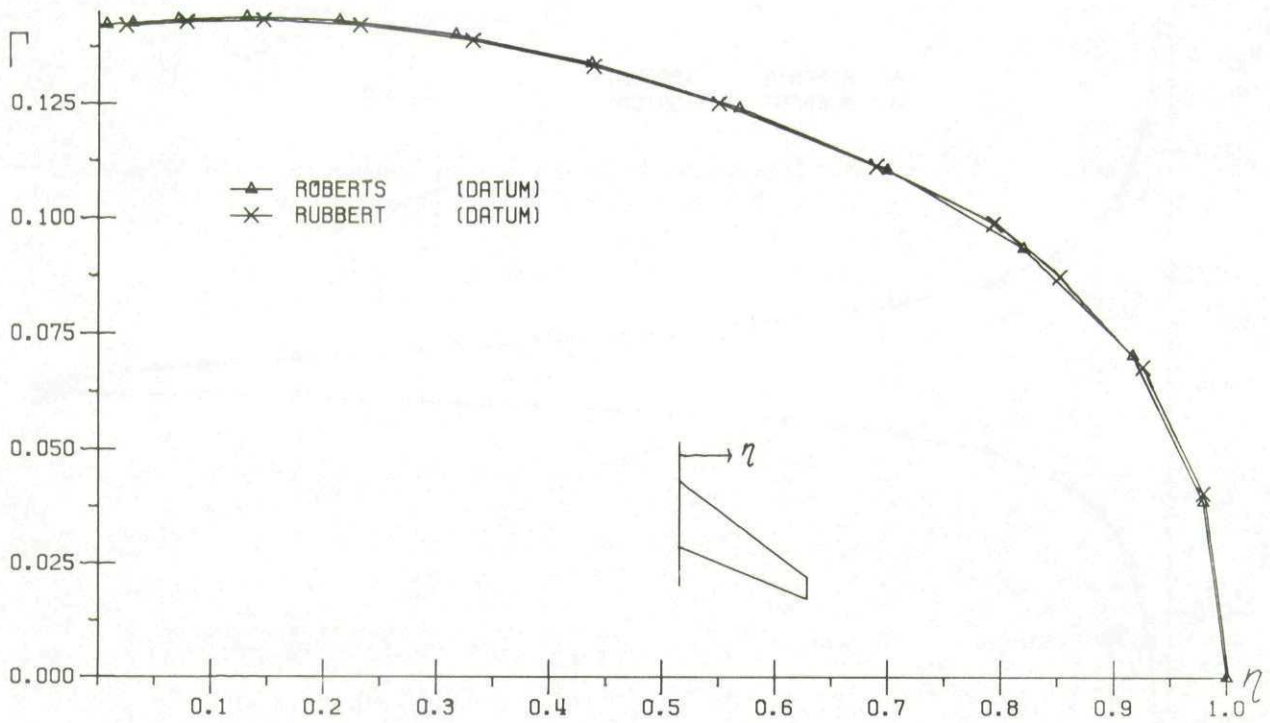


FIG. 23 COMPARISON OF DATUM RESULTS
CIRCULATION
RAE WING , T/C = .02 , $\alpha = 5.0$

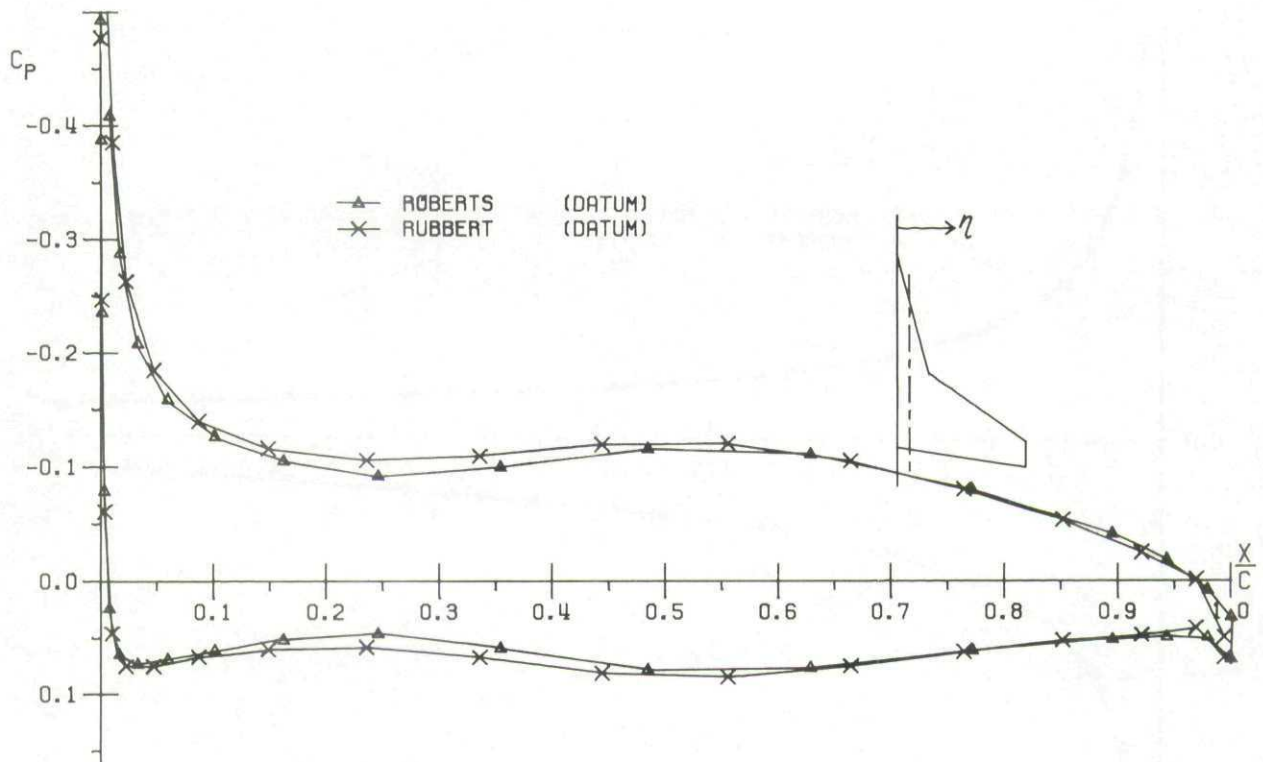


FIG. 24 COMPARISON OF DATUM RESULTS
CHORDWISE PRESSURE DISTRIBUTION
STRAKED WING , T/C = .02 , $\alpha = 5.0$, $\eta = .099$

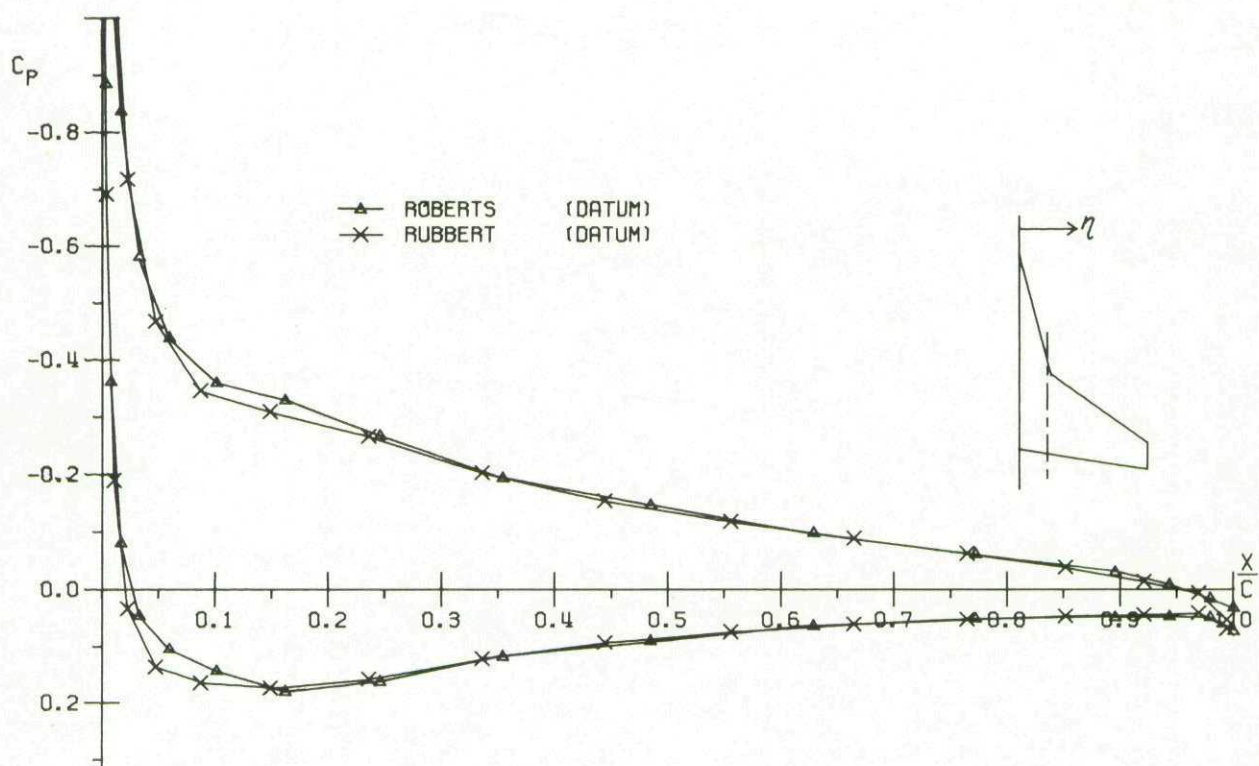


FIG. 25 COMPARISON OF DATUM RESULTS
 CHORDWISE PRESSURE DISTRIBUTION
 STRAKED WING . T/C = .02 . $\alpha = 5.0$. $\eta = .219$

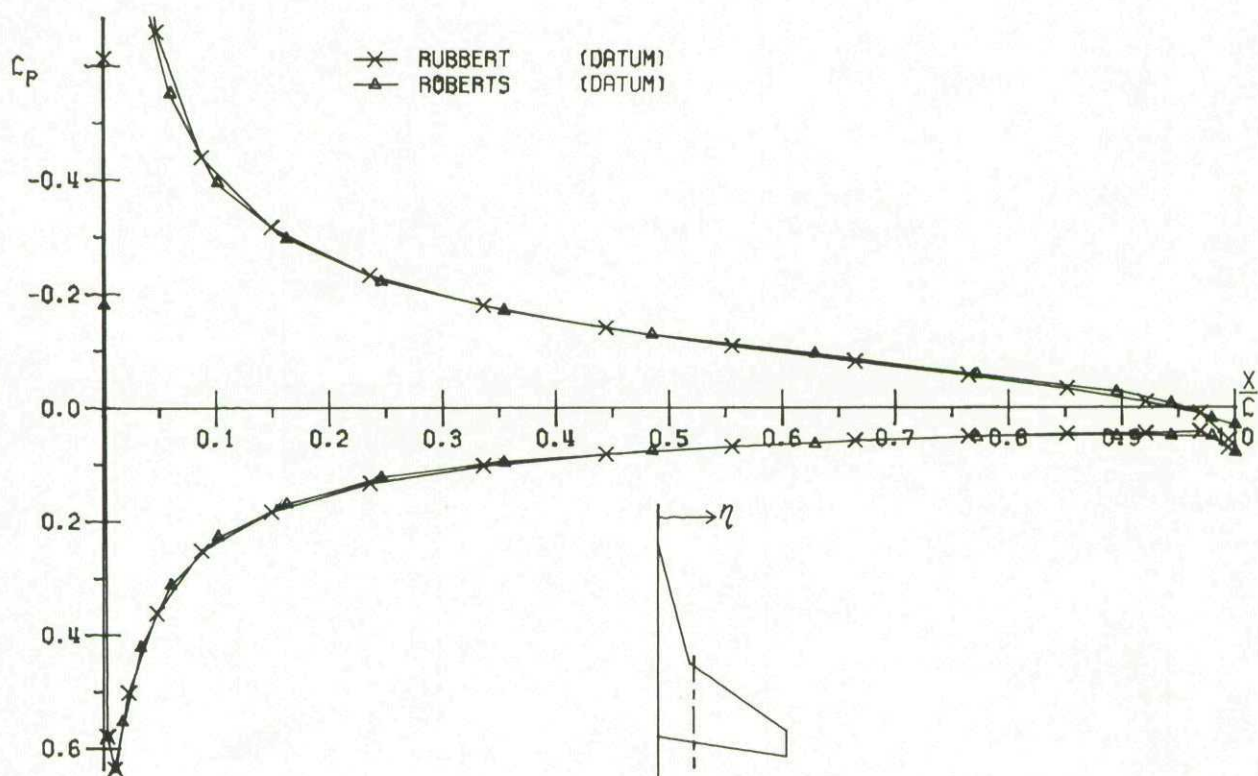


FIG. 26 COMPARISON OF DATUM RESULTS
 CHORDWISE PRESSURE DISTRIBUTION
 STRAKED WING . T/C = .02 . $\alpha = 5.0$. $\eta = .280$

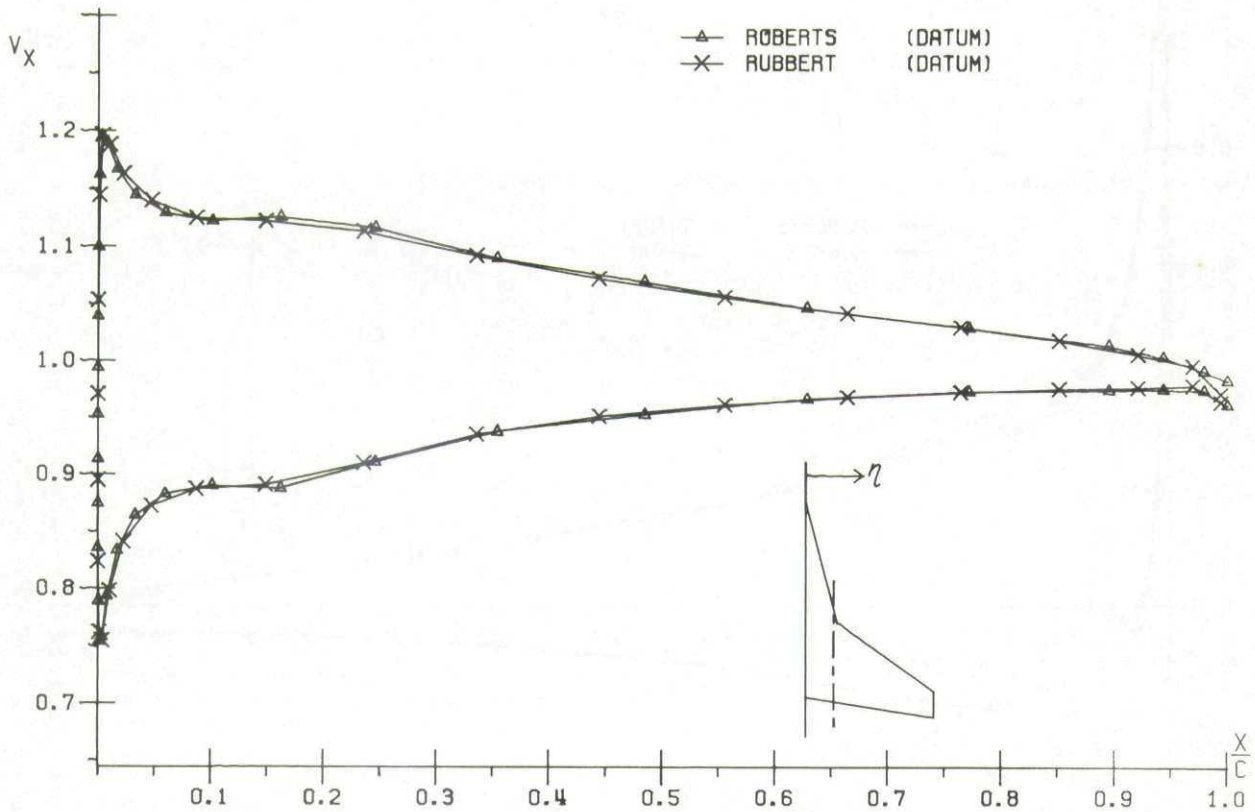


FIG. 27 COMPARISON OF DATUM RESULTS
X-COMPONENT OF VELOCITY
STRAKED WING, $T/C = .02$, $\alpha = 5.0$, $\eta = .219$

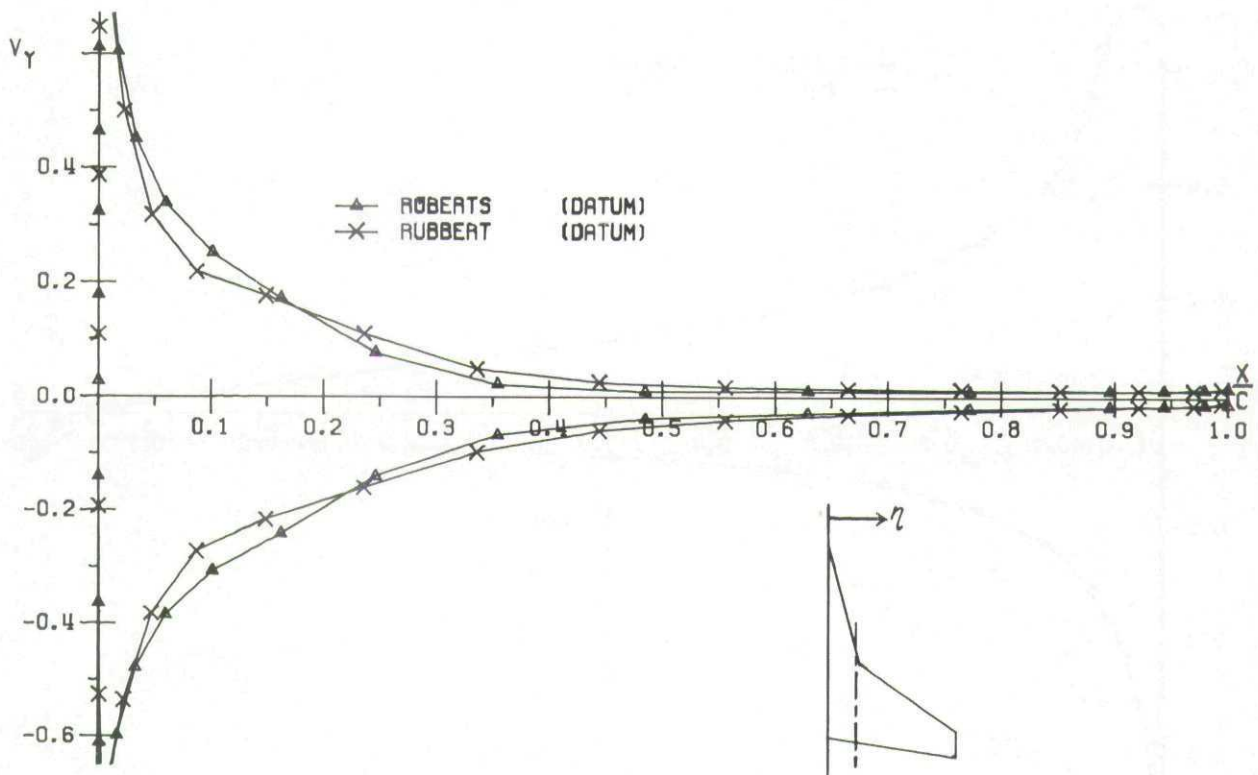


FIG. 28 COMPARISON OF DATUM RESULTS
Y-COMPONENT OF VELOCITY
STRAKED WING, $T/C = .02$, $\alpha = 5.0$, $\eta = .219$

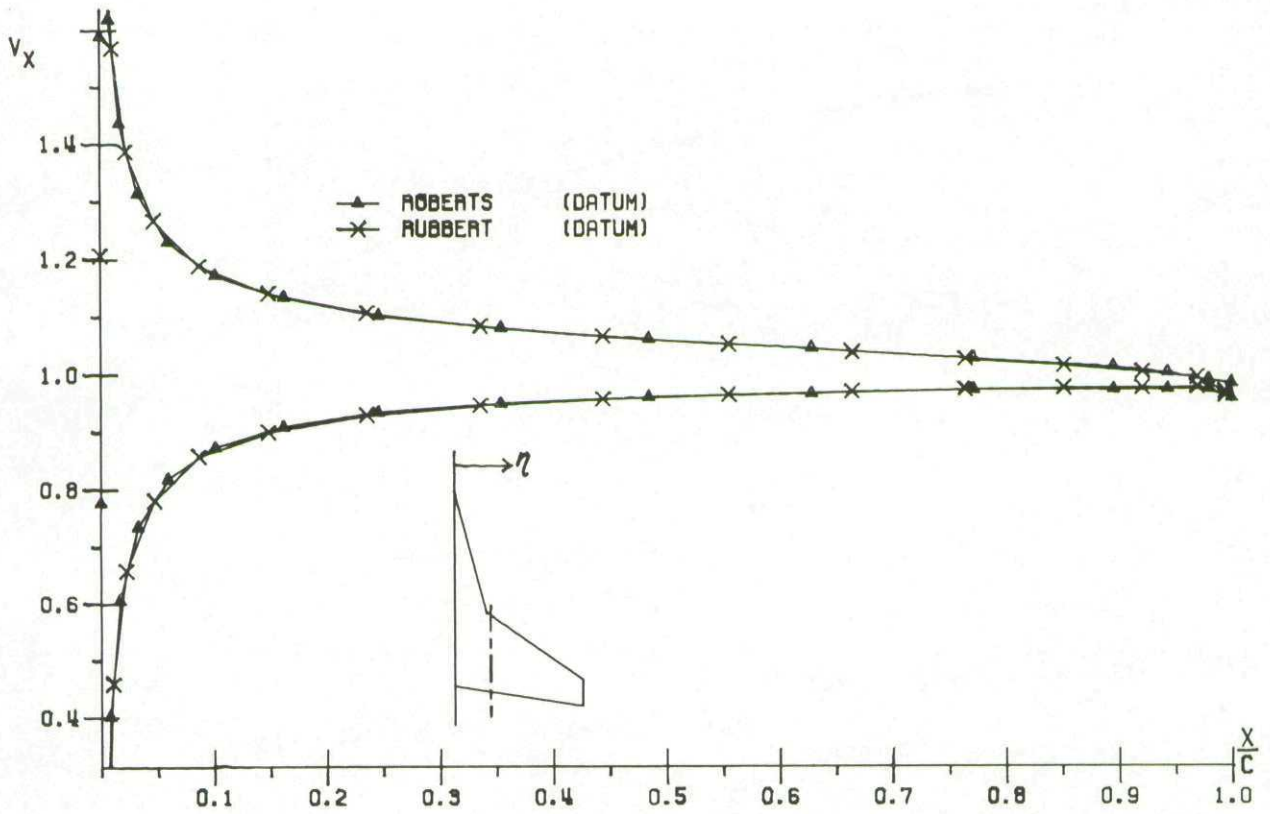


FIG. 29 COMPARISON OF DATUM RESULTS
X-COMPONENT OF VELOCITY
STRAKED WING, $T/C = .02$, $\alpha = 5.0$, $\eta = .280$

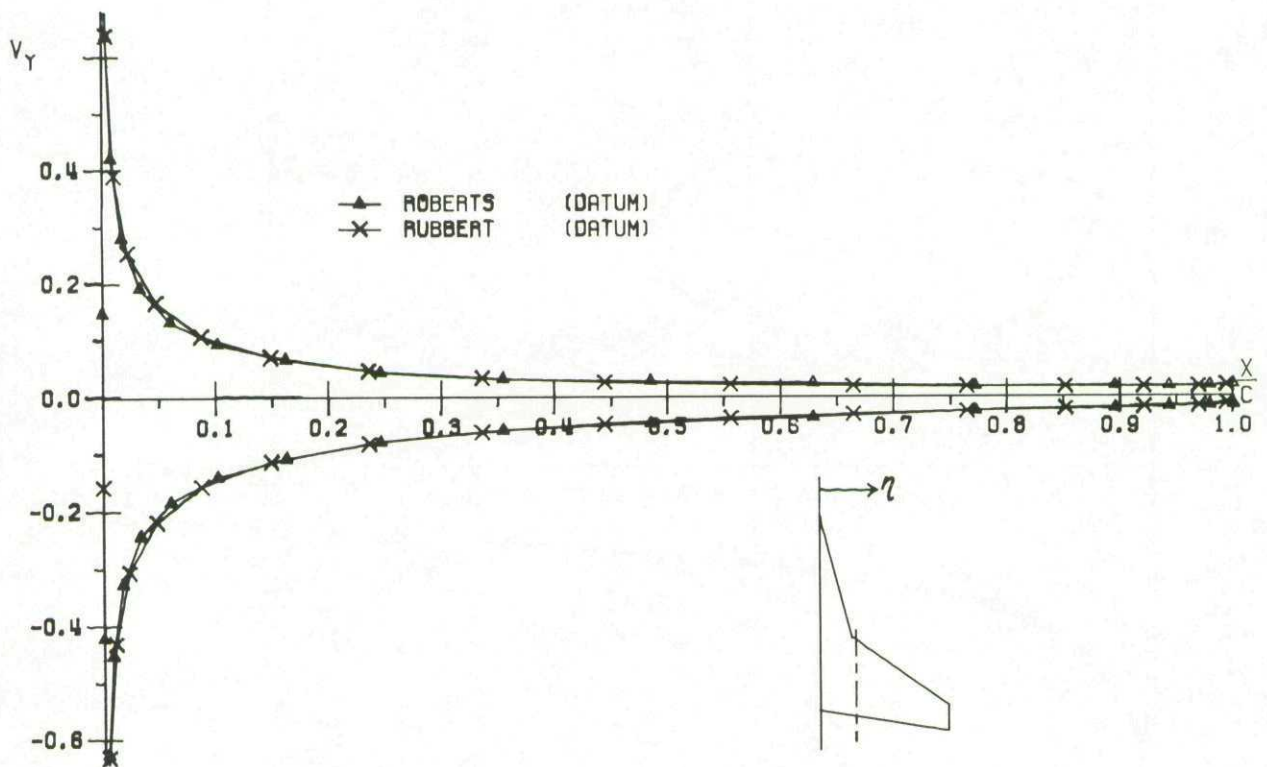


FIG. 30 COMPARISON OF DATUM RESULTS
Y-COMPONENT OF VELOCITY
STRAKED WING, $T/C = .02$, $\alpha = 5.0$, $\eta = .280$

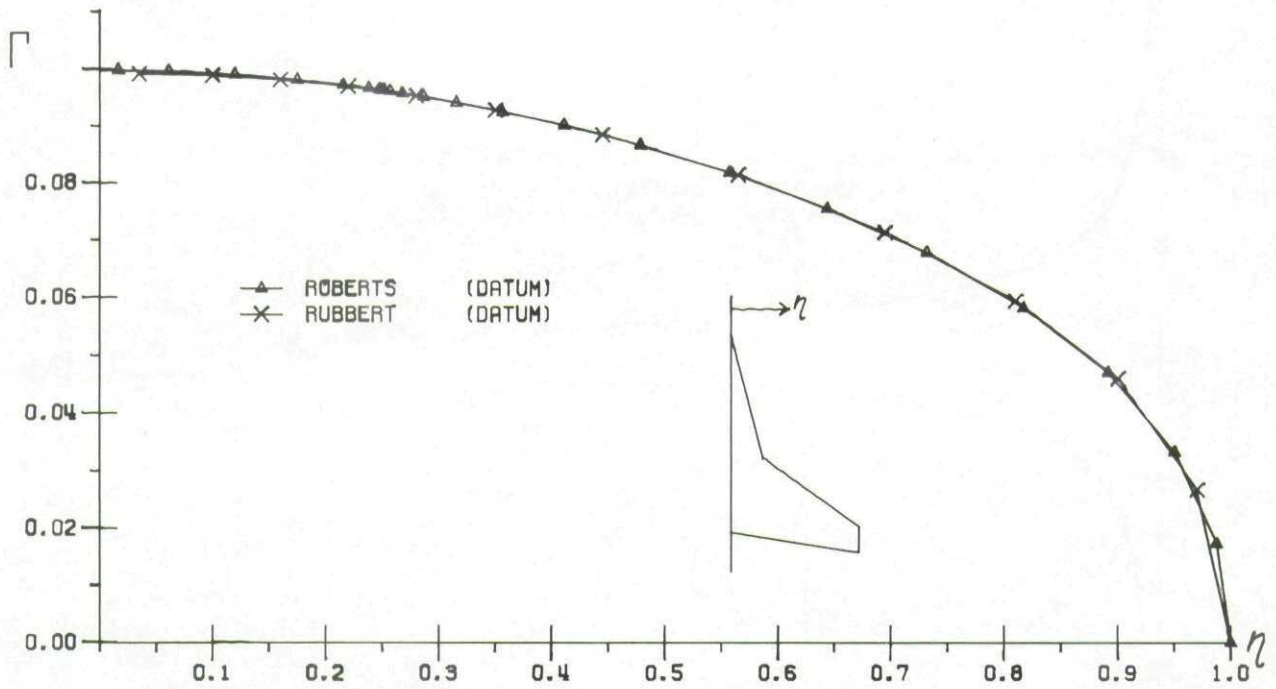


FIG. 31 COMPARISON OF DATUM RESULTS
CIRCULATION
STRAKED WING, $T/C = .02$, $\alpha = 5.0$

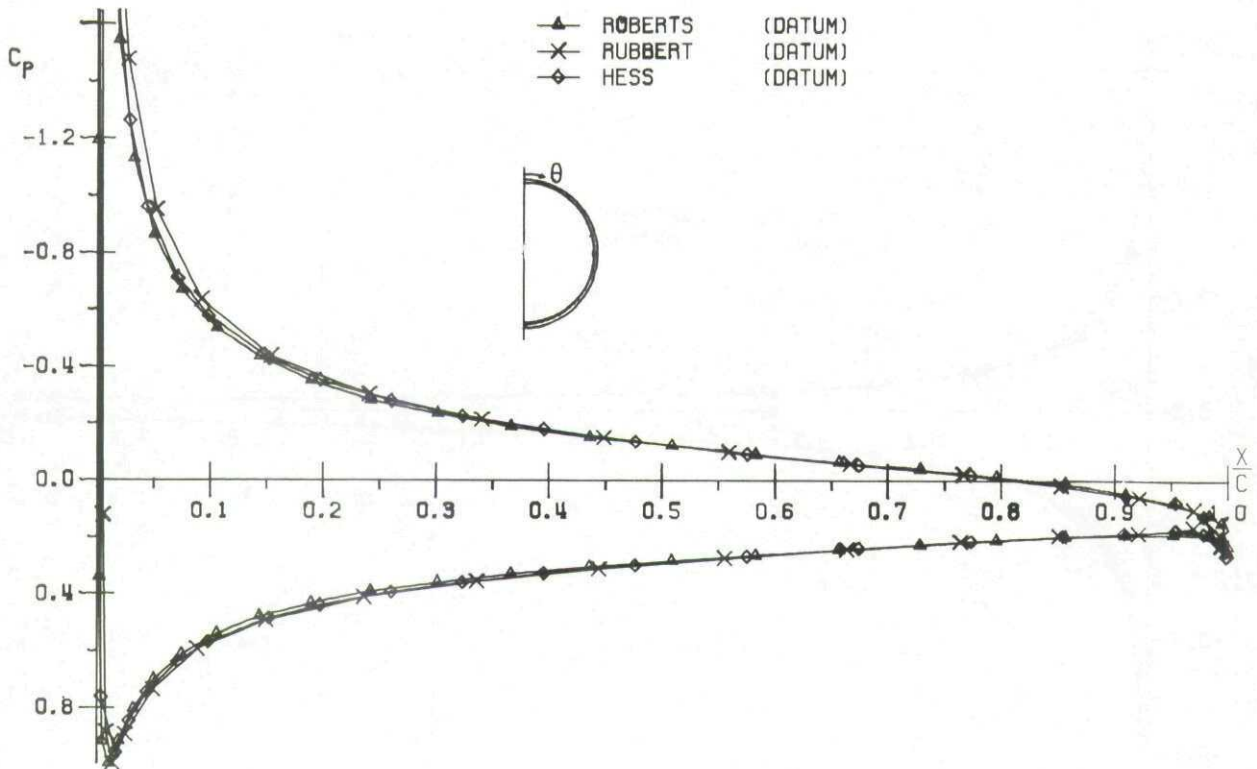


FIG. 32 COMPARISON OF DATUM RESULTS
CHORDWISE PRESSURE DISTRIBUTION
NACELLE, $C/DE = 1.0000$, $\alpha = 0.0$, $\theta = 0.000$

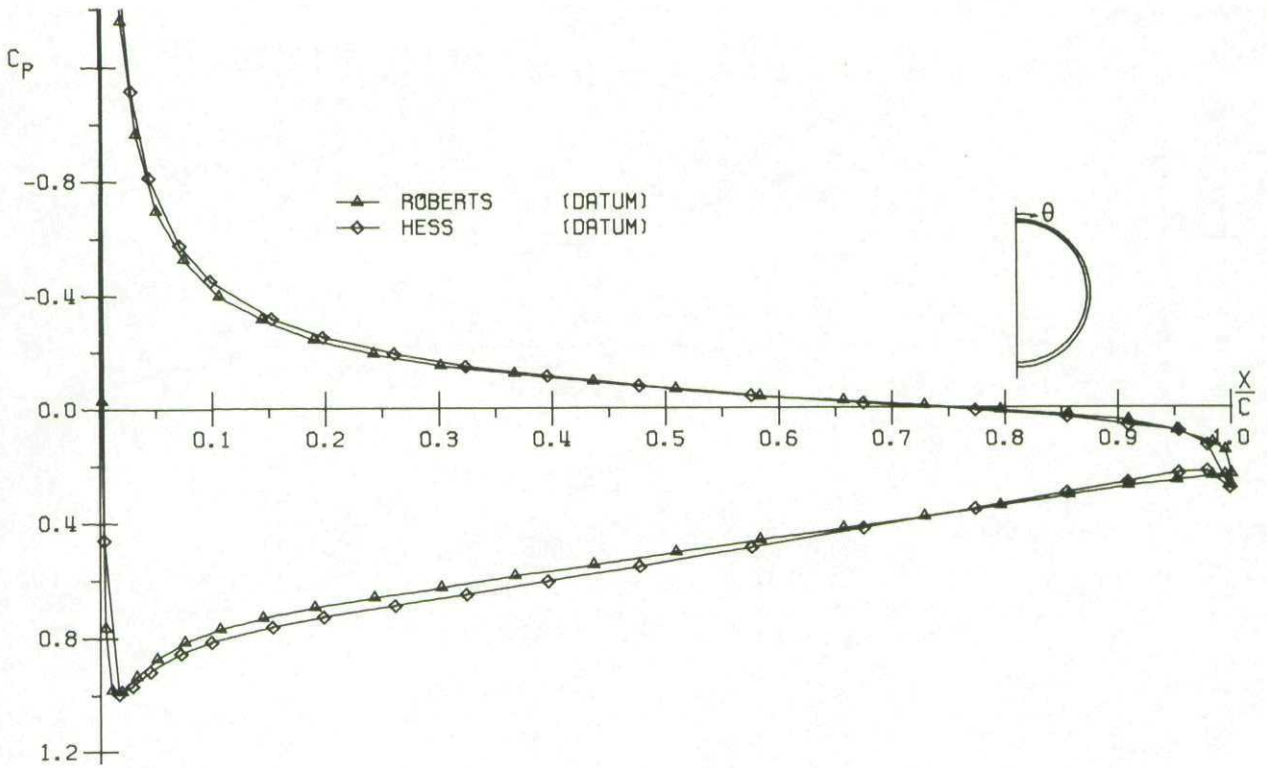


FIG. 33 COMPARISON OF DATUM RESULTS
CHORDWISE PRESSURE DISTRIBUTION
NACELLE . $C/DE = 3.3333$. $\alpha = 0.0$. $\theta = 0.000$

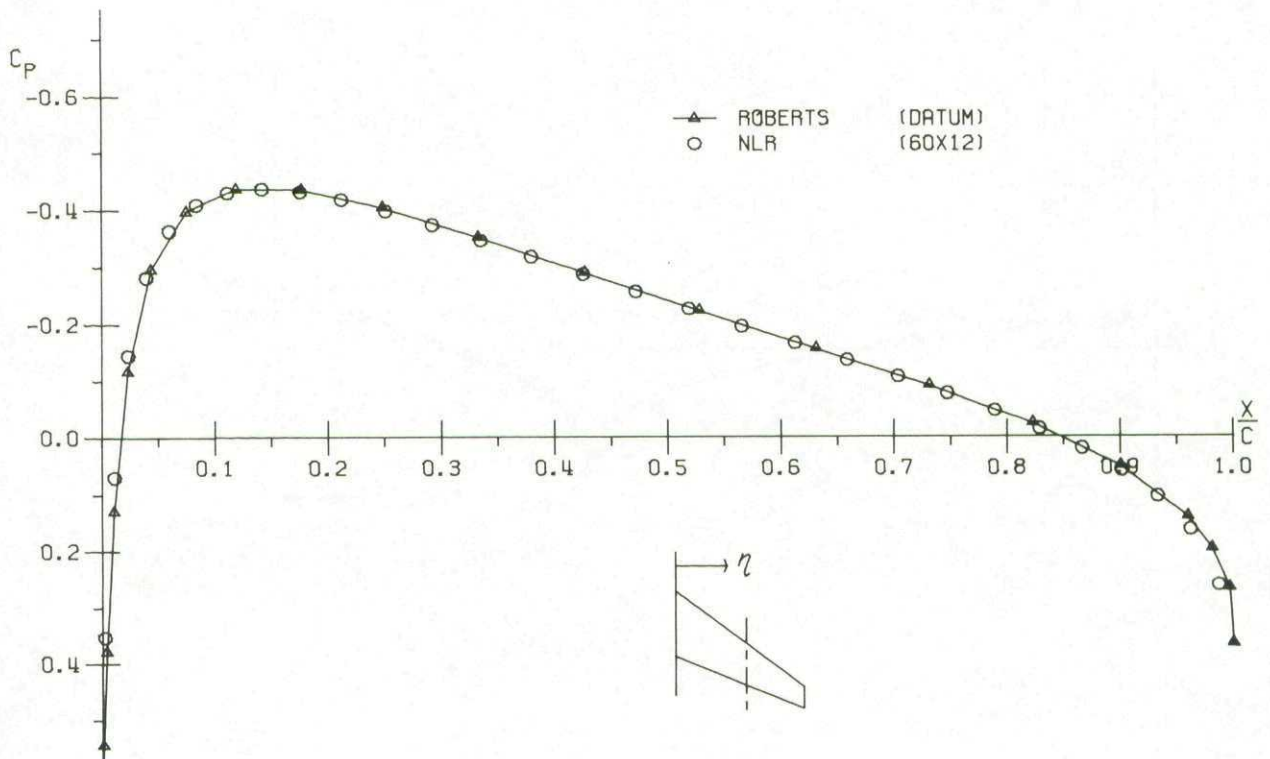


FIG. 34 FIRST ORDER METHOD COMPARISON
CHORDWISE PRESSURE DISTRIBUTION
RAE WING . $T/C = .15$. $\alpha = 0.0$. $\eta = .549$

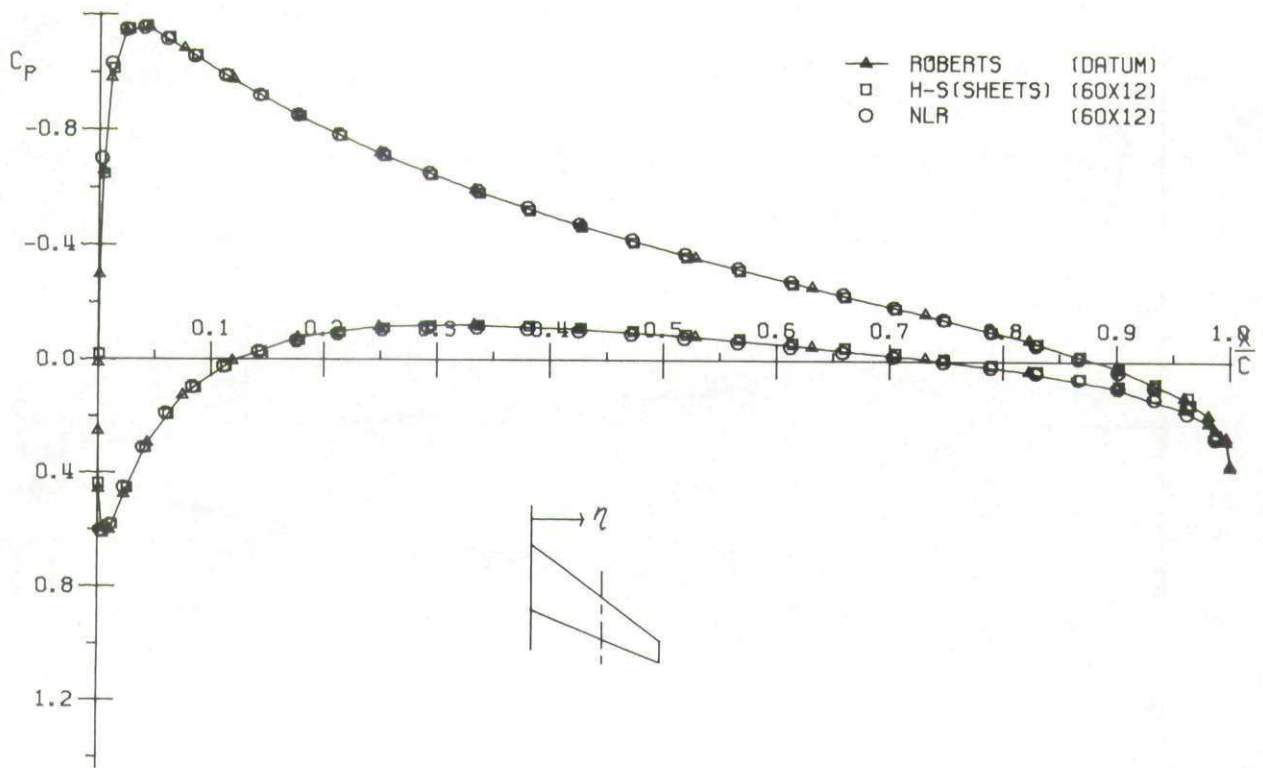


FIG. 35 FIRST ORDER METHOD COMPARISON
 CHORDWISE PRESSURE DISTRIBUTION
 RAE WING , $T/C = .15$, $\alpha = 5.0$, $\eta = .549$

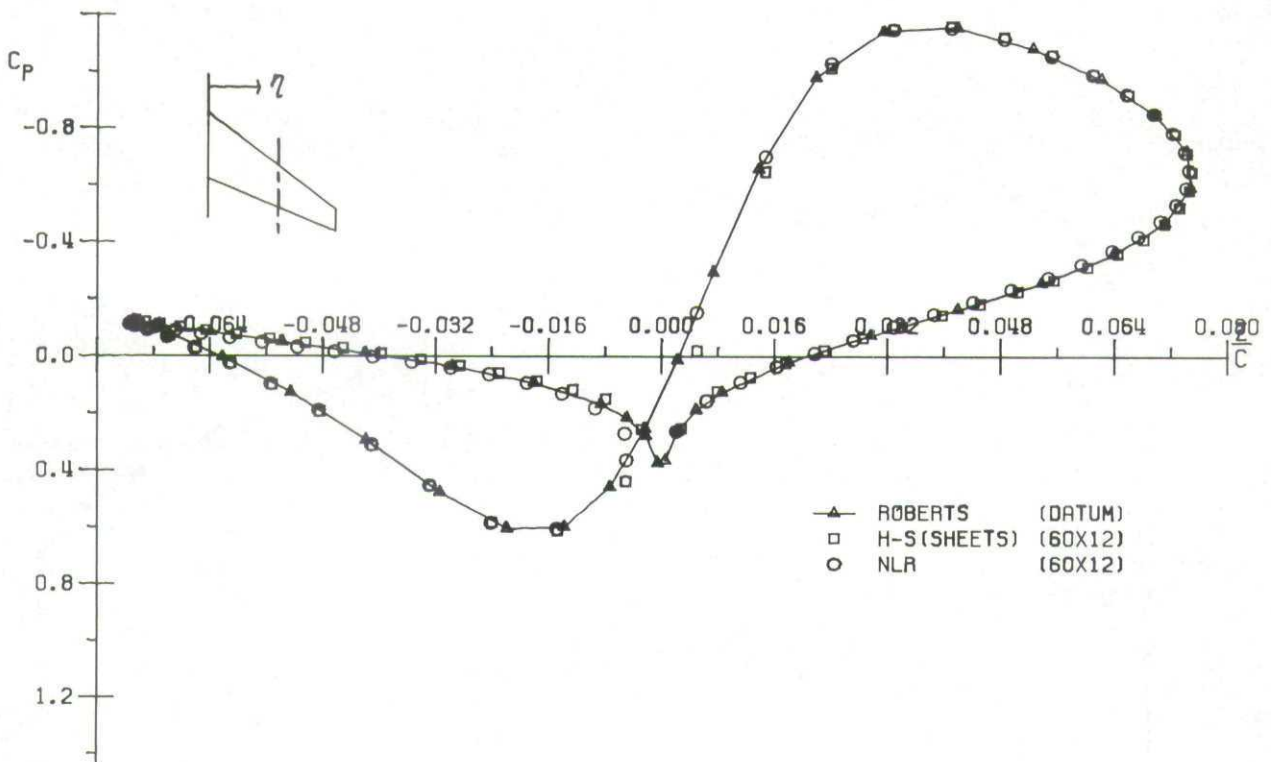


FIG. 36 FIRST ORDER METHOD COMPARISON
 DRAG LOOP
 RAE WING , $T/C = .15$, $\alpha = 5.0$, $\eta = .549$

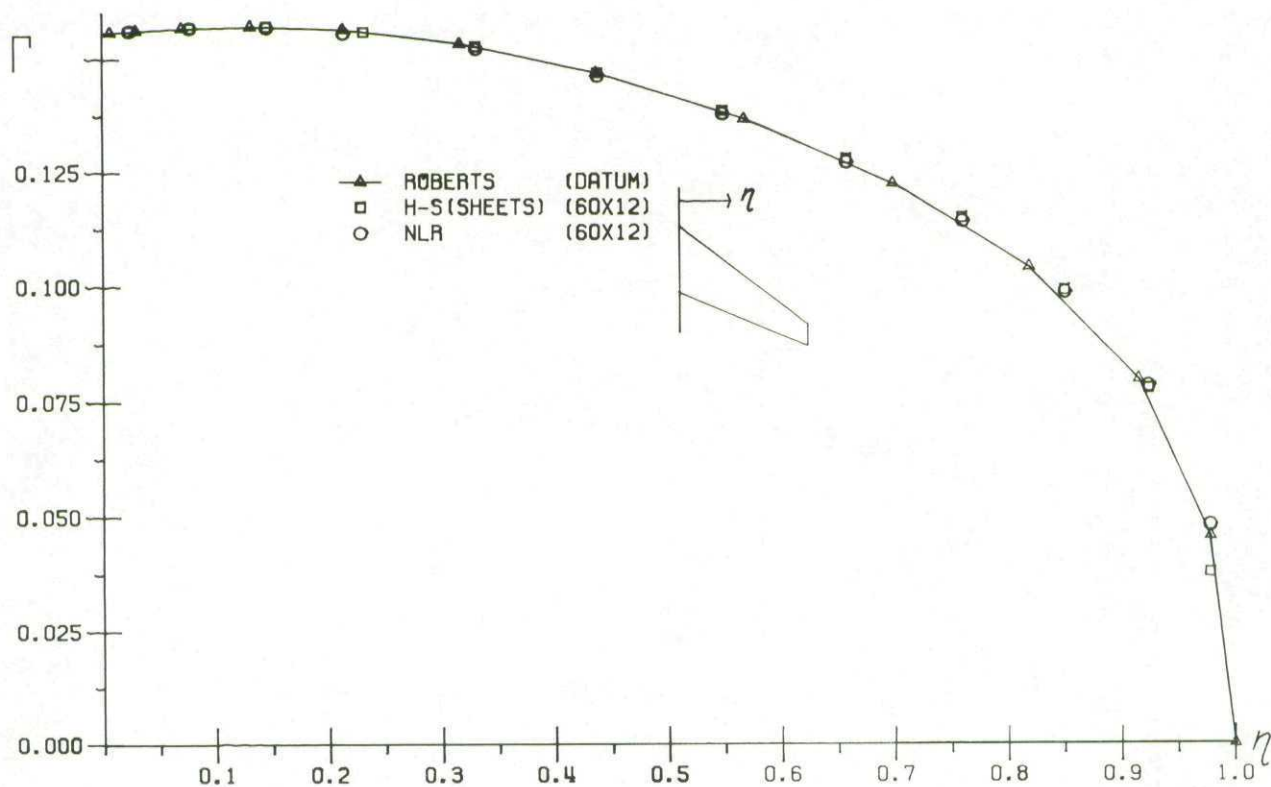


FIG. 37 FIRST ORDER METHOD COMPARISON
 CIRCULATION
 RAE WING , T/C = .15 , $\alpha = 5.0$

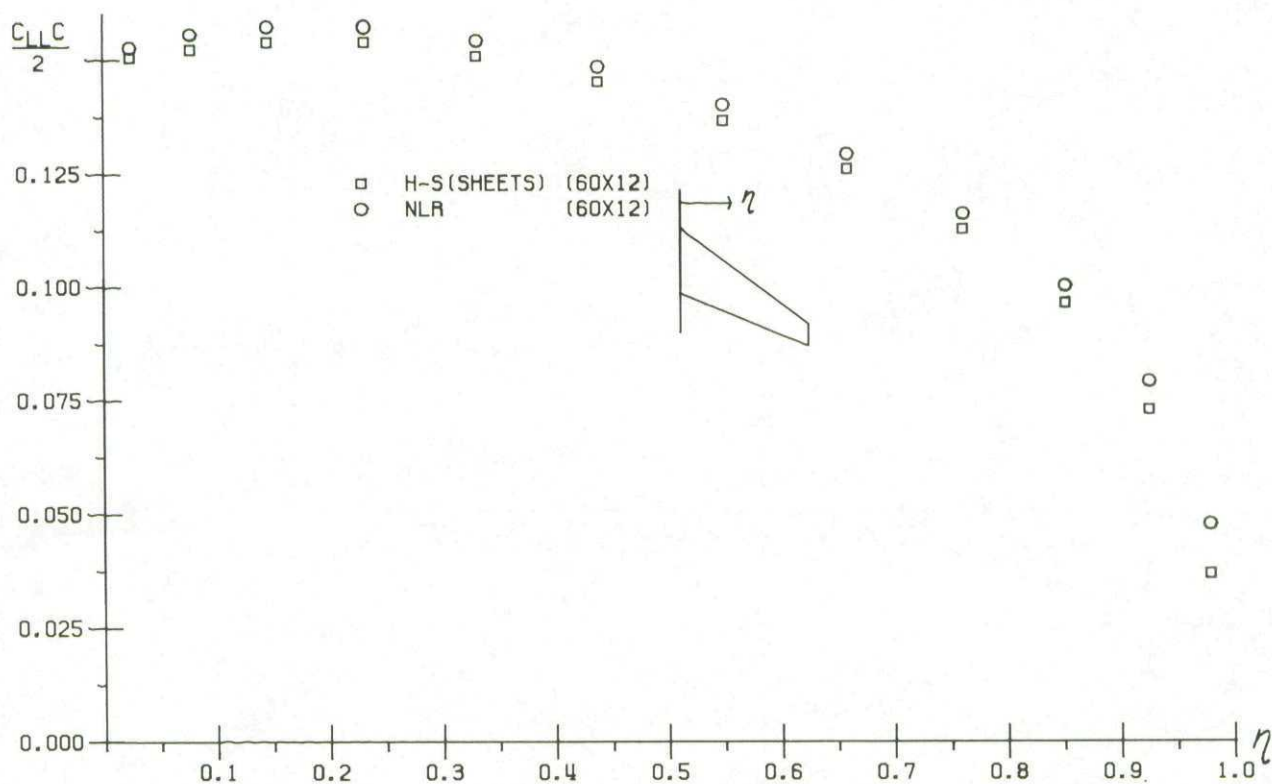


FIG. 38 FIRST ORDER METHOD COMPARISON
 SECTIONAL LOAD
 RAE WING , T/C = .15 , $\alpha = 5.0$

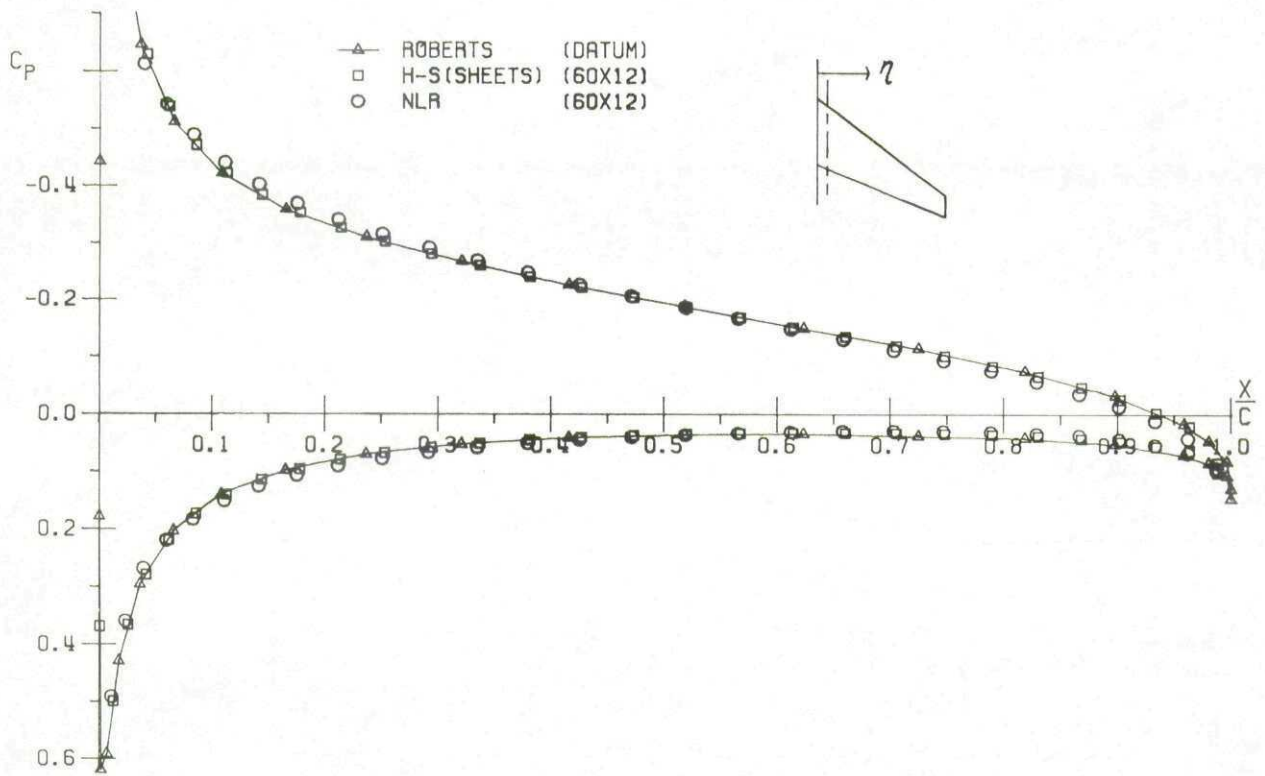


FIG. 39 FIRST ORDER METHOD COMPARISON
 CHORDWISE PRESSURE DISTRIBUTION
 RAE WING , $T/C = .05$, $\alpha = 5.0$, $\eta = .079$

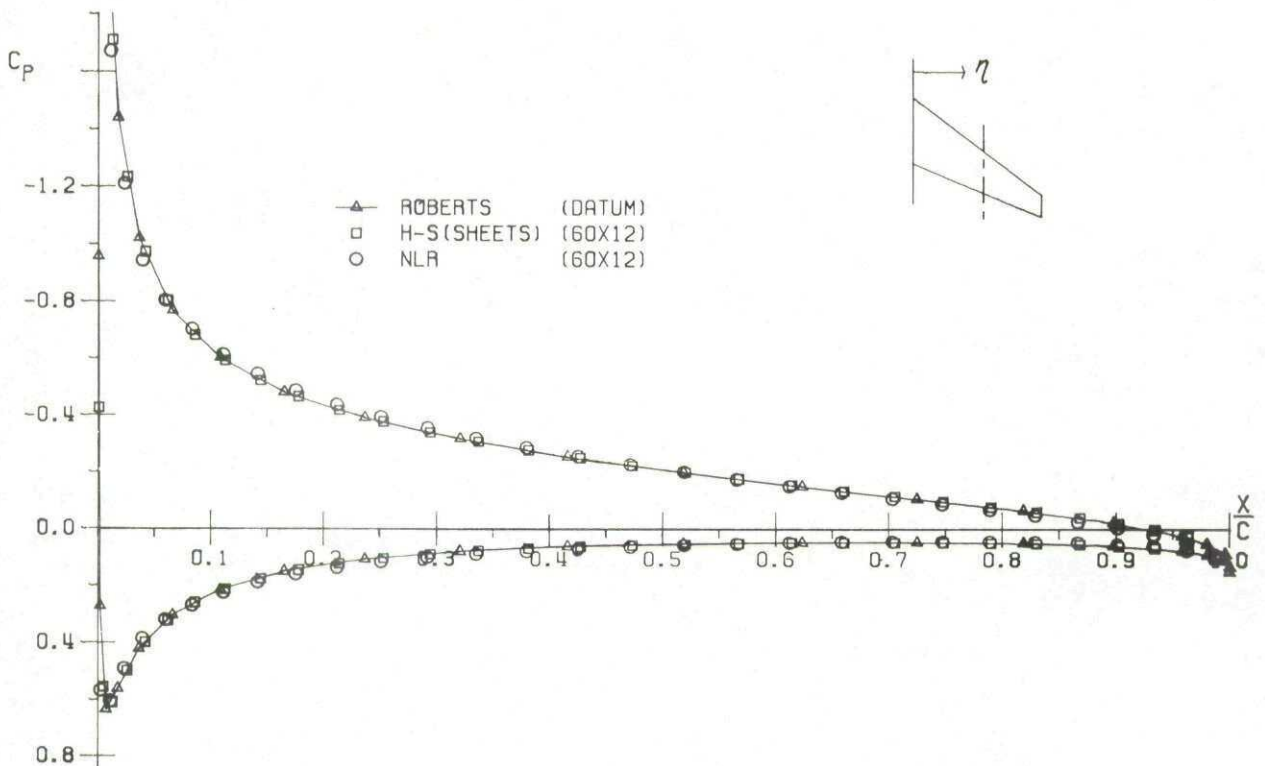


FIG. 40 FIRST ORDER METHOD COMPARISON
 CHORDWISE PRESSURE DISTRIBUTION
 RAE WING , $T/C = .05$, $\alpha = 5.0$, $\eta = .549$

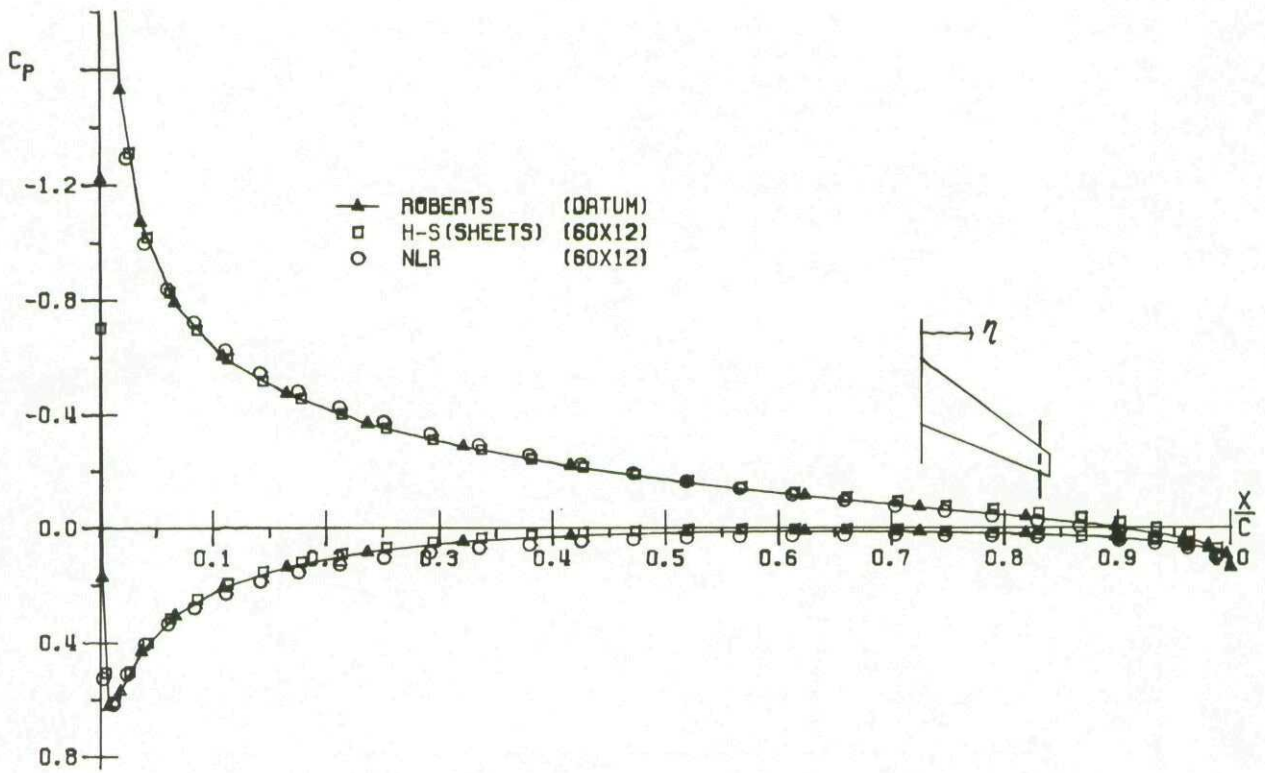


FIG. 41 FIRST ORDER METHOD COMPARISON
CHORDWISE PRESSURE DISTRIBUTION
RAE WING , T/C = .05 , $\alpha = 5.0$, $\eta = .924$

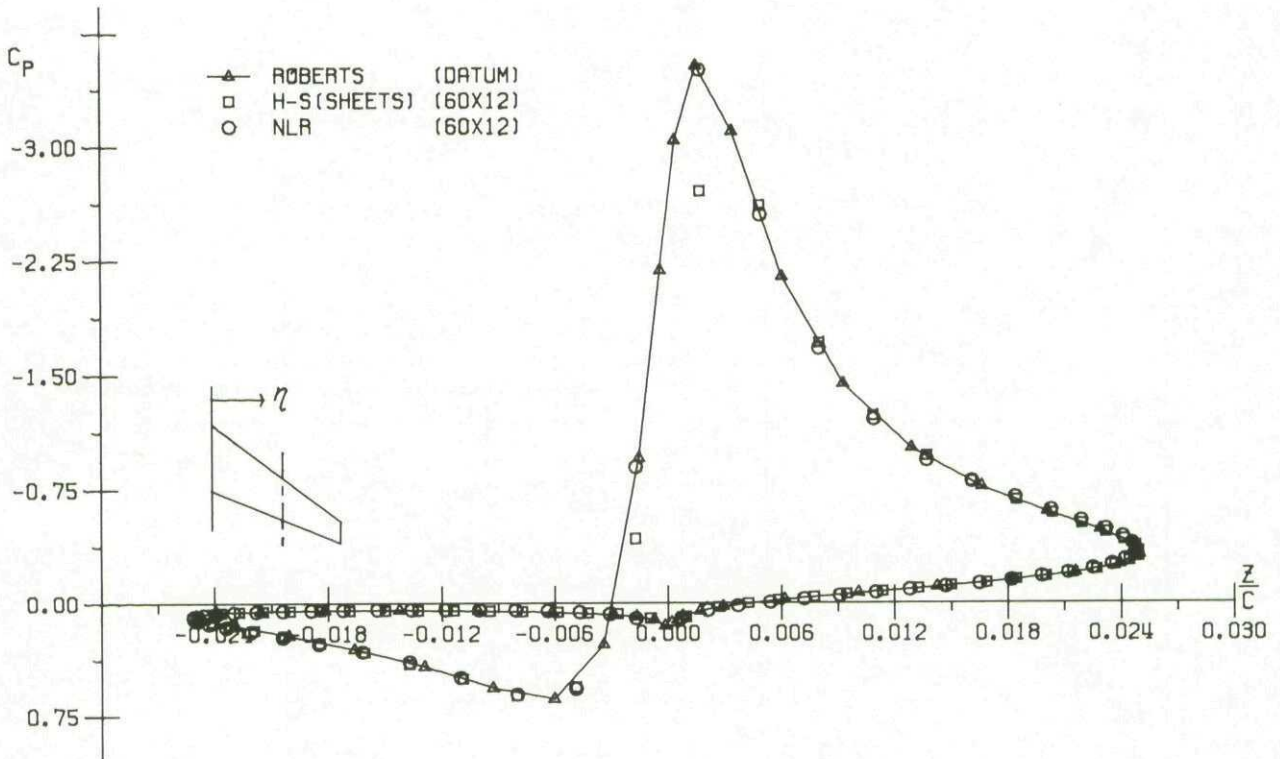


FIG. 42 FIRST ORDER METHOD COMPARISON
DRAG LOOP
RAE WING , T/C = .05 , $\alpha = 5.0$, $\eta = .549$

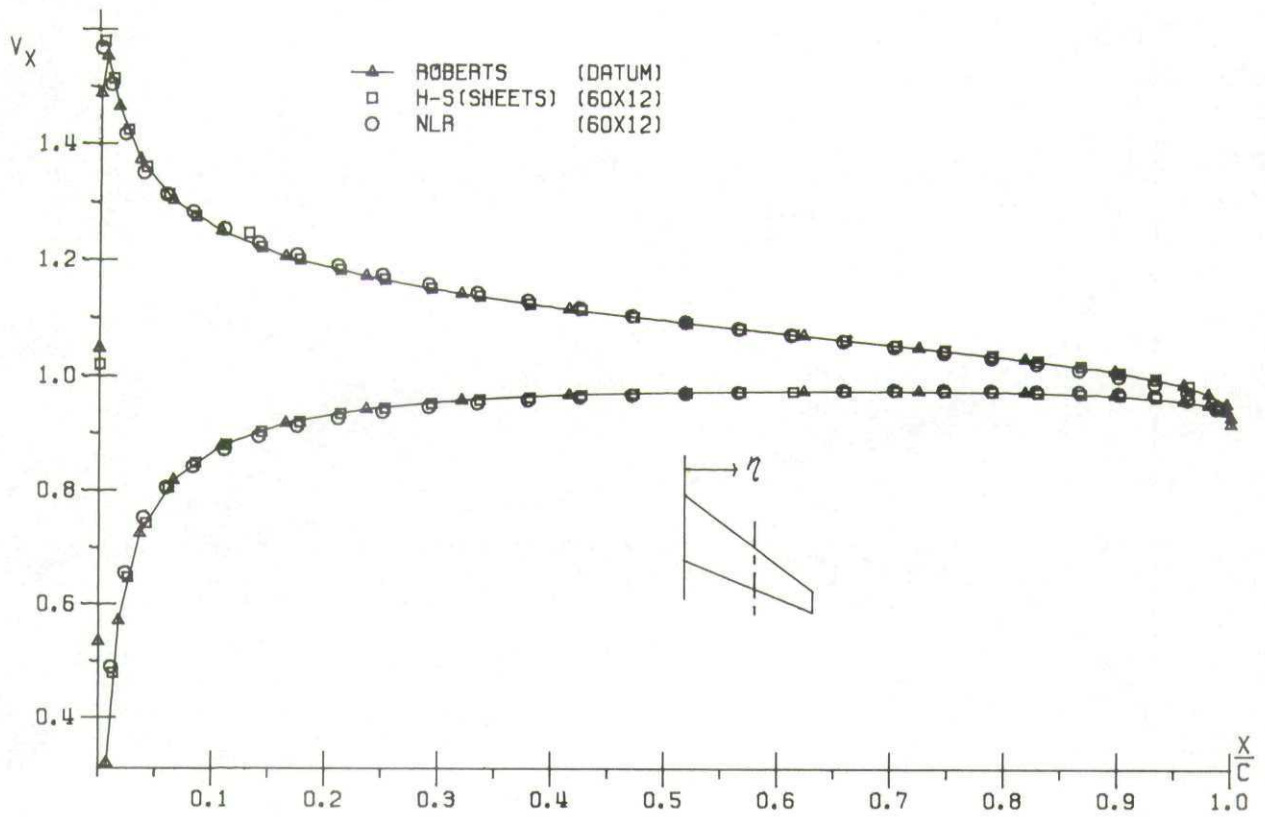


FIG. 43 FIRST ORDER METHOD COMPARISON
 X-COMPONENT OF VELOCITY
 RAE WING , $T/C = .05$, $\alpha = 5.0$, $\eta = .549$

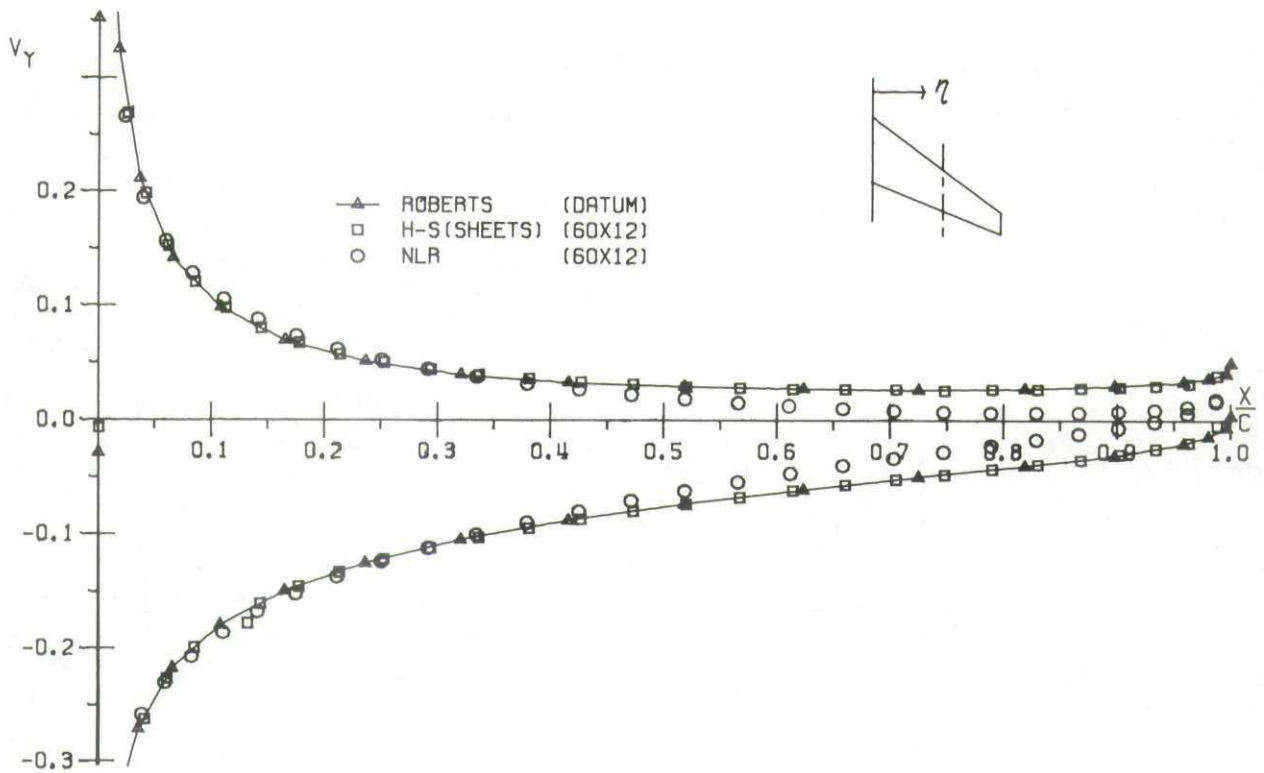


FIG. 44 FIRST ORDER METHOD COMPARISON
 Y-COMPONENT OF VELOCITY
 RAE WING , $T/C = .05$, $\alpha = 5.0$, $\eta = .549$

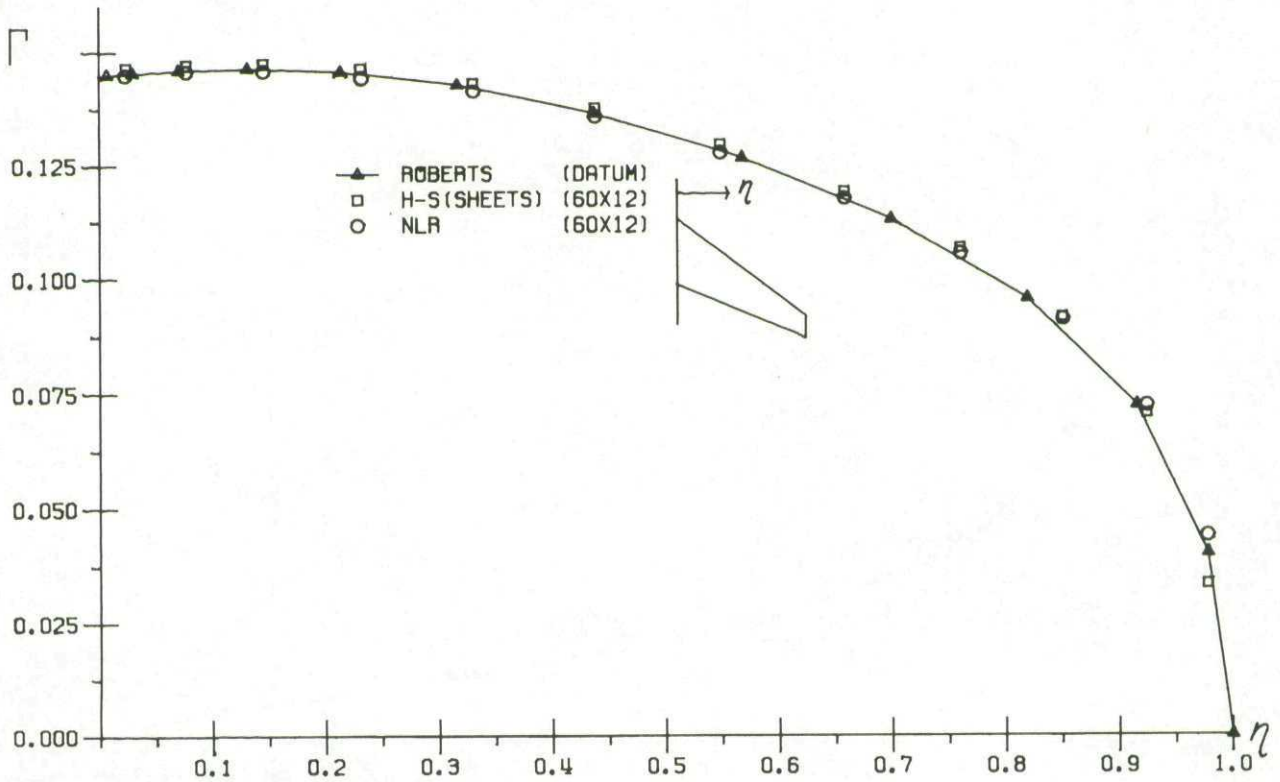


FIG. 45 FIRST ORDER METHOD COMPARISON
CIRCULATION
RAE WING , T/C = .05 , $\alpha = 5.0$

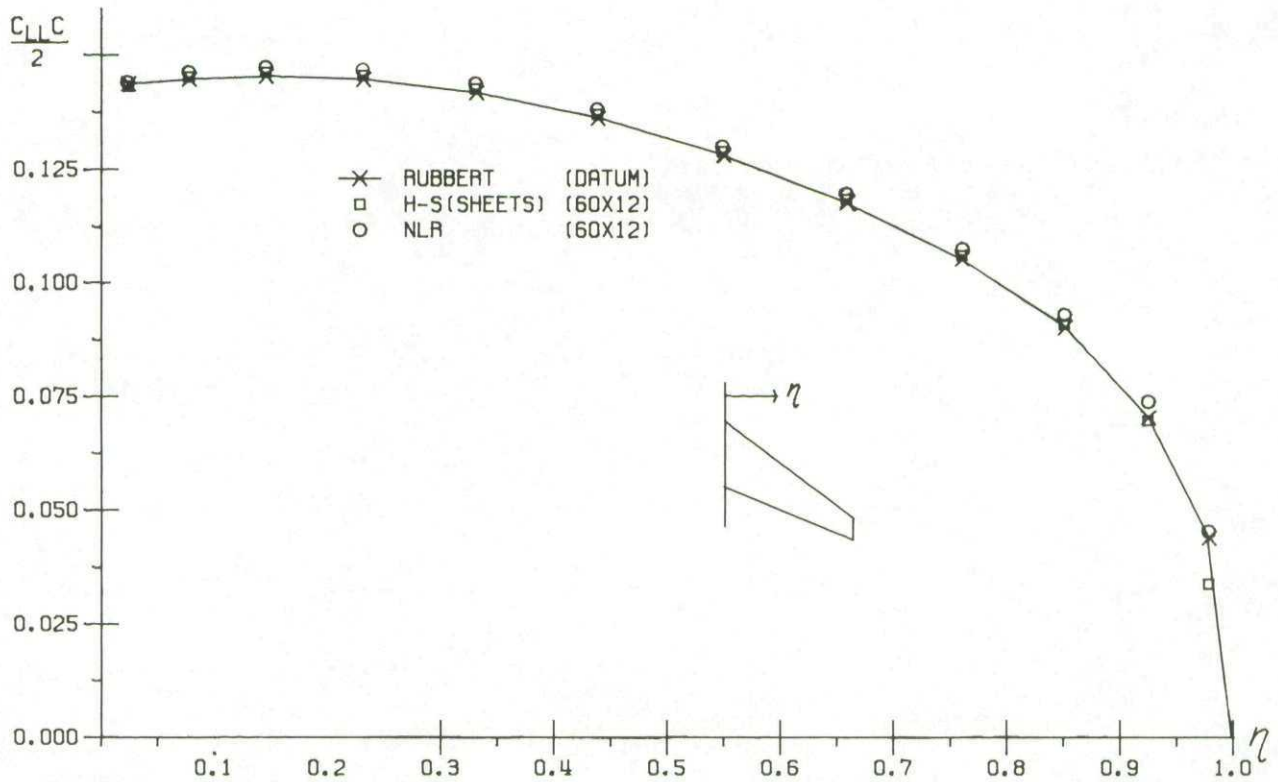


FIG. 46 FIRST ORDER METHOD COMPARISON
SECTIONAL LOAD
RAE WING , T/C = .05 , $\alpha = 5.0$

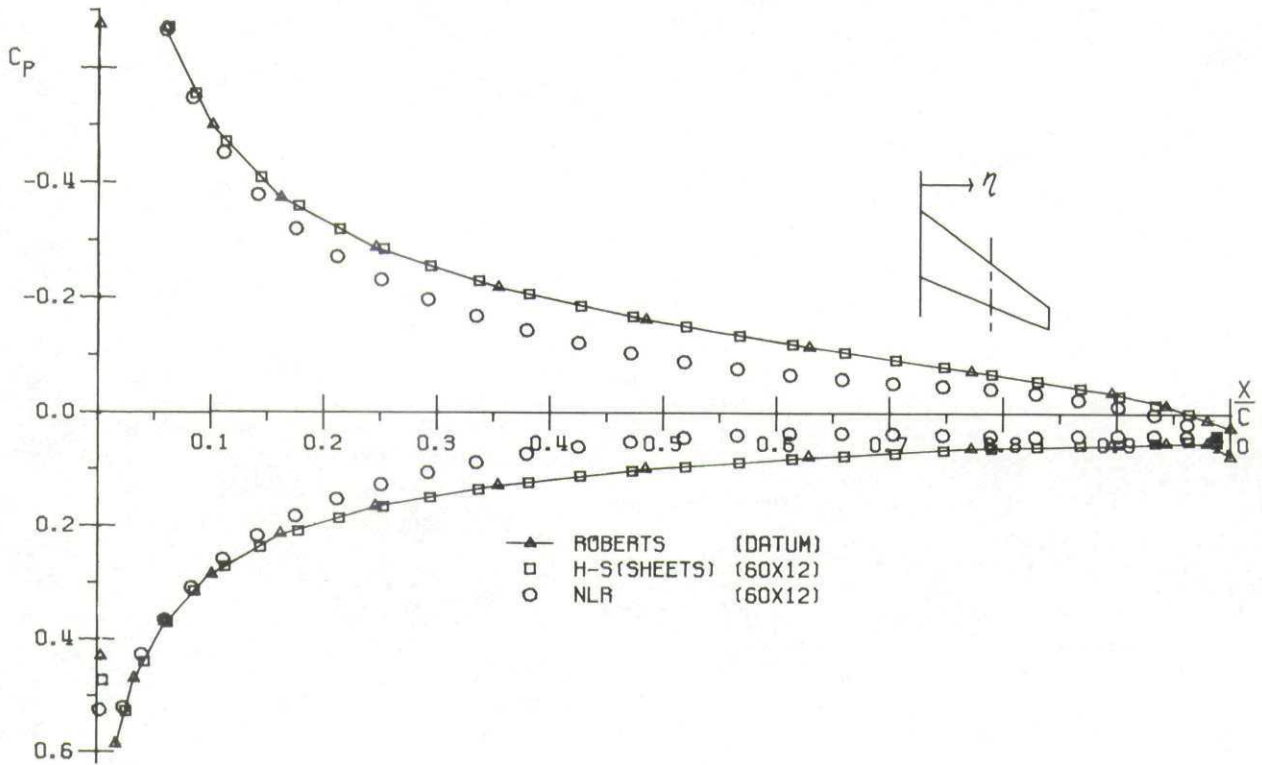


FIG. 47 FIRST ORDER METHOD COMPARISON
CHORDWISE PRESSURE DISTRIBUTION
RAE WING . T/C = .02 . $\alpha = 5.0$. $\eta = .549$

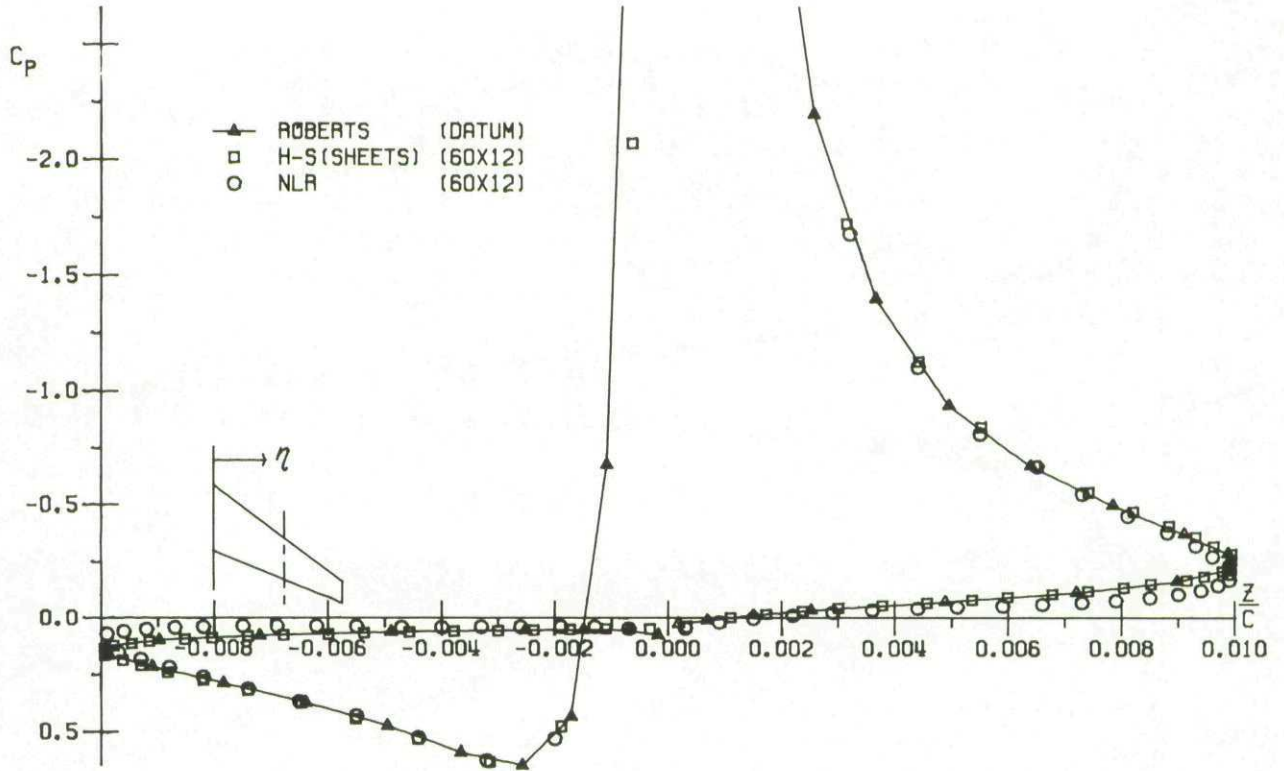


FIG. 48a FIRST ORDER METHOD COMPARISON
 DRAG LOOP
 RAE WING . T/C = .02 . α = 5.0 . η = .549

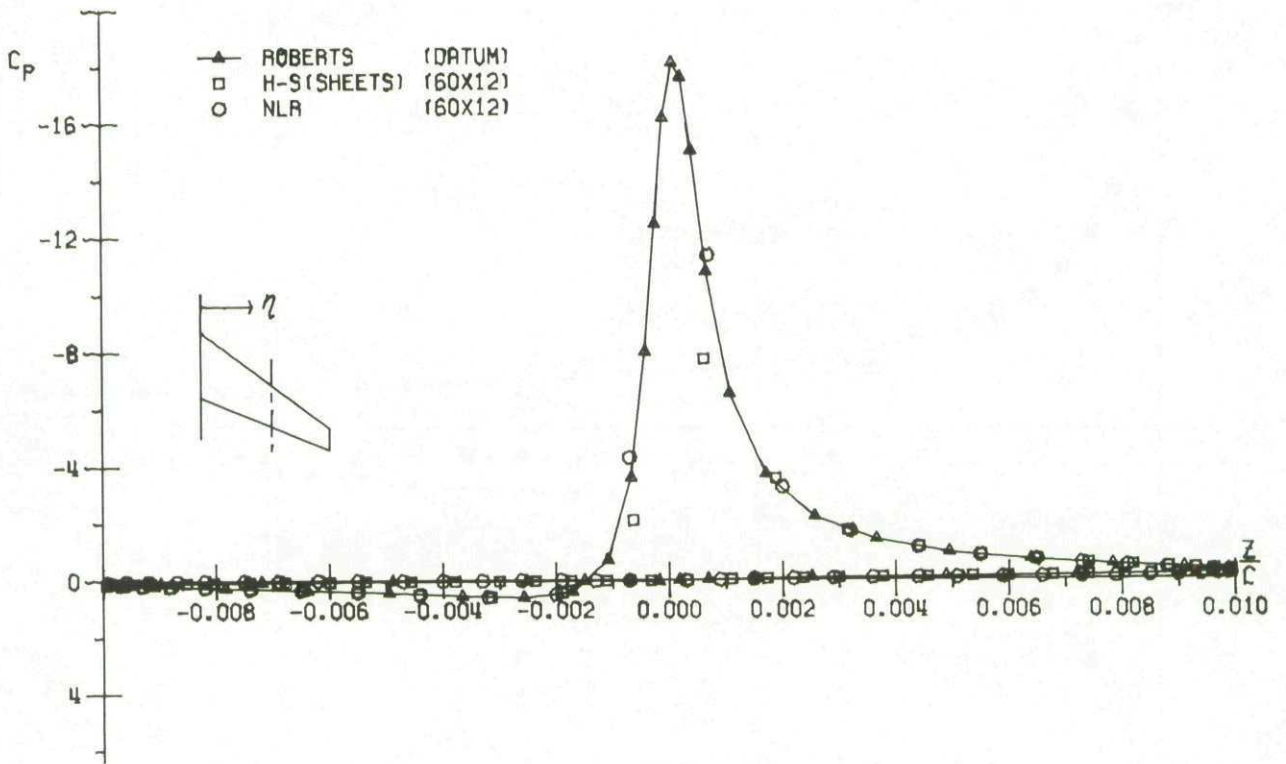


FIG. 48b FIRST ORDER METHOD COMPARISON
 DRAG LOOP
 RAE WING . T/C = .02 . α = 5.0 . η = .549

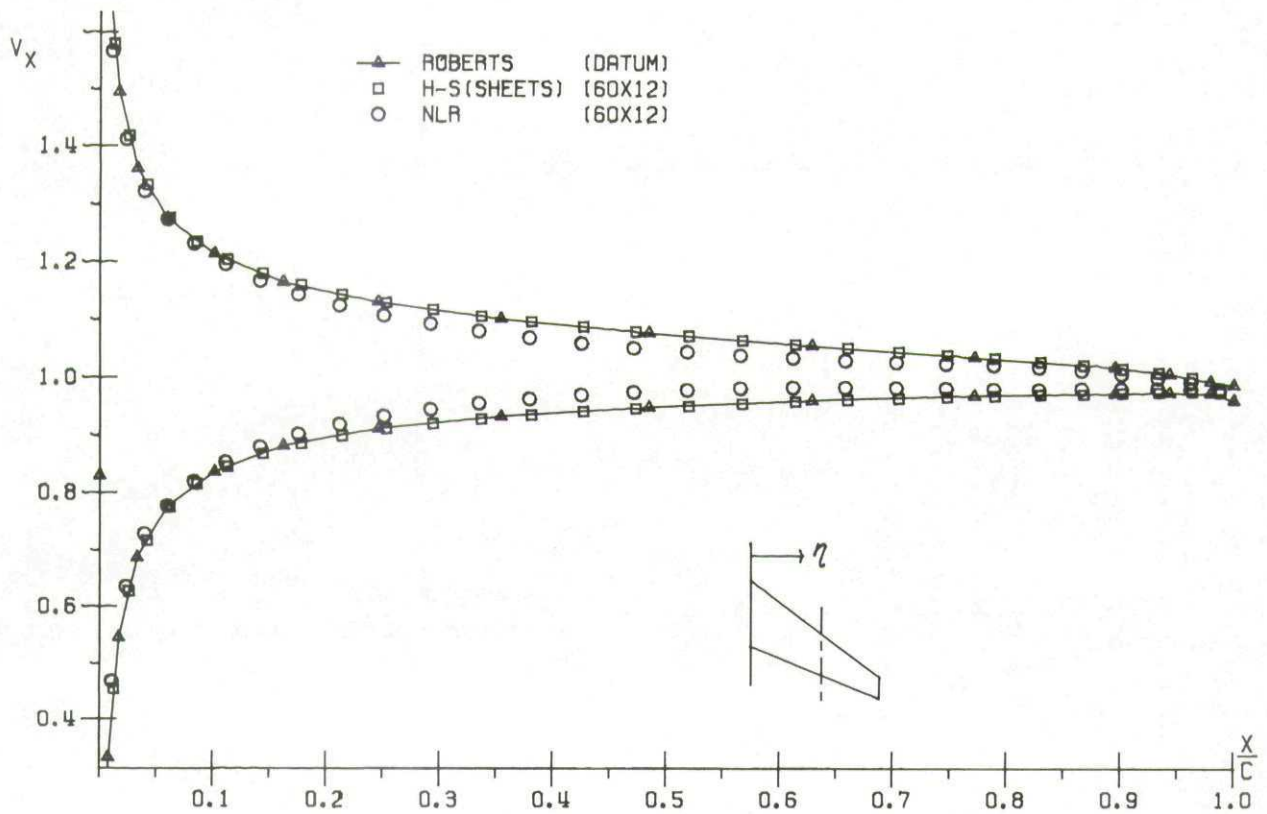


FIG. 49 FIRST ORDER METHOD COMPARISON
 X-COMPONENT OF VELOCITY
 RAE WING . T/C = .02 . $\alpha = 5.0$. $\eta = .549$

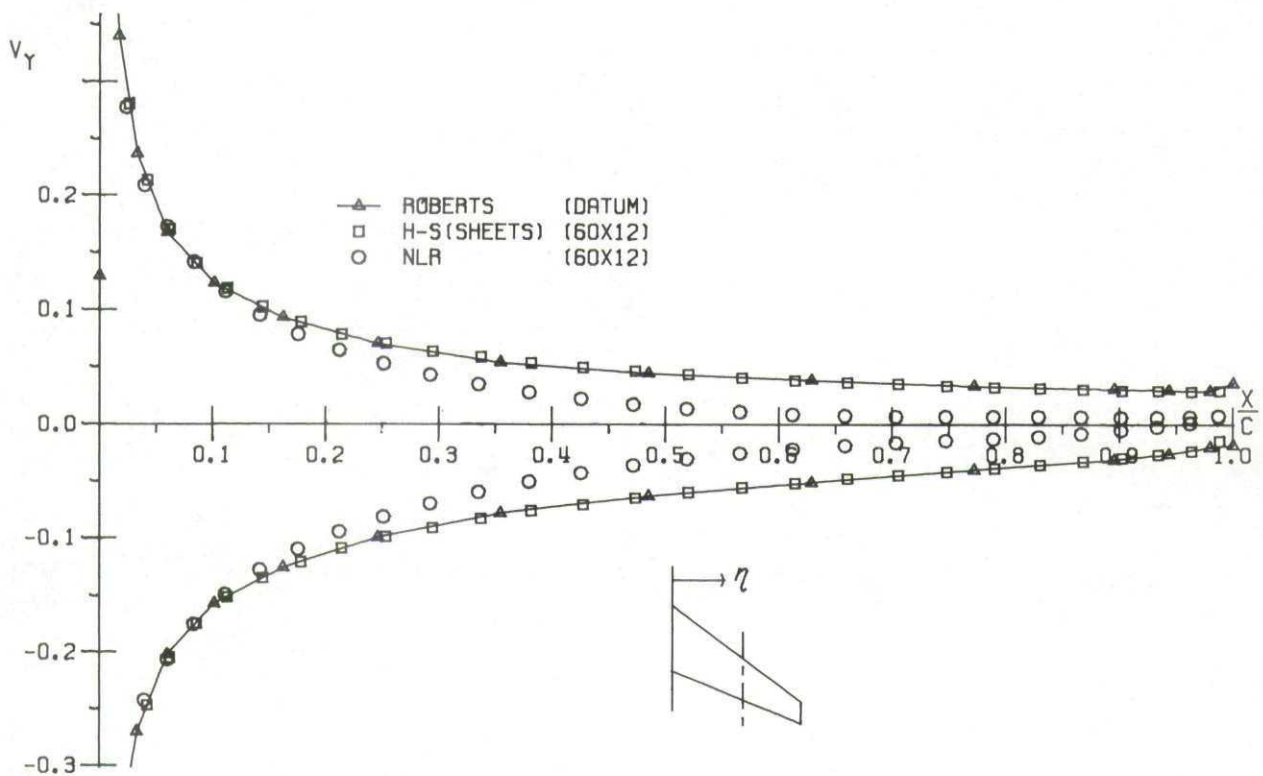


FIG. 50 FIRST ORDER METHOD COMPARISON
 Y-COMPONENT OF VELOCITY
 RAE WING . T/C = .02 . $\alpha = 5.0$. $\eta = .549$

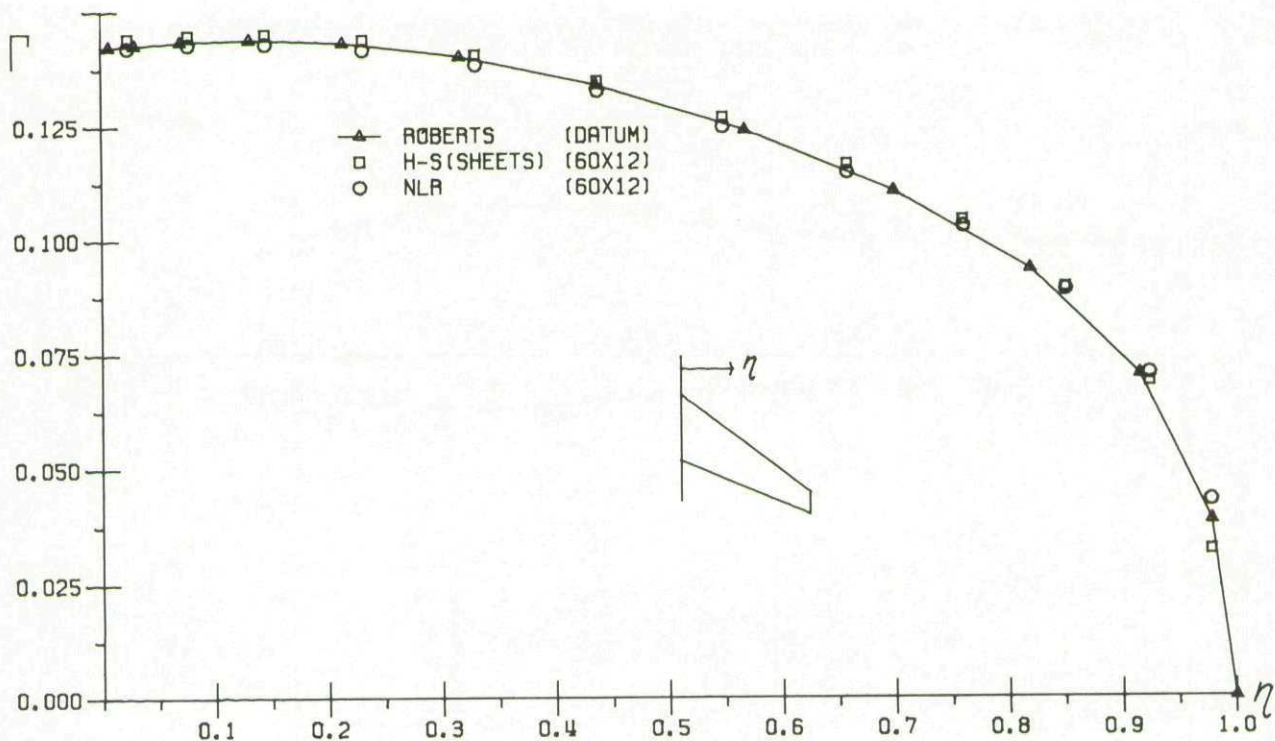


FIG. 51 FIRST ORDER METHOD COMPARISON
CIRCULATION
RAE WING . T/C = .02 . α = 5.0

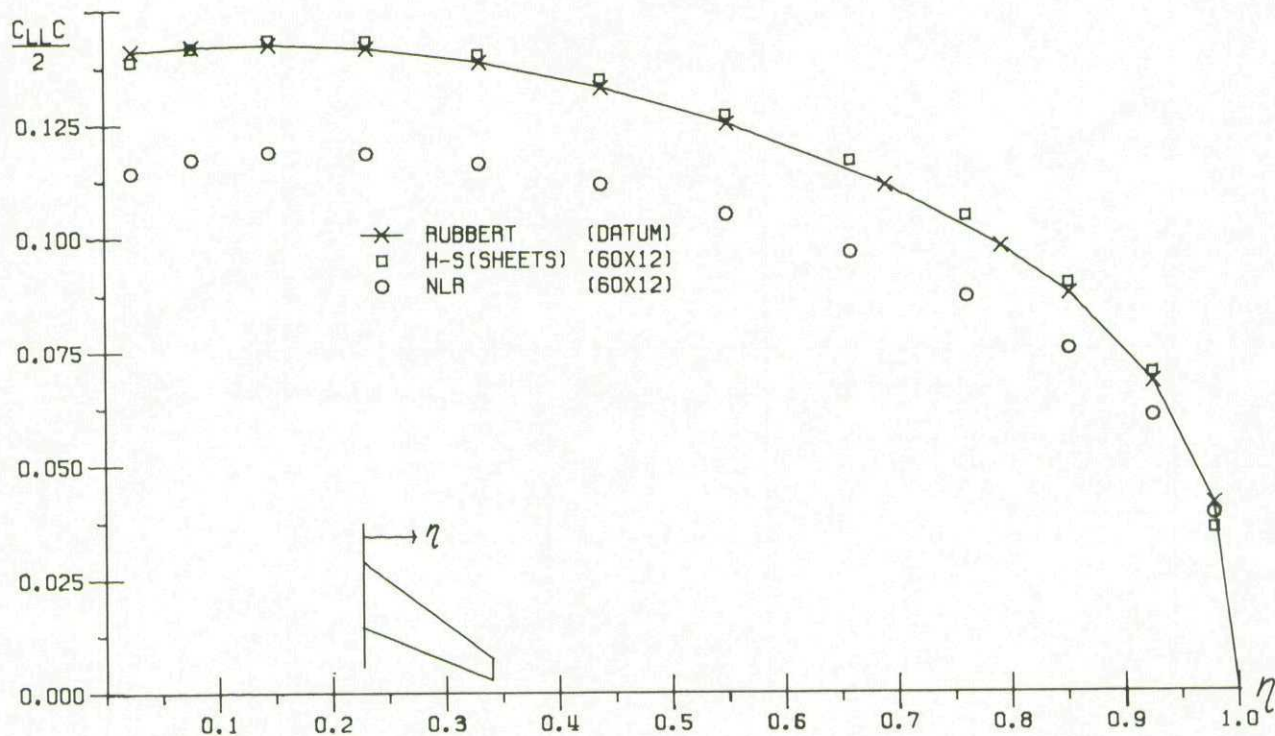


FIG. 52 FIRST ORDER METHOD COMPARISON
SECTIONAL LOAD
RAE WING . T/C = .02 . α = 5.0

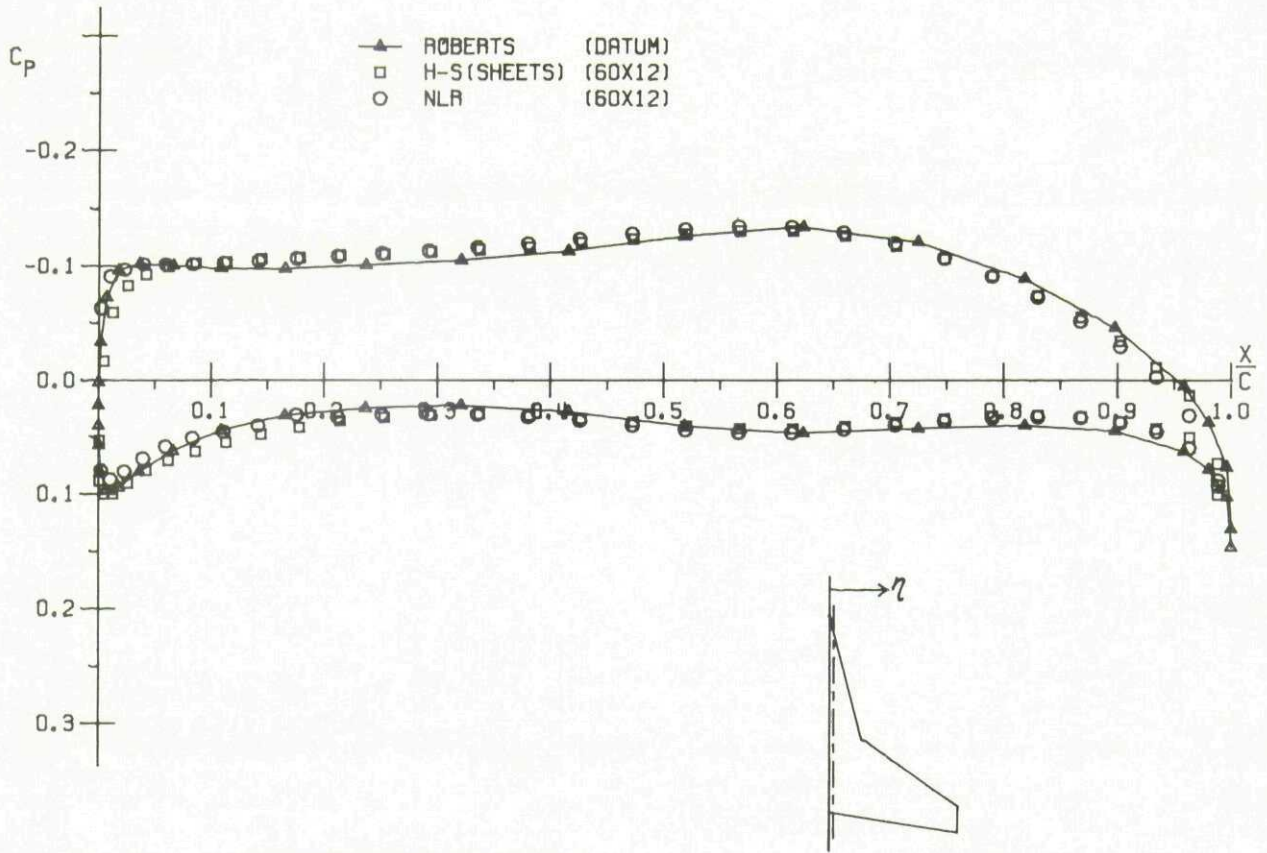


FIG. 53 FIRST ORDER METHOD COMPARISON
CHORDWISE PRESSURE DISTRIBUTION
STRAKED WING, $T/C = .05$, $\alpha = 5.0$, $\eta = .034$

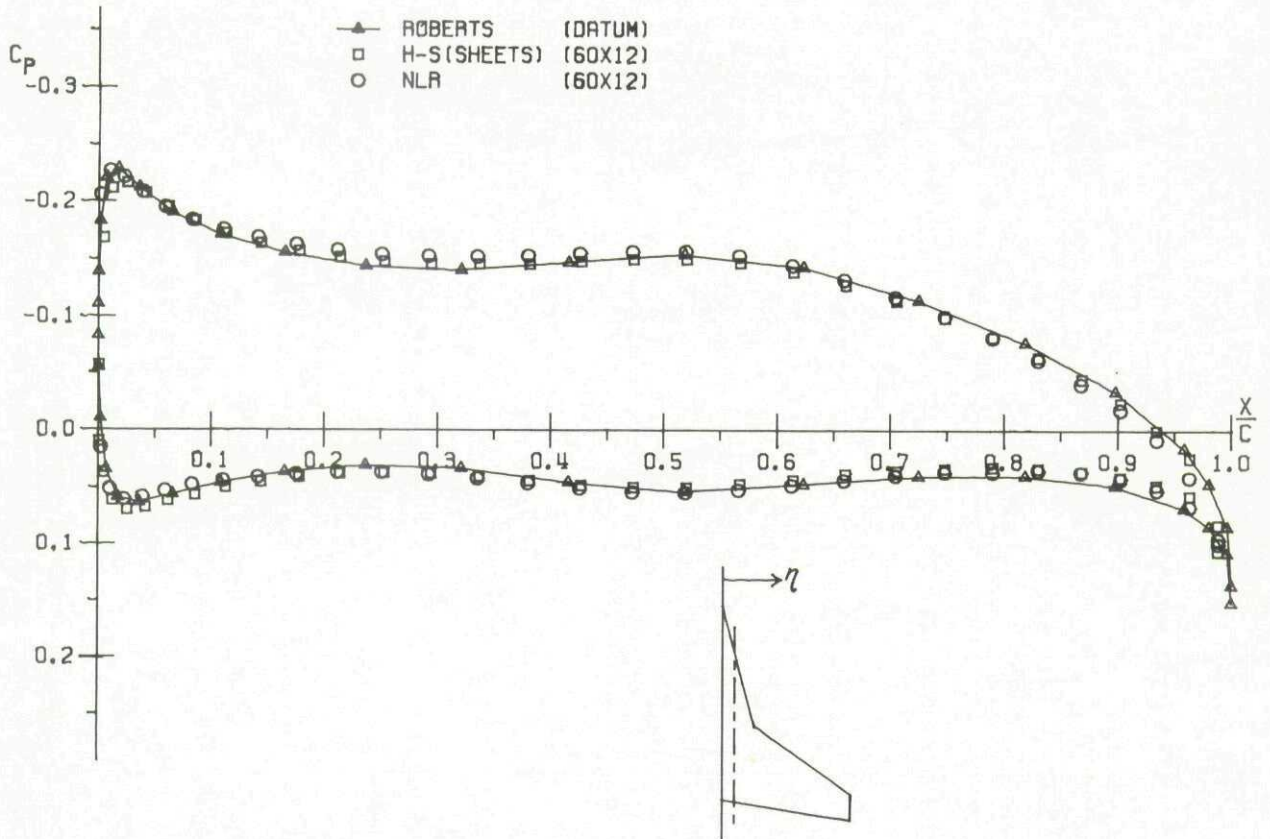


FIG. 54 FIRST ORDER METHOD COMPARISON
CHORDWISE PRESSURE DISTRIBUTION
STRAKED WING, $T/C = .05$, $\alpha = 5.0$, $\eta = .099$

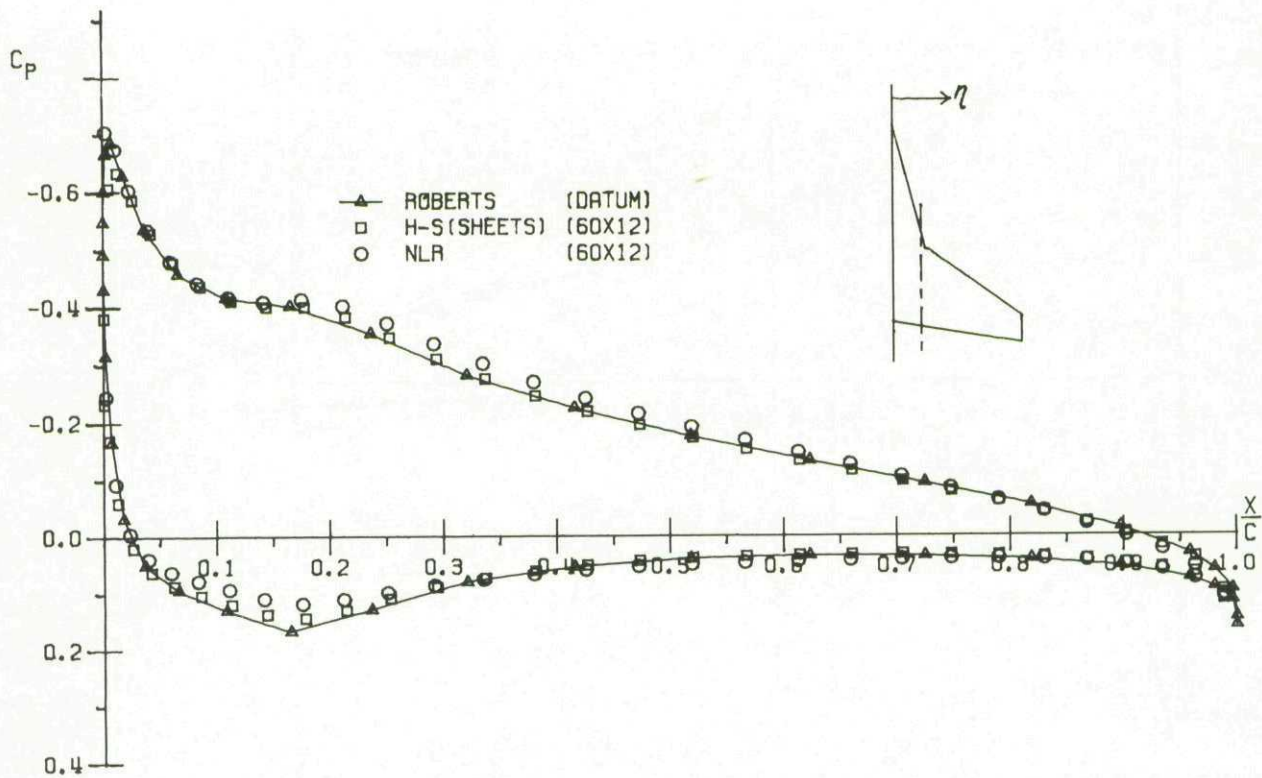


FIG. 55 FIRST ORDER METHOD COMPARISON
CHORDWISE PRESSURE DISTRIBUTION
STRAKED WING . T/C = .05 . $\alpha = 5.0$. $\eta = .219$

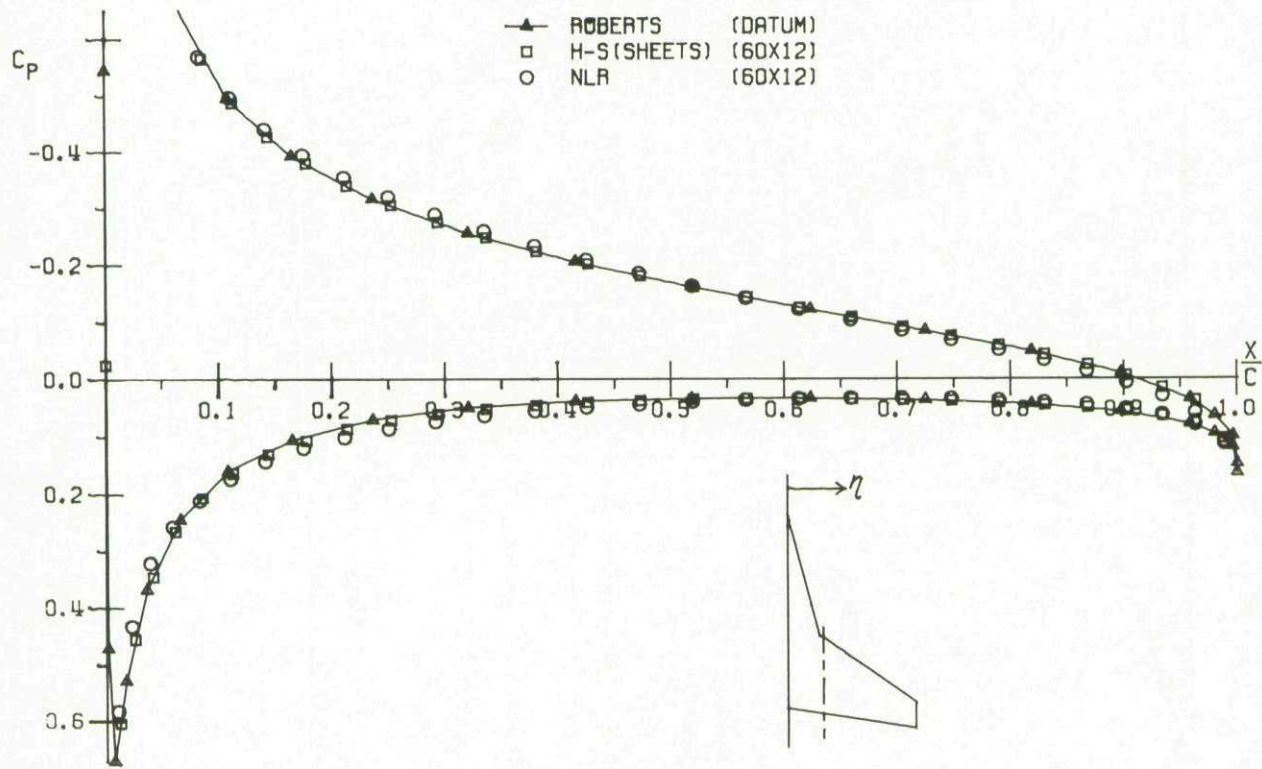


FIG. 56 FIRST ORDER METHOD COMPARISON
CHORDWISE PRESSURE DISTRIBUTION
STRAKED WING . T/C = .05 . $\alpha = 5.0$. $\eta = .280$

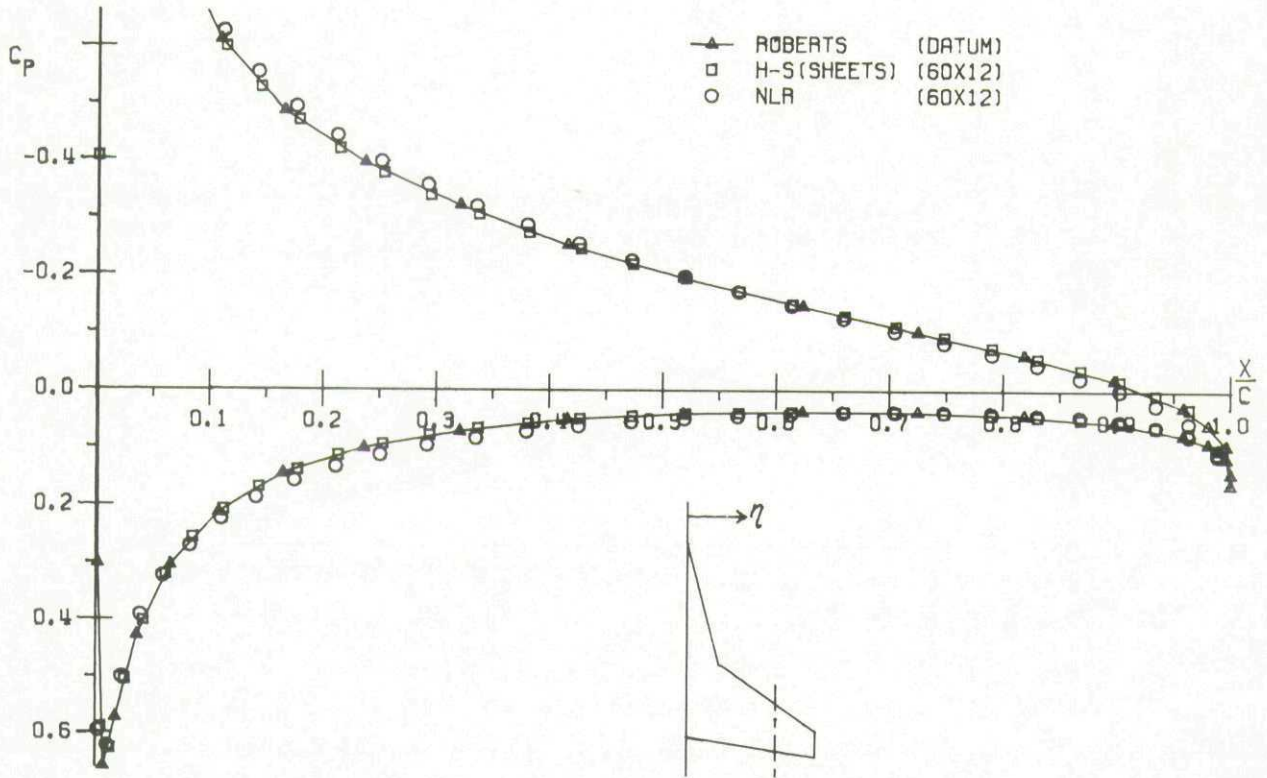


FIG. 57 FIRST ORDER METHOD COMPARISON
CHORDWISE PRESSURE DISTRIBUTION
STRAKED WING . T/C = .05 . α = 5.0 . η = .693

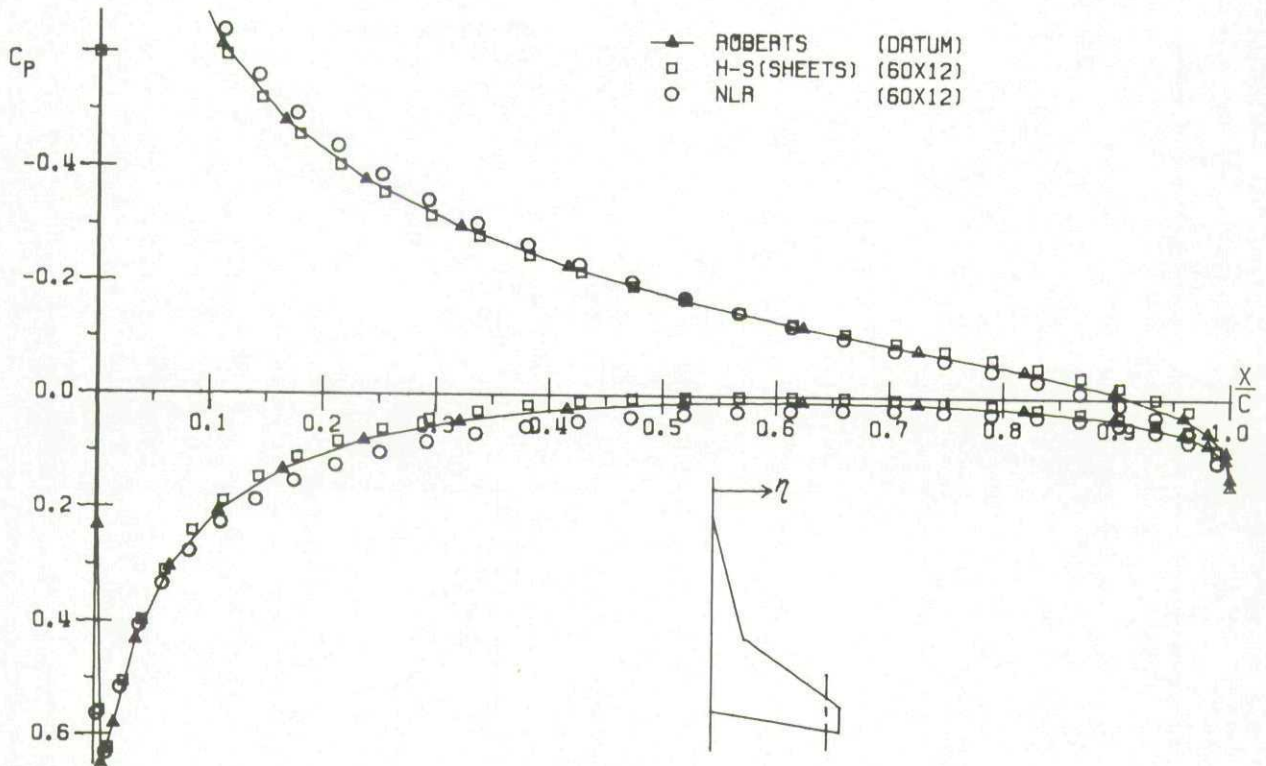


FIG. 58 FIRST ORDER METHOD COMPARISON
CHORDWISE PRESSURE DISTRIBUTION
STRAKED WING . T/C = .05 . α = 5.0 . η = .899

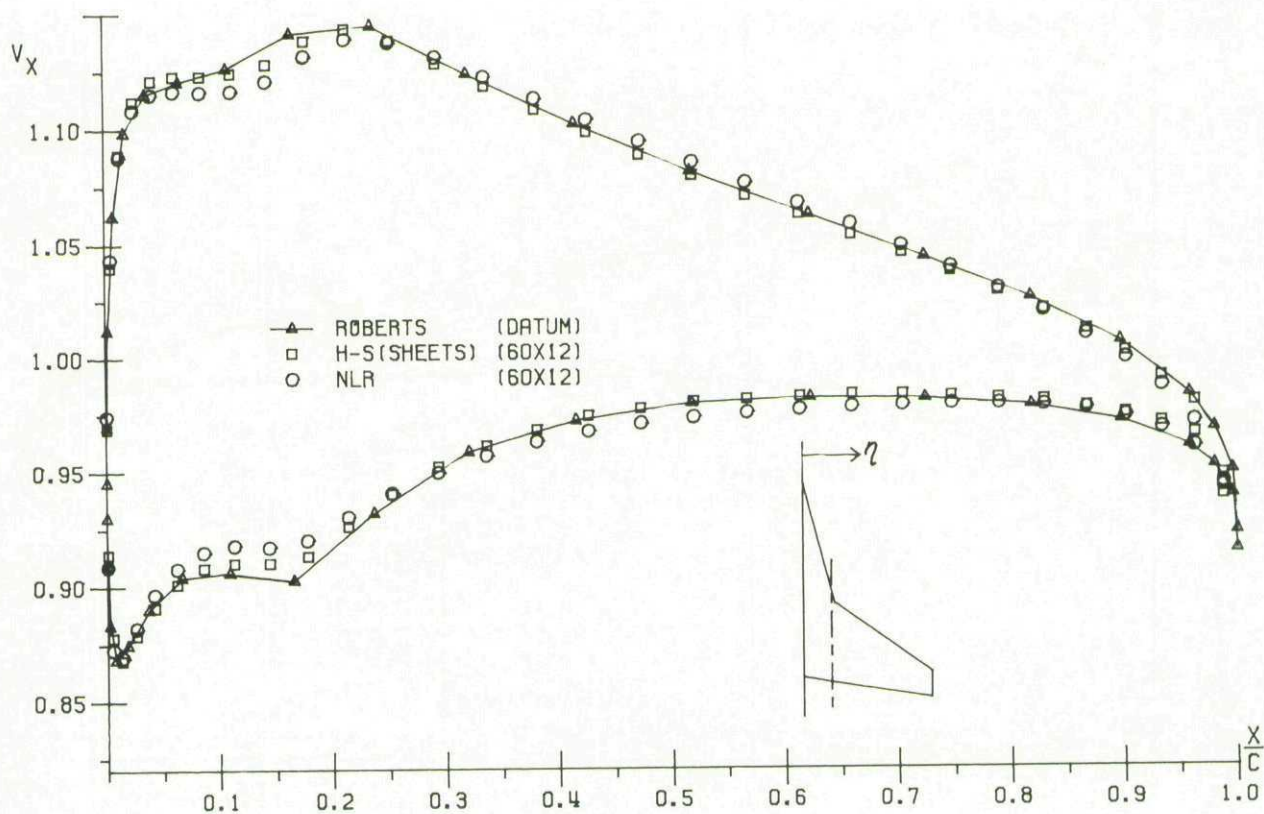


FIG. 59 FIRST ORDER METHOD COMPARISON
 X-COMPONENT OF VELOCITY
 STRAKED WING, $T/C = .05$, $\alpha = 5.0$, $\eta = .219$

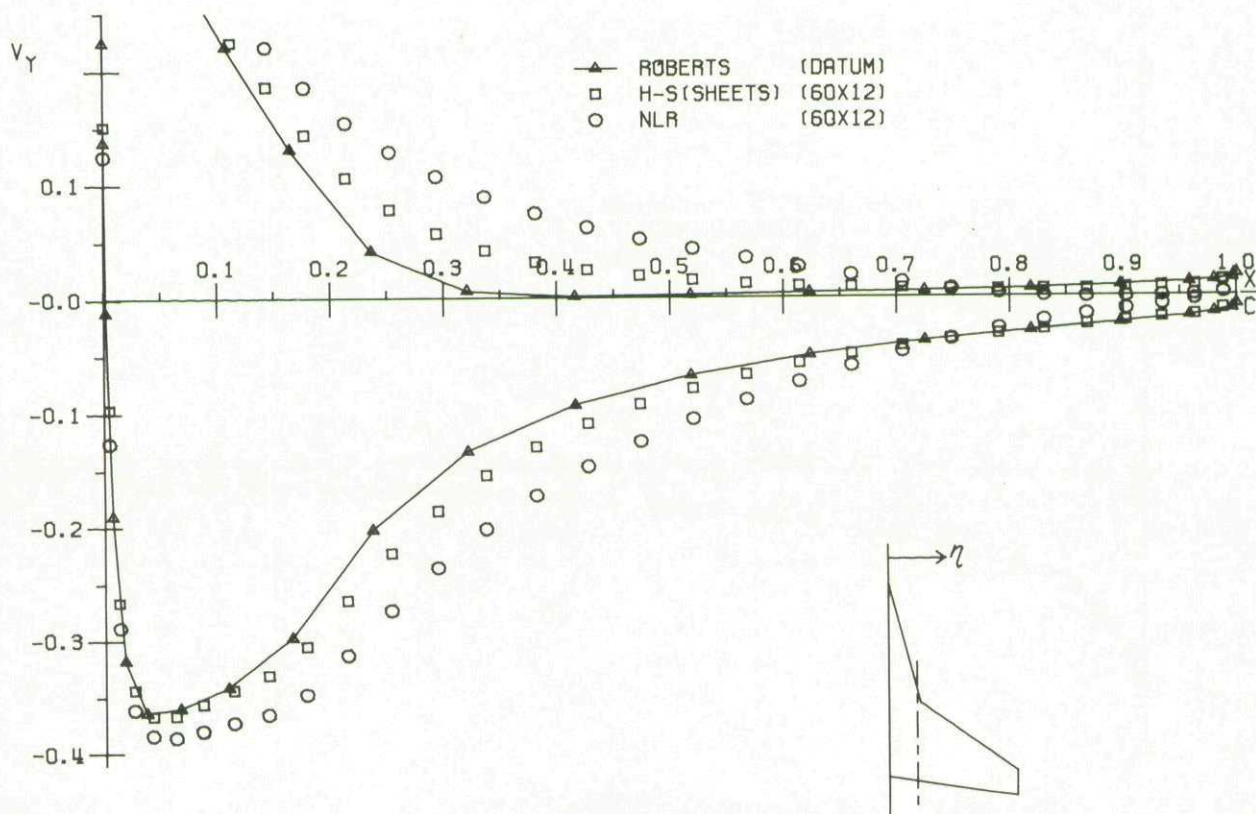


FIG. 60 FIRST ORDER METHOD COMPARISON
 Y-COMPONENT OF VELOCITY
 STRAKED WING, $T/C = .05$, $\alpha = 5.0$, $\eta = .219$

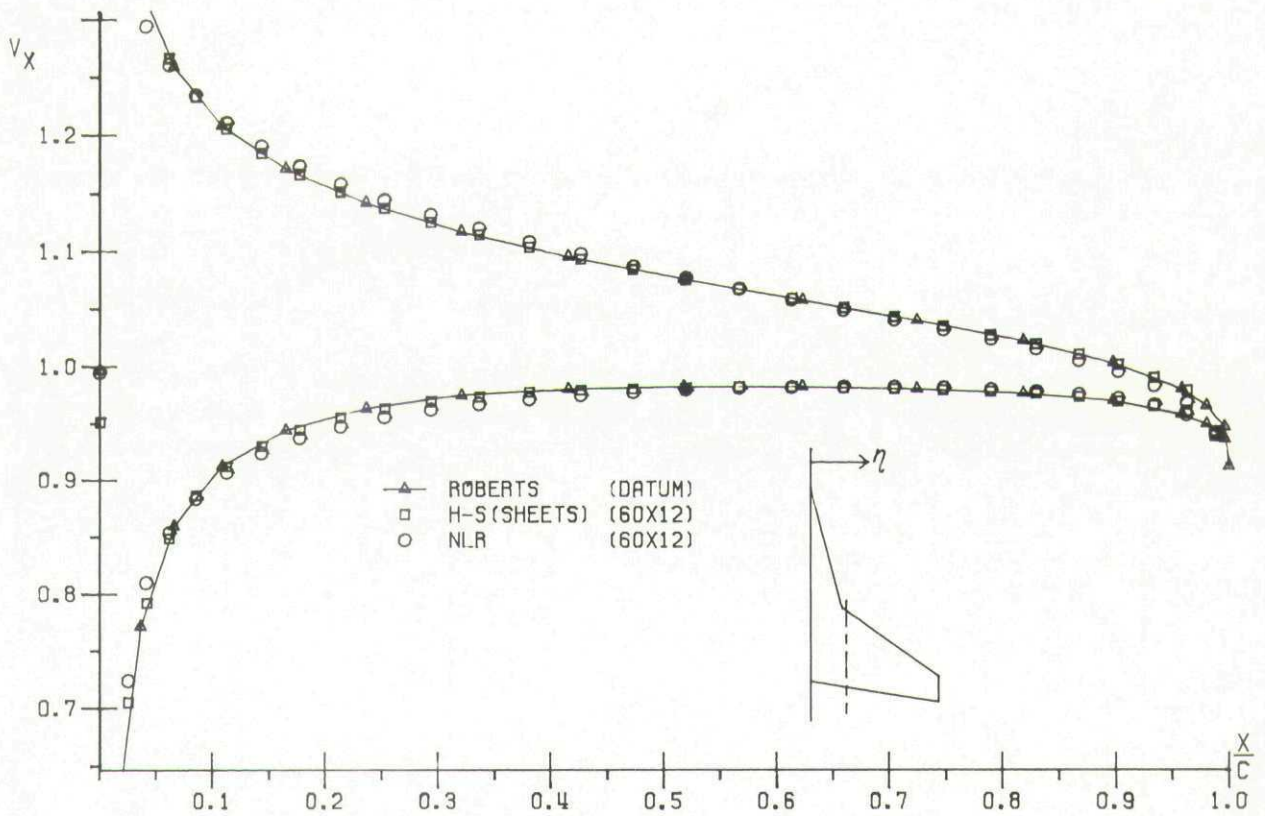


FIG. 61 FIRST ORDER METHOD COMPARISON
X-COMPONENT OF VELOCITY
STRAKED WING, T/C = .05 , $\alpha = 5.0$, $\eta = .280$

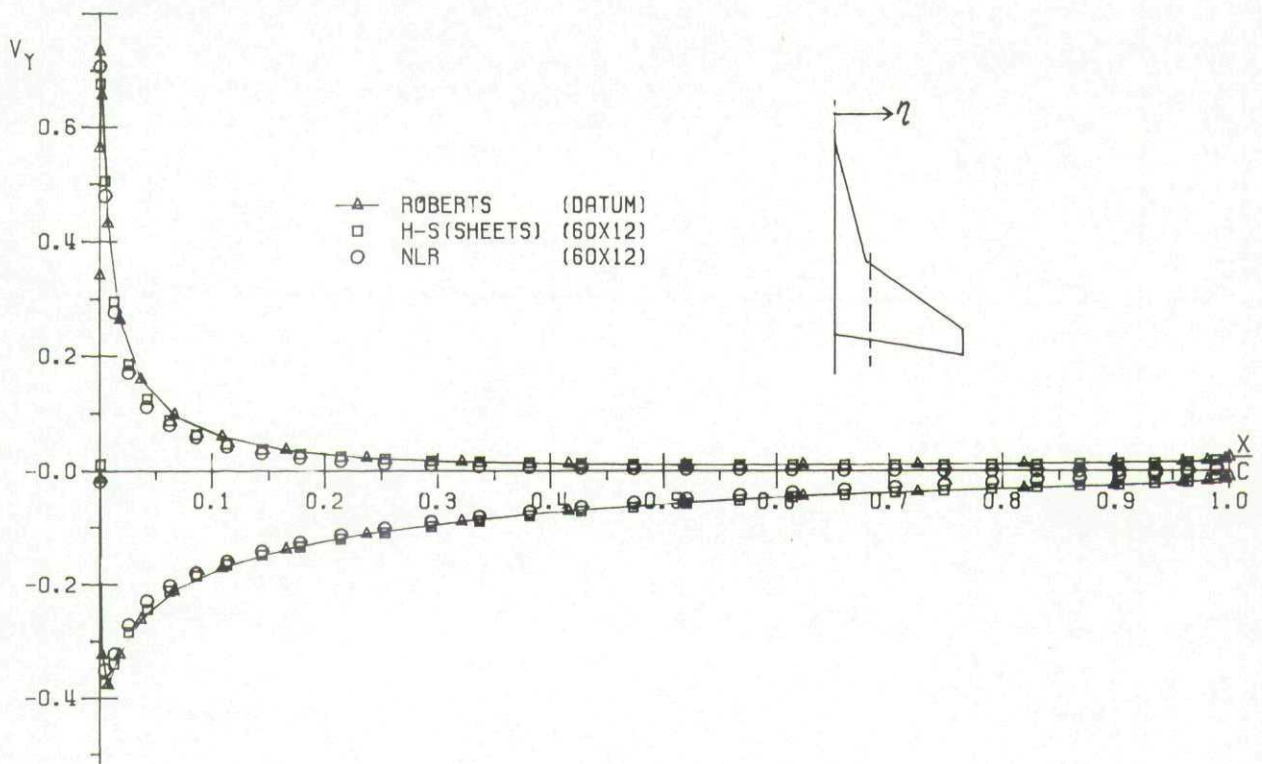


FIG. 62 FIRST ORDER METHOD COMPARISON
Y-COMPONENT OF VELOCITY
STRAKED WING, T/C = .05 , $\alpha = 5.0$, $\eta = .280$

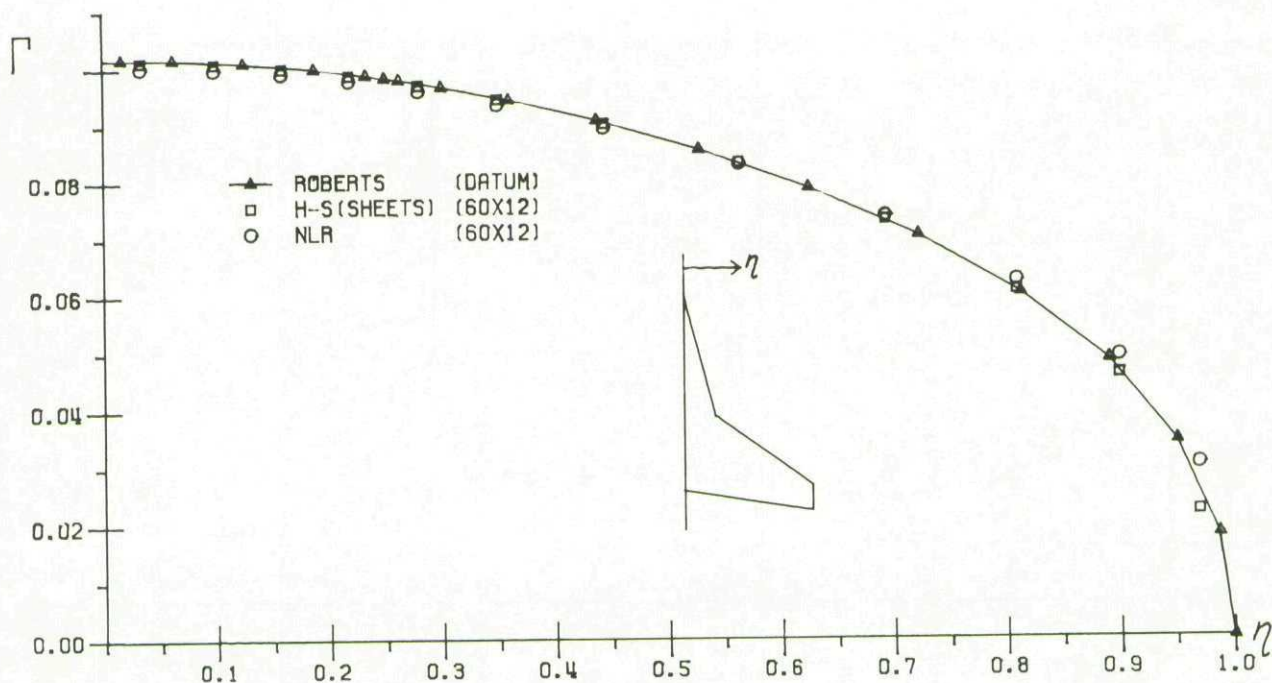


FIG. 63 FIRST ORDER METHOD COMPARISON
CIRCULATION
STRAKED WING, T/C = .05, α = 5.0

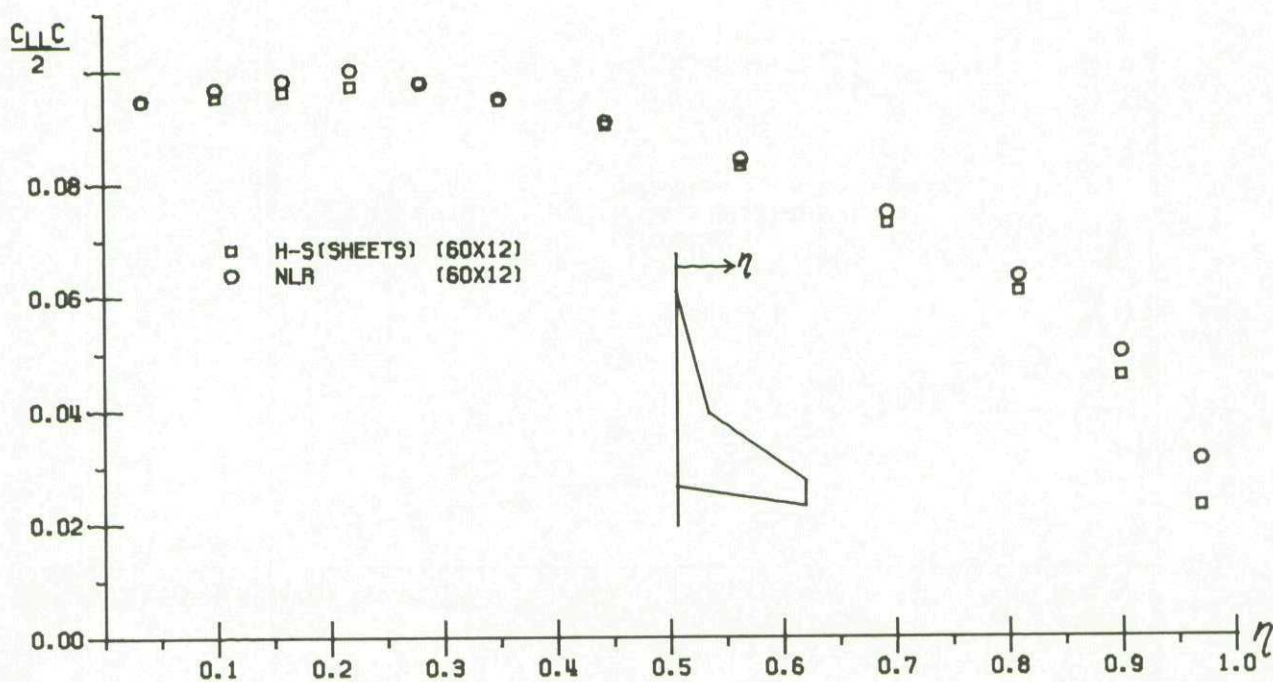


FIG. 64 FIRST ORDER METHOD COMPARISON
SECTIONAL LOAD
STRAKED WING, T/C = .05, α = 5.0

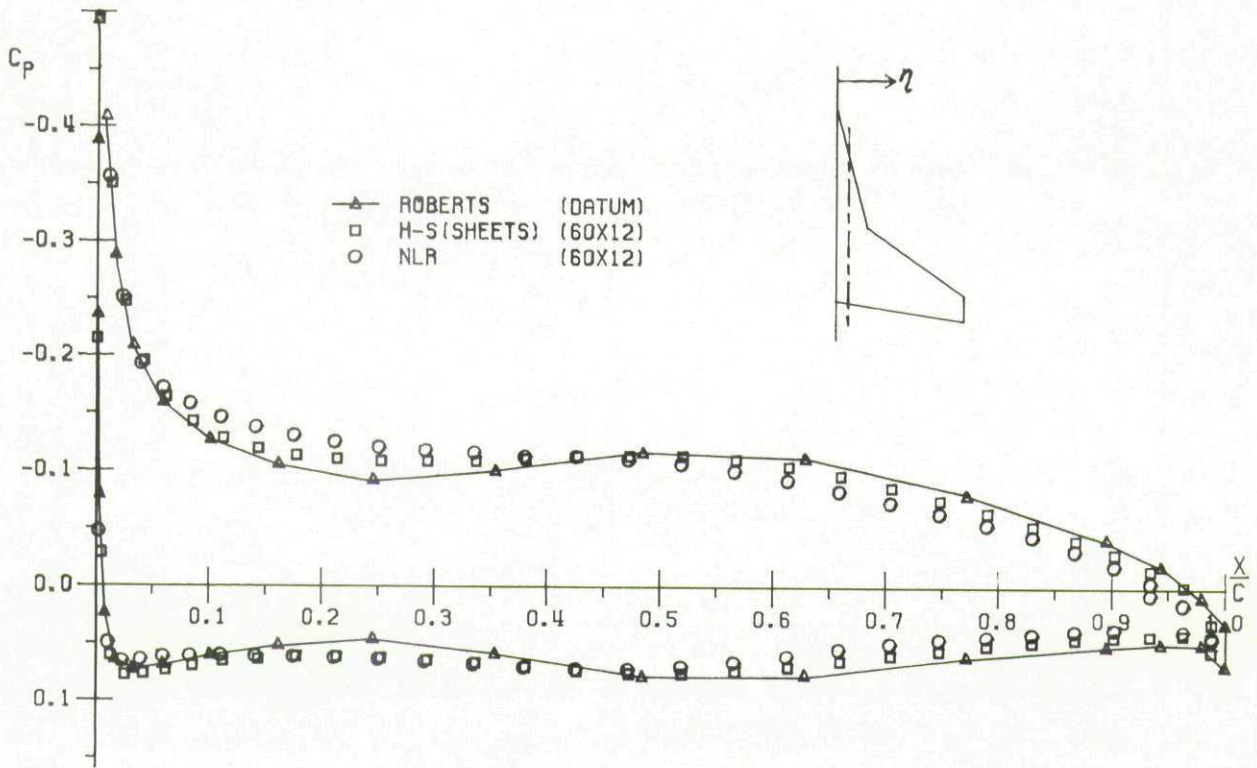


FIG. 65 FIRST ORDER METHOD COMPARISON
CHORDWISE PRESSURE DISTRIBUTION
STAKED WING, $T/C = .02$, $\alpha = 5.0$, $\eta = .099$

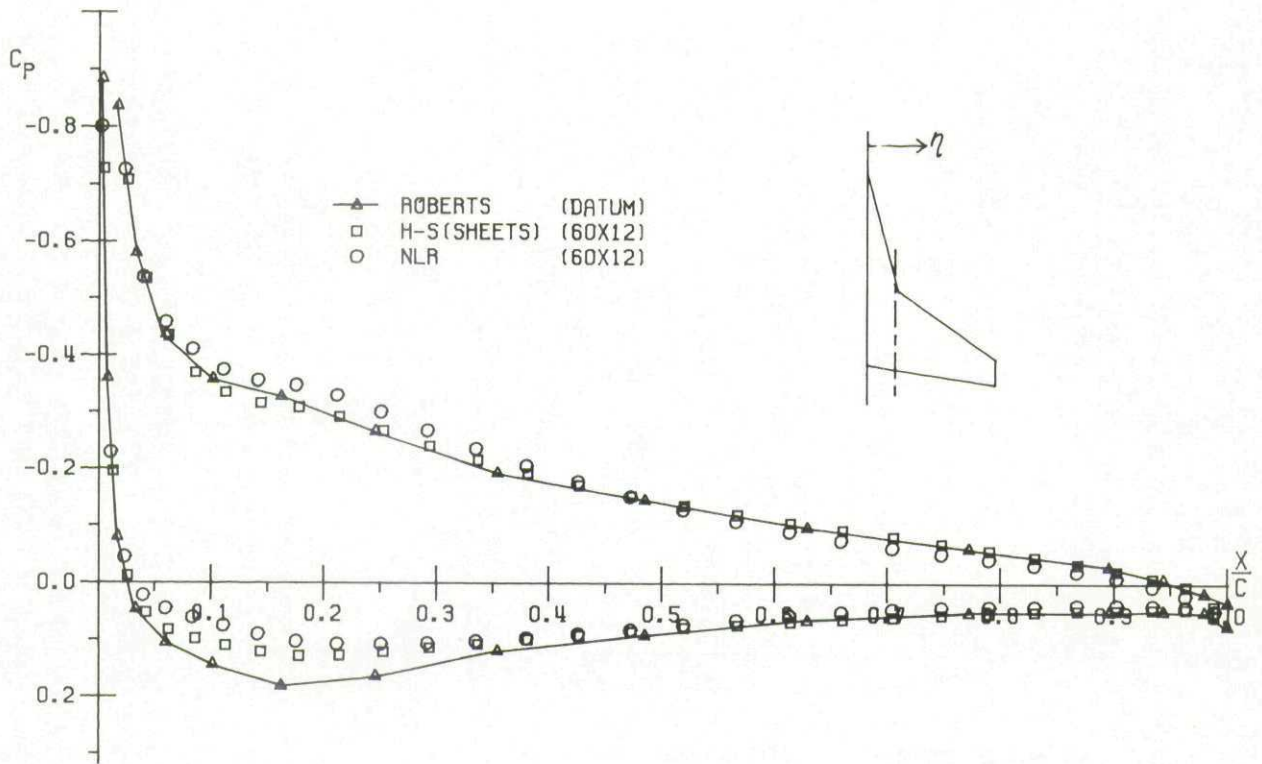


FIG. 66 FIRST ORDER METHOD COMPARISON
CHORDWISE PRESSURE DISTRIBUTION
STAKED WING, $T/C = .02$, $\alpha = 5.0$, $\eta = .219$

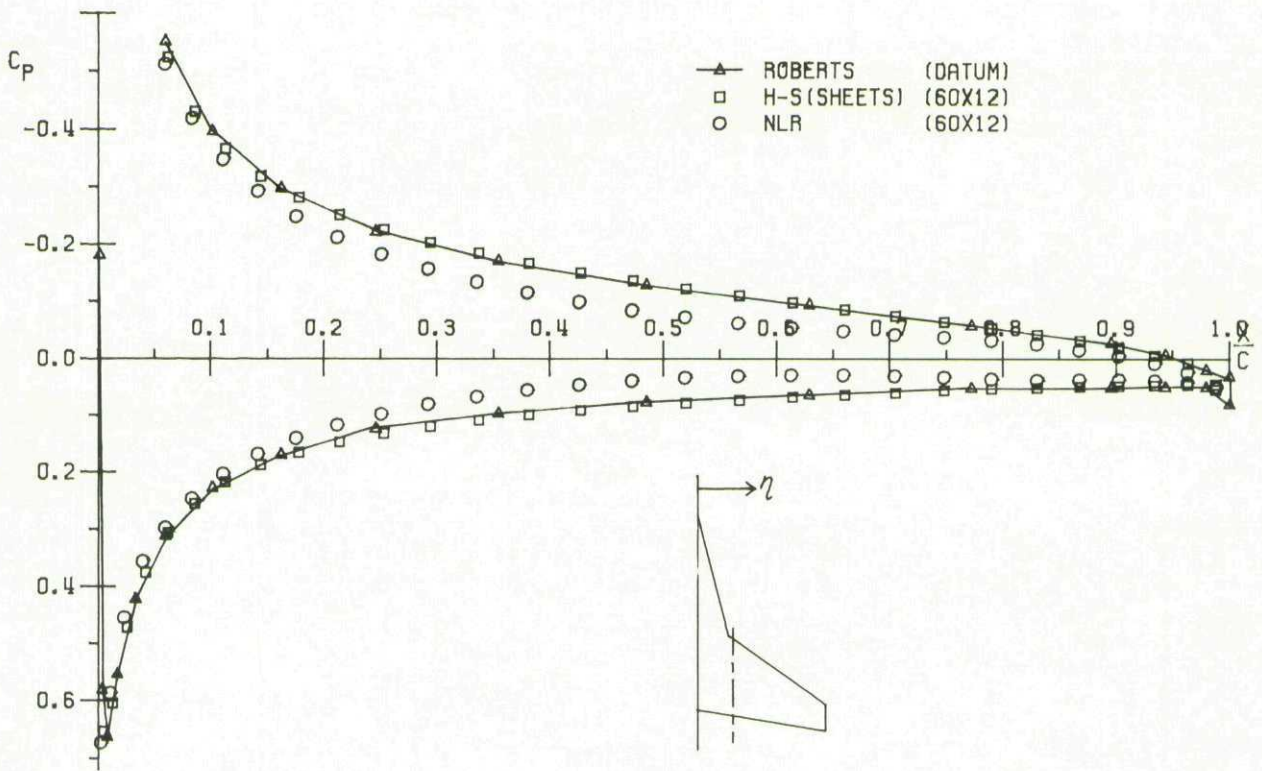


FIG. 67 FIRST ORDER METHOD COMPARISON
 CHORDWISE PRESSURE DISTRIBUTION
 STRAKED WING, $T/C = .02$, $\alpha = 5.0$, $\eta = .280$

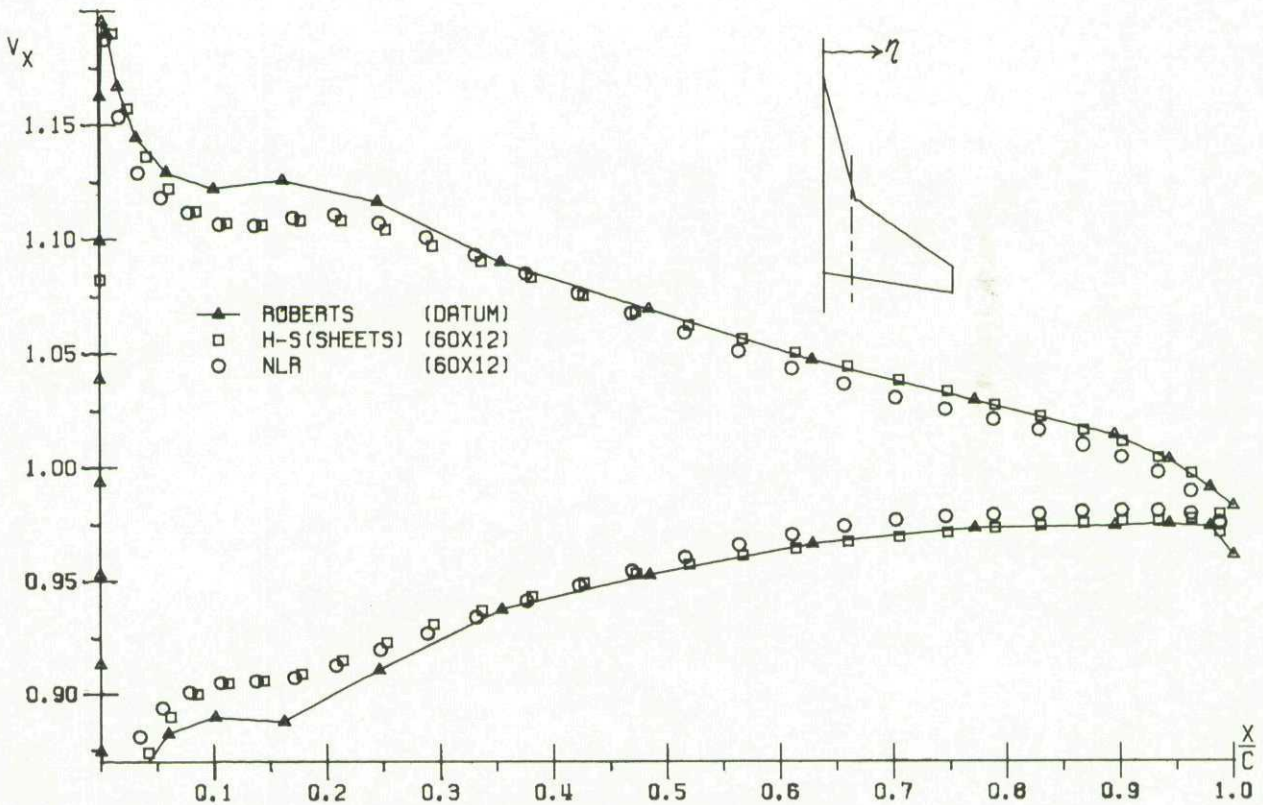


FIG. 68 FIRST ORDER METHOD COMPARISON
 X-COMPONENT OF VELOCITY
 STRAKED WING, $T/C = .02$, $\alpha = 5.0$, $\eta = .219$

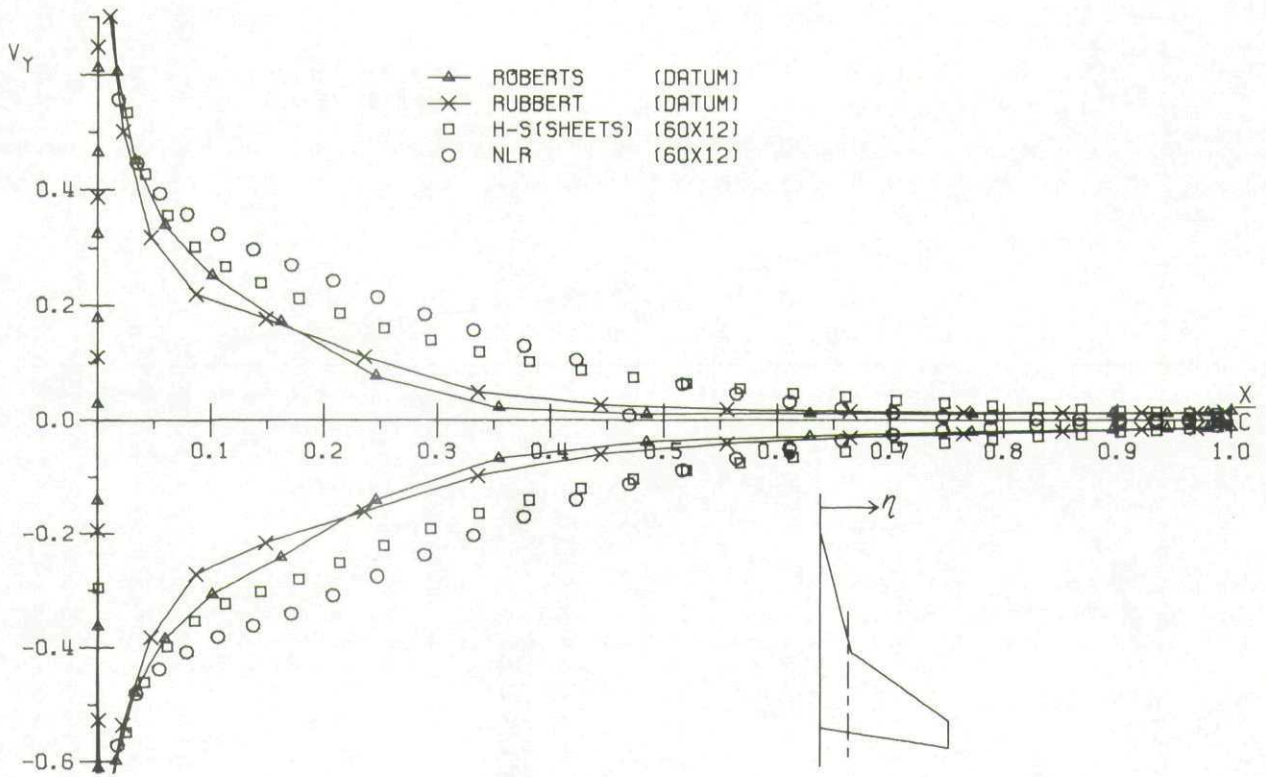


FIG. 69 FIRST ORDER METHOD COMPARISON
 Y-COMPONENT OF VELOCITY
 STRAKED WING . T/C = .02 . $\alpha = 5.0$. $\eta = .219$

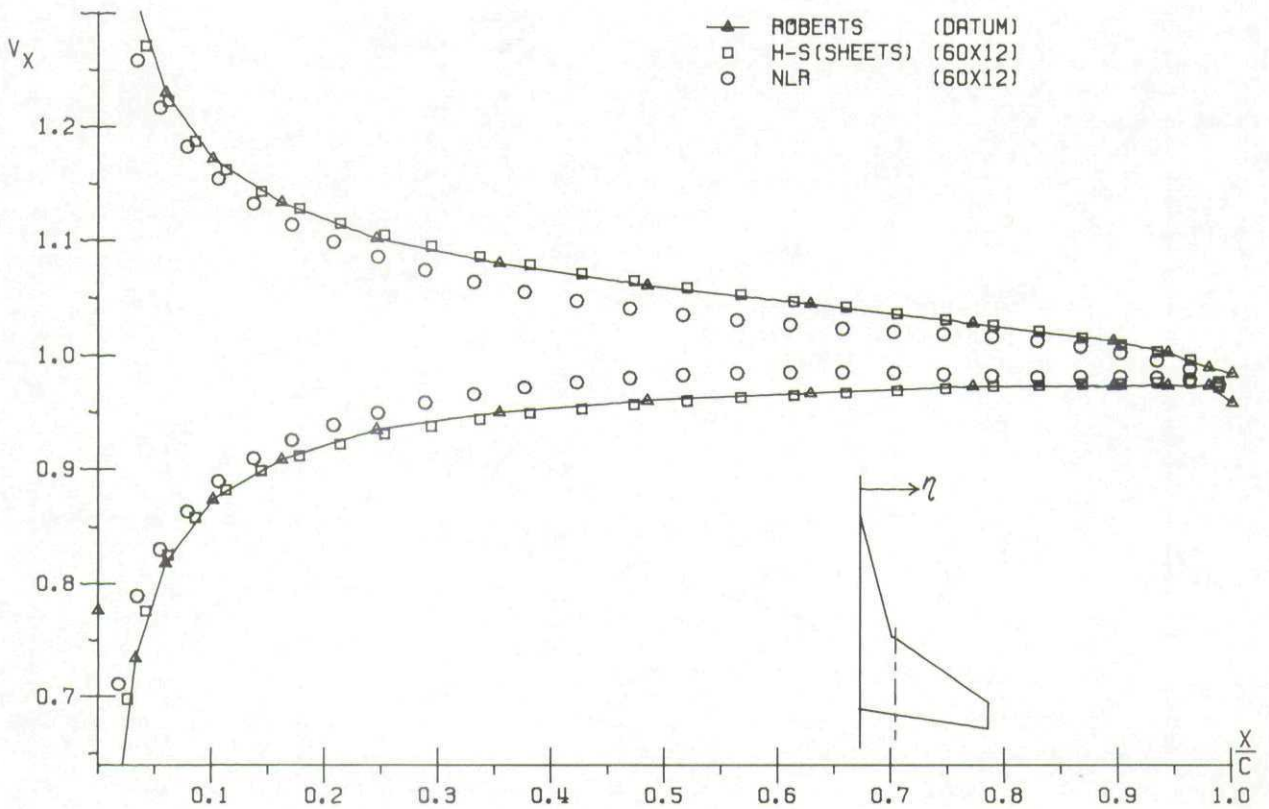


FIG. 70 FIRST ORDER METHOD COMPARISON
 X-COMPONENT OF VELOCITY
 STRAKED WING . T/C = .02 . $\alpha = 5.0$. $\eta = .280$

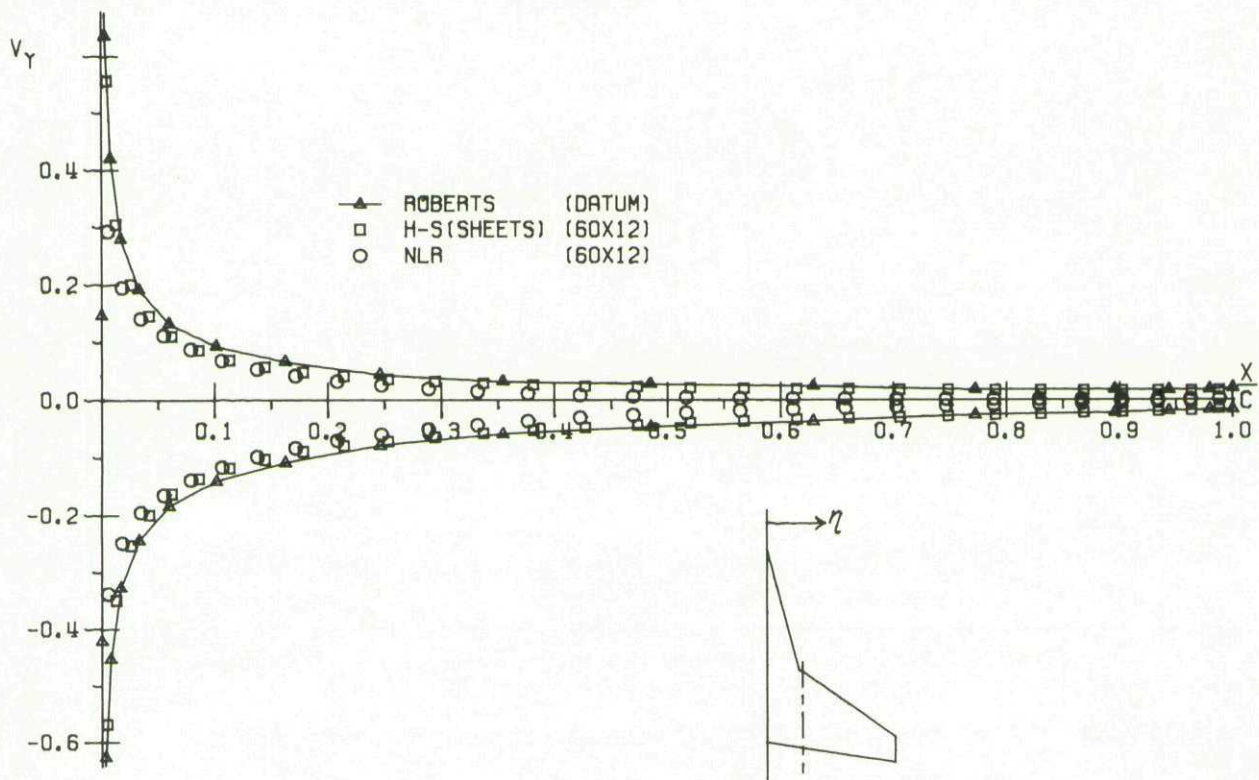


FIG. 71 FIRST ORDER METHOD COMPARISON
 Y-COMPONENT OF VELOCITY
 STRAKED WING, $T/C = .02$, $\alpha = 5.0$, $\eta = .280$

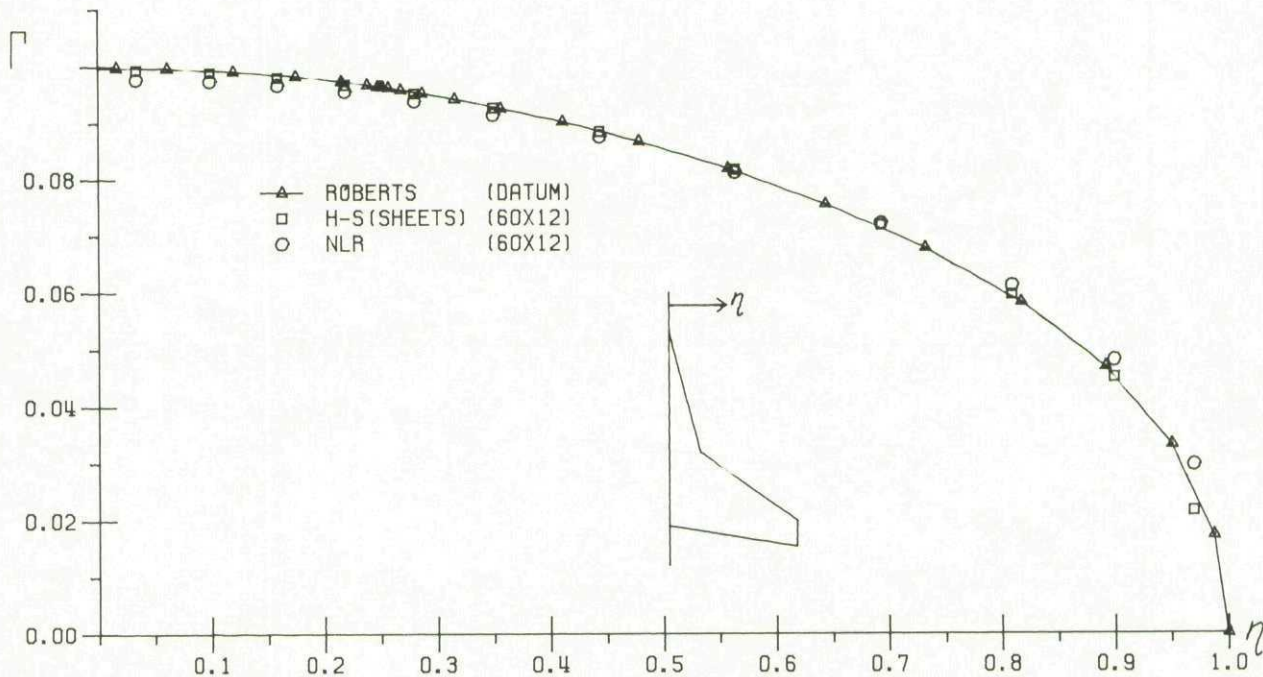


FIG. 72 FIRST ORDER METHOD COMPARISON
 CIRCULATION
 STRAKED WING, $T/C = .02$, $\alpha = 5.0$

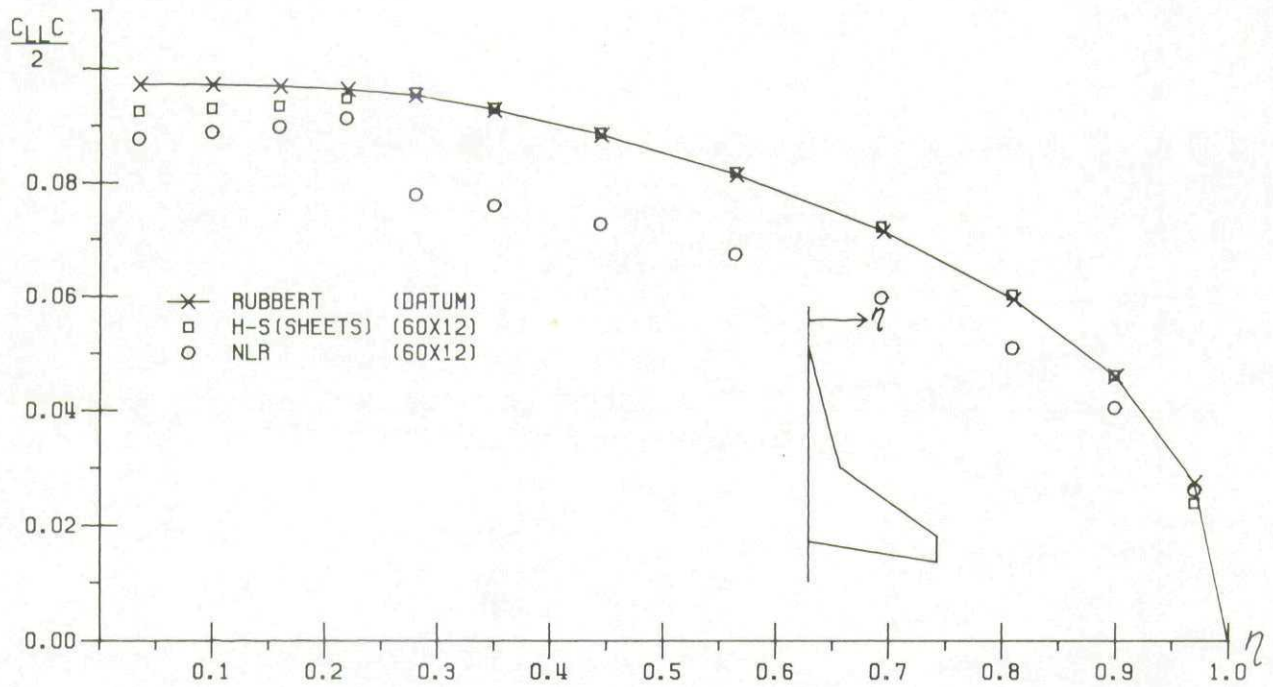


FIG. 73 FIRST ORDER METHOD COMPARISON
SECTIONAL LOAD
STRAKED WING, T/C = .02, $\alpha = 5.0$

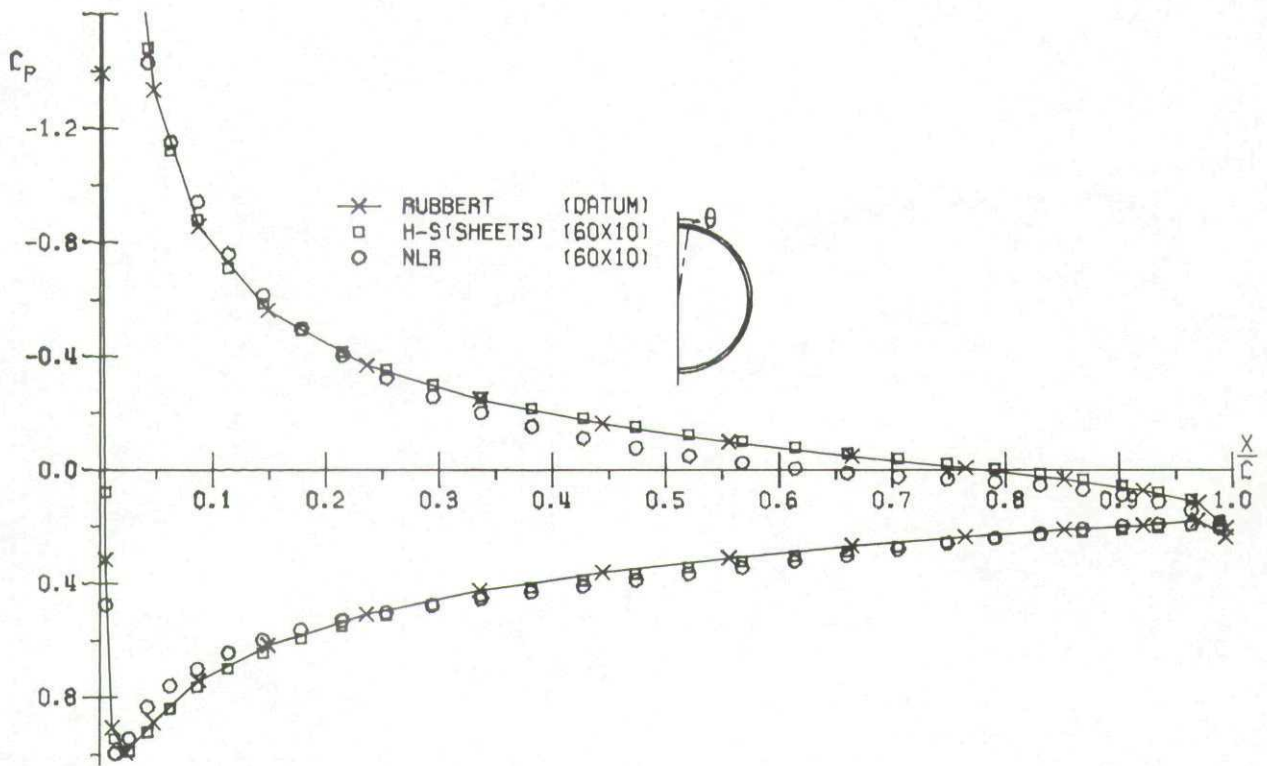


FIG. 74 FIRST ORDER METHOD COMPARISON
CHORDWISE PRESSURE DISTRIBUTION
NACELLE, C/DE = 1.000, $\alpha = 5.0$, $\theta = 9.000$

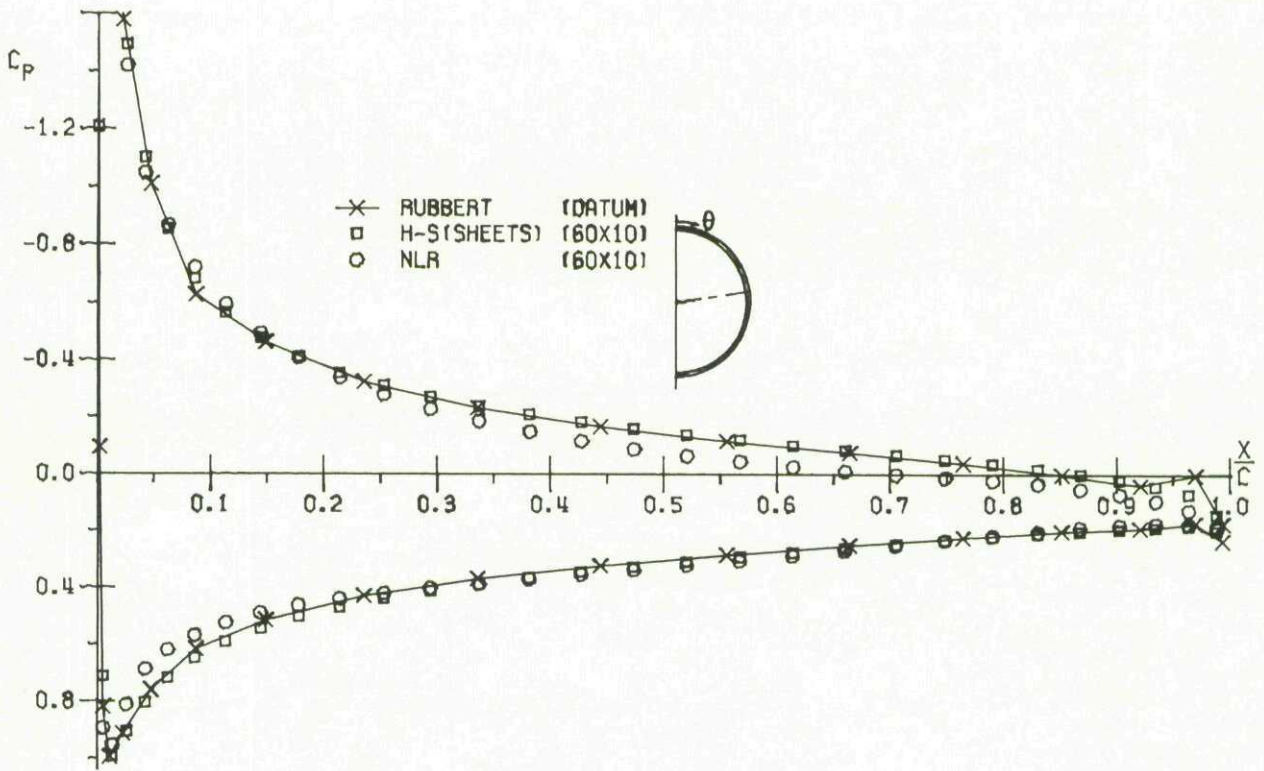


FIG. 75 FIRST ORDER METHOD COMPARISON
CHORDWISE PRESSURE DISTRIBUTION
NACELLE . $C/DE=1.0000$. $\alpha = 5.0$. $\theta = 81.000$

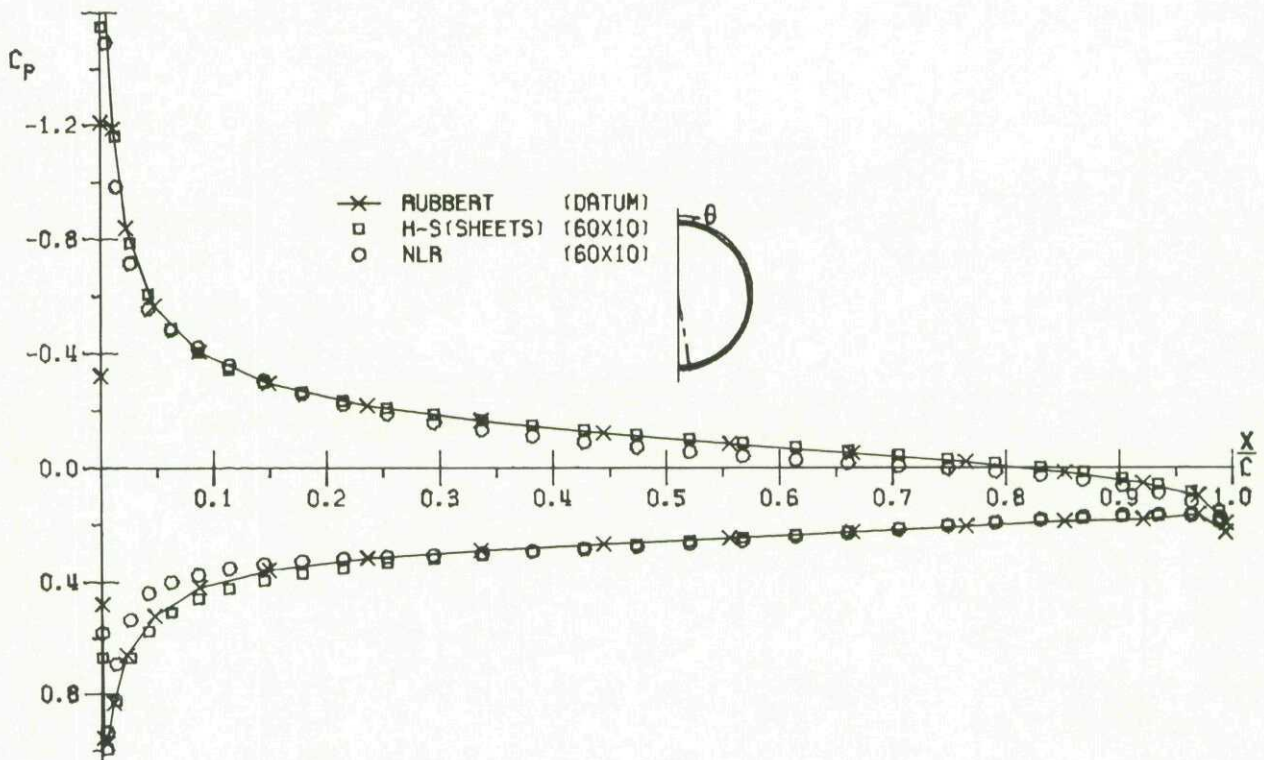


FIG. 76 FIRST ORDER METHOD COMPARISON
CHORDWISE PRESSURE DISTRIBUTION
NACELLE . $C/DE=1.0000$. $\alpha = 5.0$. $\theta = 171.000$

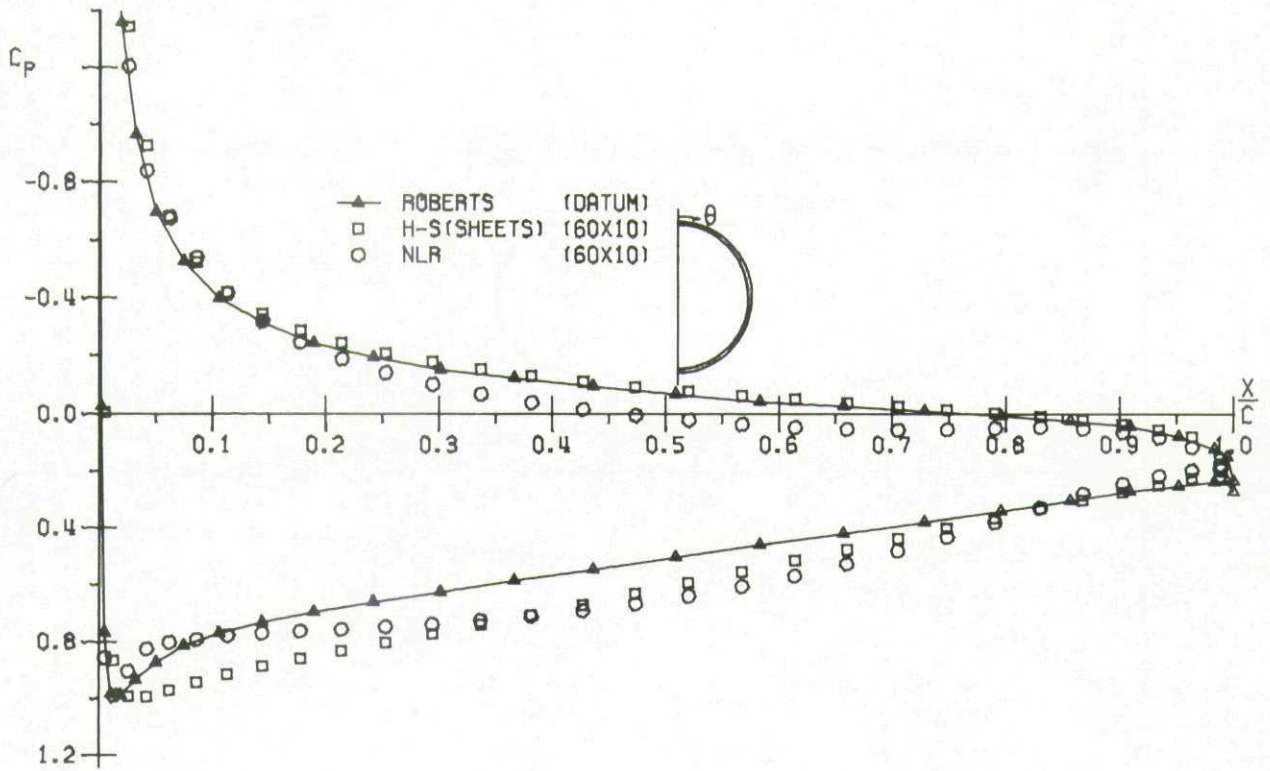


FIG. 77 FIRST ORDER METHOD COMPARISON
 CHORDWISE PRESSURE DISTRIBUTION
 NACELLE $C/DE = 3.3333$ $\alpha = 0.0$ $\theta = 0.000$

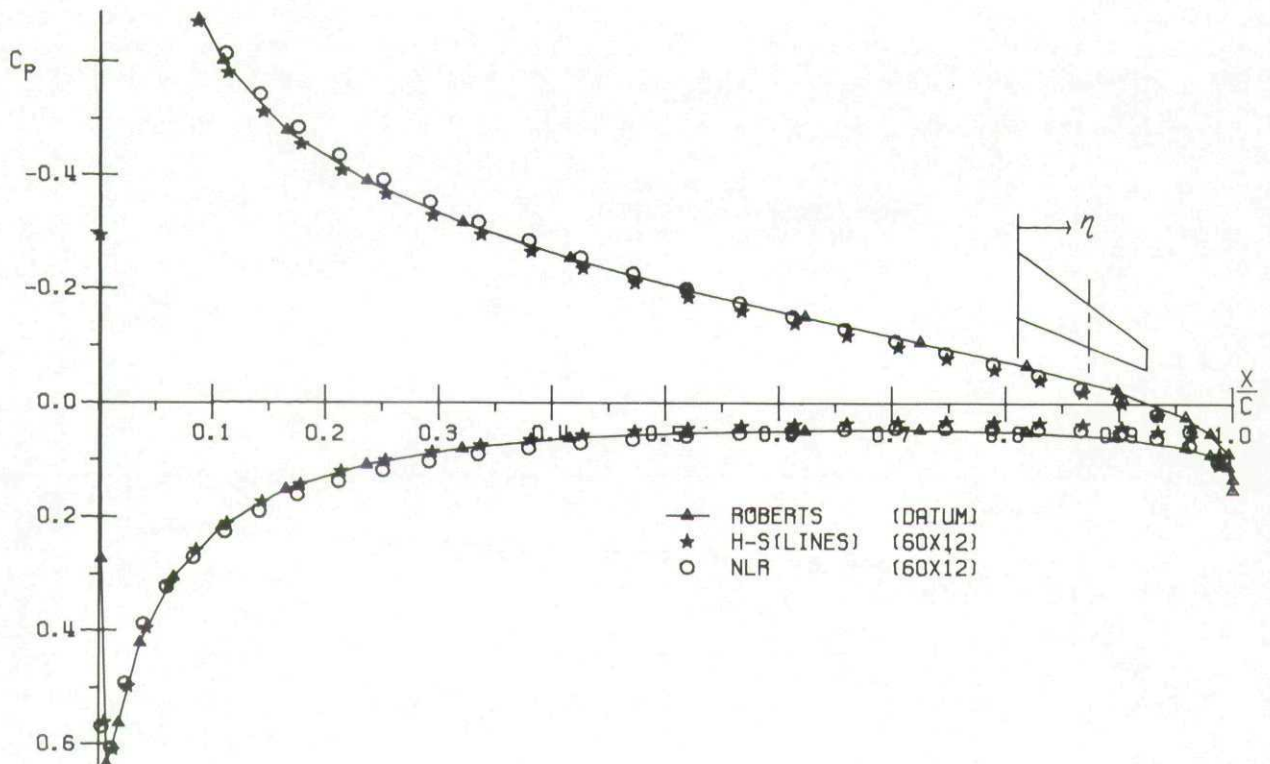


FIG. 78 FIRST ORDER METHOD COMPARISON
 CHORDWISE PRESSURE DISTRIBUTION
 RAE WING $T/C = .05$ $\alpha = 5.0$ $\eta = .549$

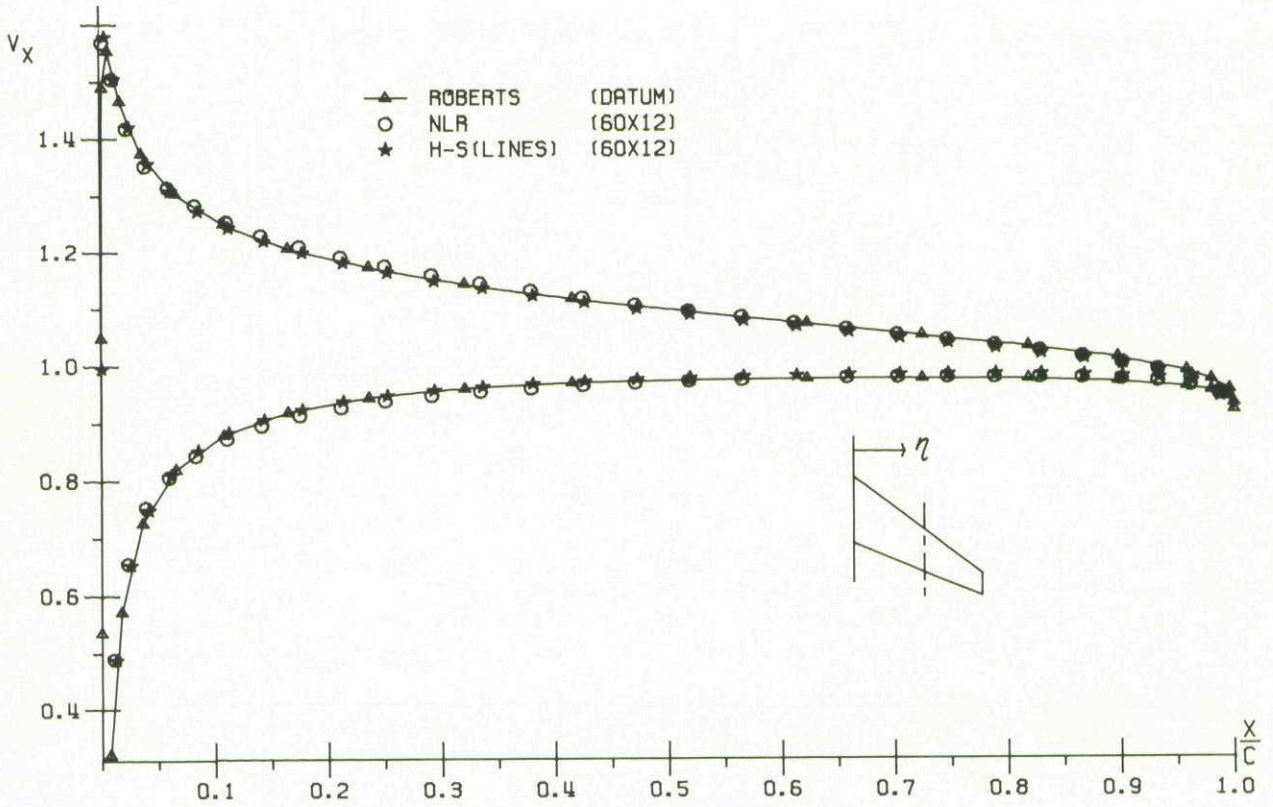


FIG. 79 FIRST ORDER METHOD COMPARISON
X-COMPONENT OF VELOCITY
RAE WING . $T/C = .05$. $\alpha = 5.0$. $\eta = .549$

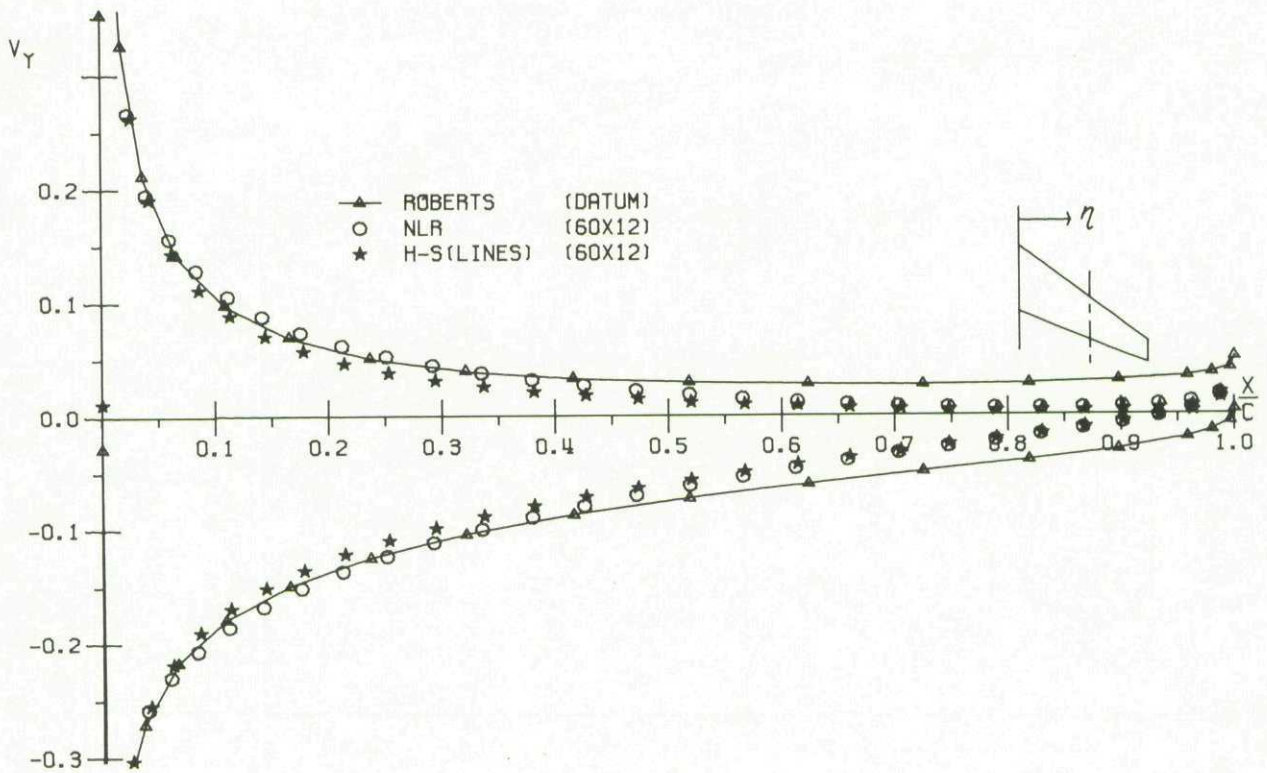


FIG. 80 FIRST ORDER METHOD COMPARISON
Y-COMPONENT OF VELOCITY
RAE WING . $T/C = .05$. $\alpha = 5.0$. $\eta = .549$

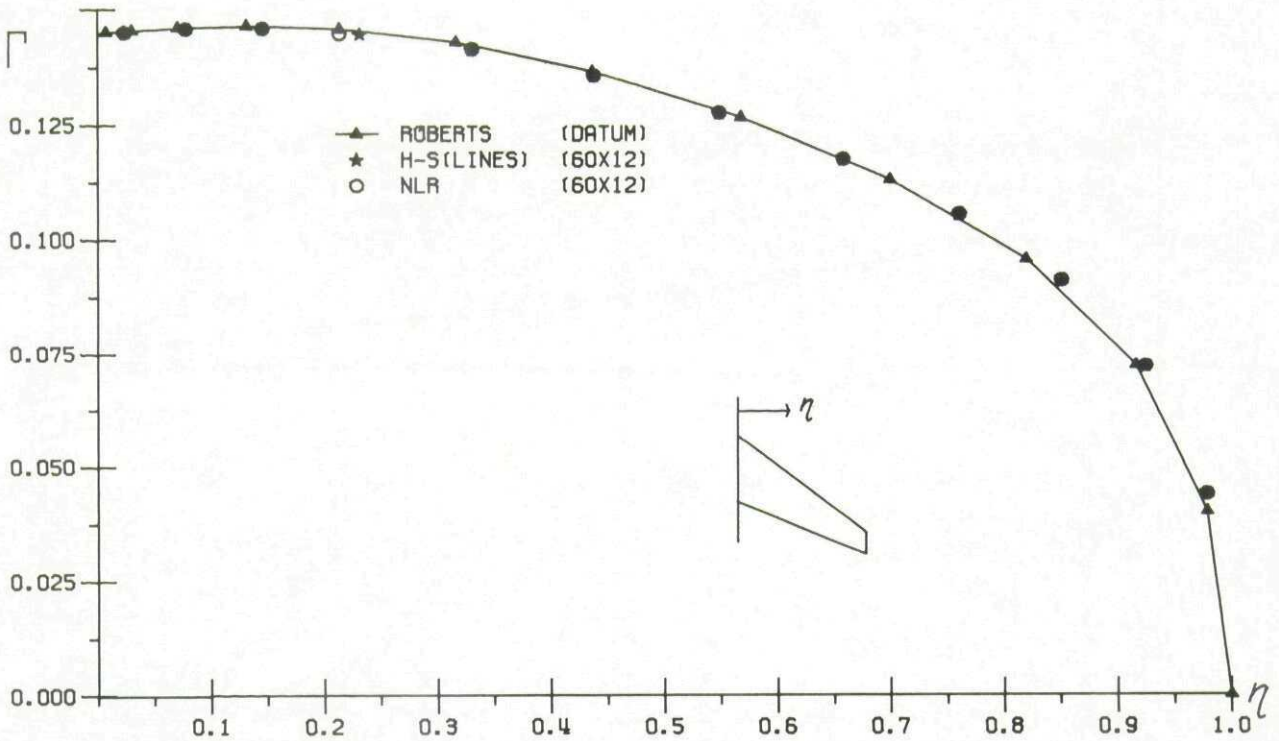


FIG. 81 FIRST ORDER METHOD COMPARISON
CIRCULATION
RAE WING . T/C = .05 . $\alpha = 5.0$

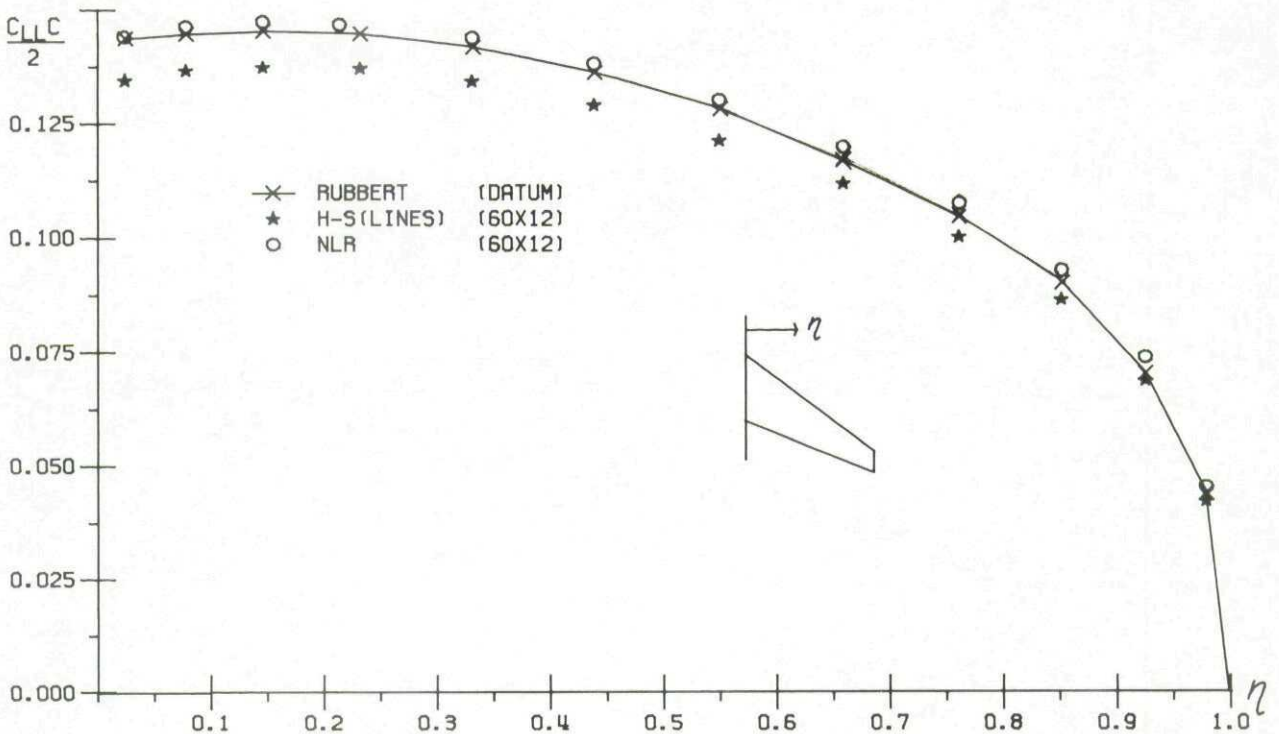


FIG. 82 FIRST ORDER METHOD COMPARISON
SECTIONAL LOAD
RAE WING . T/C = .05 . $\alpha = 5.0$

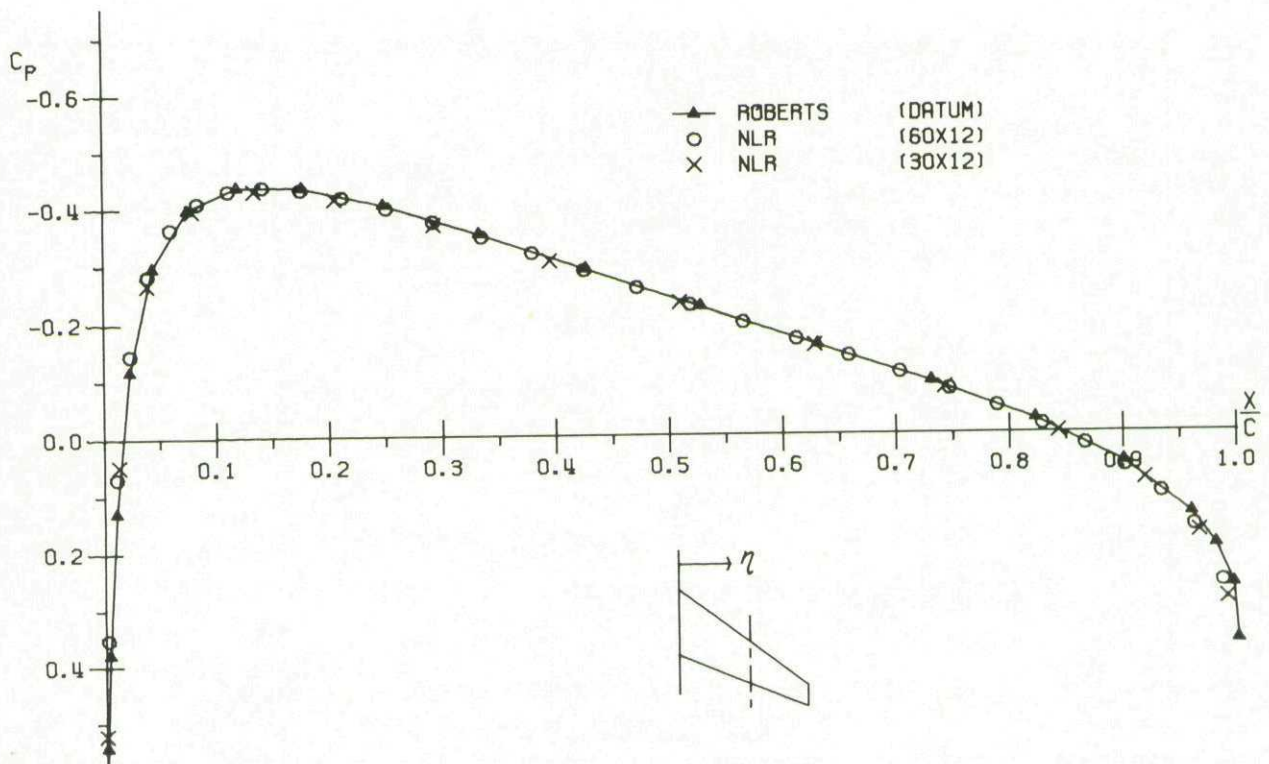


FIG. 83 CONVERGENCE STUDY
 CHORDWISE PRESSURE DISTRIBUTION
 RAE WING . $T/C = .15$. $\alpha = 0.0$. $\eta = .549$

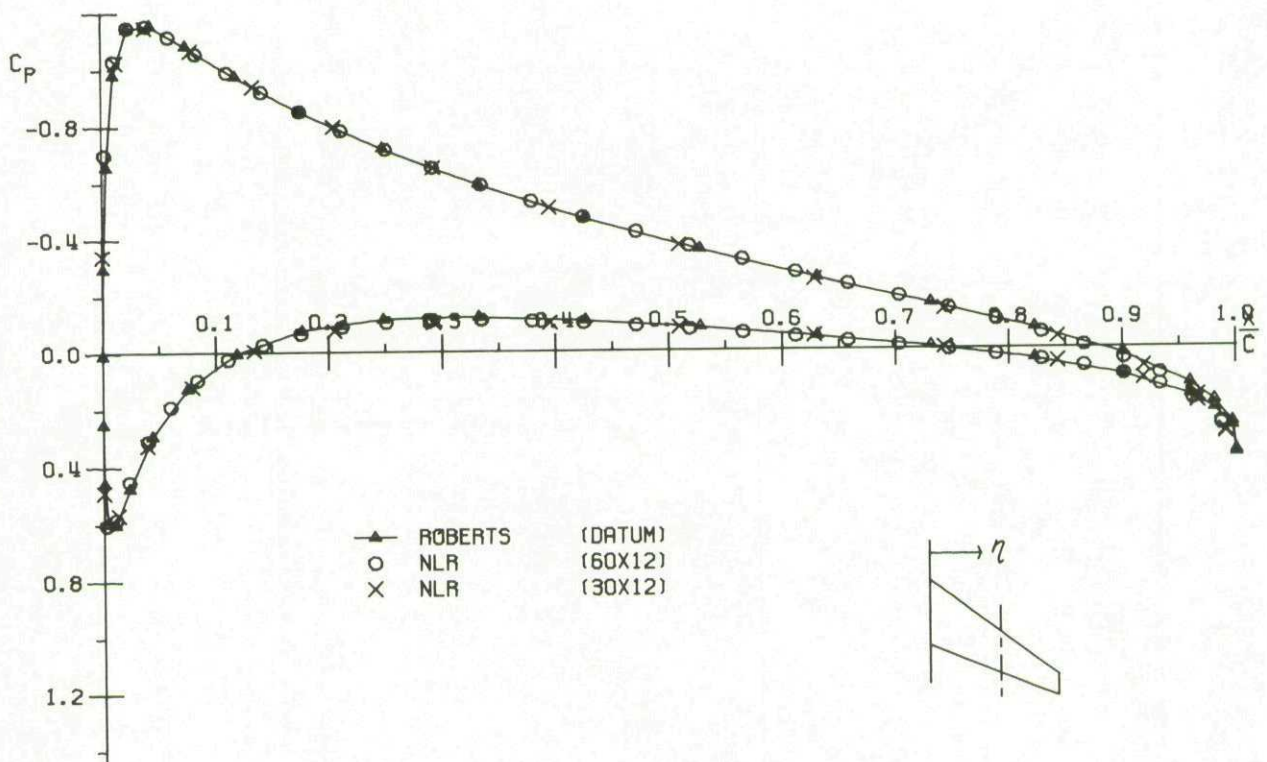


FIG. 84 CONVERGENCE STUDY
 CHORDWISE PRESSURE DISTRIBUTION
 RAE WING . $T/C = .15$. $\alpha = 5.0$. $\eta = .549$

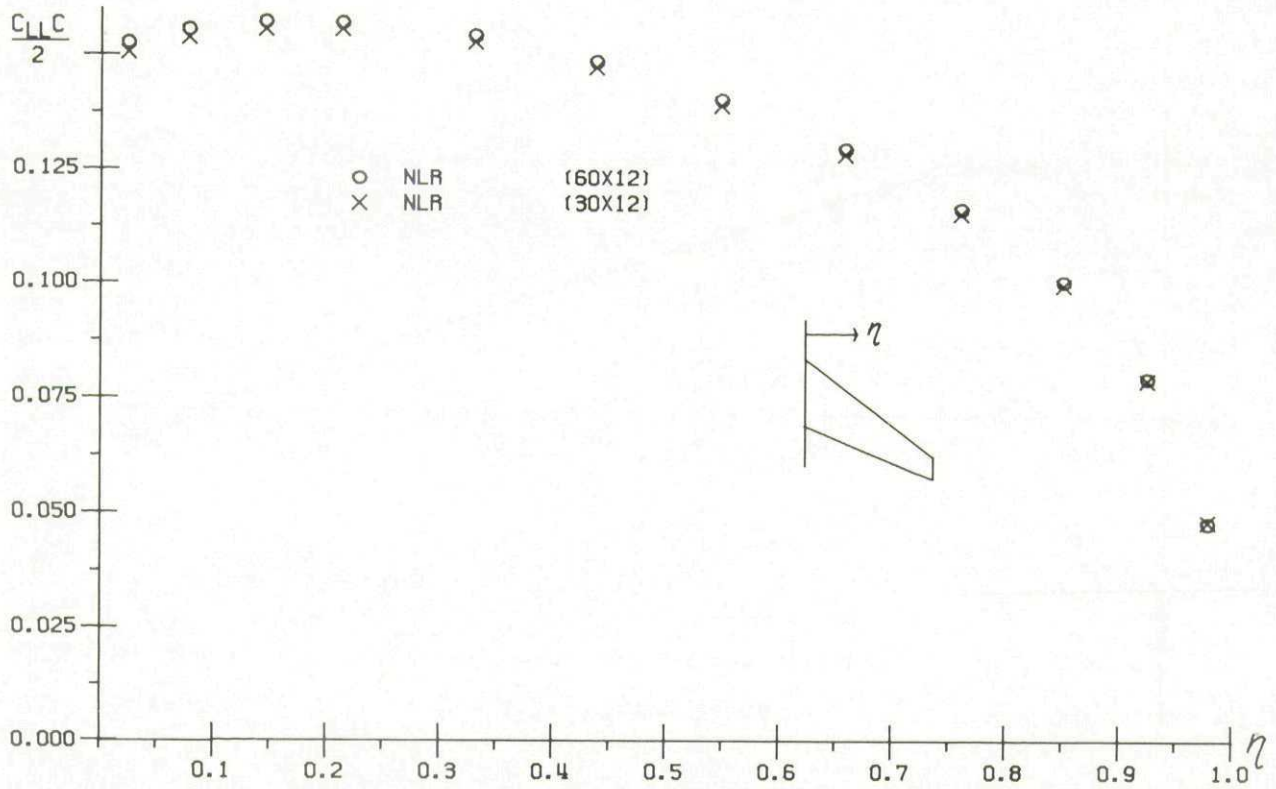


FIG. 85 CONVERGENCE STUDY
SECTIONAL LOAD
RAE WING . T/C = .15 . $\alpha = 5.0$

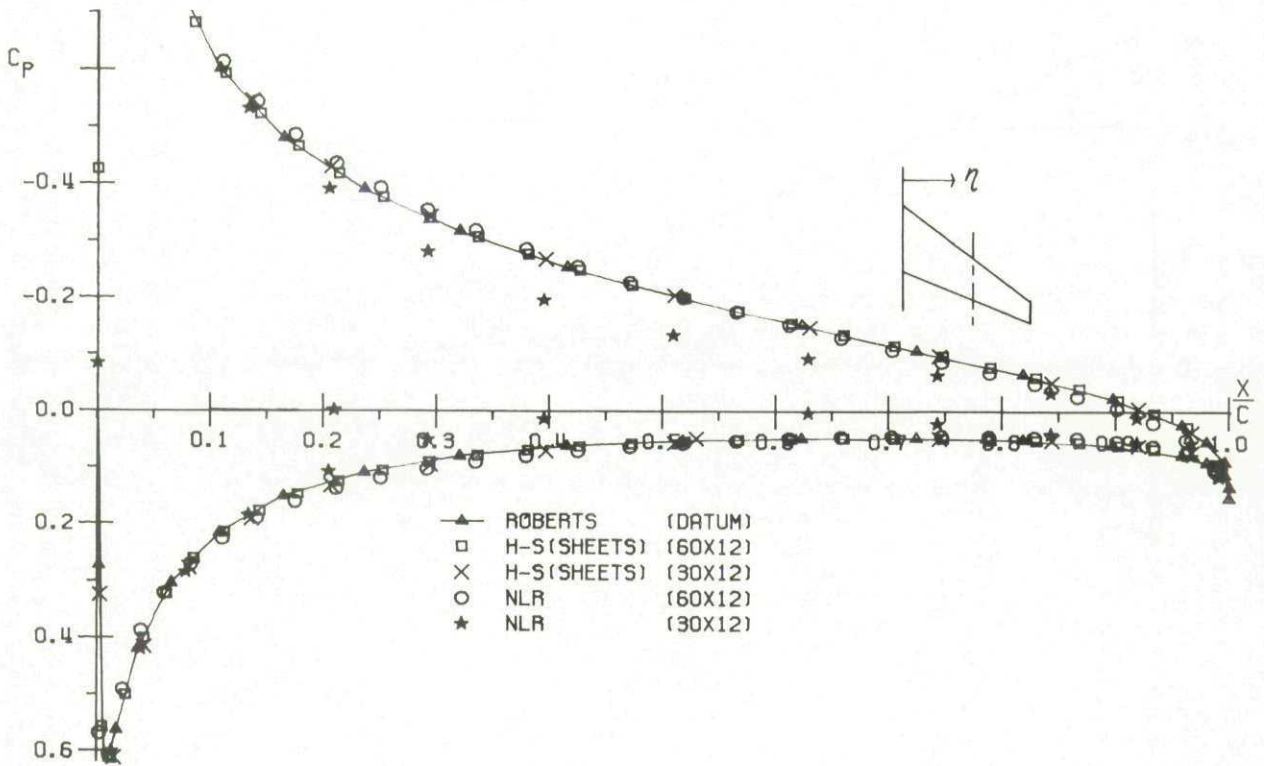


FIG. 86 CONVERGENCE STUDY
CHORDWISE PRESSURE DISTRIBUTION
RAE WING . T/C = .05 . $\alpha = 5.0$. $\eta = .549$

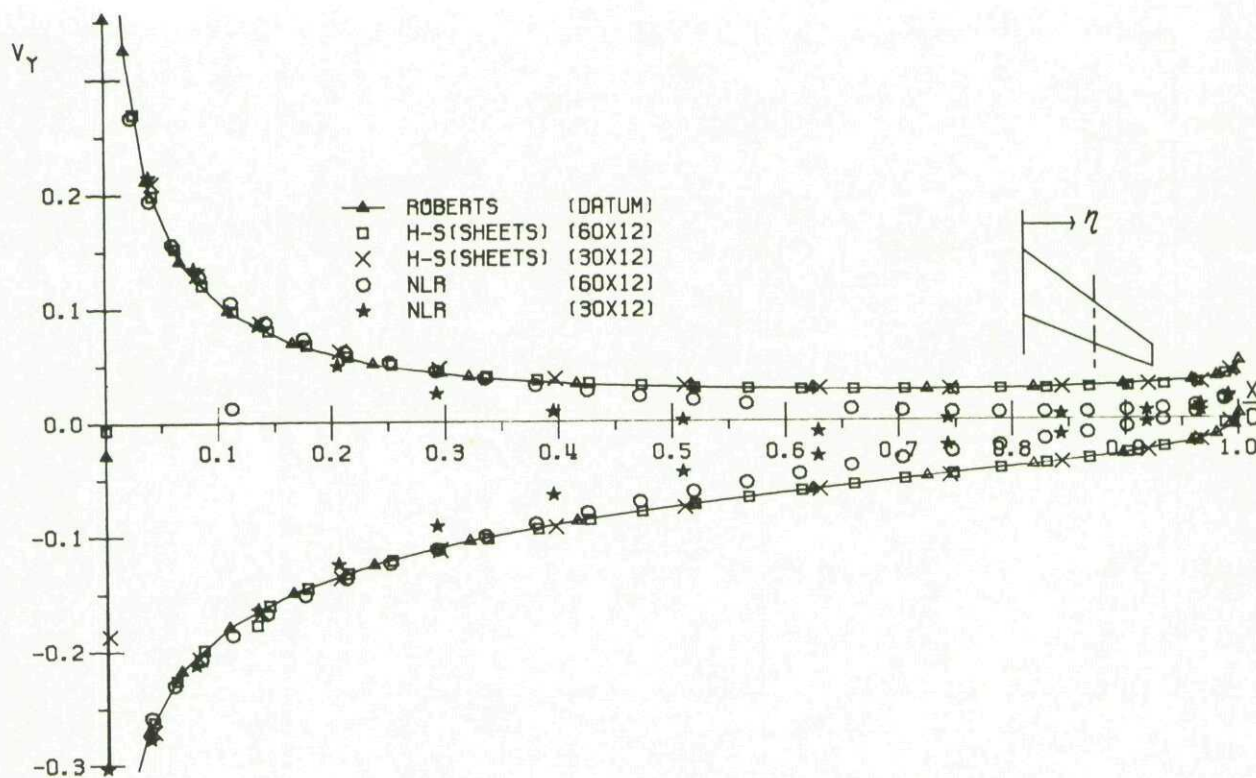


FIG. 87 CONVERGENCE STUDY
 Y-COMPONENT OF VELOCITY
 RAE WING . T/C = .05 . $\alpha = 5.0$. $\eta = .549$

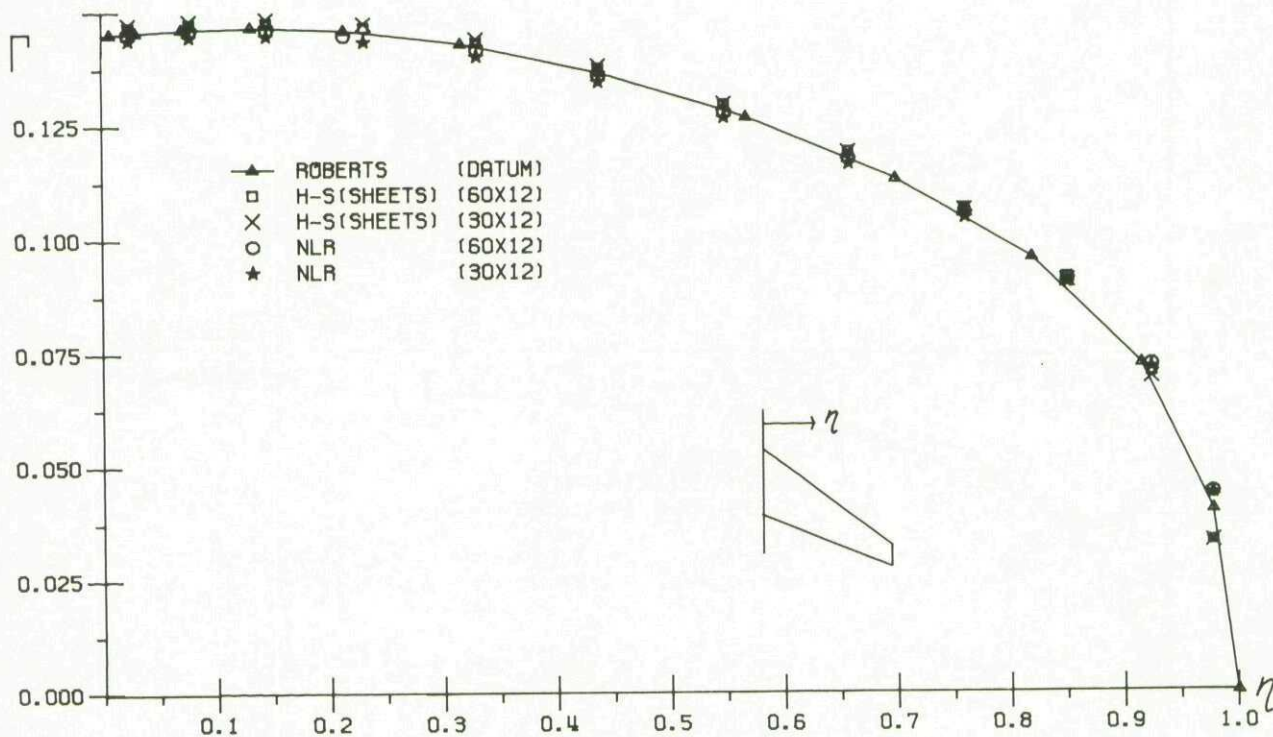


FIG. 88 CONVERGENCE STUDY
 CIRCULATION
 RAE WING . T/C = .05 . $\alpha = 5.0$

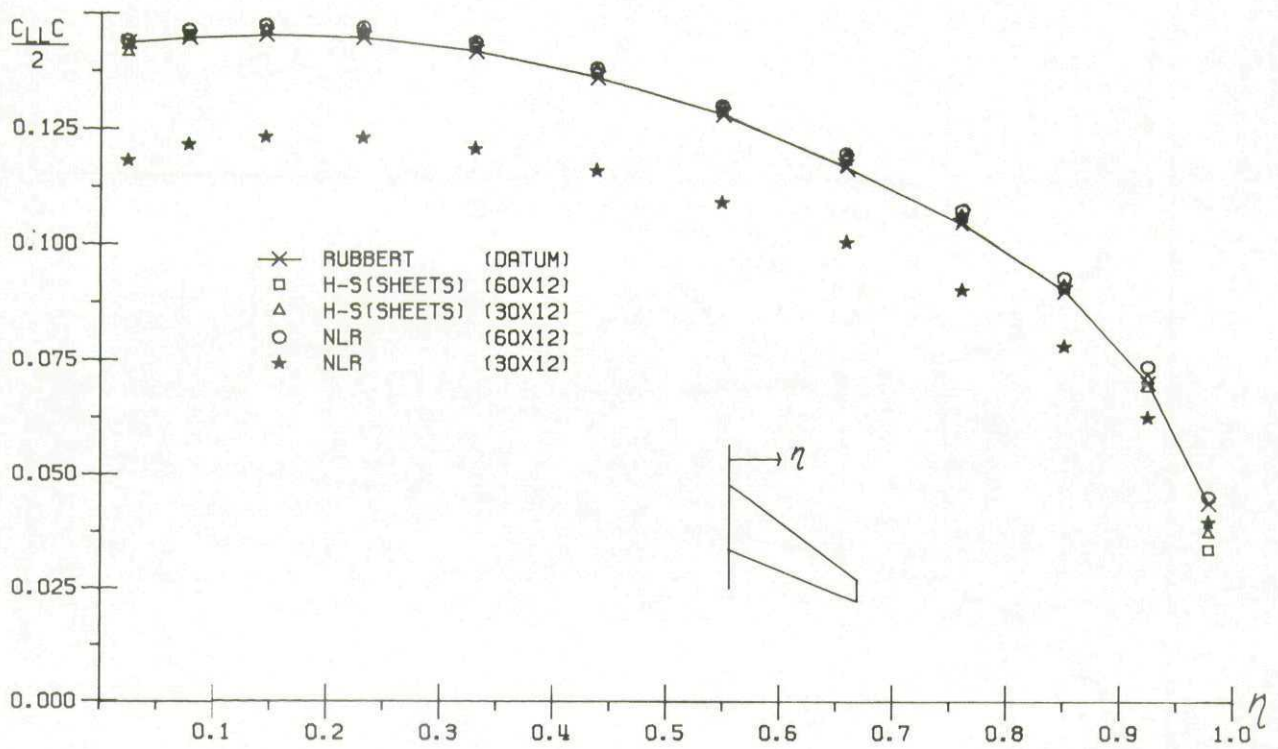


FIG. 89 CONVERGENCE STUDY
SECTIONAL LOAD
RAE WING . T/C = .05 . α = 5.0

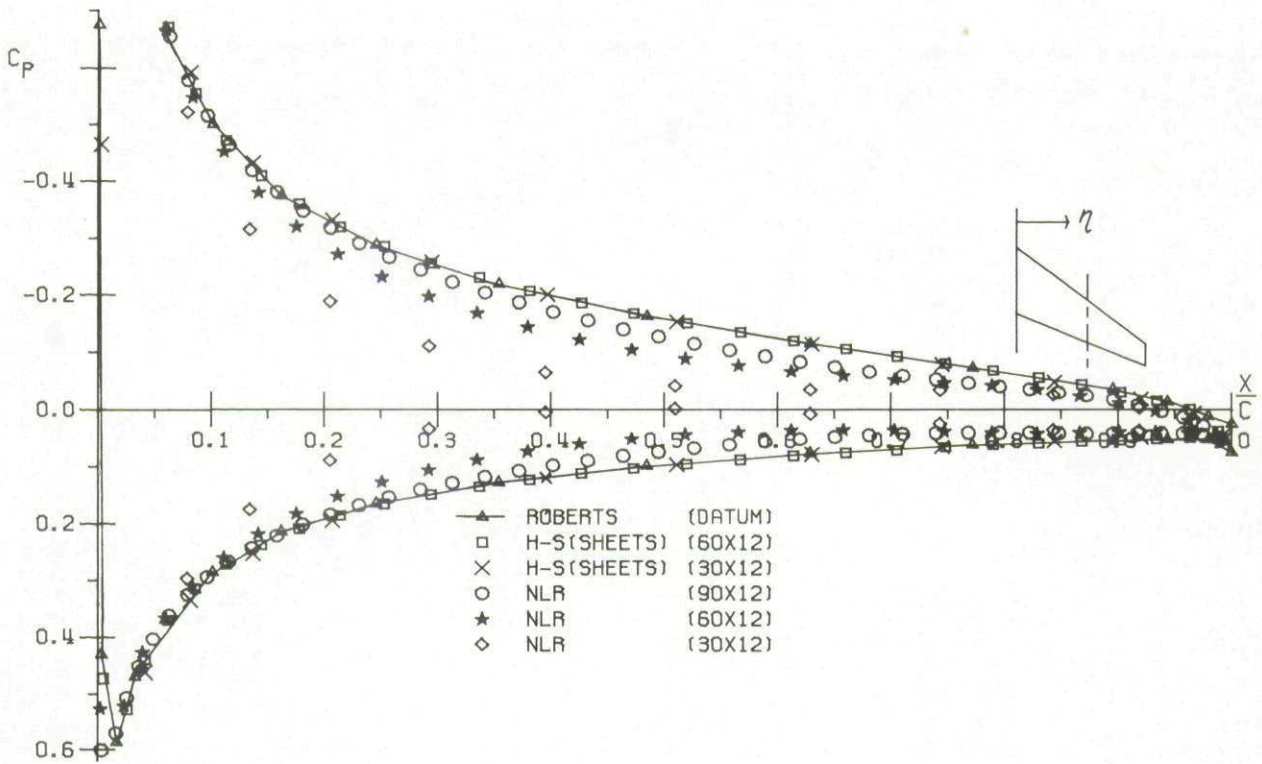


FIG. 90 CONVERGENCE STUDY
CHORDWISE PRESSURE DISTRIBUTION
RAE WING . T/C = .02 . α = 5.0 . η = .549

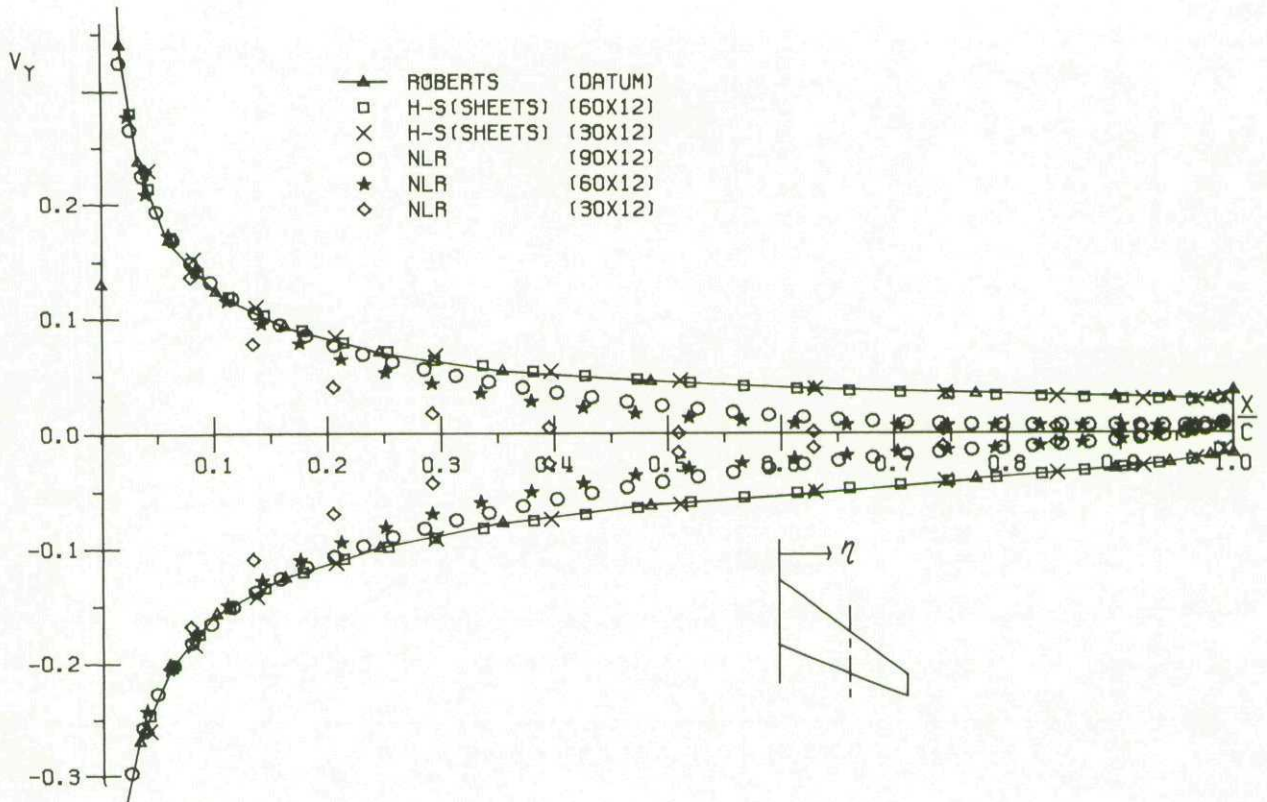


FIG. 91 CONVERGENCE STUDY
Y-COMPONENT OF VELOCITY
RAE WING . T/C = .02 . $\alpha = 5.0$. $\eta = .549$

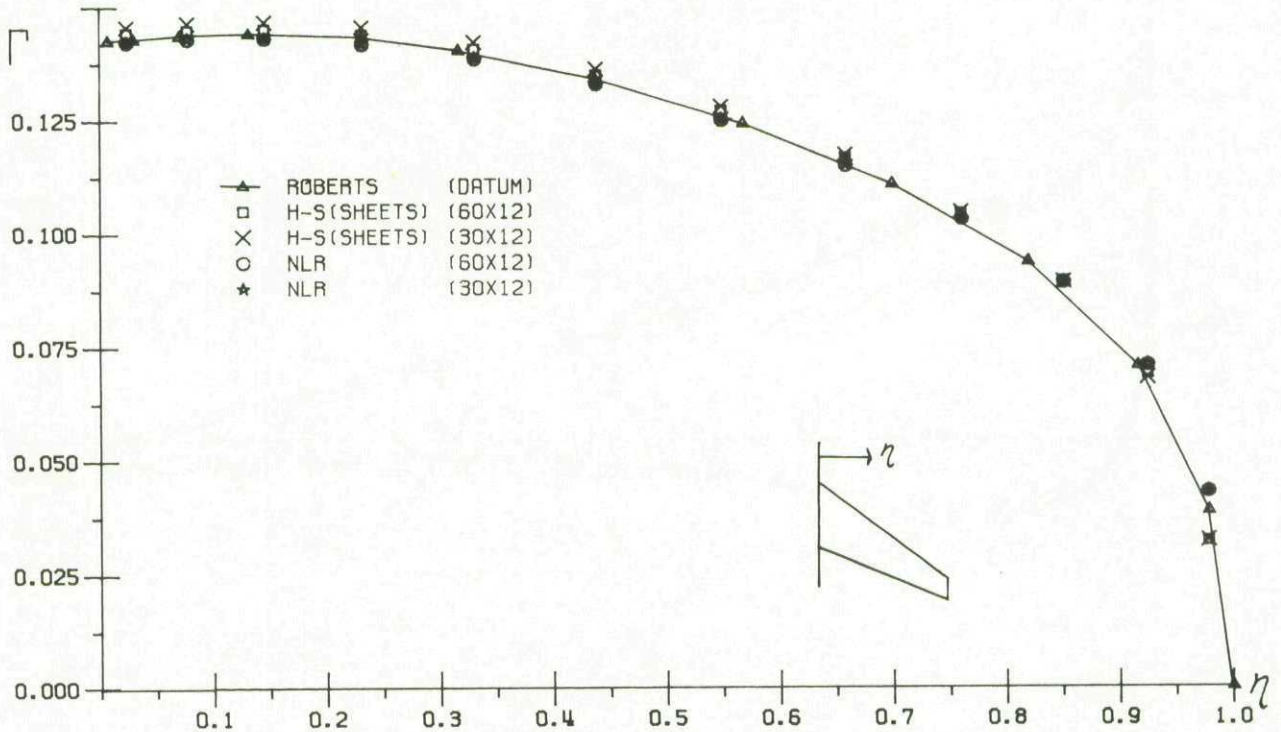


FIG. 92 CONVERGENCE STUDY
CIRCULATION
RAE WING . T/C = .02 . $\alpha = 5.0$

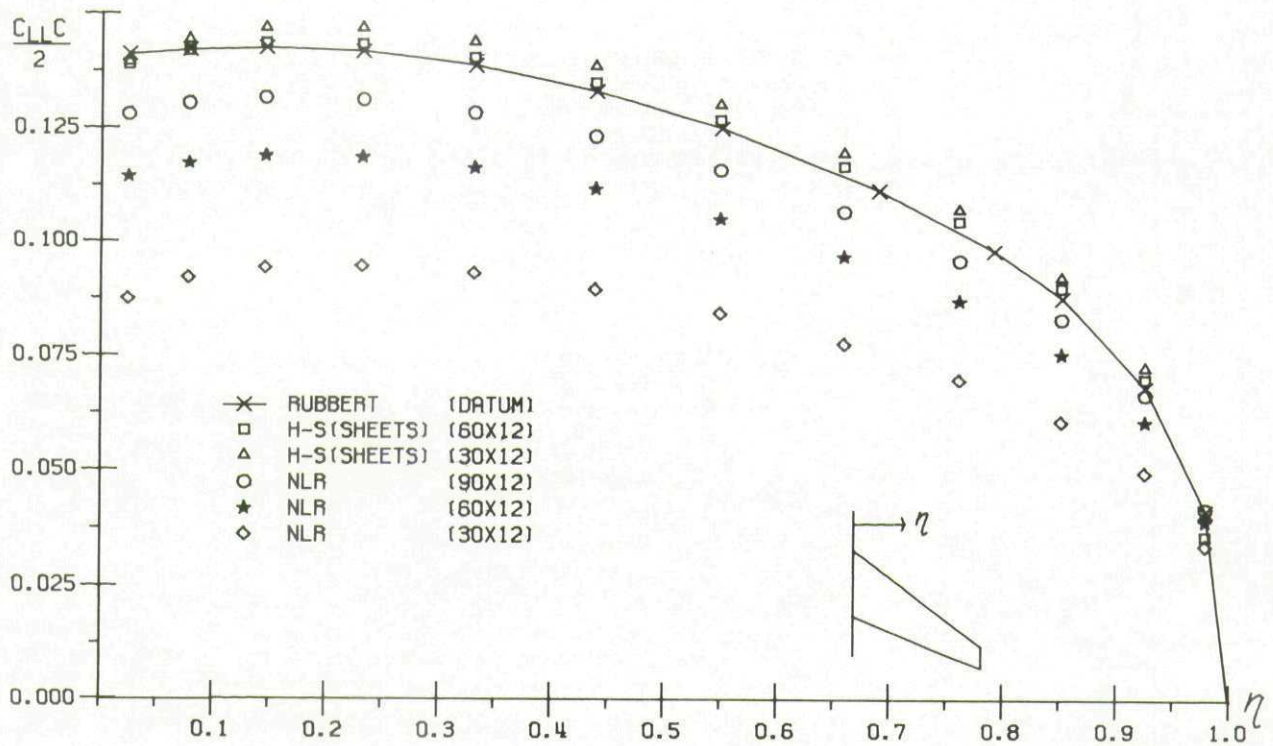


FIG. 93 CONVERGENCE STUDY
SECTIONAL LOAD
RAE WING . T/C = .02 . $\alpha = 5.0$

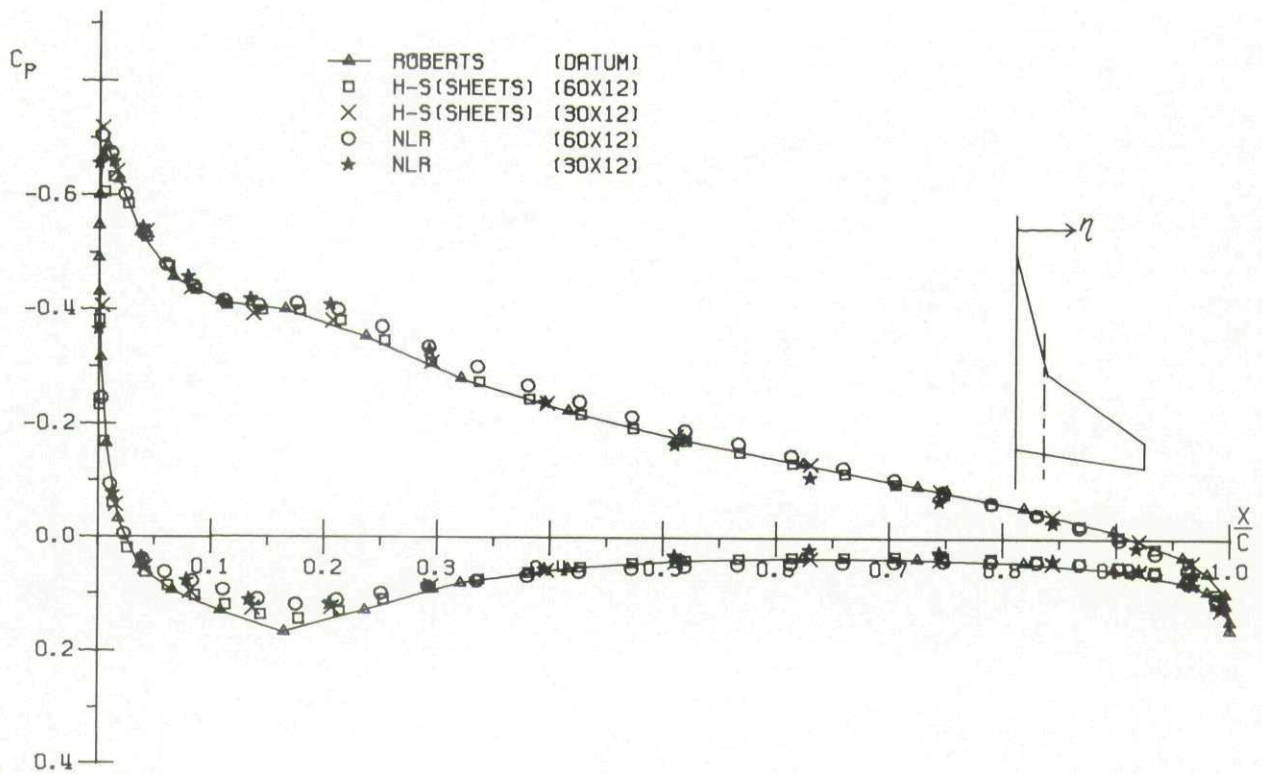


FIG. 94 CONVERGENCE STUDY
CHORDWISE PRESSURE DISTRIBUTION
STRAKED WING . T/C = .05 . $\alpha = 5.0$. $\eta = .219$

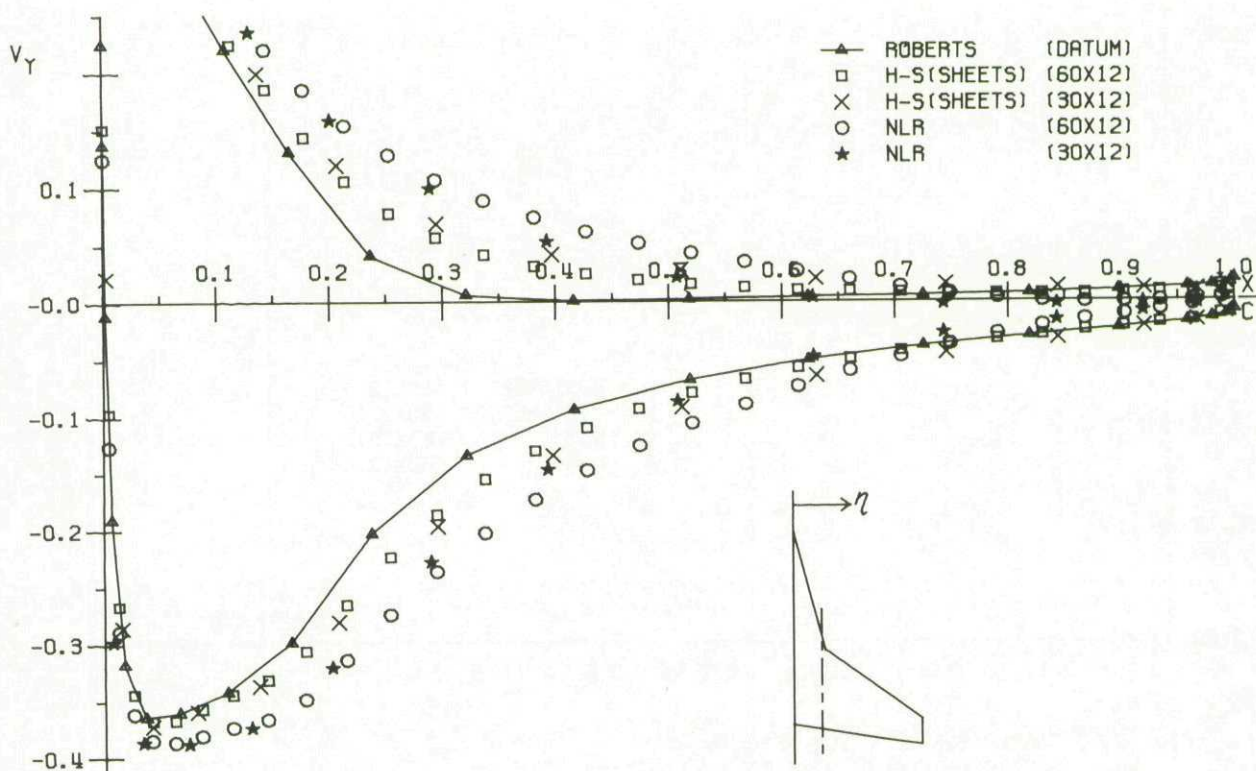


FIG. 95 CONVERGENCE STUDY
 Y-COMPONENT OF VELOCITY
 STRAKED WING . T/C = .05 . $\alpha = 5.0$. $\eta = .219$

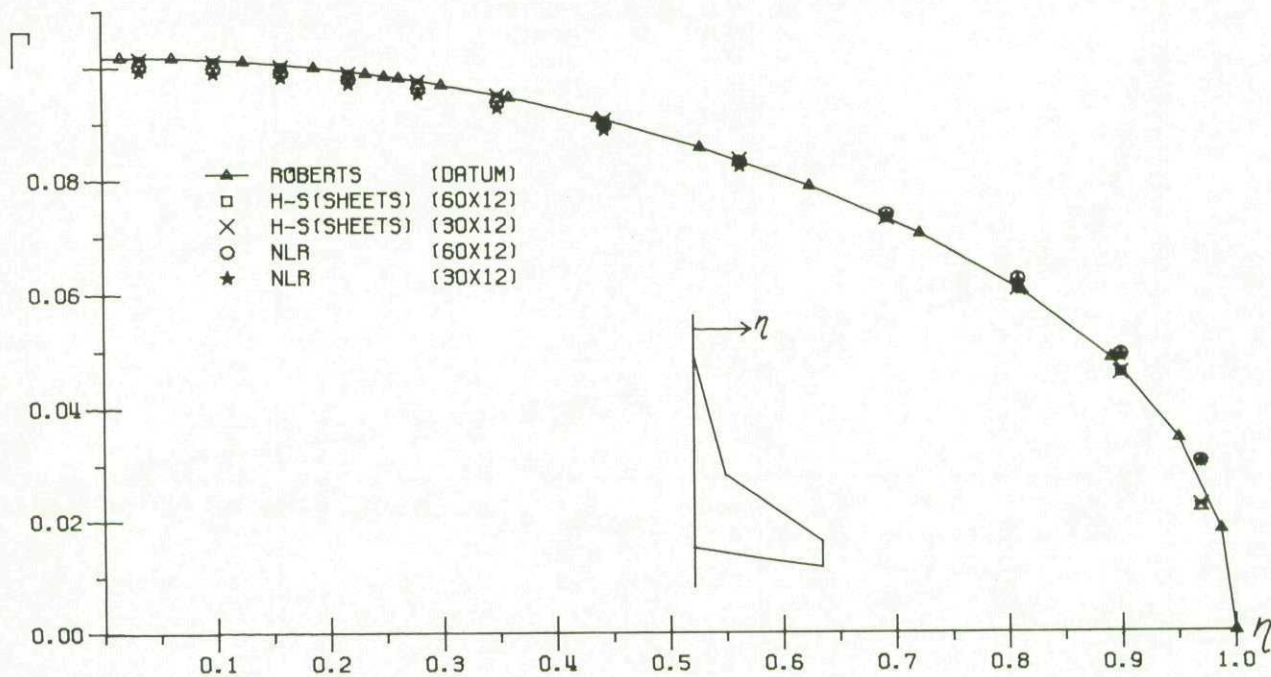


FIG. 96 CONVERGENCE STUDY
 CIRCULATION
 STRAKED WING . T/C = .05 . $\alpha = 5.0$

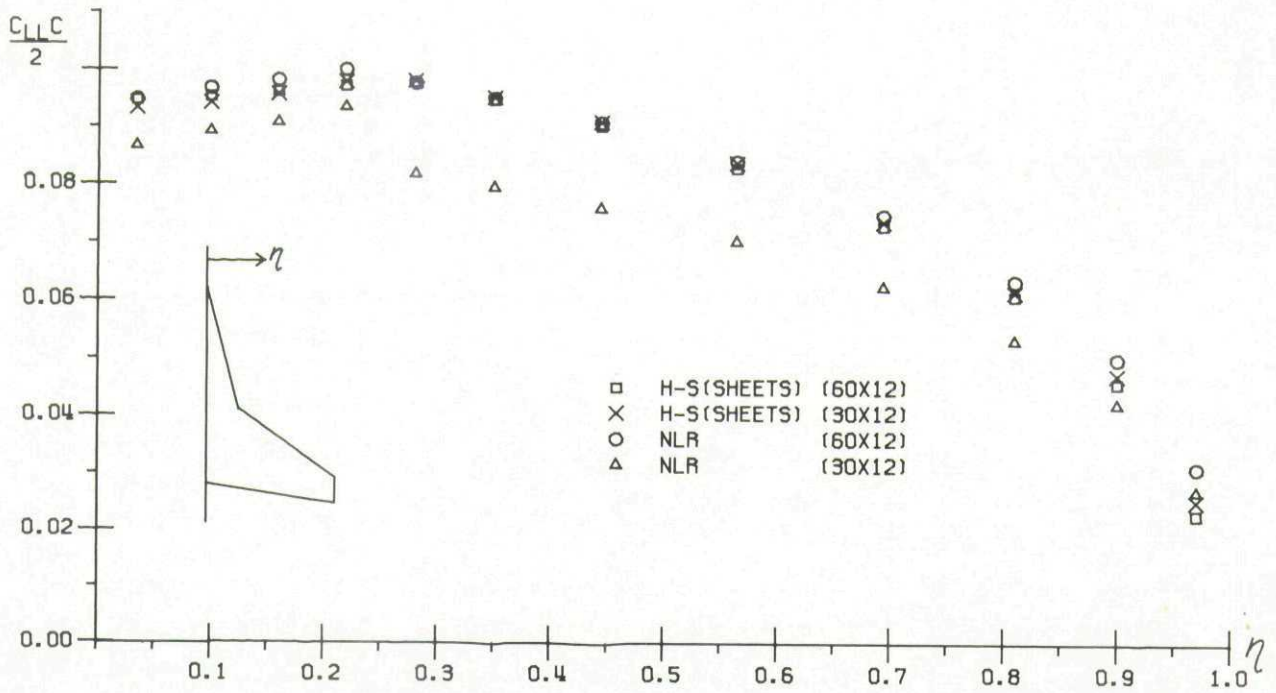


FIG. 97 COMPARISON OF DATUM RESULTS
SECTIONAL LOAD
STRAKED WING . T/C = .05 . α = 5.0

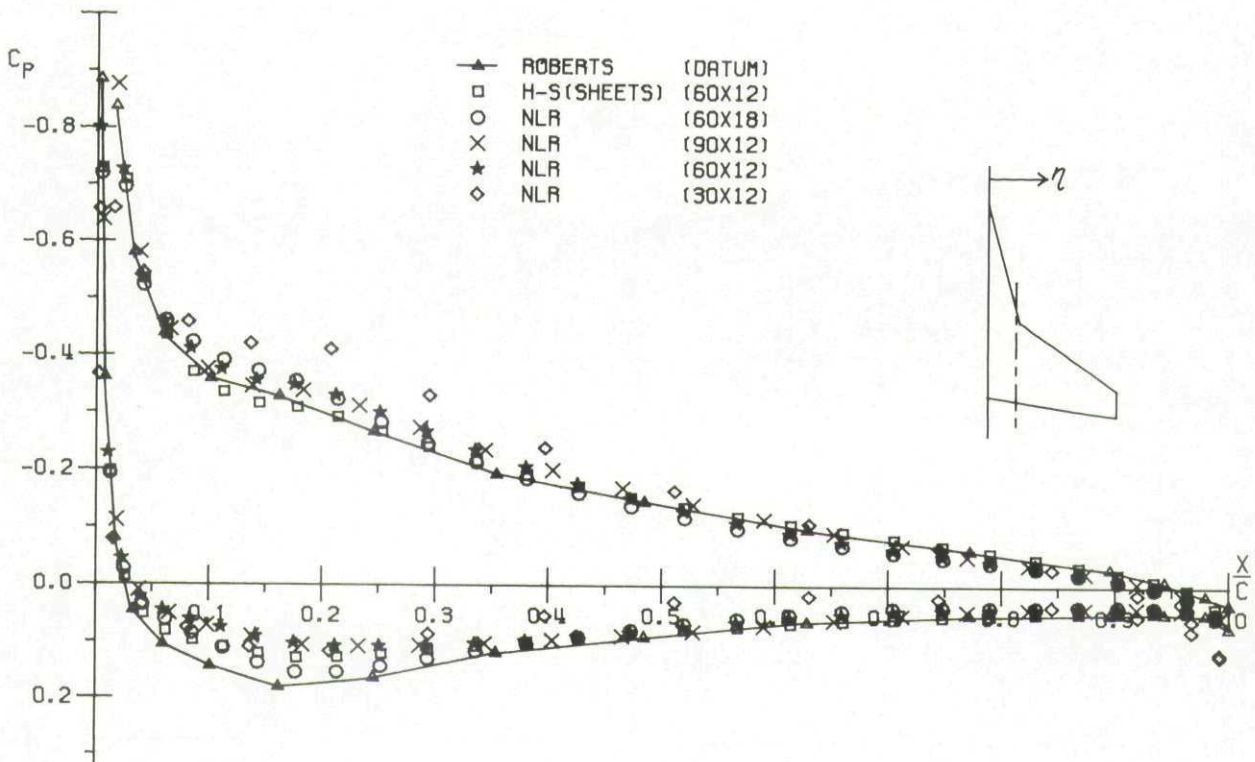


FIG. 99 CONVERGENCE STUDY
CHORDWISE PRESSURE DISTRIBUTION
STRAKED WING . T/C = .02 . α = 5.0 . η = .219

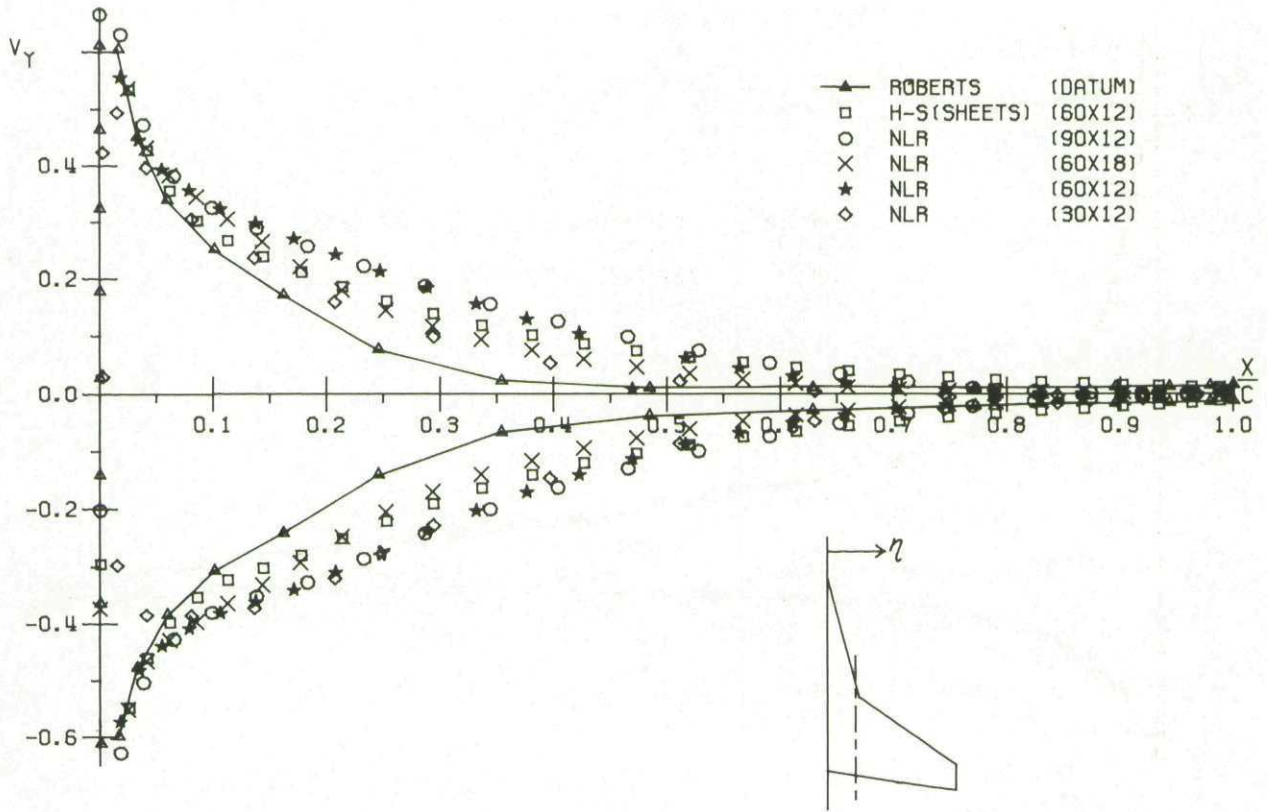


FIG. 99 CONVERGENCE STUDY
 Y-COMPONENT OF VELOCITY
 STRAKED WING . T/C = .02 . $\alpha = 5.0$. $\eta = .219$

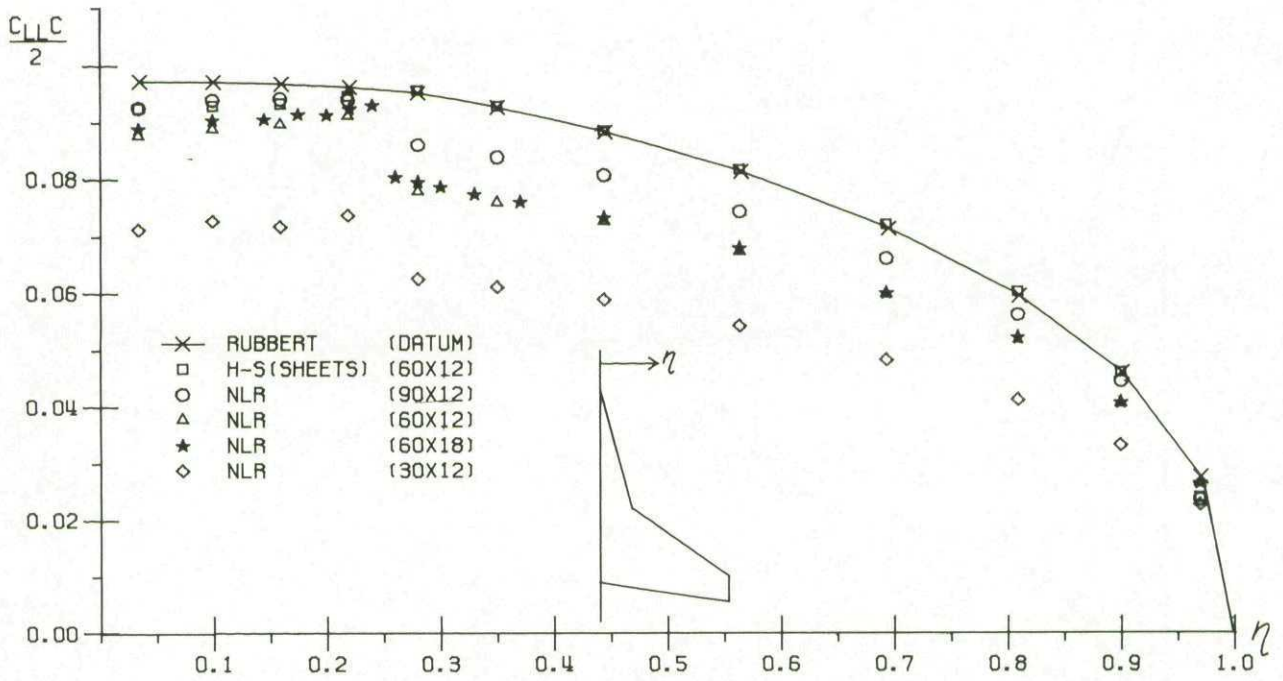


FIG. 100 CONVERGENCE STUDY
 SECTIONAL LOAD
 STRAKED WING . T/C = .02 . $\alpha = 5.0$

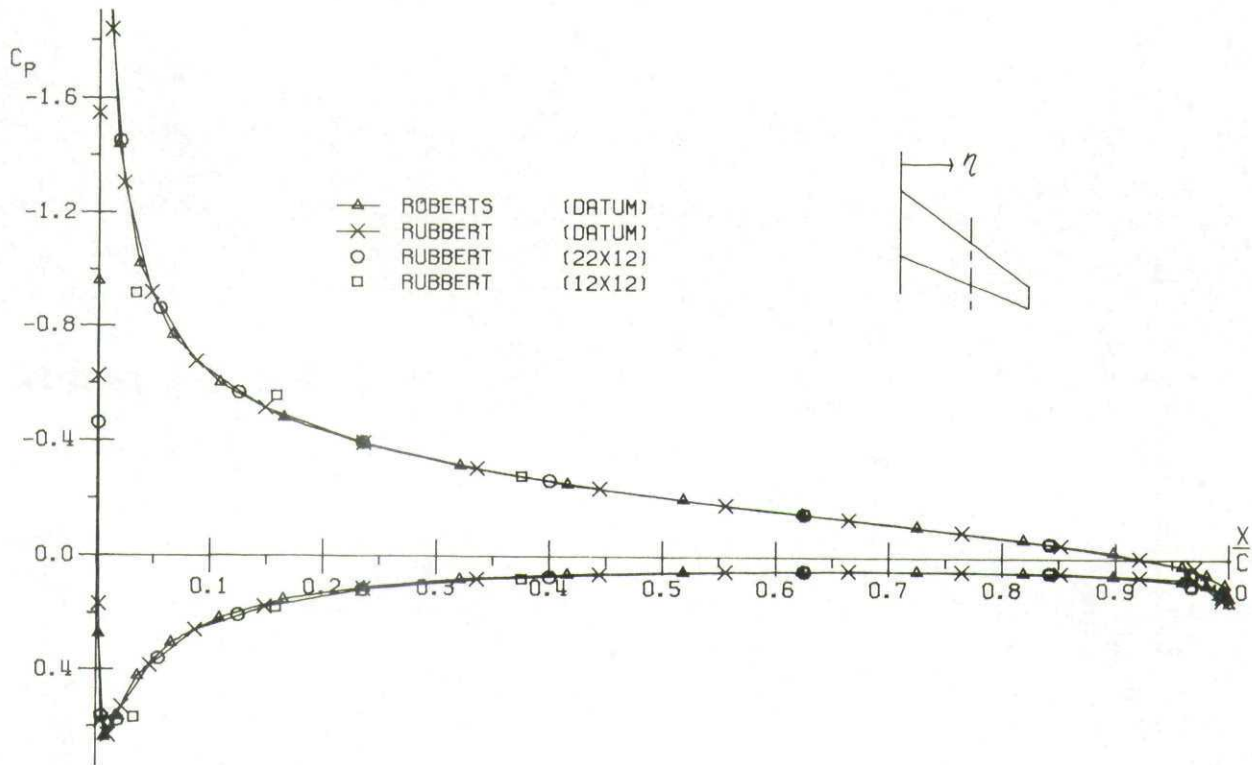


FIG. 101 CONVERGENCE STUDY
 CHORDWISE PRESSURE DISTRIBUTION
 RAE WING . T/C = .05 . α = 5.0 . η = .549

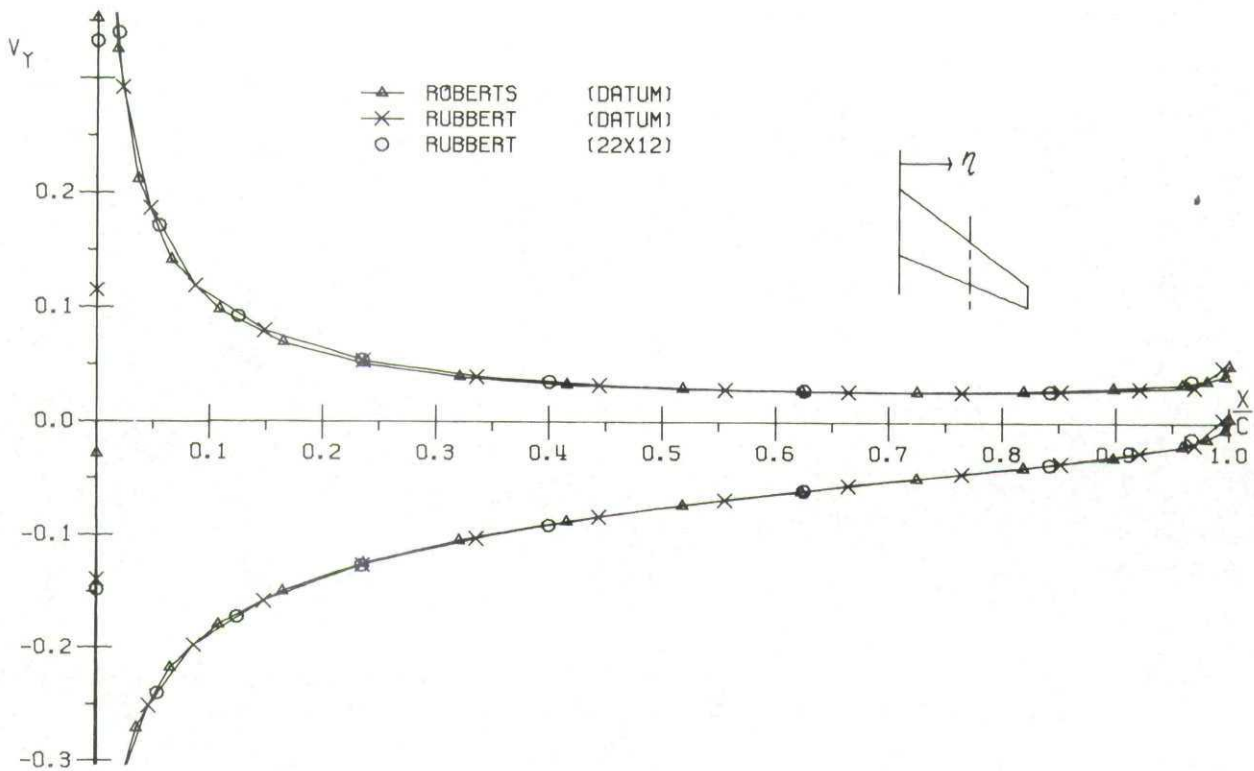


FIG. 102 CONVERGENCE STUDY
 Y-COMPONENT OF VELOCITY
 RAE WING . T/C = .05 . α = 5.0 . η = .549

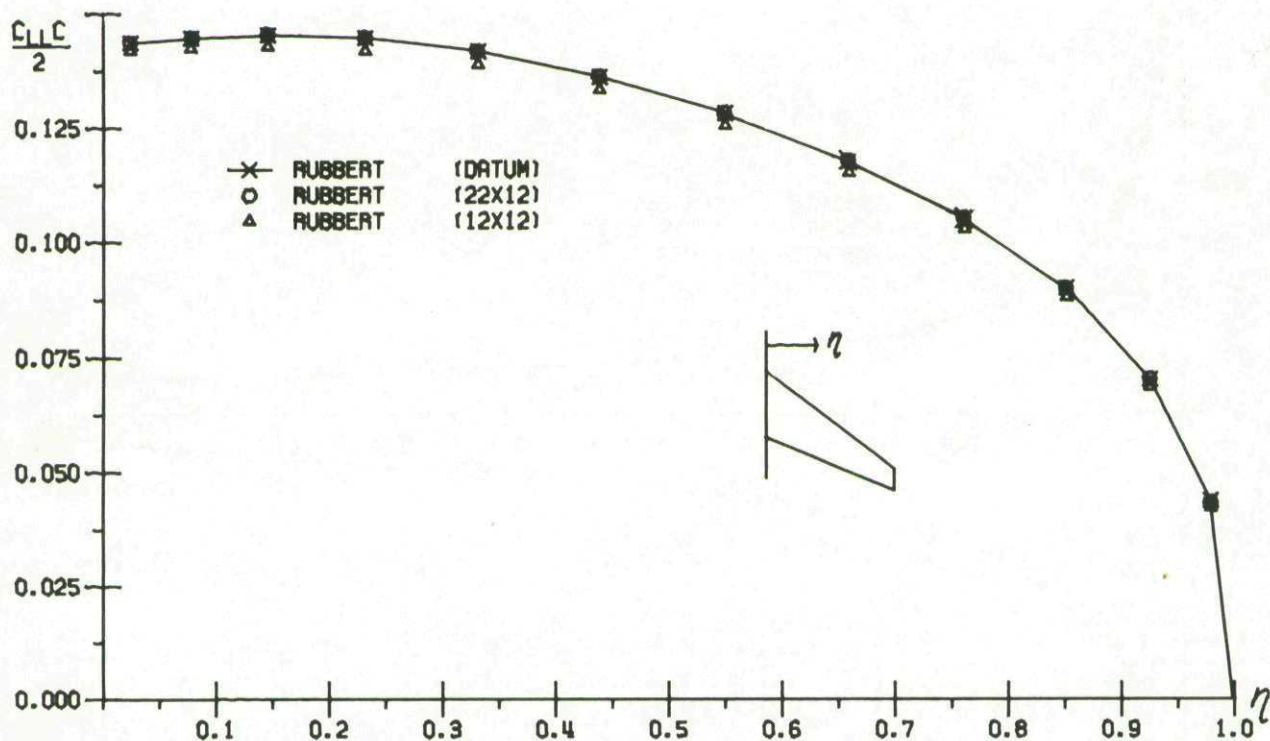


FIG. 103 CONVERGENCE STUDY
SECTIONAL LOAD
RAE WING . T/C = .05 . α = 5.0

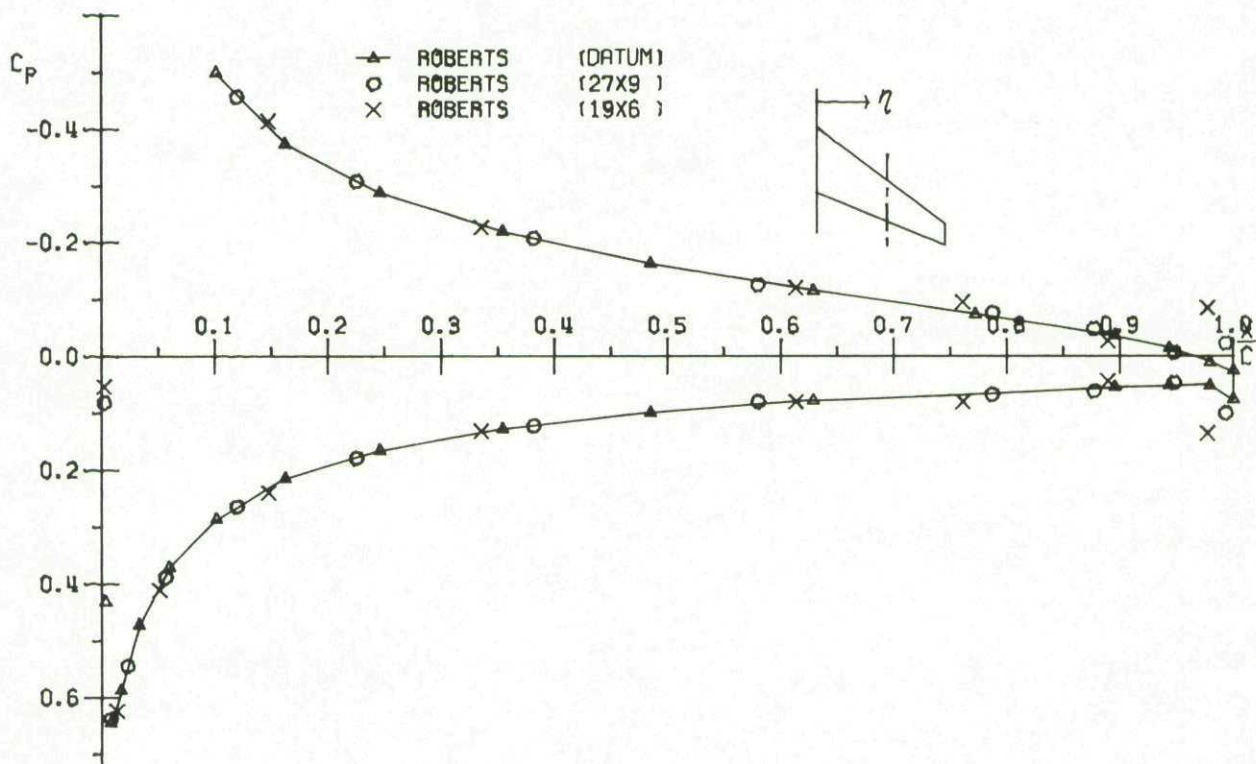


FIG. 104 CONVERGENCE STUDY
CHORDWISE PRESSURE DISTRIBUTION
RAE WING . T/C = .02 . α = 5.0 . η = .549

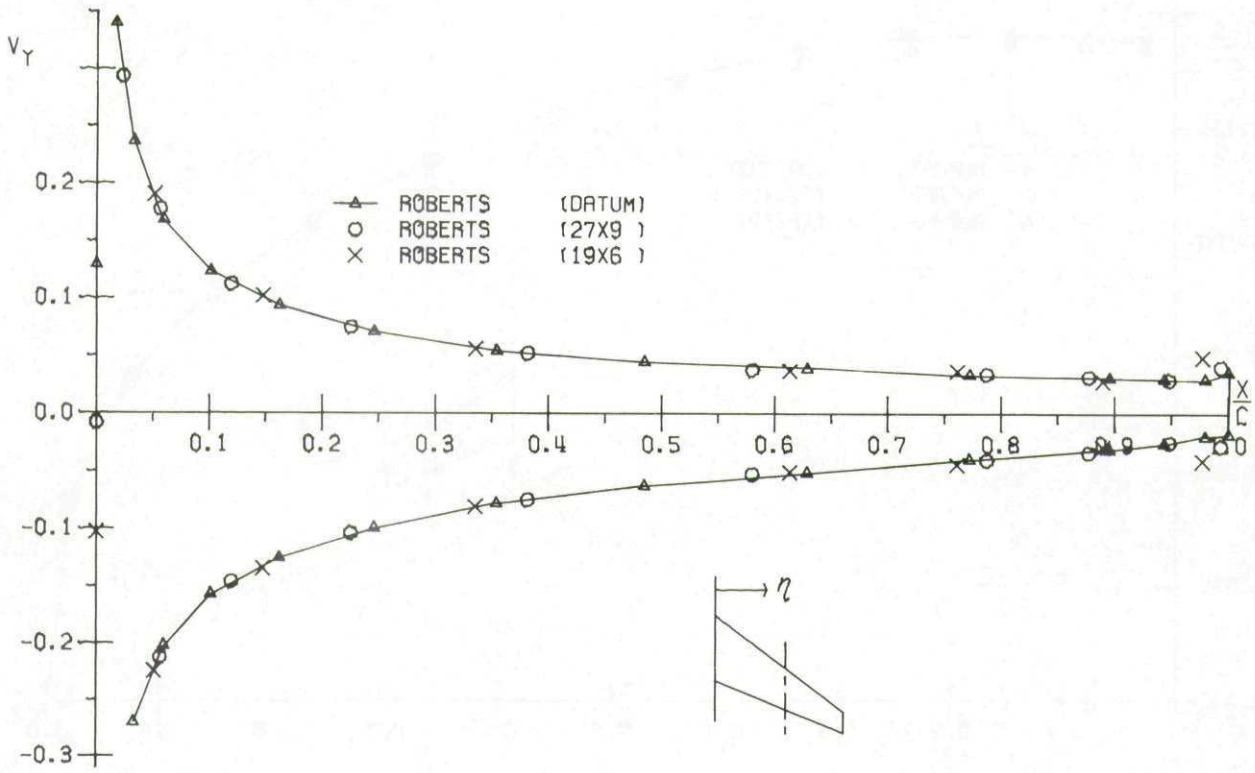


FIG. 105 CONVERGENCE STUDY
 Y-COMPONENT OF VELOCITY
 RAE WING . T/C = .02 . $\alpha = 5.0$. $\eta = .549$

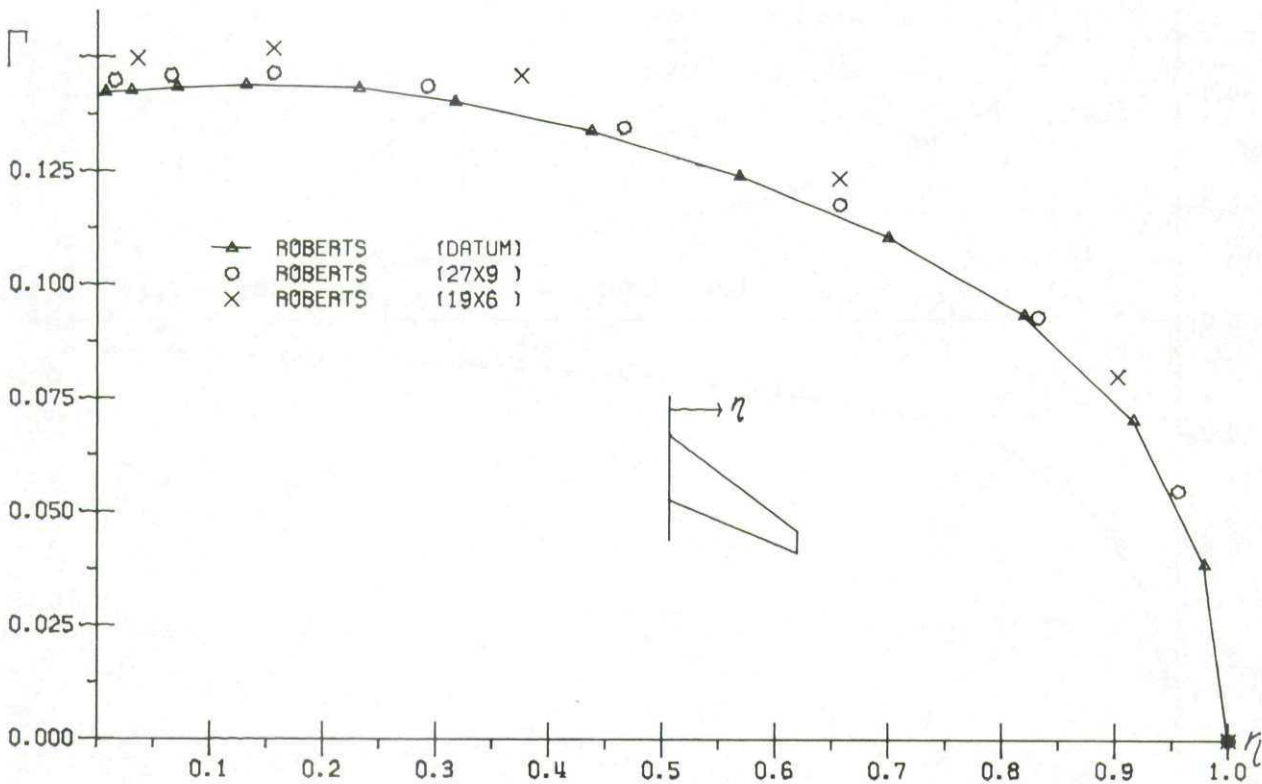


FIG. 106 CONVERGENCE STUDY
 CIRCULATION
 RAE WING . T/C = .02 . $\alpha = 5.0$

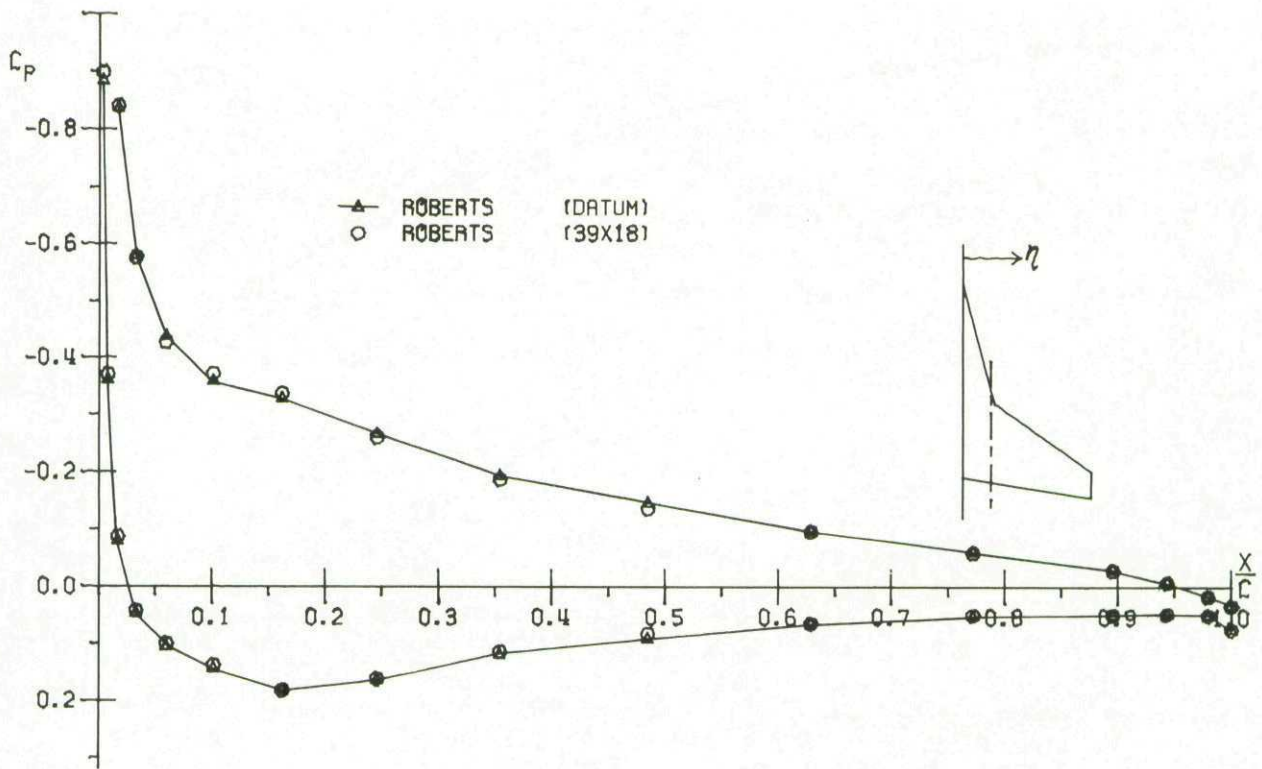


FIG. 107 CONVERGENCE STUDY
 CHORDWISE PRESSURE DISTRIBUTION
 STRAKED WING . T/C = .02 . α = 5.0 . η = .219

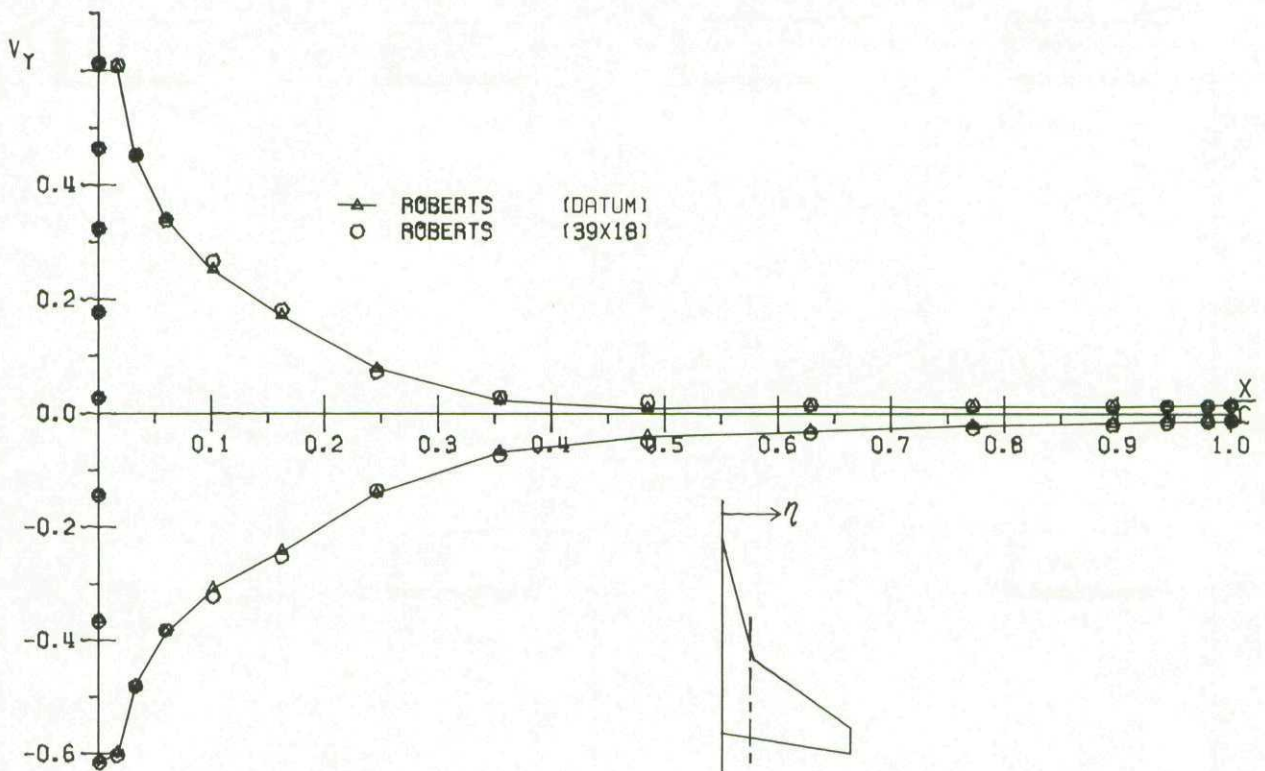


FIG. 108 CONVERGENCE STUDY
 Y-COMPONENT OF VELOCITY
 STRAKED WING . T/C = .02 . α = 5.0 . η = .219

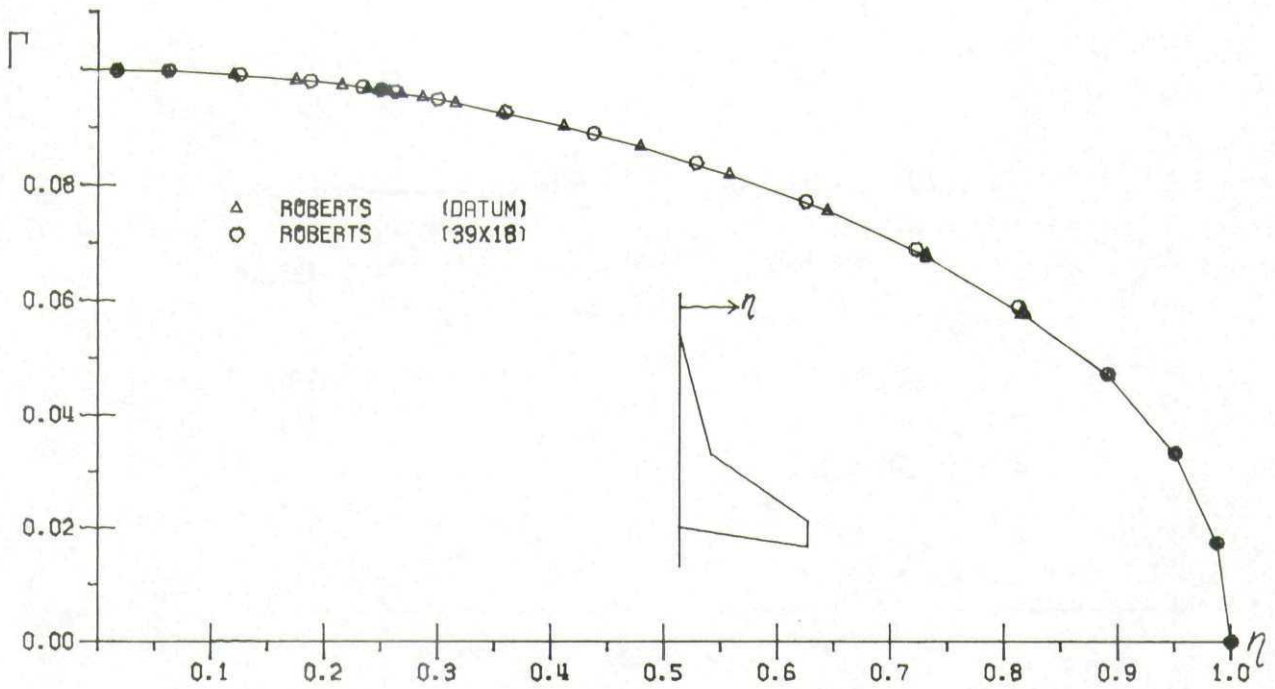


FIG. 109 CONVERGENCE STUDY
CIRCULATION
STRAKED WING . T/C = .02 . $\alpha = 5.0$

×	RUBBERT	40 x 12 (=DATUM) / 22 x 12 / 12 x 12
□	HU-SE (SHEETS)	60 x 12 / 30 x 12
■	HU-SE (LINES)	60 x 12
○	NLR	60 x 12 / 30 x 12

×	RUBBERT	40 x 12 (=DATUM)
△	ROBERTS	27 x 9 / 19 x 6
□	HU-SE (SHEETS)	60 x 12 / 30 x 12
○	NLR	90 x 12 / 60 x 12 / 30 x 12

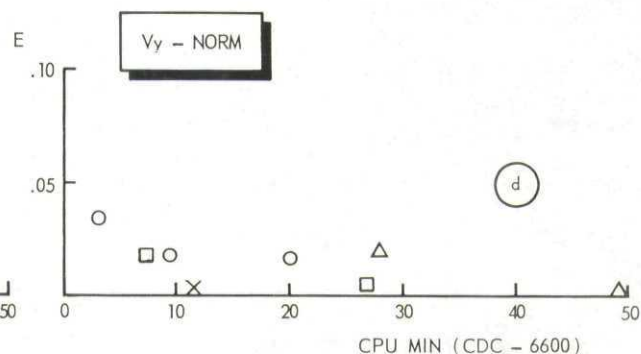
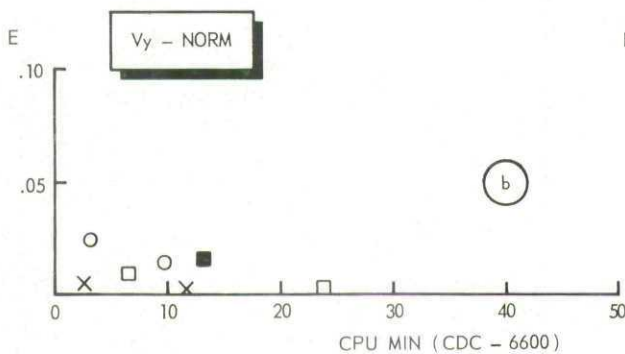
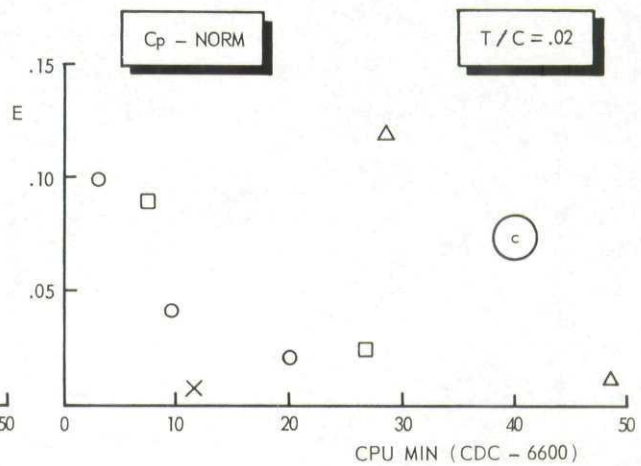
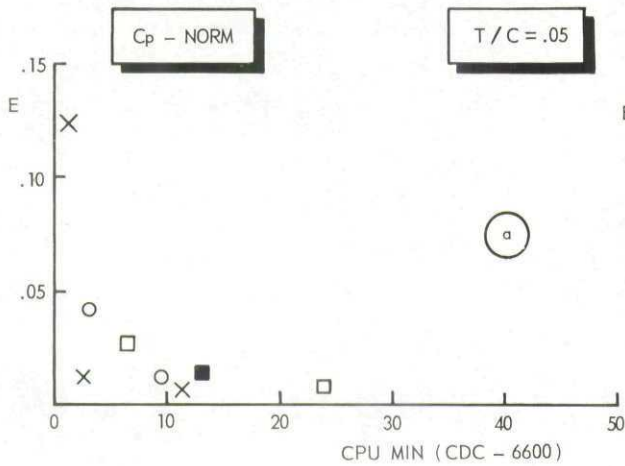


Fig. 110 L_2 -error norm E, RAE wing cases at $\eta = .549$ as function of central processor time (CDC 6600)

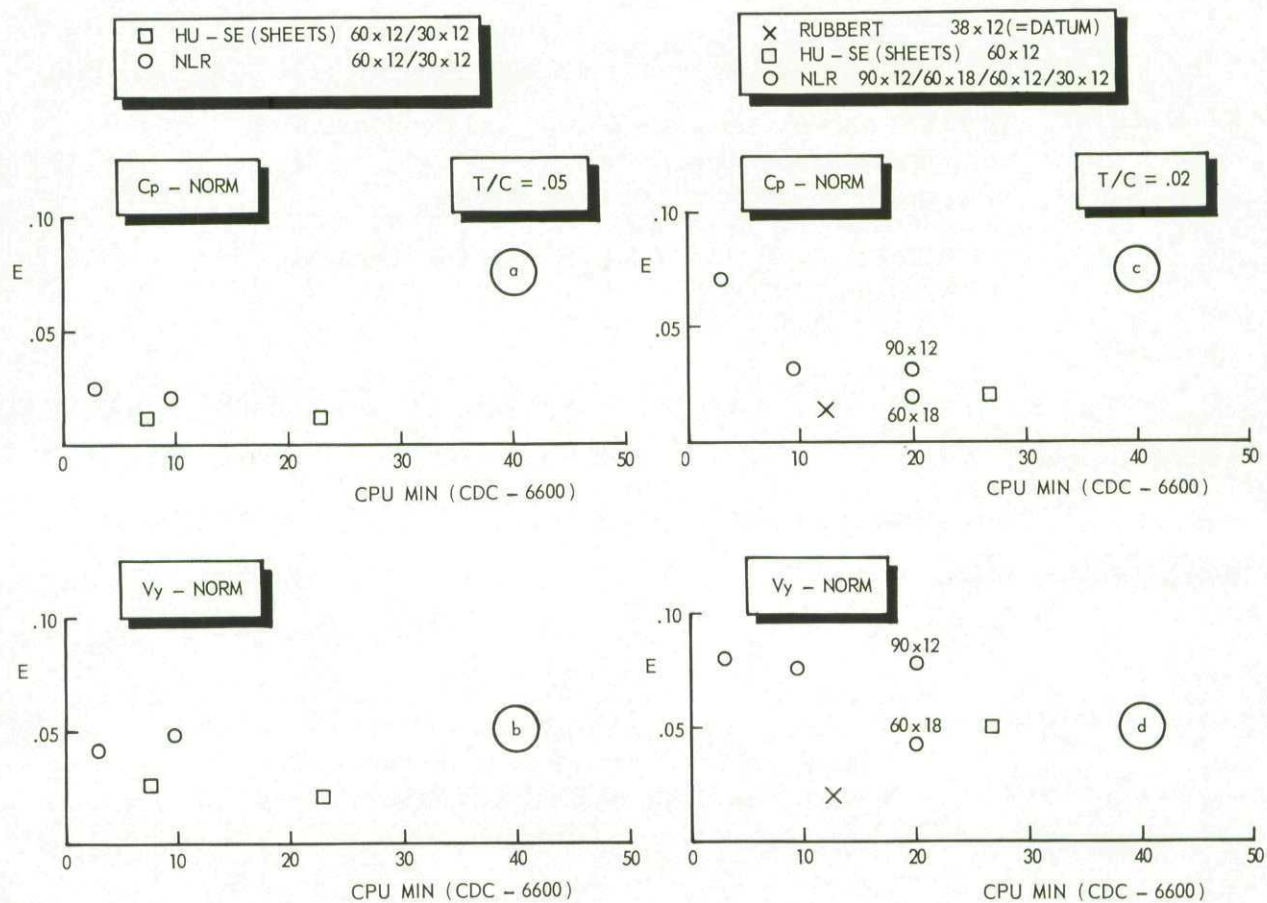


Fig. 111 L_2 -error norm E, for straked wing cases at $\eta = .218$ as function of central processor time (CDC 6600)

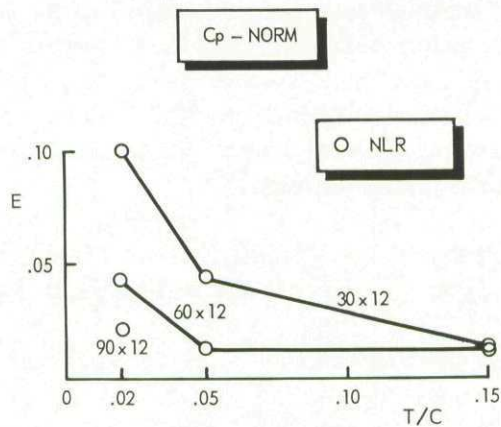


Fig. 112 L_2 -error norm E for the NLR panel method chordwise pressure distributions at $\eta = .549$ for RAE wing cases as function of thickness/chord ratio

REPORT DOCUMENTATION PAGE

1. Recipient's Reference	2. Originator's Reference AGARD-AG-241	3. Further Reference 13 ISBN 92-835-1312-6	4. Security Classification of Document UNCLASSIFIED						
5. Originator Advisory Group for Aerospace Research and Development North Atlantic Treaty Organization 7 rue Ancelle, 92200 Neuilly sur Seine, France									
6. Title 7 A COMPARISON OF PANEL METHODS FOR SUBSONIC FLOW COMPUTATION									
7. Presented at									
8. Author(s)/Editor(s) H.S. Sytsma, B.L. Hewitt and P.E. Rubbert HS 8 BL 9			9. Date 10 2. February 1979						
10. Author's/Editor's Address See Fly Leaf			11. Pages 88						
12. Distribution Statement This document is distributed in accordance with AGARD policies and regulations, which are outlined on the Outside Back Covers of all AGARD publications.									
13. Keywords/Descriptors <table border="0" style="width:100%"> <tr> <td>Numerical analysis</td> <td>Incompressible flow</td> </tr> <tr> <td>Aerodynamic configurations</td> <td>Applications of mathematics</td> </tr> <tr> <td>Subsonic characteristics</td> <td>Flow distribution</td> </tr> </table>				Numerical analysis	Incompressible flow	Aerodynamic configurations	Applications of mathematics	Subsonic characteristics	Flow distribution
Numerical analysis	Incompressible flow								
Aerodynamic configurations	Applications of mathematics								
Subsonic characteristics	Flow distribution								
14. Abstract <p>Panel, or surface singularity, methods have been developed to the stage where they provide nominally exact numerical solutions for incompressible flow potential around complicated, real aircraft configurations. A large variety of these methods are in use or under development. This report provides a data base against which the various programs may be checked and makes comparisons of several methods with the datum solutions for several simple wing configurations and nacelle configurations.</p> <p>Datum results are from the Roberts (BAe) Spline-Naumann Program, and a pilot version of the Boeing Advanced Panel-Type Influence Coefficient Method.</p> <p>This AGARDograph has been produced at the request of the Fluid Dynamics Panel of AGARD.</p> <p align="right">MAZ</p>									

<p>AGARDograph No.241 Advisory Group for Aerospace Research and Development, NATO A COMPARISON OF PANEL METHODS FOR SUBSONIC FLOW COMPUTATION by H.S.Sytsma, B.L.Hewitt and P.E.Rubbert Published February 1979 88 pages</p> <p>Panel, or surface singularity, methods have been developed to the stage where they provide nominally exact numerical solutions for incompressible flow potential around complicated, real aircraft configurations. A large variety of these methods are in use or under development. This report provides a data base against which the various programs may be checked</p> <p style="text-align: right;">P.T.O.</p>	<p style="text-align: center;">AGARD-AG-241</p> <p>Numerical analysis Aerodynamic configurations Subsonic characteristics Incompressible flow Applications of mathematics Flow distribution</p>	<p>AGARDograph No.241 Advisory Group for Aerospace Research and Development, NATO A COMPARISON OF PANEL METHODS FOR SUBSONIC FLOW COMPUTATION by H.S.Sytsma, B.L.Hewitt and P.E.Rubbert Published February 1979 88 pages</p> <p>Panel, or surface singularity, methods have been developed to the stage where they provide nominally exact numerical solutions for incompressible flow potential around complicated, real aircraft configurations. A large variety of these methods are in use or under development. This report provides a data base against which the various programs may be checked</p> <p style="text-align: right;">P.T.O.</p>	<p style="text-align: center;">AGARD-AG-241</p> <p>Numerical analysis Aerodynamic configurations Subsonic characteristics Incompressible flow Applications of mathematics Flow distribution</p>
<p>AGARDograph No.241 Advisory Group for Aerospace Research and Development, NATO A COMPARISON OF PANEL METHODS FOR SUBSONIC FLOW COMPUTATION by H.S.Sytsma, B.L.Hewitt and P.E.Rubbert Published February 1979 88 pages</p> <p>Panel, or surface singularity, methods have been developed to the stage where they provide nominally exact numerical solutions for incompressible flow potential around complicated, real aircraft configurations. A large variety of these methods are in use or under development. This report provides a data base against which the various programs may be checked</p> <p style="text-align: right;">P.T.O.</p>	<p style="text-align: center;">AGARD-AG-241</p> <p>Numerical analysis Aerodynamic configurations Subsonic characteristics Incompressible flow Applications of mathematics Flow distribution</p>	<p>AGARDograph No.241 Advisory Group for Aerospace Research and Development, NATO A COMPARISON OF PANEL METHODS FOR SUBSONIC FLOW COMPUTATION by H.S.Sytsma, B.L.Hewitt and P.E.Rubbert Published February 1979 88 pages</p> <p>Panel, or surface singularity, methods have been developed to the stage where they provide nominally exact numerical solutions for incompressible flow potential around complicated, real aircraft configurations. A large variety of these methods are in use or under development. This report provides a data base against which the various programs may be checked</p> <p style="text-align: right;">P.T.O.</p>	<p style="text-align: center;">AGARD-AG-241</p> <p>Numerical analysis Aerodynamic configurations Subsonic characteristics Incompressible flow Applications of mathematics Flow distribution</p>

AGARD

NATO  OTAN7 RUE ANCELLE · 92200 NEUILLY-SUR-SEINE
FRANCE

Telephone 745.08.10 · Telex 610176

DISTRIBUTION OF UNCLASSIFIED
AGARD PUBLICATIONS

AGARD does NOT hold stocks of AGARD publications at the above address for general distribution. Initial distribution of AGARD publications is made to AGARD Member Nations through the following National Distribution Centres. Further copies are sometimes available from these Centres, but if not may be purchased in Microfiche or Photocopy form from the Purchase Agencies listed below.

NATIONAL DISTRIBUTION CENTRES

BELGIUM

Coordonnateur AGARD – VSL
Etat-Major de la Force Aérienne
Quartier Reine Elisabeth
Rue d'Evere, 1140 Bruxelles

CANADA

Defence Scientific Information Service
Department of National Defence
Ottawa, Ontario K1A 0Z2

DENMARK

Danish Defence Research Board
Østerbrogades Kaserne
Copenhagen Ø

FRANCE

O.N.E.R.A. (Direction)
29 Avenue de la Division Leclerc
92 Châtillon sous Bagneux

GERMANY

Zentralstelle für Luft- und Raumfahrt-
dokumentation und -information
c/o Fachinformationszentrum Energie,
Physik, Mathematik GmbH
Kernforschungszentrum
7514 Eggenstein-Leopoldshafen 2

GREECE

Hellenic Air Force General Staff
Research and Development Directorate
Holargos, Athens, Greece

ICELAND

Director of Aviation
c/o Flugrad
Reykjavik

ITALY

Aeronautica Militare
Ufficio del Delegato Nazionale all'AGARD
3, Piazzale Adenauer
Roma/EUR

LUXEMBOURG

See Belgium

NETHERLANDS

Netherlands Delegation to AGARD
National Aerospace Laboratory, NLR
P.O. Box 126
Delft

NORWAY

Norwegian Defence Research Establishment
Main Library
P.O. Box 25
N-2007 Kjeller

PORTUGAL

Direcção do Serviço de Material
da Força Aérea
Rua da Escola Politecnica 42
Lisboa
Attn: AGARD National Delegate

TURKEY

Department of Research and Development (ARGE)
Ministry of National Defence, Ankara

UNITED KINGDOM

Defence Research Information Centre
Station Square House
St. Mary Cray
Orpington, Kent BR5 3RE

UNITED STATES

National Aeronautics and Space Administration (NASA)
Langley Field, Virginia 23365
Attn: Report Distribution and Storage Unit

THE UNITED STATES NATIONAL DISTRIBUTION CENTRE (NASA) DOES NOT HOLD STOCKS OF AGARD PUBLICATIONS, AND APPLICATIONS FOR COPIES SHOULD BE MADE DIRECT TO THE NATIONAL TECHNICAL INFORMATION SERVICE (NTIS) AT THE ADDRESS BELOW.

PURCHASE AGENCIES*Microfiche or Photocopy*

National Technical
Information Service (NTIS)
5285 Port Royal Road
Springfield
Virginia 22161, USA

Microfiche

Space Documentation Service
European Space Agency
10, rue Mario Nikis
75015 Paris, France

Microfiche

Technology Reports
Centre (DTI)
Station Square House
St. Mary Cray
Orpington, Kent BR5 3RF
England

Requests for microfiche or photocopies of AGARD documents should include the AGARD serial number, title, author or editor, and publication date. Requests to NTIS should include the NASA accession report number. Full bibliographical references and abstracts of AGARD publications are given in the following journals:

Scientific and Technical Aerospace Reports (STAR)
published by NASA Scientific and Technical
Information Facility
Post Office Box 8757
Baltimore/Washington International Airport
Maryland 21240; USA

Government Reports Announcements (GRA)
published by the National Technical
Information Services, Springfield
Virginia 22161, USA



Printed by Technical Editing and Reproduction Ltd
Harford House, 7-9 Charlotte St, London W1P 1HD

ISBN 92-835-1312-6